

Washington University in St. Louis

## Washington University Open Scholarship

---

Arts & Sciences Electronic Theses and  
Dissertations

Arts & Sciences

---

Summer 8-15-2021

### Enantioselective synthesis of $\beta$ -amino acid derivatives using amidine-based and bifunctional organocatalysts

Matthew Robert Straub  
*Washington University in St. Louis*

Follow this and additional works at: [https://openscholarship.wustl.edu/art\\_sci\\_etds](https://openscholarship.wustl.edu/art_sci_etds)

 Part of the [Organic Chemistry Commons](#)

---

#### Recommended Citation

Straub, Matthew Robert, "Enantioselective synthesis of  $\beta$ -amino acid derivatives using amidine-based and bifunctional organocatalysts" (2021). *Arts & Sciences Electronic Theses and Dissertations*. 2535.  
[https://openscholarship.wustl.edu/art\\_sci\\_etds/2535](https://openscholarship.wustl.edu/art_sci_etds/2535)

This Dissertation is brought to you for free and open access by the Arts & Sciences at Washington University Open Scholarship. It has been accepted for inclusion in Arts & Sciences Electronic Theses and Dissertations by an authorized administrator of Washington University Open Scholarship. For more information, please contact [digital@wumail.wustl.edu](mailto:digital@wumail.wustl.edu).

WASHINGTON UNIVERSITY IN ST. LOUIS

Department of Chemistry

Dissertation Examination Committee:

Kevin Moeller, Chair

Vladimir Birman

Marcus Foston

John-Stephen Taylor

Timothy Wencewicz

Enantioselective Synthesis of  $\beta$ -Amino Acid Derivatives Using Amidine-Based and Bifunctional Organocatalysts

by

Matthew Robert Straub

A dissertation presented to  
The Graduate School  
of Washington University in  
partial fulfillment of the  
requirements for the degree  
of Doctor of Philosophy

August 2021

Saint Louis, Missouri

© 2021, Matthew Robert Straub

# Table of Contents

List of Figures.....	vi
List of Tables.....	ix
List of Abbreviations.....	xi
Acknowledgments.....	xiii
Abstract.....	xv
<b>Chapter 1: Introduction to <math>\beta</math>-amino acids.....</b>	<b>1</b>
1.1 Structure, properties, and the practical significance of $\beta$ -amino acids.....	1
1.2 Asymmetric, catalytic approaches to $\beta$ -amino acids and their derivatives.....	5
1.3 References.....	7
<b>Chapter 2: Enantioselective synthesis of <math>\alpha</math>-fluoro-<math>\beta</math>-amino acid derivatives using amidine based- acyl transfer organocatalysts.....</b>	<b>11</b>
2.1 Properties of fluorine and its role in medicinal chemistry.....	11
2.2 Asymmetric, catalytic approaches to $\alpha$ -fluoro- $\beta$ -amino acid derivatives.....	14
2.3 Lewis base-catalyzed asymmetric synthesis of $\beta$ -lactams.....	16
2.4 Isothiourea-catalyzed formal [2+2] cycloadditions.....	17
2.5 Our approach to $\alpha$ -fluoro- $\beta$ -amino acids via asymmetric ABC-catalyzed formal [2+2] cycloaddition.....	20
2.6 Optimization of reaction conditions: Activator, base, and achiral catalyst.....	21
2.7 Optimization of reaction conditions: Chiral catalysts and exploring nucleophiles.....	23
2.8 Substrate scope of new methodology.....	25
2.9 Exploring other imines.....	26
2.10 Deprotection of nitrogen.....	27
2.11 Exploring additional uses of fluoroenolates.....	28
2.12 Substrate-dependent diastereoselectivities.....	29
2.13 Conclusions and future directions.....	31
2.14 Experimental.....	32
2.14.1 Preparation of anhydrous fluoroacetic acid.....	33

2.14.2 Enantioselective synthesis and ring opening of 3-fluoro- $\beta$ -lactams.....	34
2.14.3 Protecting group exchange.....	45
2.15 X-ray crystal structure of <b>2.51a-OMe</b> .....	47
2.16 References.....	58
<b>Chapter 3: Kinetic resolution of isoxazolidinones</b> .....	<b>62</b>
3.1 Introduction to kinetic resolution.....	64
3.2 Kinetic resolution, dynamic kinetic resolution, and desymmetrization of cyclic acyl donors via organocatalytic enantioselective alcoholysis.....	66
3.3 Introduction to bifunctional organocatalysis.....	68
3.4 Initial screening of reaction conditions.....	70
3.5 Optimization of solvent and alcohol using Takemoto's catalyst.....	73
3.6 Bifunctional catalyst survey.....	75
3.7 Substrate scope of new methodology.....	76
3.8 Reversible ring closure of <i>t</i> -Bu derivative <b>3.44-Me</b> .....	78
3.9 Additional Transformations.....	79
3.10 Conclusions and Future Directions.....	80
3.11 Experimental.....	81
3.11.1 Synthesis of new isoxazolidinones.....	82
3.11.2 Kinetic resolution experiments: Initial survey of reaction conditions.....	86
3.11.3 Kinetic resolution experiments: Exploring solvents and alcohols with Takemoto's catalyst.....	88
3.11.4 Kinetic resolution experiments: Bifunctional catalyst survey.....	89
3.11.5 Kinetic resolution experiments: Substrate scope.....	89
3.12 Interconversion of kinetic resolution products.....	90
3.12.1 Methanolysis of isoxazolidinones or esters.....	90
3.12.2 Recyclization of methyl ester <b>3.44m-Me</b> into isoxazolidinone <b>3.43f</b> .....	91
3.12.3. Recyclization of methyl ester <b>3.44m-Me</b> into <b>3.43m</b> .....	91
3.13 Hydrogenolysis of <b>3.43a</b> into $\beta$ -phenylalanine.....	92
3.14 Characterization of ester products.....	93
3.15 References.....	108

<b>Chapter 4: Organocatalyzed rearrangements of thioesters</b> .....	112
4.1 General introduction to asymmetric acyl transfer catalysis.....	112
4.2 Introduction to thioesters as acyl donors.....	115
4.3 Our previous work on rearrangements of thioesters.....	118
4.3.1 Asymmetric synthesis of thiochromenes.....	118
4.3.2 Asymmetric synthesis of thiochromanes.....	119
4.4 Synthesis and exploration of 5-aryl-DHIP derivatives.....	122
4.5 Organocatalyzed rearrangement of S-(2-oxoalkyl)-thioenoates.....	125
4.5.1 Mechanistically different rearrangement.....	125
4.5.2 Optimization of solvent and achiral catalyst.....	126
4.5.3 Initial attempts at an enantioselective variant.....	128
4.5.4 Racemic substrate scope.....	128
4.5.5 Alternative two-component approach to the same products.....	130
4.5.6 Origins of low enantioselectivity.....	130
4.6 Additional organocatalyzed rearrangements of S-aryl thioesters.....	133
4.6.1 Asymmetric synthesis of a 4-substituted thiochrome.....	133
4.6.2 Asymmetric synthesis of a 3-fluoro thiochromene.....	134
4.6.3 Synthesis of fused indanes.....	137
4.7 Conclusions and future directions.....	141
4.8 Experimental.....	143
4.8.1 Synthesis of S-phenacyl thiocinnamate derivatives <b>4.76</b> .....	144
4.8.2 Rearrangements of thioesters <b>4.76</b> .....	151
4.8.3 Synthesis of trichlorophenyl esters <b>4.85</b> .....	157
4.8.4 Two component synthesis of dihydrothiophene <b>4.82a</b> .....	159
4.8.5 Synthesis of a 4-substituted thiochromene.....	161
4.8.6 Synthesis of a 3-fluoro thiochromene.....	163
4.8.7 Synthesis of new catalysts.....	165
4.8.8 Synthesis of fused indanes <b>4.103a,b</b> .....	171
4.9 X-ray crystal structure of <b>4.100a-BnNH<sub>2</sub></b> .....	175
4.10 X-ray crystal structure of <b>4.100b</b> .....	188

4.11 References.....	199
----------------------	-----

## Appendix

A.1 Isodesmic study: An attempt to elucidate the spontaneous ring closure of <b>3.44m-Me</b> .....	202
A.2 Kinetic data for 5-aryl DHIP derivatives.....	203
A.3 HPLC chromatograms.....	209
A.4 $^1\text{H}$ and $^{13}\text{C}$ NMR spectra.....	250

# List of Figures

Figure 1.1: Pharmacologically important compounds with a $\beta$ -amino acid moiety.....	1
Figure 1.2: Comparing the structure of $\alpha$ - and $\beta$ -amino acids.....	2
Figure 1.3: Structure of CFP, an inhibitor of endopeptidase EC.....	3
Figure 1.4: Some examples of $\beta$ -peptides as peptidomimetics .....	4
Figure 1.5: Illustrative catalytic asymmetric approaches to $\beta$ -amino acids and derivatives.....	6
Figure 1.6: Additional examples of asymmetric approaches to $\beta$ -amino acids and derivatives.....	6
Figure 2.1: Effects of fluorine on a hairpin turn in a $\beta$ -tetrapeptide.....	13
Figure 2.2: Catalytic asymmetric approaches to $\alpha$ -fluoro- $\beta$ -amino acids.....	15
Figure 2.3: KR of an $\alpha$ -fluoro- $\beta$ -lactam via enantioselective methanolysis.....	15
Figure 2.4: Lewis-base catalyzed formal [2+2] cycloadditions as an approach to enantioenriched $\beta$ -lactams.....	17
Figure 2.5: Evolution of ABCs developed by our group.....	18
Figure 2.6: Homobenzotramisole-catalyzed aldol-lactonization tandem reaction.....	18
Figure 2.7: Tandem Michael-aldol-lactonization synthesis of $\beta$ -lactone fused cyclopentanes.....	19
Figure 2.8: Smith's approach to $\beta$ -lactams and $\beta$ -amino acid esters using a chiral ABC.....	19
Figure 2.9: Our proposed strategy to enantioenriched $\alpha$ -fluoro- $\beta$ -amino acids via [2+2] cycloaddition.....	20
Figure 2.10: X-ray crystal structure of <b>2.51a-OMe</b> .....	25
Figure 2.11: Exploring other imines with optimized reaction conditions.....	27
Figure 2.12: Removal of tosyl group from <b>2.51a-OBn</b> .....	28
Figure 2.13: Other electrophiles tested using this methodology.....	29
Figure 2.14: Substrate-dependent diastereoselectivities.....	31
Figure 3.1: N-carbalkoxy-isoxazolidin-5-ones as precursors to $\beta$ -amino acids.....	62
Figure 3.2: Asymmetric catalytic approaches to N-Boc-isoxazolidinones.....	63
Figure 3.3: a) Brière's racemic, one pot-multicomponent synthesis, b) Attempts at rendering this multicomponent reaction enantioselective.....	64
Figure 3.4: A graphical representation of KR and the equations used to calculate its efficacy.....	65
Figure 3.5: Examples of enantioselective alcoholysis of cyclic acyl donors. a) KR of $\alpha$ -amino	



acid carboxyanhydrides, b) desymmetrization of prochiral cyclic anhydrides, c) KR of N-acyl- $\beta$ -lactams, d) DKR of azlactones via non-covalent and covalent modes of catalysis, e) KR of oxazinones.....	67
Figure 3.6: General structure of the most common bifunctional double hydrogen bond donor-amine organocatalysts.....	69
Figure 3.7: Asymmetric Michael addition of 1,3-dicarbonyls to nitroolefins.....	69
Figure 3.8: Novel thiourea-tertiary amine organocatalyst designs.....	70
Figure 3.9: Proposed KR of N-carbalkoxy-isoxazolidin-5-ones.....	70
Figure 3.10: Ring opening of an N-Boc-isoxazolidinone with MeOH and NEt <sub>3</sub> .....	71
Figure 3.11: Catalysts used in this study.....	73
Figure 3.12: Reversible ring-closure of <i>t</i> -butyl substrate <b>3.43m</b> .....	78
Figure 3.13: Quantitative N-O bond cleavage to yield an enantioenriched $\beta$ -amino acid.....	79
Figure 3.14: Recycling of reacted enantiomer.....	80
Figure 3.15: Other acyl donors that may be amenable to KR via enantioselective alcoholysis.....	81
Figure 4.1: Three mechanistically distinct pathways involving catalytic acyl transfer.....	113
Figure 4.2: Some examples from the most common classes of achiral acyl transfer catalysts.....	114
Figure 4.3: Chiral acyl transfer catalysts developed by other groups.....	115
Figure 4.4: Conventional acyl donors and thioesters.....	116
Figure 4.5: Thioesters: An alternative approach to C <sub>1</sub> ammonium zwitterionic enolates.....	116
Figure 4.6: Organocatalyzed rearrangement of an enol ester.....	117
Figure 4.7: Organocatalyzed rearrangement of $\omega$ -hydroxy- $\alpha,\beta$ -unsaturated thioesters.....	118
Figure 4.8: Organocatalyzed enantioselective rearrangements of ortho-formylthioesters using HBTM-2.....	118
Figure 4.9: Organocatalyzed enantioselective rearrangement of S-aryl thioesters into tricyclic ene-lactones using H-PIP.....	119
Figure 4.10: Relative acylation enthalpies and relative rates of various achiral ABCs.....	121
Figure 4.11: 5- and 7-substituted DHIP derivatives.....	122
Figure 4.12: Synthesis of achiral 5-aryl-DHIP and chiral 5-aryl-PIP derivatives.....	124
Figure 4.13: Testing 5-aryl DHIP derivatives.....	124
Figure 4.14: a) Synthesis of S-phenacyl thiocinnamate, b) The expected catalyzed rearrangement	

pathway, c) The experimentally observed rearrangement pathway.....	125
Figure 4.15: Achiral catalysts used in this study.....	126
Figure 4.16: Attempts at an enantioselective variant.....	128
Figure 4.17: Alternative two-component approach the dihydrothiophenes <b>4.79</b> .....	130
Figure 4.18: Origins of low enantioselectivity.....	131
Figure 4.19: Alternative mode of catalysis used to make racemic thiochromenes.....	132
Figure 4.20: S-aliphatic thiolate capable of reacting with thioester in addition to ammonium cation: one possible explanation for the origin of low enantioselectivity.....	132
Figure 4.21: Troublesome substrates in the thiochromene synthesis.....	133
Figure 4.22: Synthesis of a 4-substituted thiochromene.....	134
Figure 4.23: Catalysts used in the fluorothiochromene study.....	135
Figure 4.24: <sup>1</sup> H NMR spectra showing formation and disappearance of <b>4.95</b> .....	136
Figure 4.25: Decarboxylation of fluorinated β-lactone intermediate.....	137
Figure 4.26: Proposed explanation for inversion of enantioselectivity.....	139
Figure 4.27: X-ray crystal structure of <b>4.100b</b> .....	141
Figure 4.28: X-ray crystal structure of <b>4.100a-BnNH<sub>2</sub></b> , analyzed as the ring-opened benzyl amide.....	141
Figure 4.29: Possible additional application for thioesters as acyl donors.....	143
Figure A.1: Linear regression for catalyst <b>4.59b</b> .....	206
Figure A.2: Linear regression for catalyst <b>4.59c</b> .....	206
Figure A.3: Comparing the kinetics between catalysts <b>4.59b</b> and <b>4.59c</b> .....	207
Figure A.4: Zoomed in graph with error bars.....	208

# List of Tables

Table 2.1: Optimization of reaction conditions: activator, base, and achiral catalyst.....	22
Table 2.2: Optimization of the enantioselective variant.....	24
Table 2.3: Substrate scope.....	26
Table 2.4: Crystal data and structure refinement for <b>2.51a-OMe</b> .....	47
Table 2.5: Atomic coordinates ( $\times 10^4$ ) and equivalent isotropic displacement parameters ( $\text{\AA}^2 \times 10^3$ ) for <b>2.51a-OMe</b> .....	48
Table 2.6: Bond lengths [ $\text{\AA}$ ] and angles [ $^\circ$ ] for <b>2.51a-OMe</b> .....	49
Table 2.7: Anisotropic displacement parameters ( $\text{\AA}^2 \times 10^3$ ) for <b>2.51a-OMe</b> .....	53
Table 2.8: Hydrogen coordinates ( $\times 10^4$ ) and isotropic displacement parameters ( $\text{\AA}^2 \times 10^3$ ) for <b>2.51a-OMe</b> .....	54
Table 2.9: Torsion angles [ $^\circ$ ] for <b>2.51a-OMe</b> .....	55
Table 2.10: Hydrogen bonds for <b>2.51a-OMe</b> [ $\text{\AA}$ and $^\circ$ ].....	56
Table 3.1: Initial screening of reaction conditions.....	72
Table 3.2: Solvent study.....	74
Table 3.3: Bifunctional catalyst survey.....	75
Table 3.4: Substrate scope.....	77
Table 3.5: Initial survey of reaction conditions. (corresponds to Table 3.1, section 3.4).....	88
Table 3.6: Survey of solvents and alcohols using Takemoto's catalyst <b>3.17</b> . (corresponds to Table 3.2, section 3.5).....	88
Table 3.7: Bifunctional catalyst survey (corresponds to Table 3.3, section 3.6).....	89
Table 3.8: Substrate scope (corresponds to Table 3.4, section 3.7).....	90
Table 4.1: Optimization of achiral catalyst and solvent.....	127
Table 4.2: Racemic substrate scope.....	129
Table 4.3: Synthesis of a 3-fluorothiochromene.....	135
Table 4.4: Synthesis of fused indanes <b>4.100a</b> and <b>4.100b</b> .....	138
Table 4.5: Crystal data and structure refinement for <b>4.100a-BnNH<sub>2</sub></b> .....	175
Table 4.6: Atomic coordinates ( $\times 10^4$ ) and equivalent isotropic displacement parameters ( $\text{\AA}^2 \times$	

10 <sup>3</sup> ) for <b>4.100a-BnNH<sub>2</sub></b> .....	176
Table 4.7: Bond lengths [Å] and angles [°] for <b>4.100a-BnNH<sub>2</sub></b> .....	178
Table 4.8: Anisotropic displacement parameters (Å <sup>2</sup> x 10 <sup>3</sup> ) for <b>4.100a-BnNH<sub>2</sub></b> .....	183
Table 4.9: Hydrogen coordinates ( x 10 <sup>4</sup> ) and isotropic displacement parameters (Å <sup>2</sup> x 10 <sup>3</sup> ) for <b>4.100a-BnNH<sub>2</sub></b> .....	184
Table 4.10: Torsion angles [°] for <b>4.100a-BnNH<sub>2</sub></b> .....	185
Table 4.11: Hydrogen bonds for <b>4.100a-BnNH<sub>2</sub></b> [Å and °].....	187
Table 4.12: Crystal data and structure refinement for <b>4.100b</b> .....	188
Table 4.13: Atomic coordinates ( x 10 <sup>4</sup> ) and equivalent isotropic displacement parameters (Å <sup>2</sup> x 10 <sup>3</sup> ) for <b>4.100b</b> .....	189
Table 4.14: Bond lengths [Å] and angles [°] for <b>4.100b</b> .....	190
Table 4.15: Anisotropic displacement parameters (Å <sup>2</sup> x 10 <sup>3</sup> ) for <b>4.100b</b> .....	194
Table 4.16: Hydrogen coordinates ( x 10 <sup>4</sup> ) and isotropic displacement parameters (Å <sup>2</sup> x 10 <sup>3</sup> ) for <b>4.100b</b> .....	195
Table 4.17: Torsion angles [°] for <b>4.100b</b> .....	196
Table 4.18: Hydrogen bonds for <b>4.100b</b> [Å and °].....	198
Table A.1: Results of isodesmic study.....	202
Table A.2: Conversion data obtained for catalyst <b>4.59b</b> .....	204
Table A.3: Conversion data obtained for catalyst <b>4.59c</b> .....	205

# List of Abbreviations

ABC: Amidine-based catalyst

Ac: Acetyl

Alloc: Allyloxycarbonyl

Ar: Aryl

BTM: Benzotetramisole

Bn: Benzyl

Boc: *tert*-butyloxycarbonyl

Bz: Benzoyl

Cbz: Benzyloxycarbonyl

CF<sub>3</sub>-PIP: 2-Phenyl-6-(trifluoromethyl)-2,3-dihydroimidazo[1,2-a]pyridine

Cl-PIQ: 7-Chloro-2-phenyl-1,2-dihydroimidazo[1,2-a]quinoline

COD: 1,5-cyclooctadiene

DABCO: 1,4-Diazabicyclo[2.2.2]octane

DBU: 1,8-Diazabicyclo[5.4.0]undec-7-ene

DFT: density functional theory

DHIP: 2,3-Dihydroimidazo[1,2-a]pyridine

DHPB: 3,4-Dihydro-2H-benzo[4,5]thiazolo[3,2-a]pyrimidine

(DHQD)<sub>2</sub>AQN: Hydroquinidine (anthraquinone-1,4-diyl) diether

DKR: dynamic kinetic resolution

DMAP: 4-(dimethylamino)pyridine

dppa: bis(diphenylphosphanyl)amine

dr: diastereomeric ratio

*ent*: enantiomer of

*ee*: enantiomeric excess

Et: ethyl

EtOAc: ethyl acetate

Fmoc: 9-fluorenylmethoxycarbonyl

HBTM: Homobenzotetramisole  
HOMO: Highest Occupied Molecular Orbital  
H-PIP: 2-Phenyl-2,3-dihydroimidazo[1,2-a]pyridine  
HPLC: High Performance Liquid Chromatography  
*i*-Pr: isopropyl  
KR: Kinetic resolution  
LiHMDS: lithium bis(trimethylsilyl)amide  
LUMO: Lowest Unoccupied Molecular Orbital  
Me: methyl  
NFSI: N-fluorobenzenesulfonimide  
NHC: N-heterocyclic carbene  
Nosyl: nitrobenzenesulfonyl  
p: para  
Ph: phenyl  
Piv: Pivaloyl  
s: selectivity factor  
Salen: 2,2'-ethylenebis(nitriloomethylidene)diphenol  
TBDPS: *tert*-butyldiphenylsilyl  
TBME: *tert*-butyl methyl ether  
*t*-Bu: *tert*-butyl  
TCBC: trichlorobenzoyl chloride  
TFA: trifluoroacetic acid  
TFE: trifluoroethanol  
TMS: trimethylsilyl  
Ts: tosyl

# Acknowledgments

First, I would like to express my gratitude to my Ph.D. advisor, Professor Vladimir Birman, for all of the guidance, mentorship, knowledgeable insight, and financial and emotional support during my Ph.D. studies at Washington University. From group meetings to countless hours talking about chemistry in the lab, the invaluable knowledge I gained under his direction allowed me to achieve success in many research projects. I am eternally grateful.

I would also like to thank the two members of my Ph.D. advisory committee, Professor Kevin Moeller and Professor John-Stephen Taylor, for their valuable feedback and insightful discussions that always took place during my committee meetings. I would also like to thank Dr. Marcus Foston and Dr. Timothy Wencewicz for serving on my Dissertation Defense committee and providing constructive criticism and useful comments.

I also deeply appreciate the support of Jingwei Yin and Ruth Son, two incredibly hard-working colleagues who have always inspired me to be the best chemist I could be. In addition to current coworkers, I also want to acknowledge David Leace and Benjamin Matz for their collaborative efforts on organocatalyzed rearrangements of thioesters, in addition to giving me mentorship experience. I also wish to recognize Dr. Nicholas Ahlemeyer, Dr. Muthupandi Pandi and Dr. Krishnah Sharmah Gautam for their initial guidance and support when I first joined the group.

I want to express thanks to the chemistry faculty for the knowledge that I gained taking their courses. For this I would like to additionally thank Dr. Jonathan Barnes, Dr. John Bleeke, and Dr. Dewey Holten.

I also gratefully acknowledge the National Science Foundation (CHE 1566588) and Washington University in Saint Louis for their financial support. We also thank Dr. Nigam Rath (University of Missouri-Saint Louis) for providing crystallographic data.

Lastly, I wish to express my sincere gratitude to my parents, brother, extended family, friends, and my significant other. I would not have obtained my Ph.D. without their continuous emotional support.

*Washington University in St. Louis*

*August, 2021*



## ABSTRACT OF THE DISSERTATION

Enantioselective Synthesis of  $\beta$ -Amino Acid Derivatives Using Amidine-Based and Bifunctional Organocatalysts

for Arts & Sciences Graduate Students

by

Matthew Robert Straub

Doctor of Philosophy in Chemistry

Washington University in St. Louis, 2021

Professor Vladimir B. Birman, Principal Investigator

Two new enantioselective methodologies have been developed that have important implications for the asymmetric synthesis of  $\beta$ -amino acids and their derivatives. First, chiral amidine-based catalyst (ABC) HBTM-2 catalyzed an asymmetric cyclocondensation between in situ activated fluoroacetic acid and N-sulfonyl aldimines to give  $\alpha$ -fluoro- $\beta$ -lactams in highly enantioenriched form, achieving modest to excellent diastereoselectivities. These reactive lactams can then be quenched with various alcohols and amines to deliver the  $\alpha$ -fluoro- $\beta$ -amino acid derivatives in moderate isolated yields. Secondly, bifunctional double hydrogen bond donor-amine organocatalysts enable the catalytic alcoholysis of various racemic N-carbalkoxy-3-substituted isoxazolidin-5-ones, resulting in their kinetic resolution. The enantioenriched unreacted isoxazolidinone and product (easily recyclable via a two-step transesterification-cyclization process) can undergo quantitative N-O bond cleavage by hydrogen to give  $\beta$ -amino acids in N-protected form.

The fourth chapter of this dissertation, an extension of previous achievements in our group, describes the development of an organocatalyzed rearrangement of S-phenacyl thioesters that is mechanistically distinct from our previously published work. Additionally, more examples of asymmetric tandem rearrangements of S-aryl thioesters were demonstrated.

# Chapter 1: Introduction to $\beta$ -amino acids

## 1.1 Structure, properties, and the practical significance of $\beta$ -amino acids

Compared to the more well-known  $\alpha$ -amino acids,  $\beta$ -amino acids are much less abundant in the natural world. In fact, polymers of  $\beta$ -amino acids,  $\beta$ -peptides, are virtually nonexistent in Nature. Some  $\beta$ -amino acids, such as  $\beta$ -alanine (mostly in the form of the dipeptide carnosine), a catabolite of uracil, are quite plentiful in mammals. However,  $\beta$ -amino acids are not incorporated into mammalian proteins.<sup>1</sup> Despite all this, the  $\beta$ -amino acid moiety itself is quite prevalent in Nature and has been found in bioactive natural products such as the anticancer agent taxol **1.01** (paclitaxel)<sup>2</sup>, the antifungal cispentacin **1.02**<sup>3</sup>, and the known aminopeptidase inhibitors bestatin **1.03**<sup>4</sup> and amastatin **1.04**<sup>4</sup> (Figure 1.1).

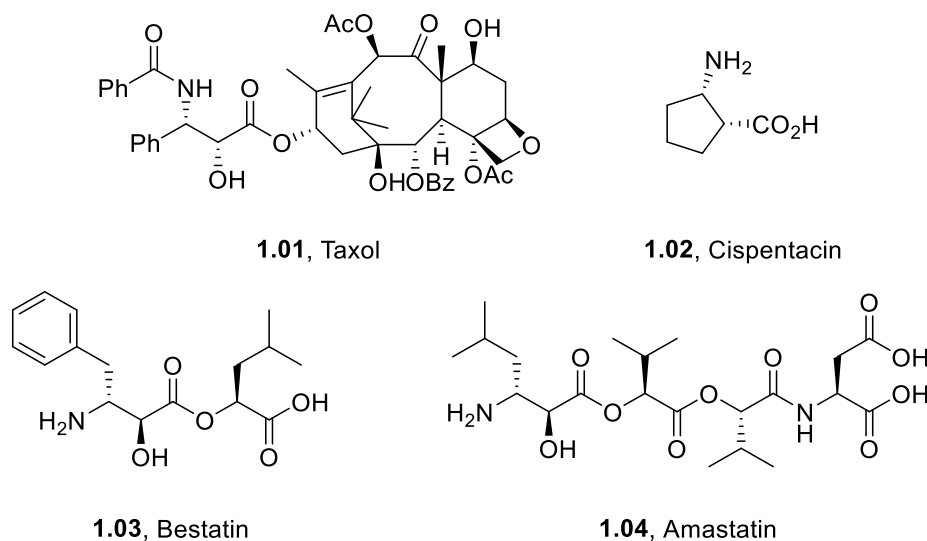


**Figure 1.1.** Pharmacologically important compounds with a  $\beta$ -amino acid moiety.

$\beta$ -amino acids are similar to  $\alpha$ -amino acids in that both have an amino terminus (called the N terminus) and a carboxyl terminus (called the C terminus); however,  $\beta$ -amino acids contain an

extra carbon between these two termini (Figure 1.2). The  $\beta$ -amino acid may be further categorized based on its substitution pattern.

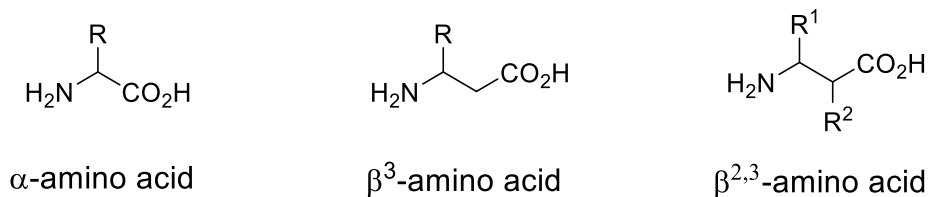


**Figure 1.2.** Comparing the structure of  $\alpha$ - and  $\beta$ -amino acids.

This extra carbon is a structural feature of  $\beta$ -amino acids that bestows a greater potential for molecular design compared to homologous  $\alpha$ -amino acids.<sup>5</sup> For example, with the additional carbon a total of four stereoisomers (two diastereomers each as a pair of enantiomers) is possible for each  $\beta$ -amino acid residue in a peptide chain, assuming each stereocenter is monosubstituted. Extra structural diversity can be achieved with di- and polysubstitution. This contrasts with  $\alpha$ -amino acids, which can exist as only one of two stereoisomers, the R or S enantiomer. As such, the construction of peptides containing  $\beta$ -amino acids is a developing method to meticulously adjust physicochemical properties, three-dimensional structure, and conformational preferences.<sup>6</sup> Consequently, there has been much interest in utilizing  $\beta$ -amino acids, and  $\alpha$ -peptides incorporating them, for therapeutical and pharmacological applications.

One significant property of  $\beta$ -amino acids that increases their prospects in medicinal chemistry is their proteolytic and hydrolytic stability. One potential application for this is enzyme inhibition. For example, since proteases and peptidases often play a huge role in inter- and intracellular processes, inhibitors of these enzymes would be ideal for probing cellular networks, in addition to treating certain diseases.<sup>7</sup> This resistance to enzymatic degradation was first reported in the 1960s, when naturally occurring polypeptide hormones adrenocorticotropin and angiotensin

II incorporating N-terminus  $\beta$ -amino acids were shown to be resistant to aminopeptidase degradation.<sup>8</sup> In the late 1990s, Seebach et al. also demonstrated the resistance of  $\beta$ -peptides to degradation by proteases such as trypsin, chymotrypsin, and pepsin. Interestingly, these  $\beta$ -peptides stayed intact for several days, whereas analogous  $\alpha$ -peptides were completely consumed within minutes.<sup>9</sup>

For another example, EP 24.15 (commonly called CFP, **1.05**, Figure 1.3) is an  $\alpha$ -peptide that serves as an inhibitor of the enzyme endopeptidase EC.<sup>10</sup> CFP undergoes hydrolysis by an enzyme known as neprilysin. In one study, many substitutions of CFP involving  $\beta$ -amino acids were made, almost all of them preventing any proteolytic degradation by neprilysin.<sup>11</sup>

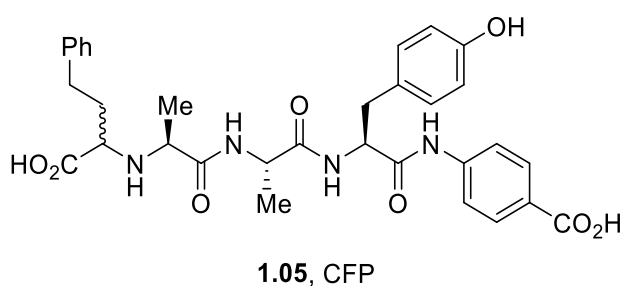


**Figure 1.3.** Structure of CFP, an inhibitor of endopeptidase EC.

Their biological stability, coupled with their structural homology to naturally occurring  $\alpha$ -amino acids, has allowed  $\beta$ -amino acids and  $\beta$ -amino acid-containing proteins to be used as peptidomimetics, or protein mimics. This is arguably their most studied pharmacological application. For some examples,  $\beta$ -amino acid-containing (aminobenzamidino)succinyl compound **1.06** (Figure 1.4) was discovered as a peptidomimetic for the Arg-Gly-Asp-Phe sequence of fibrinogen, a glycoprotein complex necessary for proper blood clot formation.<sup>12</sup> In the mid-1990s this orally active fibrinogen receptor antagonist's ability to inhibit platelet aggregation was studied

in vitro and in vivo, where 35% reduction in platelet count was observed after 9 days in canine studies.<sup>13</sup> In the late 1990s Seebach showed that cyclic  $\beta$ -tetrapeptide **1.07** has the potential to serve as an enterobactin-type  $C_3$ -symmetrical ligand, mimicking compounds that certain species of bacteria use to sequester iron from the environment.<sup>14</sup> Lastly, this same group showed that hexapeptide **1.08** can fold in such a way such that it mimics the amphipathic  $\alpha$ -peptide helix binding motifs required to inhibit membrane-bound proteins that facilitate lipid transport. When tested with CaCo-2 cells, model cells often used to simulate the epithelial lining of mammalian small intestines, this hexapeptide was shown to inhibit fat and cholesterol absorption.<sup>15</sup>

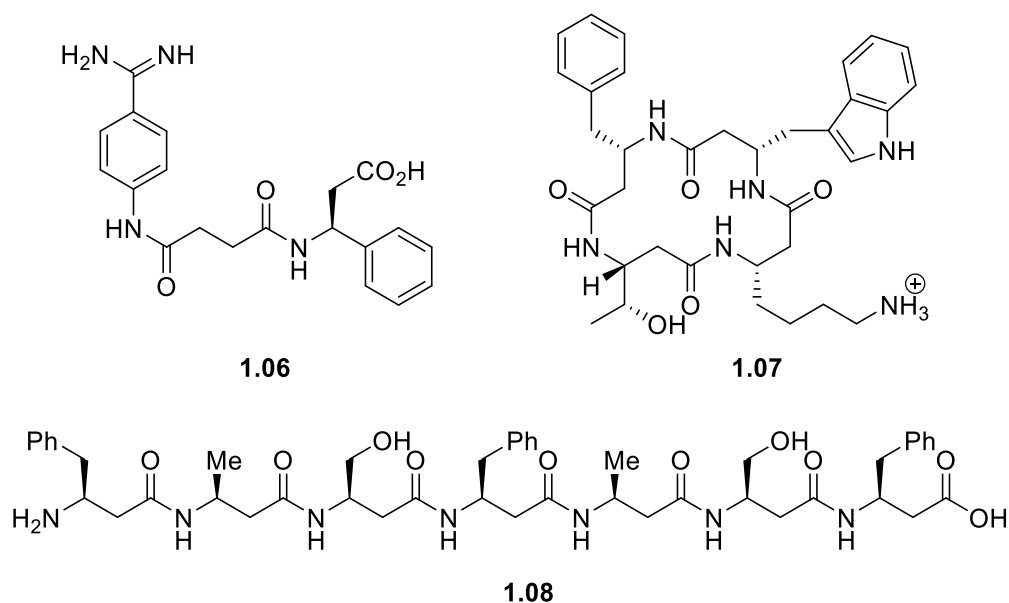


**Figure 1.4.** Some examples of  $\beta$ -peptides as peptidomimetics.

Additionally,  $\beta$ -peptide and  $\beta$ -amino acid-containing  $\alpha$ -peptide protein hormones have been studied as membrane-targeting peptides and receptor ligands. Peptides containing  $\beta$ -amino acid moieties have even adopted secondary structures seen in analogous  $\alpha$ -peptides, essentially mimicking their function. Within these broad categories of biological exploration,  $\beta$ -amino acid-

containing peptides have displayed antimicrobial activity, anti-angiogenic behavior, and inhibition of protein-protein interactions, just to name a few specific uses.<sup>16</sup>

In conclusion, given their increased biological stability, increased structural diversity, and ease of incorporation using standard solid-phase peptide synthesis,  $\beta$ -amino acids (and peptides consisting of) are key candidates for pharmacological and therapeutic exploration, most notably and expectedly as peptidomimetics. Since the discovery of the practical significance of  $\beta$ -amino acids, the synthetic community has explored asymmetric syntheses of these compounds.

## 1.2 Asymmetric, catalytic approaches to $\beta$ -amino acids and their derivatives

Some of the first methods developed to synthesize enantiomerically enriched  $\beta$ -amino acids relied on classical resolution, stoichiometric amounts of chiral auxiliaries, or homologations (e.g. Arndt-Eistert) of  $\alpha$ -amino acids. However, in recent years, the catalytic asymmetric syntheses of these compounds using transition metals, organocatalysts, and biocatalysts have rapidly expanded.<sup>17</sup> Generally speaking, the most common modern-day, catalytic, asymmetric approaches to  $\beta$ -amino acids and their derivatives fall into one of these categories: 1) addition of nucleophiles to imines or  $\alpha,\beta$ -unsaturated imides/esters (Eq. 1)<sup>18</sup>, 2) ring-opening of  $\beta$ -lactams (Eq. 2)<sup>19</sup>, 3) kinetic resolutions (Eq. 3)<sup>20</sup>, 4) reduction of enamines (Eq. 4)<sup>21</sup>, and 5) aza-Michael addition to enals (Eq. 5)<sup>22</sup>. Illustrative examples of each category are given in Figure 1.5.

Though less thoroughly investigated, the Baylis-Hillman reaction (Figure 1.6, Eq. 1)<sup>23</sup>, ring-expansive carbonylation of oxazolines (Eq.2)<sup>24</sup>, and using sulfoxides as chiral auxiliaries (Eq. 3)<sup>25</sup> have also been explored as a means of obtaining these compounds in enantioenriched form.

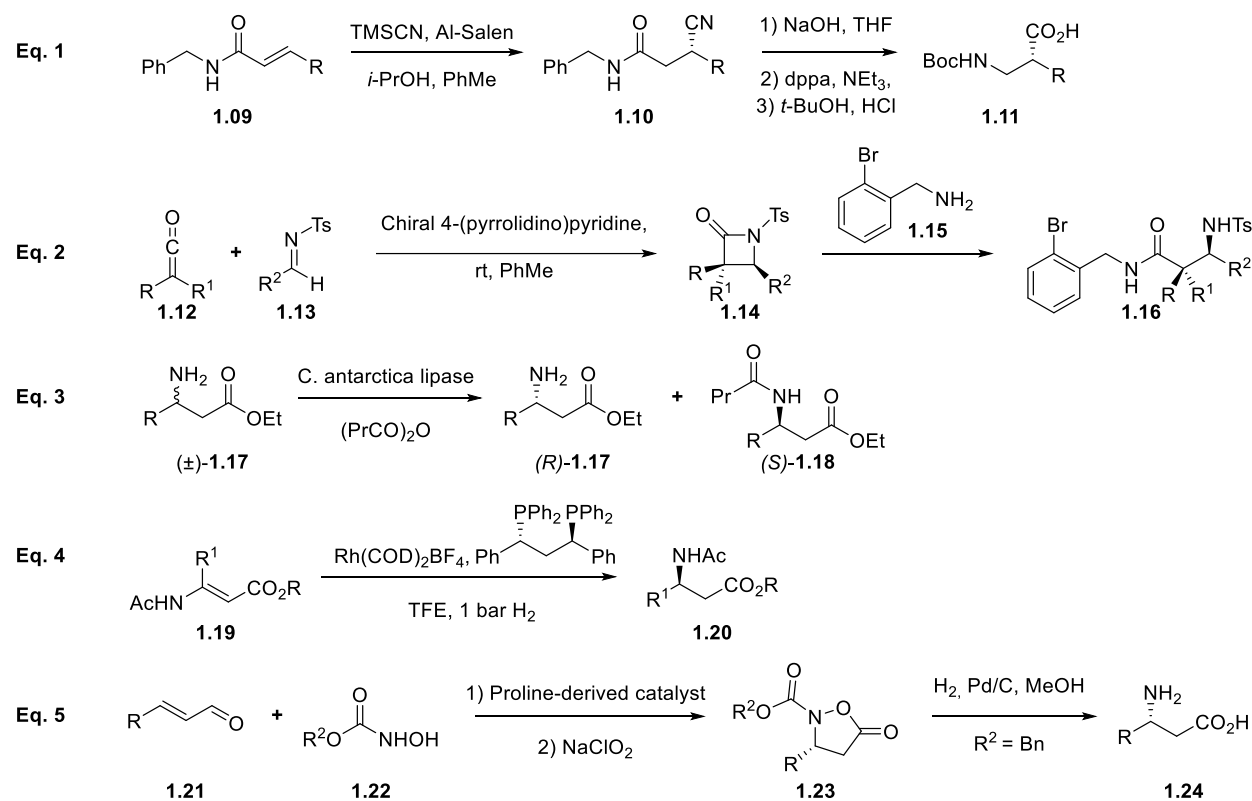


**Figure 1.5.** Illustrative catalytic asymmetric approaches to  $\beta$ -amino acids and derivatives.

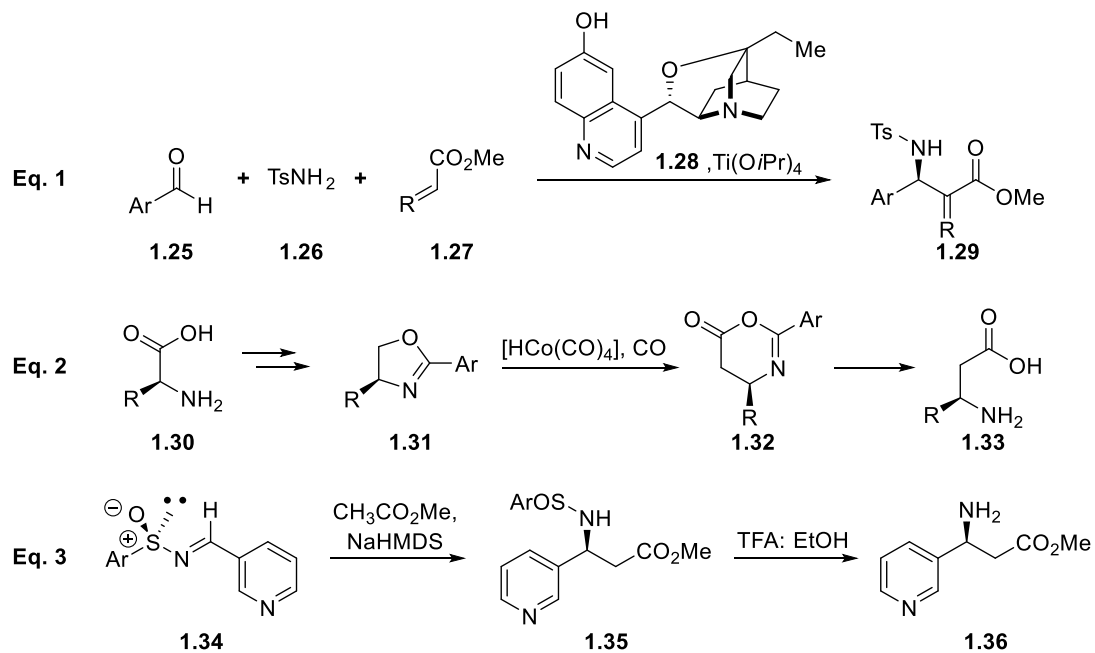


**Figure 1.6.** Additional examples of asymmetric approaches to  $\beta$ -amino acids and derivatives.

The numerous methodologies to obtain enantioenriched  $\beta$ -amino acids and their derivatives indicate the significance of these compounds.<sup>26</sup> Nevertheless, our group realized that some methods had remained unreported in the literature. These complementary organocatalytic methods we had envisioned offered distinct advantages such as obviating the need for transition metals and utilizing more easily available/synthesizable chiral catalysts.

## 1.3 References

1. Griffith, O. W. *Annu. Rev. Biochem.* **1986**, *55*, 855.
2. Kudo, F.; Miyanaga, A.; Eguchi, T. *Nat. Prod. Rep.* **2014**, *31*, 1056.
3. E. Juaristi (Ed.). *Enantioselective Synthesis of  $\beta$ -Amino Acids*; Wiley-VCH: New York, 1997.
4. Roers, R.; Verdine, G. L. *Tetrahedron Lett.* **2001**, *42*, 3563.
5. Steer, D. L.; Lew, R. A.; Perlmutter, P.; Smith, A. I.; Aguilar, M.-I. *Curr. Med. Chem.* **2002**, *9*, 811.
6. (a) Cheng, R. P.; Gellman, S. H.; DeGrado, W. F. *Chem. Rev.* **2001**, *101*, 3219. (b) Goodman, C. M.; Choi, S.; Shandler, S.; DeGrado, W. F. *Nat. Chem. Biol.* **2007**, *3*, 252. (c) Koyack, M. J.; Cheng, R. P. *Methods Mol. Biol.* **2006**, *340*, 95. (d) Horne, W. S. *Expert Opin. Drug Discov.* **2011**, *6*, 1247.
7. Steer, D. L.; Lew, R. A.; Perlmutter, P.; Smith, A. I.; Aguilar, M.-I. *Lett. Pept. Sci.* **2002**, *8*, 241.
8. (a) Doepfner, W. *Progr. Endocrinol., Proc. Int. Congr. Endocrinol.*, *3<sup>rd</sup>*. **1969**, 407.



- (b) Riniker, B.; Schwyzer, R. *Helv. Chim. Acta.* **1964**, 2357.
9. (a) Seebach, D.; Abele, S.; Schreiber, J. V.; Martinoni, B.; Nussbaum, A. K.; Schild, H.; Schulz, H.; Hennecke, H.; Woessner, R.; Bitsch, F. *Chimia.* **1998**, 52, 734. (b) Hintermann, T.; Seebach, D. *Chimia.* **1997**, 51, 244.
10. Orłowski, M.; Michand, C.; Molineaux, C. J. *Biochemistry*, **1988**, 27, 597.
11. Steer, D. L.; Lew, R. A.; Perlmutter, P.; Smith, A. I.; Aguilar, M.-I. *Lett. Pept. Sci.* **2002**, 8, 241.
12. Rico, J. G.; Lindmark, R. J.; Rogers, T. E.; Bovy, P. R. *J. Org. Chem.* **1993**, 58, 7948.
13. Zablocki, J. A.; et al. *J. Med. Chem.* **1995**, 38, 2378.
14. Gademann, K.; Seebach, D. *Helv. Chim. Acta.* **1999**, 82, 957.
15. Werder, M.; Hauser, H.; Abele, S.; Seebach, D. *Helv. Chim. Acta.* **1999**, 82, 1774.
16. (a) Cabrele, C.; Martinek, T. A.; Reiser, O.; Berlicki, L. *J. Med. Chem.* **2014**, 57, 9718.  
(b) Steer, D. L.; Lew, R. A.; Perlmutter, P.; Smith, A. I.; Aguilar, M.-I. *Curr. Med. Chem.* **2002**, 9, 811.
17. Weiner, B.; Szymanski, W.; Janssen, D. B.; Minnaard, A. J.; Feringa, B. L. *Chem. Soc. Rev.* **2010**, 39, 1656.
18. (a) Sammis, G. M. Jacobsen, E. N. *J. Am. Chem. Soc.* **2003**, 125, 4442. (b) Hamashima, Y.; Somei, H.; Shimura, Y.; Tamura, T.; Sodeoka, M. *Org. Lett.* **2004**, 6, 1861. (c) Wenzel, A. G.; Jacobsen, E. N. *J. Am. Chem. Soc.* **2002**, 124, 12964. (d) Hamashima, Y.; Sasamoto, N.; Hotta, D.; Somei, H.; Umebayashi, N.; Sodeoka, M. *Angew. Chem. Int.*

- Ed.* **2005**, *44*, 1525. (e) France, S.; Wack, H.; Hafez, A. M.; Taggi, A. E.; Witsil, D. R.; Lectka, T. *Org. Lett.* **2002**, *4*, 1603.
19. Hodous, B. L.; Fu, G. C. *J. Am. Chem. Soc.* **2002**, *124*, 1578.
20. (a) Gedey, S.; Liljebblad, A.; Lazar, L.; Fulop, F.; Kanerva, L. T. *Tetrahedron Asymmetry* **2001**, *12*, 105. (b) Forro, E.; Fueloep, F. *Org. Lett.* **2003**, *5*, 1209.
21. (a) Holz, J.; Monsees, A.; Jiao, H.; You, J.; Komarov, I. V.; Fischer, C.; Drauz, K.; Borner, A. *J. Org. Chem.* **2003**, *68*, 1701. (b) Dubrovina, N. V.; Tararov, V. I.; Monsees, A.; Kadyrov, R.; Fischeher, C.; Borner, A. *Tetrahedron Asymmetry* **2003**, *14*, 2739. (c) Heller, D.; Holz, J.; Drexler, H.-J.; Lang, J.; Drauz, K.; Krimmer, H.-P.; Boerner, A. *J. Org. Chem.* **2001**, *66*, 6816. (d) Davies, S. G. Smith, A. D.; Price, P. D. *Tetrahedron Asymmetry* **2005**, *16*, 2833.
22. Ibrahim, I.; Rios, R.; Vesely, J.; Zhao, G.-L.; Cordova, A. *Synthesis* **2008**, 1153.
23. Balan, D.; Adolfsson, H. *Tetrahedron Lett.* **2003**, *44*, 2521.
24. Byrne, C. M.; Church, T. L.; Kramer, J. W.; Coates, G. W. *Angew. Chem. Int. Ed.* **2008**, *47*, 3979.
25. (a) Davis, F. A.; Szewczyk, J. M.; Reddy, R. E. *J. Org. Chem.* **1996**, *61*, 2222. (b) Davis, F. A.; Szewczyk, J. M.; Reddy, R. E. *Tetrahedron Lett.* **1997**, *38*, 5139.
26. (a) Kim, S. M.; Yang, J. W. *Org. Biomol. Chem.* **2013**, *11*, 4737. (b) Ma, J.-A. *Angew. Chem. Int. Ed.* **2003**, *42*, 4290. (c) Sleebbs, B. E.; Van Nguyen, T. T.; Hughes, A. B. *Org. Prep. Proced. Int.* **2009**, *41*, 429. (d) Noda, H.; Shibasaki, M. *Eur. J. Org. Chem.* **2020**,

2020, 2350. (e) Liu, M.; Sibi, M. P. *Tetrahedron* **2002**, 58, 7991. (f) Lelais, G.; Seebach, D.; *Biopolymers* **2004**, 76, 206.

# **Chapter 2: Enantioselective synthesis of $\alpha$ -fluoro- $\beta$ -amino acid derivatives using amidine based acyl transfer organocatalysts<sup>1</sup>**

## **2.1 Properties of fluorine and its role in medicinal chemistry**

It has been known for quite some time that the introduction of fluorine into organic molecules can greatly alter chemical and physical properties, especially those of bioactive molecules. In fact, the greatest exploitation of fluorine's unique properties has been seen in the field of medicinal chemistry.<sup>2</sup> In 2014, it was estimated that approximately 20% of new pharmaceuticals entering the market contained at least one fluorine atom. The reason fluorine plays such an important role in drug development is because fluorinated substituents can greatly increase the efficacy of a drug. The role of fluorine is usually to enhance lipophilicity, increase metabolic stability, and change the pKa of nearby functional groups.<sup>3</sup>

Fluorine's high electronegativity is mostly responsible for the unique properties it confers to organofluorine compounds. Because fluorine is the most electronegative element that can be incorporated into organic molecules, the C-F bond has a very large dipole compared to other carbon-heteroatom bonds. Simple consideration of this large dipole and its interaction with other nearby dipoles can allow for a reasonable prediction of favorable conformations of fluorine-containing moieties. Another consideration to make when predicting conformations is the low lying  $\sigma^*_{\text{C-F}}$  antibonding orbital, which often likes to stereoelectronically align itself with electron rich bonds (e.g C-H bonds).<sup>4</sup> The C-F bond is also very strong compared to other carbon-heteroatom bonds, which may bode well for biological applications. In addition to its effects on bond polarization and bond strength, fluorine's size also makes it the best isosteric replacement

for both hydrogen and oxygen, being intermediate in size. Replacing hydrogen with fluorine can greatly alter chemical properties of nearby functional groups, oftentimes advantageously.<sup>5</sup>

One interesting fact about fluorine is its absence in biology. Since naturally occurring organofluorine compounds are near non-existent in nature, biological systems never evolved to incorporate fluorine into biopolymers such as proteins nor their constituent amino acids.<sup>6</sup> As such, the integration of man-made fluorinated amino acids is a distinctive way to modify proteins.<sup>7</sup> In addition to protein modification, incorporation of fluorinated amino acids has also aided in studying local protein environments and dynamics by <sup>19</sup>F NMR since the early 1990s.<sup>8</sup> Furthermore, coupled with the unique effects that  $\beta$ -amino acids can have on protein structure and properties (vide supra, Chapter 1), fluorinated  $\beta$ -amino acids offer an even greater opportunity for protein alteration. Incorporation of fluorine into biomolecules such as amino acids and proteins can be very advantageous since the ability to control their conformation is of great interest for biomedical applications.

While many fluorinated  $\beta$ -amino acids contain fluorine on aromatic rings as part of their side chain, the monofluorinated, monosubstituted  $\alpha$ -fluoro- $\beta$ -amino acids are relatively less explored and have less published procedures pertaining to their synthesis. However, like other fluorinated amino acids,  $\alpha$ -fluoro- $\beta$ -amino acids also have a lot of potential biological promise.<sup>9</sup> For example, the incorporation of a single fluorine on the  $\alpha$ -carbon of a  $\beta$ -amino acid can have a marked effect on the conformation of said moiety. This fluorine incorporation has been known to stabilize, for example, secondary structures; however, this can often be unpredictable. As a case in point, the fluorinated  $\beta$ -tetrapeptide **2.01a** and non-fluorinated analog **2.01b** were prepared to analyze the effect that fluorine has on a hairpin turn, an important secondary structure that is often used as a recognition motif. After performing solution NMR experiments, it was discovered that

the fluorinated tetrapeptide adopted a more stable hairpin structure on account of the more stable central fluorinated amide bond (Figure 2.1).<sup>10</sup>

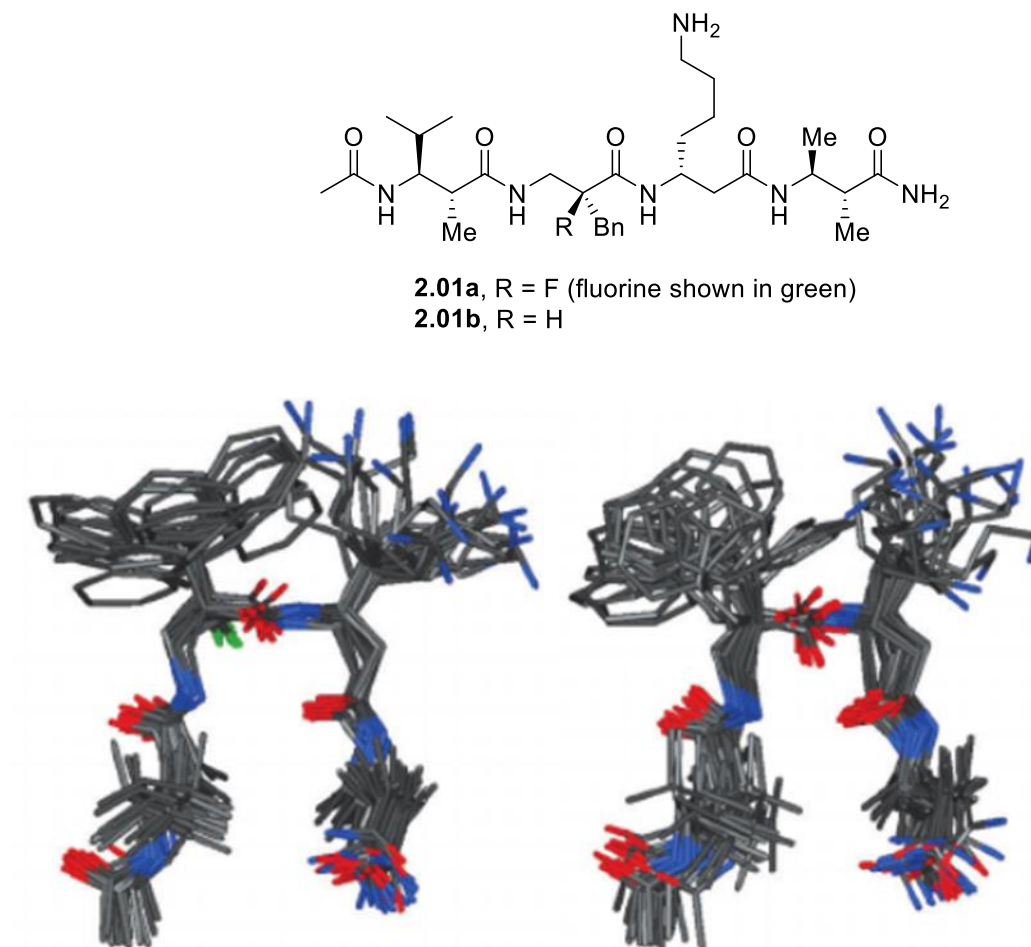


**Figure 2.1:** Effects of fluorine on a hairpin turn in a  $\beta$ -tetrapeptide. All credit for this graphic goes to Mathad, et al.<sup>10</sup>

Oftentimes it is hard to predict the behaviors/properties that incorporation of a single fluorine atom at the  $\alpha$ -position will have on a  $\beta$ -amino acid. Nevertheless, a lot of effort has been devoted to catalytic enantioselective syntheses of these compounds with the intent of further study.

## 2.2 Asymmetric, catalytic approaches to $\alpha$ -fluoro- $\beta$ -amino acid derivatives

Though less common than syntheses of other fluorinated amino acids, there still exist many methods for making enantiomerically enriched  $\alpha$ -fluoro- $\beta$ -amino acids and their derivatives. It should come as no surprise that a lot of the catalytic approaches used to make enantioenriched  $\beta$ -amino acids have also been applied to make  $\alpha$ -fluoro- $\beta$ -amino acids. Some illustrative examples are in Figure 2.2. In 2010, Brenner-Moyer et al. disclosed an enantioselective iminium ion catalysis approach (Eq. 1).<sup>11</sup> Formation of the iminium cation from the prolinol-derived catalyst and enal, followed by Michael addition of the Cbz-protected hydroxylamine generates an intermediate enamine. This enamine can react with NFSI (N-fluorobenzenesulfonimide), an electrophilic fluorinating agent (“F<sup>+</sup>” equivalent). The workup delivers the fluorinated aldehyde **2.04** which undergoes Pinnick oxidation to the carboxylic acid. Another approach disclosed in 2010 involved using a C<sub>2</sub>-symmetrical guanidine to catalyze the asymmetric addition of fluorinated  $\beta$ -ketoazolidinone **2.07** to reactive N-carbamate imine **2.06** (Eq. 2).<sup>12</sup> Subsequent selective deacylations delivered the final product. Along with these methodologies, another common approach to these compounds involves asymmetric reduction of  $\alpha$ -fluoro- $\beta$ -enamino esters. This has been achieved in two ways, either using N-sulfinyl urea-catalyzed asymmetric hydrosilylation (Eq. 3)<sup>13</sup> or via asymmetric hydrogenation using iridium and ZhaoPhos (Eq. 4).<sup>14</sup> In addition to these asymmetric catalytic approaches,  $\alpha$ -fluoro- $\beta$ -amino acids have also been synthesized via kinetic resolution (KR, vide infra, section 3.1). Enantioselective methanolysis of mono-fluorinated N-unprotected  $\beta$ -lactam **2.16** was achieved by *Burkholderia cepacia* lipase (Figure 2.3).<sup>15</sup> Interestingly, the non-fluorinated analogue of this  $\beta$ -lactam did not react, possibly indicating the activating effect that fluorine has on the electrophilicity of the nearby carbonyl.

---

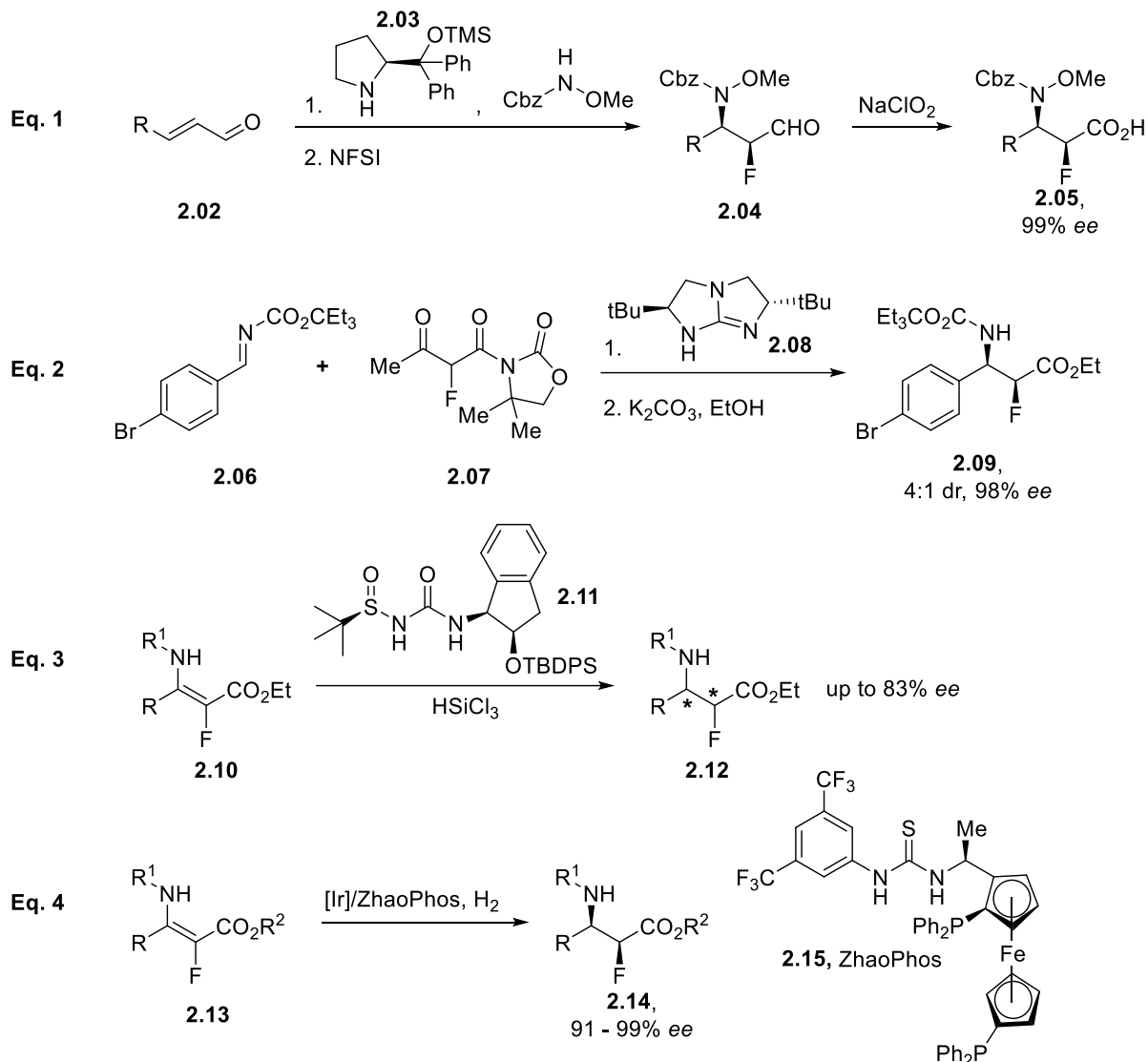


**Figure 2.2.** Catalytic asymmetric approaches to  $\alpha$ -fluoro- $\beta$ -amino acids.

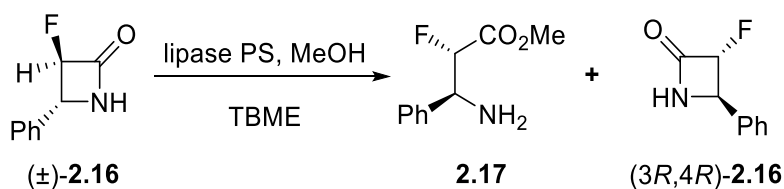


**Figure 2.3.** KR of an  $\alpha$ -fluoro- $\beta$ -lactam via enantioselective methanolysis.

While the most illustrative examples were described, more methods exist for the catalytic, asymmetric synthesis of these compounds.<sup>9</sup>



## 2.3 Lewis base-catalyzed asymmetric synthesis of $\beta$ -lactams

As aforementioned in subchapter 1.2 (Figure 1.5, Eq. 2), the ring-opening of  $\beta$ -lactams is a practical approach to enantioenriched  $\beta$ -amino acid derivatives. In 2002, Fu demonstrated for the first time that a chiral organic Lewis base could catalyze an asymmetric Staudinger reaction, or an overall formal [2+2] cycloaddition between an imine and ketene, to deliver  $\beta$ -lactams in enantioenriched form (Figure 2.4, Eq. 1). Prior to this work, most enantioselective approaches to  $\beta$ -lactams via the Staudinger reaction relied on stoichiometric amounts of chiral auxiliaries.<sup>16</sup> The mechanism is straightforward and starts with the nucleophilic catalyst **2.20** attacking the electrophilic ketene **2.18**. The resulting zwitterionic enolate will react with imine **2.19**. Subsequent ring closure turns over the catalyst and generates the  $\beta$ -lactam. One disadvantage of this work, however, was the laborious synthesis of the chiral catalyst **2.20**.

Since 2002, others have shown the efficacy of this asymmetric Lewis base-catalyzed Staudinger reaction. For example, in 2004 Lectka et. al demonstrated analogous asymmetric Staudinger reactions using the much more accessible cinchona alkaloid derivative O-benzoylquinine **2.26** as Lewis base catalyst (Figure 2.4, Eq. 2). Starting with acid chlorides rather than ketenes, non-nucleophilic proton sponge (1,8-bis(dimethylamino)naphthalene) served as a proton sink, aiding in the formation of the key intermediate zwitterionic enolate and preventing protonation of the catalyst.<sup>17</sup> For several years, these two approaches remained the state of the art for the asymmetric Lewis base-catalyzed synthesis of  $\beta$ -lactams and capitalized on the chiral Lewis bases available at the time. However, around 2004, another important class of Lewis basic catalysts were being put to the forefront of asymmetric organocatalysis.

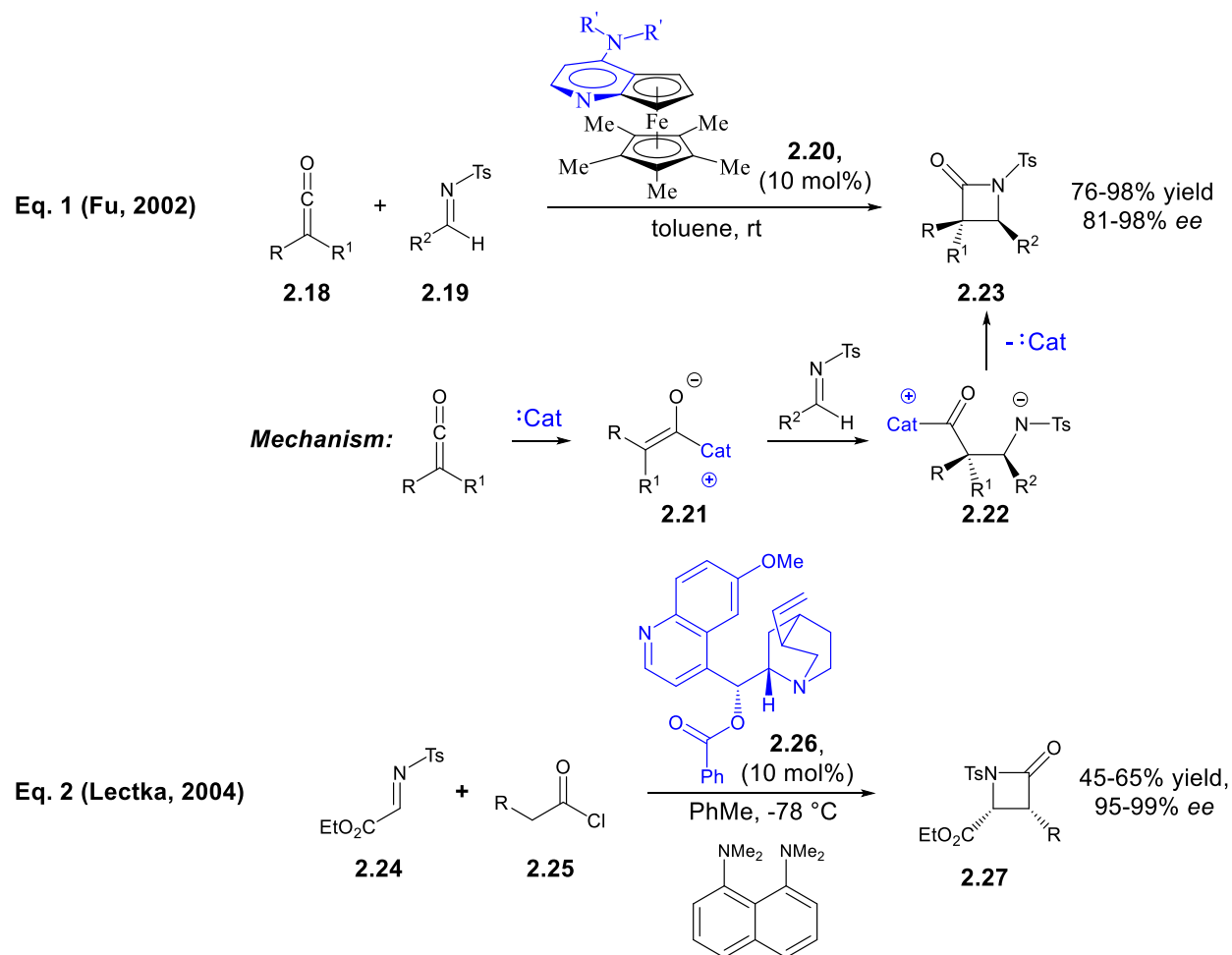


**Figure 2.4.** Lewis-base catalyzed formal [2+2] cycloadditions as an approach to enantioenriched  $\beta$ -lactams.

## 2.4 Amidine base-catalyzed formal [2+2] cycloadditions

Since their inception by our group in 2004 (Figure 2.5), amidine-based catalysts (ABCs) have been utilized in a myriad of enantioselective organocatalytic processes. These processes include, but are not limited to, kinetic resolutions, dynamic kinetic resolutions, desymmetrizations, asymmetric Michael additions, rearrangements, and domino reactions.<sup>18</sup> Additionally, ABCs have displayed their success in enantioselective formal [2+2] and [4+2] cycloadditions, exemplifying their ability to catalyze transformations leading to synthetically useful heterocycles.

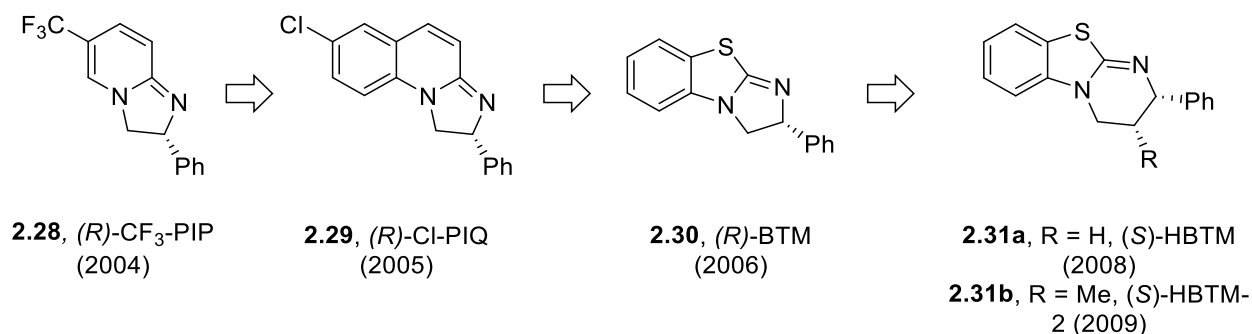


**Figure 2.5.** Evolution of ABCs developed by our group.

The first use of ABCs in a formal [2+2] cycloaddition was demonstrated by Romo et al. A homobenzotetramisole (HBTM)-catalyzed intramolecular aldol-lactonization tandem reaction converted keto acids **2.32** into bi- and tricyclic  $\beta$ -lactones (Figure 2.6).<sup>19</sup> This methodology was later used in the total synthesis of (–)-Curcumanolide A and (–)-Curcumalactone.<sup>20</sup>

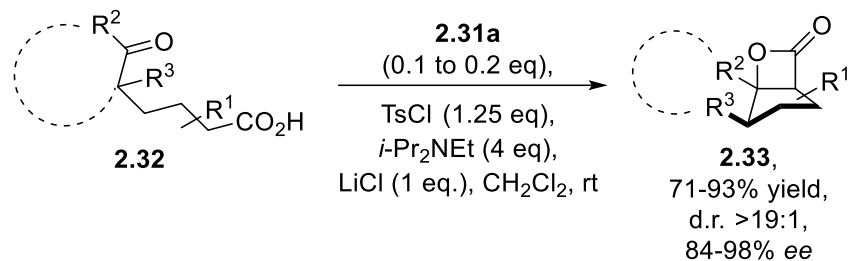


**Figure 2.6.** Homobenzotetramisole-catalyzed aldol-lactonization tandem reaction.

A couple years later, Romo's group published another impressive tandem transformation that involved an asymmetric Michael addition followed by an aldol-lactonization process (Figure 2.7).<sup>21</sup>

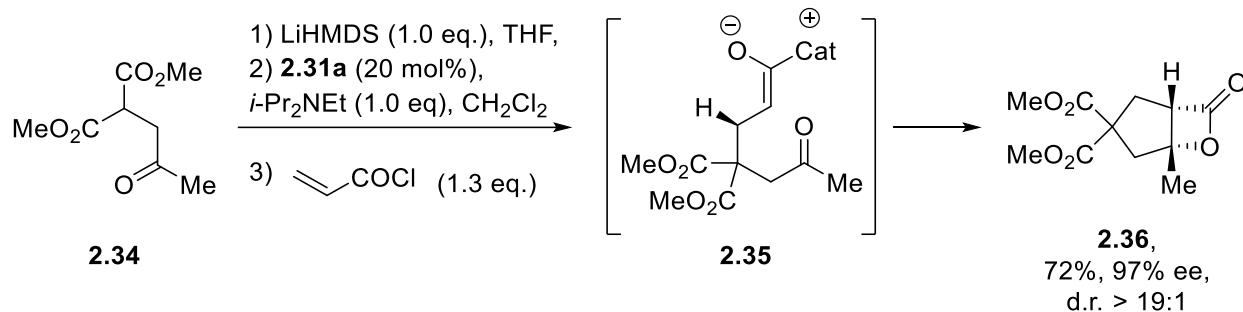


**Figure 2.7.** Tandem Michael-aldol-lactonization synthesis of  $\beta$ -lactone fused cyclopentanes.

Furthermore, in 2014, Smith et. al expanded upon the currently available methods for the Lewis-base catalyzed synthesis of  $\beta$ -lactams by using a modified ABC known as HBTM-2.1 (or Hyper BTM, **2.31c**), where the Me group in HBTM-2 was replaced with a sterically bulkier isopropyl group.<sup>22</sup> Here, they demonstrated that in situ activated aryl-, alkenyl-, and thioaryl acetic acid derivatives could be used in a manner similar to the work of Fu and Lectka (Figure 2.4) to make reactive N-sulfonyl  $\beta$ -lactams (Figure 2.8). These reactive lactams were opened with lithium methoxide to generate the  $\beta$ -amino acid esters **2.40**.<sup>23</sup>

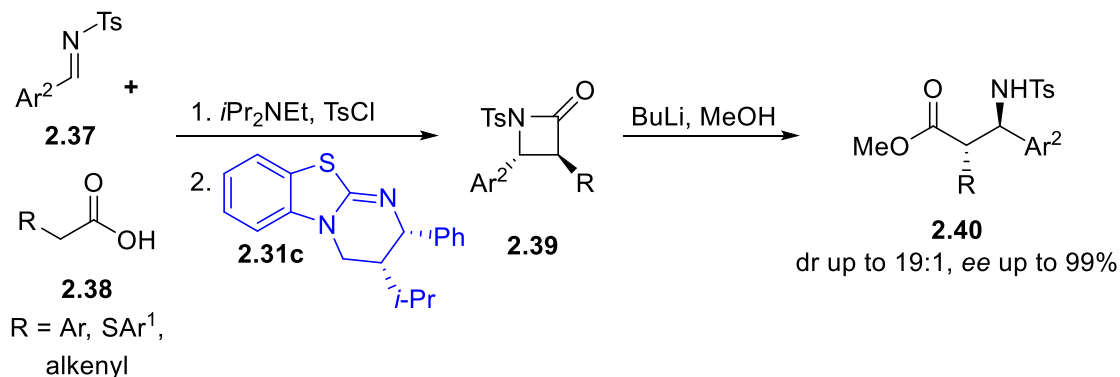


**Figure 2.8.** Smith's approach to  $\beta$ -lactams and  $\beta$ -amino acid esters using a chiral ABC.

## 2.5 Our approach to $\alpha$ -fluoro- $\beta$ -amino acids via asymmetric ABC-catalyzed formal [2+2] cycloaddition

With all the asymmetric approaches to  $\alpha$ -fluoro- $\beta$ -amino acids outlined in Section 2.2, there is one enantioselective catalytic approach that had remained uninvestigated. Given the literature precedent outlined in section 2.3, it was envisaged that enantioenriched  $\alpha$ -fluoro- $\beta$ -amino acids could be made by quenching  $\alpha$ -fluoro- $\beta$ -lactams **2.42** with nucleophiles (Figure 2.9). While this method has been used to prepare enantioenriched non-fluorinated  $\beta$ -amino acid esters (e.g. see Figure 1.5, Eq. 2), this reaction had yet to be explored with the analogous fluorinated  $\beta$ -lactams, which were expected to be even more reactive.

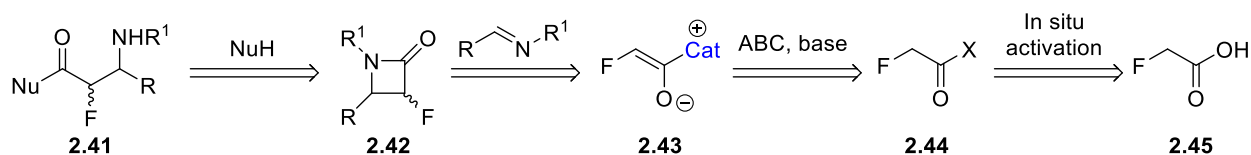


**Figure 2.9.** Our proposed strategy to enantioenriched  $\alpha$ -fluoro- $\beta$ -amino acids via [2+2] cycloaddition.

This lactam, in turn, could be synthesized via a Lewis base-catalyzed Staudinger [2+2] formal cycloaddition between reactive imines and a fluorinated zwitterionic enolate **2.43**. This enolate could be obtained from in situ activation of fluoroacetic acid, followed by nucleophilic attack of a Lewis basic catalyst and subsequent deprotonation. Though having scarce literature precedent, especially in the context of asymmetric catalysis, fluoroenolates have found use in synthesis. For example, Welch et al. discovered that the lithium enolate of ethyl fluoroacetate can be used in diastereoselective aldol reactions with variously substituted aldehydes and ketones.<sup>24</sup> Given how attractive this approach was on paper, it was astonishing to see nearly non-existent literature precedent for this strategy. Nevertheless, there did exist some precedent to suggest the

viability of this approach. For example, Lectka et al. managed to synthesize the  $\alpha$ -fluorinated- $\beta$ -lactam using their methodology (Figure 2.4, Eq. 2, R=F, obtained in 97% *ee*); however, no effort was made to further explore the substrate tolerance of this fluoroenolate. It was also unclear if this fluoroenolate would be well-behaved using a structurally different class of acyl transfer catalysts, namely ABCs. Furthermore, Smith's group demonstrated for the first time that ABCs can be used in formal [2+2] cycloadditions leading to  $\beta$ -lactams (Figure 2.8). However, a fluorine at the  $\alpha$ -carbon (**2.38**, R=F) remained unexplored. They showed that an electron-stabilizing substituent at the  $\alpha$ -carbon in **2.38** (R=aryl, alkenyl) was well tolerated. This group most likely further acidifies the  $\alpha$ -proton, facilitating deprotonation of the acyl ammonium cation and formation of the key zwitterionic enolate intermediate. However, other electron withdrawing groups, such as a fluorine substituent, can be envisioned to serve the same purpose. Our group wanted to explore this possibility; however, it was unknown if the different reactivity between fluoroenolates and the enolates employed in Smith's work would necessitate the optimization of a different set of reaction conditions.

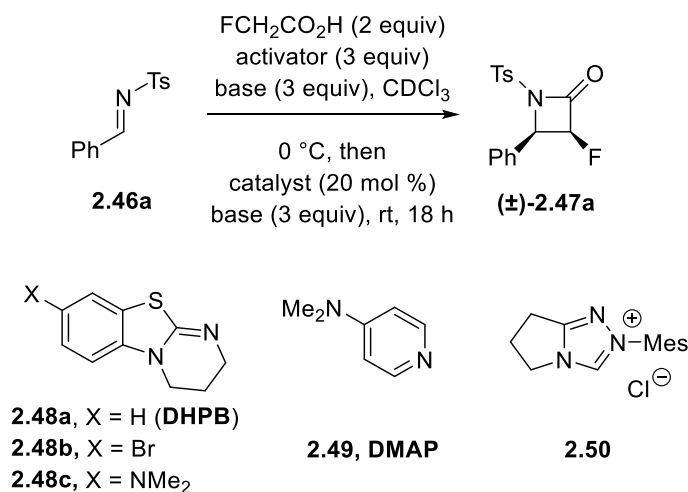
## 2.6 Optimization of reaction conditions: Activator, base, and achiral catalyst

Fluoroacetic acid had never been used as an acyl donor in Lewis base-catalyzed reactions. Therefore, we needed to establish a procedure to activate it in situ and avoid reaction conditions that lead to uncatalyzed, racemic background reactions. We started by exploring different activators, bases, and achiral acyl transfer catalysts (Table 2.1).

First, we treated fluoroacetic acid with tosyl chloride<sup>23,25</sup> and excess triethylamine. Upon addition of N-tosyl benzaldimine **2.46a**, without any acyl transfer catalyst, we observed formation of  $\beta$ -lactam **2.47a** by <sup>1</sup>H NMR (entry 1). This racemic background reaction was a pleasant

observation, but would not be suitable for developing an asymmetric version of this reaction. No lactam formation was observed in the presence of DBU or Hünig's base (N,N-diisopropylethylamine) in the absence of acyl transfer catalyst (entries 2 and 3). Interestingly, with DBU all of the imine was consumed. It was proposed that the  $\alpha$ -fluoro  $\beta$ -lactam did form, but was rapidly consumed in side reactions as a result of the nucleophilicity of DBU. This imine disappearance, however, was not observed with Hünig's base. Addition of 20 mol % of DHPB<sup>26</sup> **2.48a** led to rapid lactam formation in the presence of Hünig's base, but again, not with DBU (entries 4 and 5). Thus, Hünig's base was the optimal choice of base for this study.

**Table 2.1:** Optimization of reaction conditions: activator, base, and achiral catalyst.



entry	catalyst	activator	base	<b>2.47a/2.46a</b>
1	none	TsCl	NEt <sub>3</sub>	94:6 <sup>a</sup>
2	none	TsCl	DBU	NR
3	none	TsCl	<i>i</i> -Pr <sub>2</sub> NEt	NR
4	<b>2.48a</b>	TsCl	DBU	NR
5	<b>2.48a</b>	TsCl	<i>i</i> -Pr <sub>2</sub> NEt	66:34
6	<b>2.48a</b>	PivCl	<i>i</i> -Pr <sub>2</sub> NEt	NR
7	<b>2.48a</b>	TCBC	<i>i</i> -Pr <sub>2</sub> NEt	NR
8	<b>2.48b</b>	TsCl	<i>i</i> -Pr <sub>2</sub> NEt	22:78
9	<b>2.48c</b>	TsCl	<i>i</i> -Pr <sub>2</sub> NEt	57:43
10	<b>2.49</b>	TsCl	<i>i</i> -Pr <sub>2</sub> NEt	72:28
11	<b>2.50</b>	TsCl	<i>i</i> -Pr <sub>2</sub> NEt	NR

<sup>a</sup>After 24 hours.

At this point, extensive analyses of crude reaction mixtures by  $^{19}\text{F}$  NMR showed several byproducts, suggesting that fluoroacetic acid was being consumed in unproductive pathways. To overcome this, excess fluoroacetic acid was used. This immediately translated into higher isolated yields of the fluorinated  $\beta$ -lactam after chromatography. Other activating agents such as pivaloyl chloride<sup>27</sup> and 2,4,6-trichlorobenzoyl chloride<sup>28</sup> (TCBC, Yamaguchi reagent) were completely ineffective activators (entries 6 and 7). Other achiral catalysts were briefly explored. Electron-poor and electron-rich derivatives of DHPB produced lower conversion (entries 8 and 9). DMAP **2.49** gave slightly higher conversions than DHPB (entry 10). No reaction was observed with the triazolium salt **2.50**, a precursor to an NHC (N-heterocyclic carbene) catalyst (entry 11).

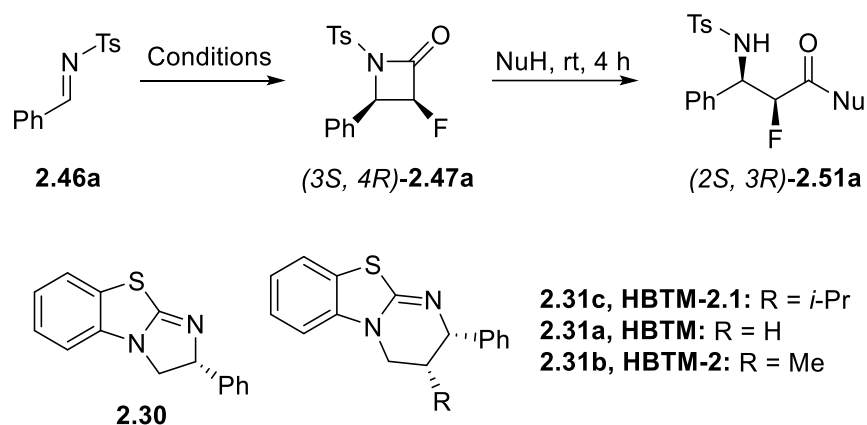
## 2.7 Optimization of reaction conditions: Chiral catalysts and exploring nucleophiles

We next explored chiral DHPB derivatives and analogues to devise an enantioselective approach to these compounds (Table 2.2). BTM<sup>29</sup> **2.30** and HBTM-2.1<sup>22</sup> **2.31c** gave excellent enantioselectivities, but stalled before all imine was consumed (entries 1 and 2). HBTM<sup>30</sup> **2.31a** and HBTM-2<sup>31</sup> **2.31b** brought the reaction to completion (entries 3 and 4). Despite high conversion being observed by  $^1\text{H}$  NMR,  $\beta$ -lactam **2.47a** was being isolated in relatively low yield (~40%). This is most likely due to decomposition during the work up and chromatography. Therefore, we converted the lactams into stable esters and amides in situ by introducing an alcohol or amine respectively into the reaction mixture. These esters and amides were isolated in moderate overall yields and with excellent enantioselectivities (entries 4-7). The ring-opened methyl ester **2.51a-OMe** produced X-ray quality crystals, allowing us to validate its expected relative and absolute stereochemistry (Figure 2.10). The absolute configuration was determined from the Flack parameters.<sup>32</sup>



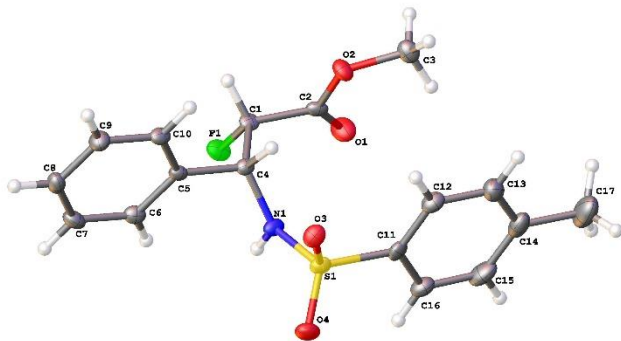
Furthermore, analysis of the crude reaction mixture by  $^{19}\text{F}$  NMR showed that both the lactam **2.47a** and benzyl ester **2.51a-OBn** were produced with 15:1 diastereoselectivity in favor of the *syn*-diastereomer. This proved that no epimerization was taking place during the ring opening.<sup>33</sup> Comparable yields of product were observed with a larger scale (2.64 mmol, entry 8) and at lower catalyst loadings (entries 9 and 10), though reaction times were appropriately adjusted.

**Table 2.2:** Optimization of the enantioselective variant.<sup>a</sup>



entry	Catalyst (mol %)	<b>2.47a/2.46a</b>	% yield <sup>b</sup>	NuH	% ee
1	<b>2.30</b> (20)	73:27	50	BnOH	99
2	<i>ent</i> - <b>2.31c</b> (20)	68:32	38	BnOH	-99
3	<i>ent</i> - <b>2.31a</b> (20)	99:1	45	BnOH	-99
4	<b>2.31b</b> (20)	99:1	60	BnOH	>99
5	<b>2.31b</b> (20)	99:1	61	MeOH	96
6	<b>2.31b</b> (20)	99:1	53	BnNH <sub>2</sub>	98
7	<b>2.31b</b> (20)	99:1	55	Et <sub>2</sub> NH	>99
8 <sup>c</sup>	<b>2.31b</b> (20)	99:1	58	BnOH	>99
9 <sup>d</sup>	<b>2.31b</b> (10)	99:1	55	BnOH	99
10 <sup>d</sup>	<b>2.31b</b> (5)	99:1	54	BnOH	98

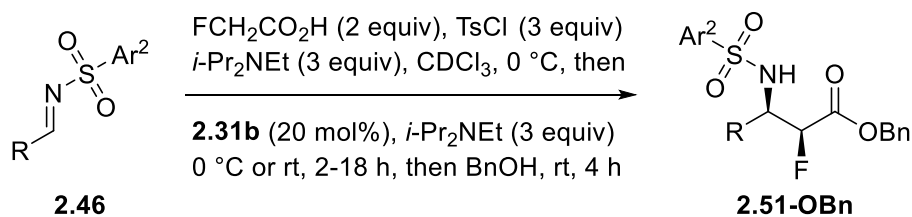
<sup>a</sup> General conditions: FCH<sub>2</sub>CO<sub>2</sub>H (0.5 mmol), TsCl (0.75 mmol), *i*-Pr<sub>2</sub>NEt (0.75 mmol), CDCl<sub>3</sub>, 0 °C, then catalyst, *i*-Pr<sub>2</sub>NEt (0.75 mmol), **2.46a** (0.25 mmol), 0 °C, 18 h, then NuH (1.2 equiv of BnOH or 10 equiv of MeOH, BnNH<sub>2</sub>, or Et<sub>2</sub>NH), rt, 4 h. <sup>b</sup> Isolated yields of the pure major diastereomer. <sup>c</sup> Performed on 10× scale (2.64 mmol substrate). <sup>d</sup> Reaction times extended to 28 h.



**Figure 2.10:** X-ray crystal structure of **2.51a-OMe**.

## 2.8 Substrate scope of new methodology

With the optimization studies completed, we next explored the substrate scope of the new methodology (Table 2.3). Arylsulfonyl groups with a *p*-methoxy or *p*-bromo substituent were tolerated but produced lower yields compared to tosyl (entries 2 and 3). *N*-Nosyl benzaldimine reacted very quickly to form the corresponding lactam; however, this lactam was also quickly consumed via side reactions (entry 4). Variation of the R group showed that while electron-withdrawing and mildly electron-donating groups were well tolerated (entries 5-11), a *p*-methoxy group rendered the imine unreactive (entry 12). *N*-tosylfuraldimine was also unreactive and underwent mostly side reactions (entry 13). No reaction was observed with *N*-tosylcinnamaldimine, a unique case where a formal [2+2] or formal [4+2] cycloaddition could be expected to compete (entry 14). An alicyclic substituent with an  $\alpha$ -proton reacted but did not give the desired product. Instead, deprotonation and subsequent fluoroacetylation delivered the *N*-fluoroacetyl-*N*-tosylenamine (entry 15). Besides entries 9 and 11, excellent enantioselectivities and moderate to high *syn*-diastereoselectivities were observed.

**Table 2.3:** Substrate scope

entry	R	Ar <sup>2</sup>	% yield	dr	% ee
1	Ph	4-MeC <sub>6</sub> H <sub>4</sub>	60 <sup>b</sup>	14.9:1	>99
2	Ph	4-MeOC <sub>6</sub> H <sub>4</sub>	50	12.6:1	>99
3	Ph	4-BrC <sub>6</sub> H <sub>4</sub>	38	11.5:1	95
4	Ph	4-O <sub>2</sub> NC <sub>6</sub> H <sub>4</sub>	<5 <sup>d</sup>	ND	ND
5	4-O <sub>2</sub> NC <sub>6</sub> H <sub>4</sub>	4-MeC <sub>6</sub> H <sub>4</sub>	32	13.8:1	>99
6	4-O <sub>2</sub> NC <sub>6</sub> H <sub>4</sub>	4-MeOC <sub>6</sub> H <sub>4</sub>	48	7.5:1	>99
7	4-BrC <sub>6</sub> H <sub>4</sub>	4-MeC <sub>6</sub> H <sub>4</sub>	52 <sup>b</sup>	>20:1	98
8	4-ClC <sub>6</sub> H <sub>4</sub>	4-MeC <sub>6</sub> H <sub>4</sub>	53 <sup>b</sup>	>20:1	>99
9 <sup>a</sup>	2-ClC <sub>6</sub> H <sub>4</sub>	4-MeC <sub>6</sub> H <sub>4</sub>	38	1.1:1	99
10 <sup>a</sup>	2-MeC <sub>6</sub> H <sub>4</sub>	4-MeC <sub>6</sub> H <sub>4</sub>	43	18.8:1	99
11 <sup>a</sup>	1-naphthyl	4-MeC <sub>6</sub> H <sub>4</sub>	39	9.1:1	74
12	4-MeOC <sub>6</sub> H <sub>4</sub>	4-MeC <sub>6</sub> H <sub>4</sub>	<5 <sup>d</sup>	ND	ND
13	2-furyl	4-MeC <sub>6</sub> H <sub>4</sub>	<5 <sup>d</sup>	ND	ND
14	styryl	4-MeC <sub>6</sub> H <sub>4</sub>	0	ND	ND
15 <sup>a</sup>	cyclohexyl	4-MeC <sub>6</sub> H <sub>4</sub>	0 <sup>c</sup>	ND	ND

<sup>a</sup> Reactions performed at rt. <sup>b</sup> Yield of the major diastereomer only. <sup>c</sup> N-Fluoroacetyl-N-tosylenamine was produced instead in 68% yield. <sup>d</sup> Complex reaction mixture.

## 2.9 Exploring other imines

As evidenced in section 2.8, *N*-sulfonyl aldimines were well tolerated in this methodology. However, even then, some of these imines failed to react (e.g. see Table 2.3, entries 12-14). There do exist reliable methods for removing an arylsulfonyl group (e.g. Birch reduction).<sup>34</sup> However, they are not the most ideal protecting groups, especially considering the relative ease with which other nitrogen protecting groups can be removed. As aforementioned, more easily removable arylsulfonyl groups such as *p*-nosyl were tested (Table 2.3, entry 4), but this resulted in lactams that were too reactive and consumed in side reactions. Furthermore, classical reagents to remove an arylsulfonyl group such as samarium iodide<sup>35</sup>, sodium naphthalenide<sup>36</sup>, and hot concentrated

acids<sup>37</sup> were not expected to bode well for compounds containing a fluorine substituent and epimerizable stereocenter. With this in mind, we explored the behavior of other imines such as those shown in Figure 2.11.

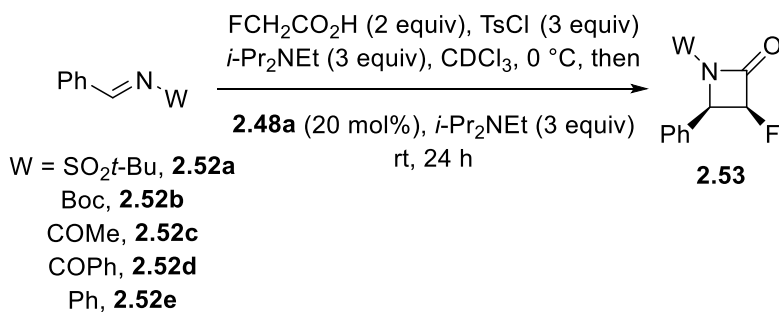


**Figure 2.11.** Exploring other imines with optimized reaction conditions.

*t*-Butylsulfonyl imine **2.52a** was well tolerated, giving moderate conversions to the desired lactam by <sup>1</sup>H NMR. Unfortunately, major purification issues of the ring-opened product were observed when both alcohols and amines were used to quench the lactam. *N*-Boc benzaldimine **2.52b** suffered the same disadvantage as *N*-nosyl benzaldimine in that the resulting lactam formed very quickly, but was quickly consumed in side reactions. *N*-acyl benzaldimines **2.52c** and **2.52d** were surprisingly completely unreactive. *N*-phenylbenzaldimine **2.52e** stalled at low 20-25% conversions. While the phenyl group is not a standard protecting group for a nitrogen atom, it was nonetheless interesting to compare how an *N*-aryl imine would react.

## 2.10 Deprotection of nitrogen

Being unable to find imines that would lead to products with relatively easier-to-remove protecting groups, we were tasked with finding a convenient deprotection protocol. A two-step procedure was devised that first involved installation of an electron withdrawing group on the nitrogen (Figure 2.12). A Boc group was chosen for convenience. Following a published

procedure,<sup>38</sup> intermediate **2.54a-OBn** was sonicated with magnesium metal in methanol to deliver the detosylated **2.55a-OMe** product with concomitant transesterification of the benzyl ester. No evidence of defluorination or epimerization was observed over these two steps. This is in stark contrast to other attempted methods to remove the tosyl group, such as samarium iodide or sodium naphthalenide, which gave very complex mixtures and oftentimes removed the fluorine from the desired product.

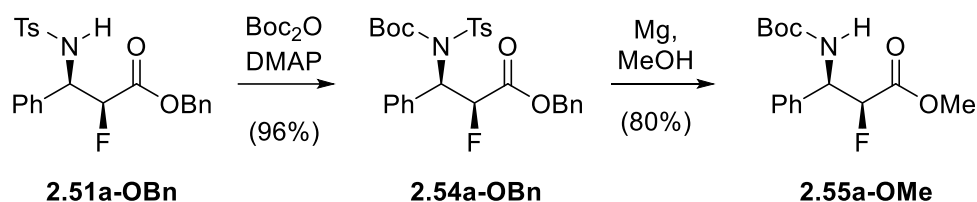


**Figure 2.12.** Removal of tosyl group from **2.51a-OBn**.

## 2.11 Exploring additional uses of fluoroenolates

Encouraged by our success with using fluoroacetic acid in the beta-lactam synthesis described above, we decided to explore the reactivity of the putative fluoroenolate with other electrophiles. As alluded to in Section 2.8, one of the biggest limitations of this new methodology is the seemingly exclusive tolerance of *N*-sulfonyl aldimines. In addition to imines with different electron-withdrawing groups on the nitrogen (section 2.9), other electrophiles were also explored using the optimized reaction conditions and DHPB as catalyst. These electrophiles and their expected products are shown in Figure 2.13. Unfortunately, all of these electrophiles failed to react with the fluoroenolate in the expected manner, allowing for 100% recovery of the unreacted electrophile.

Aldehydes, even those with strong electron-withdrawing groups such as *p*-nitrobenzaldehyde **2.56**, would not react with the fluoroenolates in the expected manner, indicating

the importance of an anion-stabilizing group on the electrophile. The resulting formal [2+2] cycloaddition to give the analogous  $\alpha$ -fluoro- $\beta$ -lactone **2.56a** would be a captivating approach to another class of synthetically useful fluorinated four membered rings. Lastly, it was discovered that fluoroenolates fail to react with Michael acceptors that contain anion-stabilizing groups. Methyl cinnamate **2.57**, cinnamitrile **2.58**, and ethyl 2-cyano-3-phenylacrylate **2.59** were all unreactive substrates and did not deliver the fluorinated cyclobutanones. However, this is not surprising given their relatively low electrophilicity compared to N-sulfonyl imines.

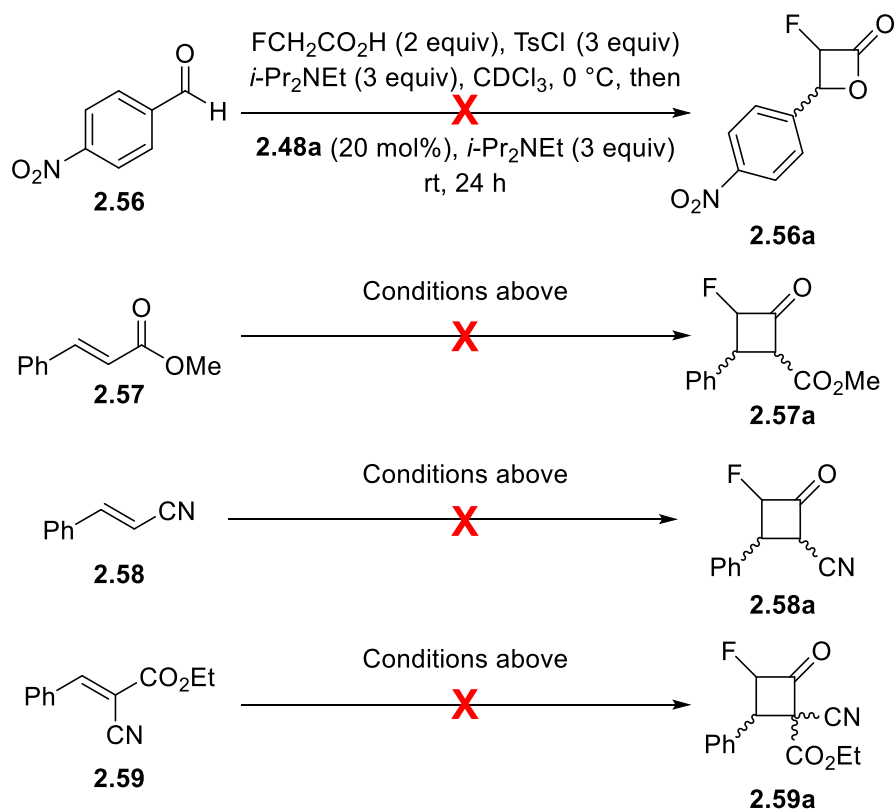


**Figure 2.13:** Other electrophiles tested using this methodology.

## 2.12 Substrate-dependent diastereoselectivities

The *syn*-diastereoselectivity observed in this study is consistent with the published work of Lectka et al.<sup>17</sup>, even though they used a different class of acyl transfer catalyst. This stands in stark

contrast to the stereochemical outcome observed by Smith et al.<sup>23</sup> (see **2.60a-c**, Figure 2.14). The [2+2] cycloadditions demonstrated by our group and Smith's group employ essentially the same reaction conditions and amidine-based acyl transfer catalysts, but produce different diastereoselectivities. In other words, the fluoroenolate seems to force a change in the transition state compared to the enolates of aryl-, arylthio-, and alkenylacetic acids. The absolute configuration at C3 is the same in both cases, demonstrating the same catalyst-controlled facial selectivity with respect to the zwitterionic Z-enolates in the transition state. Hence, the imine must approach the zwitterionic enolate from the less hindered face of the catalyst. However, the opposite stereochemistry at C4 suggests that this imine's orientation in the transition state is different (see models **2.61** and **2.62**, Figure 2.14). Even though it is not definitive, there are possible explanations for this transition state behavior. Because the fluoroenolate is not as stabilized as the aryl- or alkenyl-enolate (inductive vs resonance argument), it is expected to be a relatively more reactive nucleophile. Consequently, the C-C bond forming step is predicted to be more exothermic than in the aryl/alkenyl case. According to the Hammond postulate, this will result in an earlier open transition state, one which resembles the starting materials more than the products and one in which the C-C bond is not close to forming.<sup>39</sup> In Smith's case, the relatively later transition state may help govern the preference for the more thermodynamically stable trans-diastereomer; however, due to fluorine's small size, this thermodynamic bias may be overridden by minimum steric encumbrance in an open transition state. For example, in transition state **2.62**, the small fluorine atom can more easily accommodate the sterically bulky -NTs group in a gauche conformation. Additionally, fluorine's other unique properties (see section 2.1), such as its high electronegativity and effects on nearby dipoles, may also be contributing in unpredictable manners. Further

computational studies will need to be performed to further elucidate this diastereoselective predilection (see footnote<sup>1</sup>).

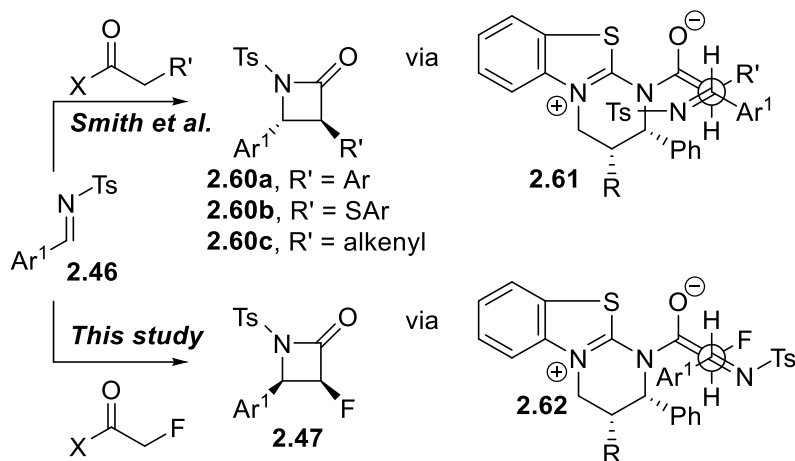


**Figure 2.14.** Substrate-dependent diastereoselectivities.

## 2.13 Conclusions and future directions

In conclusion, we have developed a new enantioselective approach to esters and amides of  $\alpha$ -fluoro- $\beta$ -amino acids. The methodology involves asymmetric synthesis of  $\alpha$ -fluoro- $\beta$ -lactams via an amidine base-catalyzed [2+2] cycloaddition, followed by quenching of the intermediate lactam with an alcohol or amine. This methodology did have some limitations, namely in restricted substrate scope. In this regard of failed substrates, either the imine is too unreactive, or the resulting fluoro- $\beta$ -lactam is too unstable and undergoes rapid decomposition. The reactivity of fluoroenolates also seems to restrict their use given the broad range of other electrophiles that do not react with these enolates. Nevertheless, this methodology greatly expanded upon the use of fluoroenolates in asymmetric catalysis. Prior to our work, only one known example of a fluoroenolate being used in this manner was known. The

<sup>1</sup> Alternative concerted asynchronous transition states are being considered.



diastereoselectivity of the [2+2] cycloaddition in favor of the syn-diastereomer is also fascinating and requires further study.

In terms of future directions, it would be intriguing to analyze other haloenolates in the exact same context. While fluorine is the most attractive halogen for this application, analogous halolactams would arguably be more stable and may even display different substrate-dependent diastereoselectivities. Furthermore, it would be interesting to see what other types of nucleophiles could be used to quench these reactive intermediate lactams. For example, thiols can be used in lieu of alcohols as nucleophiles to make fluorinated thioesters. It would also be compelling to explore fluoroenolates with other catalysts such as bifunctional primary amine-thiourea organocatalysts (see section 3.3 for an introduction to bifunctional organocatalysis) to try to overcome these limitations with the electrophiles listed in Section 2.11. For example, if a double hydrogen bond donor serves to activate an aldehyde carbonyl, then the fluoroenolate, which would be expected to be in close proximity if employing a bifunctional catalyst, is given a better chance to react with said electrophilic moiety. This would introduce a mechanistically distinct approach to  $\alpha$ -fluorinated- $\beta$ -lactones that has never been disclosed.

## 2.14 Experimental

All reagents were obtained commercially and used as received unless specified otherwise. Catalysts **2.30**, **2.31a-c**, and **2.48a-c** were prepared as previously described.<sup>22,26,29,30,31,40,41</sup> All N-sulfonylaldimines used were prepared according to published procedures.<sup>42</sup> Deuterated chloroform used as the reaction medium and diisopropylethylamine were freshly distilled from calcium hydride. p-toluenesulfonyl chloride was recrystallized from hexanes. Solvents used for chromatography were ACS or HPLC grade, as appropriate. Reactions were carried out under inert atmosphere and monitored by <sup>1</sup>H NMR. Uniplate HLF (2  $\mu$ m) silica gel plates were used for TLC

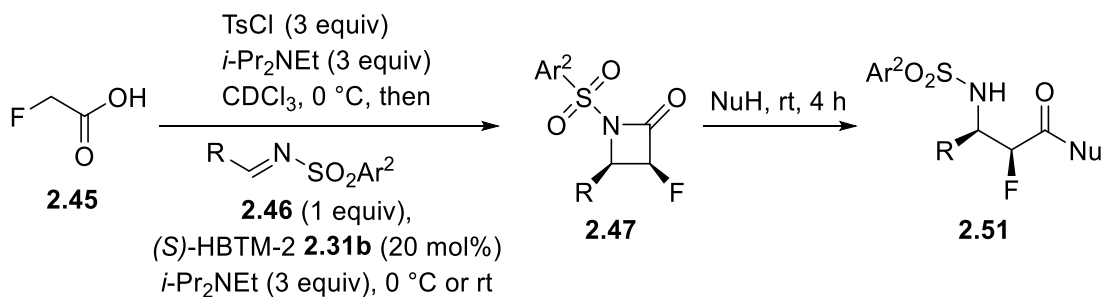
analyses. Flash column chromatography was performed over Sorbent Technologies silica gel (40-63 mm). HPLC analyses were performed on a Shimadzu LC system using Chiralcel OD-H, Chiralpak AD-H, and Chiralpak AS-H analytical chiral stationary phase columns (4.6x250 mm, Chiral Technologies, Inc.) with UV detectors at 254 nm and 204 nm, as appropriate, with a flow rate of 1.0 mL/min.  $^1\text{H}$  and  $^{13}\text{C}$  NMR spectra were recorded on Mercury 300 MHz and DD2 500 MHz Agilent spectrometers. The chemical shifts are reported as  $\delta$  values (ppm) relative to TMS using residual  $\text{CHCl}_3$  peak as the reference (7.26 ppm for  $^1\text{H}$  NMR, 77.16 ppm for  $^{13}\text{C}$  NMR). The chemical shifts for  $^{19}\text{F}$  NMR are reported as  $\delta$  values (ppm) relative to fluoroacetic acid (-230.00 ppm). Melting points were measured on a Stuart SMP10 melting point apparatus. High-Resolution mass spectral analyses were performed at Washington University MS Center on a Bruker MaXis QTOF mass spectrometer using Electrospray Ionization (ESI). Infrared spectra were recorded on a Bruker Alpha Platinum-ATR. Optical rotations were determined on a Rudolph Autopol III polarimeter.

### **2.14.1 Preparation of anhydrous fluoroacetic acid 2.45**

A published procedure<sup>43</sup> was followed with minor modifications. A solution of ethyl fluoroacetate (13.6 mL, 141 mmol) in 180 mL of 95% EtOH was treated with 20 mL of aqueous NaOH (6.72 g, 168 mmol) and stirred at rt for 1 day. The solvent was rotary evaporated to dryness. The sodium fluoroacetate thus obtained was redissolved in 120 mL of 3 M aqueous HCl, the solution was saturated with NaCl and then extracted four times with  $\text{Et}_2\text{O}$  (4x25 mL). The organic extract was dried with  $\text{MgSO}_4$ , filtered, and the filtrate was rotary evaporated to produce fluoroacetic acid as a clear oil. This crude product, which was still slightly wet, was redissolved in anhydrous  $\text{Et}_2\text{O}$ , dried with copious amounts of  $\text{MgSO}_4$  overnight, filtered, and rotary evaporated to dryness to produce crystalline fluoroacetic acid, which was stored in a desiccator over large amounts of

phosphorus pentoxide until ready to use. Note: the dryness of fluoroacetic acid is critical to ensure reproducibility of reactions described below. Also note that fluoroacetic acid and its derivatives are highly toxic!

### 2.14.2 Enantioselective synthesis and ring opening of 3-fluoro- $\beta$ -lactams



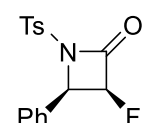
**Optimized procedure:** An oven-dried round bottom flask was charged with fluoroacetic acid (39 mg, 0.50 mmol) and 2.5 mL of  $\text{CDCl}_3$ , placed under an inert atmosphere, and cooled to  $0^\circ\text{C}$ . The mixture was treated with TsCl (143 mg, 0.75 mmol) followed by  $i\text{-Pr}_2\text{NEt}$  (124  $\mu\text{L}$ , 97 mg, 0.75 mmol) and stirred at  $0^\circ\text{C}$  for 30 min. Then, (*S*)-HBTM-2 **2.31b** (14 mg, 0.05 mmol), *N*-sulfonylimine **2.46** (0.25 mmol), and additional  $i\text{-Pr}_2\text{NEt}$  (124  $\mu\text{L}$ , 97 mg, 0.75 mmol) were added sequentially. The mixture was left to stir at the temperature indicated below, and the reaction progress was monitored by  $^1\text{H}$  NMR. Upon reaching complete conversion (>9:1 ratio of  $\beta$ -lactam **2.47** to *N*-sulfonylimine **2.46**), the reaction mixture was brought to room temperature and either worked up directly or treated with an alcohol or amine in the amount indicated. Stirring was continued until  $^1\text{H}$  NMR analysis indicated complete consumption of  $\beta$ -lactam **2.47**. The reaction was quenched with 1M aqueous HCl and the aqueous phase was extracted twice with  $\text{CH}_2\text{Cl}_2$ . The organic extract was dried with  $\text{Na}_2\text{SO}_4$  and concentrated by rotary evaporation. The crude products were purified by column chromatography or recrystallization. The major diastereomer was

isolated, at least in part, in pure form using these methods. The diastereomeric ratios reported in Table 2.3 in Section 2.8 were determined by  $^1\text{H}$  and  $^{19}\text{F}$  NMR analysis of crude reaction mixtures.

### *$\beta$ -lactam 2.47a*

After addition of *N*-tosylimine **2.46a**, the reaction was stirred at 0 °C for 9 hours and then quenched and worked up as described above. Isolated as a colorless, crystalline solid (43 mg, 40% combined yield, 39 mg isolated as pure major diastereomer shown) after chromatography (5→20% EtOAc/hexanes). Other ring opened products listed below were prepared analogously. Reaction times and temperatures to make the  $\beta$ -lactam and the nucleophile used are listed below.

### **(3*S*,4*R*)-3-fluoro-4-phenyl-1-tosylazetid-2-one (2.47a)**

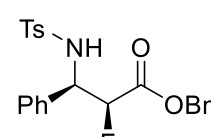
 Colorless, crystalline solid.  $^1\text{H}$  NMR (500 MHz,  $\text{CDCl}_3$ )  $\delta$  7.62 (d,  $J = 8$  Hz, 2H), 7.37-7.33 (m, 1H), 7.30-7.22 (m, 4H), 7.13 (d,  $J = 8$  Hz, 2H), 5.68 (dd,  $J = 54$  Hz, 6 Hz, 1H), 5.35 (dd,  $J = 6$  Hz, 5 Hz, 1H), 2.43 (s, 3H);  $^{13}\text{C}\{^1\text{H}\}$  NMR (125 MHz,  $\text{CDCl}_3$ ):  $\delta$  160.00 (d,  $J = 23$  Hz), 145.91, 135.39, 130.28, 130.04, 129.63, 128.70, 128.56, 127.80, 91.08 (d,  $J = 232$  Hz), 63.84 (d,  $J = 23$  Hz), 21.87;  $^{19}\text{F}$  NMR (282 MHz,  $\text{CDCl}_3$ ): Major diastereomer: -198.65 (dd,  $J = 54$  Hz, 5 Hz), Minor diastereomer: -189.98 (dd,  $J = 53$  Hz, 13 Hz); IR ( $\text{cm}^{-1}$ ): 1784, 1363, 1163, 1140, 545; MS: HR-ESI calculated for  $[\text{C}_{16}\text{H}_{14}\text{FNO}_3\text{S}+\text{Na}]^+$ : 342.0570, found 342.0554; mp: 148- 149 °C;  $[\alpha]_D^{23} = -70.5^\circ$  ( $c=0.400$ ,  $\text{CH}_2\text{Cl}_2$ ).

### *Ester 2.51a-OBn*

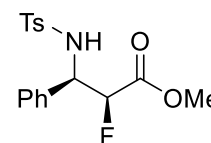
**Small-scale preparation:** The reaction was conducted as described above at 0 °C for 24 hours. Treated with 1.2 equiv of BnOH. Product isolated as a white solid (64 mg; 60% yield, single diastereomer) after chromatography (5→50% EtOAc/hexanes). **Large-scale preparation:** The reaction was carried out analogously to the small-scale procedure using the following quantities:

FCH<sub>2</sub>CO<sub>2</sub>H (412 mg, 5.28 mmol), CDCl<sub>3</sub> (26 mL), TsCl (1.51 g, 7.92 mmol), *i*-Pr<sub>2</sub>NEt (1.38 mL, 1.02 g, 7.92 mmol), (*S*)-HBTM-2 **2.31b** (1.66 mL of 0.318 M stock solution in CDCl<sub>3</sub>, 0.53 mmol), PhCH=NTs **2.46a** (684 mg, 2.64 mmol), *i*-Pr<sub>2</sub>NEt (1.38 mL, 1.02 g, 7.92 mmol), PhCH<sub>2</sub>OH (329 μL, 3.17 mmol). After workup and chromatography, 654 mg of the product was isolated as a single diastereomer (58% yield).

**benzyl (2*S*,3*R*)-2-fluoro-3-((4-methylphenyl)sulfonamido)-3-phenylpropanoate (2.51a-OBn)**

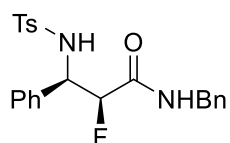
 White solid. <sup>1</sup>H NMR (500 MHz, CDCl<sub>3</sub>) δ 7.57 (d, *J* = 8 Hz, 2H), 7.41 – 7.35 (m, 3H), 7.35-7.31 (m, 2H), 7.23-7.14 (m, 3H), 7.14-7.06 (m, 4H), 5.96 (d, *J* = 10 Hz, 1H), 5.21 (d, *J* = 12 Hz, 1H), 5.12- 4.98 (m, 2H), 5.05 (d, *J* = 12 Hz, 1H), 2.32 (s, 3H); <sup>13</sup>C{<sup>1</sup>H} NMR (125 MHz, CDCl<sub>3</sub>): δ 166.95 (d, *J* = 25 Hz), 143.37, 137.42, 135.56, 134.62, 129.42, 128.75, 128.73, 128.62, 128.26, 127.12, 127.09, 127.08, 90.91 (d, *J* = 193 Hz), 67.93, 58.60 (d, *J* = 20 Hz), 21.49; <sup>19</sup>F NMR (282 MHz, CDCl<sub>3</sub>): Major diastereomer: -199.82 (dd, *J* = 50 Hz, 27 Hz), Minor diastereomer: -202.15 (dd, *J* = 52 Hz, 28 Hz); IR (cm<sup>-1</sup>): 3327, 1758, 1322, 1151, 1085, 1059, 697, 665, 549; MS: HR-ESI calculated for [C<sub>23</sub>H<sub>22</sub>FNO<sub>4</sub>S+Na]<sup>+</sup>: 450.1146, found: 450.1149; mp: 131-134 °C; HPLC: (25 % isopropanol/hexanes, AS-H): Minor enantiomer: 21.3 min; Major enantiomer: 32.0 min; >99% ee; [α]<sub>D</sub><sup>23</sup> = -11.2° (c=1.13, CH<sub>2</sub>Cl<sub>2</sub>).

**methyl (2*S*,3*R*)-2-fluoro-3-((4-methylphenyl)sulfonamido)-3-phenylpropanoate (2.51a-OMe)**

 The reaction was conducted at 0 °C for 10 hours. Treated with 10 equiv of MeOH. Isolated as a white solid (58 mg, 61% combined yield of diastereomers) after chromatography (5→30% EtOAc/hexanes). Major

diastereomer:  $^1\text{H}$  NMR (500 MHz,  $\text{CDCl}_3$ ),  $\delta$  7.55 (d,  $J = 8$  Hz, 2H), 7.24-7.19 (m, 3H), 7.15-7.10 (m, 4H), 5.53 (d,  $J = 10$  Hz, 1H), 5.03 (dd,  $J = 47$  Hz, 3 Hz, 1H), 4.97 (ddd,  $J = 26$  Hz, 10 Hz, 3 Hz, 1H), 3.68 (s, 3H), 2.34 (s, 3H);  $^{13}\text{C}\{^1\text{H}\}$  NMR (125 MHz,  $\text{CDCl}_3$ ): 167.44 (d,  $J = 24$  Hz), 143.56, 137.49, 135.90, 129.54, 128.79, 128.46, 127.17, 127.00, 90.95 (d,  $J = 193$  Hz), 58.46 (d,  $J = 20$  Hz), 52.91, 21.58; IR ( $\text{cm}^{-1}$ ): 3230, 1747, 1234, 1158, 670; MS: HR-ESI calculated for  $[\text{C}_{17}\text{H}_{18}\text{FNO}_4\text{S}+\text{H}]^+$ : 352.1013, found 352.1002; mp: 147-149  $^\circ\text{C}$ ; HPLC: (10% isopropanol/hexanes, AD-H): Major enantiomer: 31.0 min; Minor enantiomer: 42.1 min; 96% ee;  $[\alpha]_D^{24} = -28.3^\circ$  ( $c = .400$ ,  $\text{CH}_2\text{Cl}_2$ ).

**(2S,3R)-N-benzyl-2-fluoro-3-((4-methylphenyl)sulfonamido)-3-phenylpropanamide (2.51a-NHBn)**

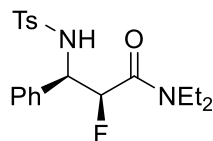


The reaction was conducted at 0  $^\circ\text{C}$  for 10 hours. Treated with 10 equiv. of  $\text{BnNH}_2$ . Isolated as a white powder (62 mg, 53% yield, single diastereomer) after recrystallization (50%  $\text{CH}_2\text{Cl}_2$ /hexanes) from the crude reaction

mixture.  $^1\text{H}$  NMR (500 MHz,  $\text{CDCl}_3$ )  $\delta$  7.59 (d,  $J = 9$  Hz, 2H), 7.25- 7.20 (m, 4H), 7.19-7.14 (m, 2H), 7.14-7.08 (m, 4H), 6.95-6.90 (m, 2H), 6.38 (d,  $J = 10$  Hz, 1H), 6.29 (br s, 1H), 5.09-4.97 (m, 2H), 4.36 (dd,  $J = 15$  Hz, 7 Hz, 1H), 4.19 (dd,  $J = 15$  Hz, 6 Hz, 1H), 2.34 (s, 3H);  $^{13}\text{C}\{^1\text{H}\}$  NMR (125 MHz,  $\text{CDCl}_3$ ): 167.61 (d,  $J = 19$  Hz), 143.40, 137.89, 136.75, 135.20, 129.57, 128.83, 128.49, 128.25, 127.84, 127.71, 127.53, 127.11, 90.76 (d,  $J = 196$  Hz), 57.45 (d,  $J = 24$  Hz), 42.97, 21.59; IR ( $\text{cm}^{-1}$ ): 3348, 3325, 1659, 1156, 702; MS: HR-ESI calculated for  $[\text{C}_{23}\text{H}_{23}\text{FN}_2\text{O}_3\text{S}+\text{Na}]^+$ : 449.1306, found 449.1313; mp: 213-215  $^\circ\text{C}$ ; HPLC: (20% isopropanol/hexanes, AD-H): Minor enantiomer: 17.5 min; Major enantiomer: 24.5 min; 98% ee;  $[\alpha]_D^{24} = -33.6^\circ$  ( $c = .500$ ,  $\text{CH}_3\text{CN}$ ).

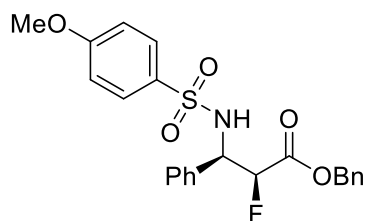
**(2S,3R)-N,N-diethyl-2-fluoro-3-((4-methylphenyl)sulfonamido)-3-phenylpropanamide**

**(2.51a-NEt<sub>2</sub>)**



The reaction was conducted at 0 °C for 10 hours. Treated with 10 equiv of HNEt<sub>2</sub>. Isolated as a white solid (57 mg, 55% yield, single diastereomer) after chromatography (5→50% EtOAc/hexanes) and subsequent recrystallization (50% CH<sub>2</sub>Cl<sub>2</sub>/hexanes). <sup>1</sup>H NMR (500 MHz, CDCl<sub>3</sub>) δ 7.56 (d, J = 8 Hz, 2H), 7.22-7.12 (m, 5H), 7.10 (d, J = 8 Hz, 2H), 6.38 (br s, 1H), 5.14 (dd, J = 48 Hz, 6 Hz, 1H), 4.90-4.82 (m, 1H), 3.25-3.14 (m, 2H), 3.03-2.88 (m, 2H), 2.33 (s, 3H), 0.96 (t, J = 7 Hz, 3H), 0.93 (t, J = 7 Hz, 3H); <sup>13</sup>C{<sup>1</sup>H} NMR (125 MHz, CDCl<sub>3</sub>): 165.68 (d, J = 20 Hz), 143.21, 137.47, 135.48, 129.40, 128.32, 128.24, 128.06, 127.19, 89.51 (d, J = 193 Hz), 58.80 (d, J = 23 Hz), 41.5, 41.32, 21.52, 14.41, 12.4; IR (cm<sup>-1</sup>): 3239, 1642, 1451, 1326, 1155, 1089, 700, 547; MS: HR-ESI calculated for [C<sub>20</sub>H<sub>25</sub>FN<sub>2</sub>O<sub>3</sub>S+H]<sup>+</sup>: 393.1643, found: 393.1632; mp: 146-147 °C; HPLC: (20% isopropanol/hexanes, AD-H): Minor enantiomer: 17.0 min; Major enantiomer: 25.7 min; >99% ee; [α]<sub>D</sub><sup>24</sup> = -30.0° (c=.800, CH<sub>2</sub>Cl<sub>2</sub>).

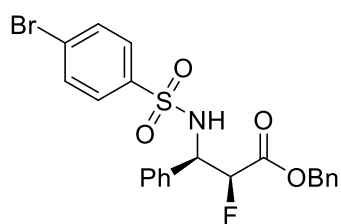
**benzyl (2S,3R)-2-fluoro-3-((4-methoxyphenyl)sulfonamido)-3-phenylpropanoate (2.51b-OBn)**



The reaction was conducted at rt for 5 hours. Treated with 1.2 equiv of BnOH. Isolated as a white solid (44 mg, 50% combined yield of diastereomers) after chromatography (5→30% EtOAc/hexanes). Major diastereomer: <sup>1</sup>H NMR (500 MHz, CDCl<sub>3</sub>) δ 7.57 (d, J = 9 Hz, 2H), 7.40-7.29 (m, 5H), 7.23-7.15 (m, 3H), 7.12- 7.07 (m, 2H), 6.75 (d, J = 9 Hz, 2H), 5.60 (d, J = 10 Hz, 1H), 5.20 (d, J = 12 Hz, 1H), 5.05 (dd, J = 47 Hz, 3 Hz, 1H), 5.06 (d, J = 12 Hz, 1H), 5.03-4.94 (m, 1 H), 3.78 (s, 3H); <sup>13</sup>C{<sup>1</sup>H} NMR(125 MHz, CDCl<sub>3</sub>):

166.97 (d, J = 24 Hz), 162.93, 135.63, 134.62, 132.03, 129.30, 128.84, 128.81, 128.80, 128.75, 128.44, 127.11, 114.07, 90.88 (d, J = 193 Hz), 68.03, 58.51 (d, J = 20 Hz), 55.70; IR (cm<sup>-1</sup>): 3316, 1757, 1144, 1086, 1060, 929, 699, 552; MS: HR-ESI calculated for [C<sub>23</sub>H<sub>22</sub>FNO<sub>5</sub>S+Na]<sup>+</sup>: 466.1095, found: 466.1084; mp: 141-142 °C; HPLC: (25% isopropanol/hexanes, AS-H): Minor enantiomer: 30.0 min; Major enantiomer: 55.5 min; >99% ee;  $[\alpha]_D^{22} = -13.5^\circ$  (c=.267, CH<sub>2</sub>Cl<sub>2</sub>).

**benzyl (2S,3R)-3-((4-bromophenyl)sulfonamido)-2-fluoro-3-phenylpropanoate (2.51c-OBn)**



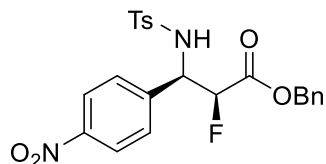
The reaction was conducted at 0 °C for 4 hours. Treated with 1.2 equiv of BnOH. Isolated as a white solid (47 mg, 38% combined yield of diastereomers) after chromatography (5→20%

EtOAc/hexanes). Major diastereomer: <sup>1</sup>H NMR (500 MHz, CDCl<sub>3</sub>)

δ 7.45 (d, J = 9 Hz, 2H), 7.41-7.36 (m, 5H), 7.34-7.31 (m, 2H), 7.25-7.21 (m, 1H), 7.20-7.15 (m, 2H), 7.06 (d, J = 8 Hz, 2H), 5.72 (br s, 1H), 5.21 (d, J = 12 Hz, 1H), 5.09 (d, J = 12 Hz, 1H), 5.06 (dd, J = 47 Hz, 3 Hz, 1H), 5.02 (ddd, J = 25 Hz, 10 Hz, 3 Hz, 1H); <sup>13</sup>C{<sup>1</sup>H} NMR (125 MHz, CDCl<sub>3</sub>): 166.88 (d, J = 25 Hz), 139.47, 135.17, 134.54, 132.11, 128.93, 128.87, 128.81, 128.66, 128.64, 127.66, 127.16, 127.15, 90.81 (d, J = 194 Hz), 68.16, 58.75 (d, J = 20 Hz); IR (cm<sup>-1</sup>): 3241, 2930, 1750, 1244, 1156, 707, 524; MS: HR-ESI calculated for [C<sub>22</sub>H<sub>19</sub>BrFNO<sub>4</sub>S+Na]<sup>+</sup>: 514.0094, found: 514.0100; mp: 124- 126 °C; HPLC: (7% isopropanol/hexanes, OD-H): Minor enantiomer: 27.5 min; Major enantiomer: 41.3 min; 95% ee;  $[\alpha]_D^{22} = -15.4^\circ$  (c=.267, CH<sub>2</sub>Cl<sub>2</sub>).



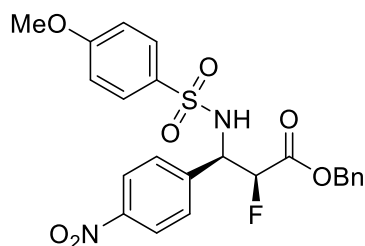
**benzyl (2S,3R)-2-fluoro-3-((4-methylphenyl)sulfonamido)-3-(4-nitrophenyl)propanoate**  
**(2.51d-OBn)**



The reaction was conducted at 0 °C for 3 hours. Treated with 1.2 equiv of BnOH. Isolated as a white solid (36 mg, 32 % combined yield of diastereomers) after chromatography (5→20% EtOAc/hexanes).

Major diastereomer: <sup>1</sup>H NMR (300 MHz, CDCl<sub>3</sub>) δ 7.98 (d, J = 9 Hz, 2H), 7.56 (d, J = 8 Hz, 2H), 7.41-7.33 (m, 3H), 7.30- 7.23 (m, 4H), 7.15 (d, J = 9 Hz, 2H), 5.70 (d, J = 9 Hz, 1H), 5.16 (d, J = 12 Hz, 1H), 5.13-4.95 (m, 2H), 5.00 (d, J = 12 Hz, 1H), 2.34 (s, 3H); <sup>13</sup>C{<sup>1</sup>H} NMR (125 MHz, CDCl<sub>3</sub>): 166.48 (d, J = 24 Hz), 147.83, 144.23, 142.53, 137.16, 134.24, 129.75, 129.12, 128.96, 128.86, 128.24, 127.13, 123.75, 89.93 (d, J = 195 Hz), 68.33, 57.81 (d, J = 21 Hz), 21.59; IR (cm<sup>-1</sup>): 3223, 1756, 1513, 1347, 1225, 1165, 1068, 694, 553; MS: HR-ESI calculated for [C<sub>23</sub>H<sub>21</sub>FN<sub>2</sub>O<sub>6</sub>S+Na]<sup>+</sup>: 495.0997, found: 495.1001; mp: 154-157 °C; HPLC: (20% isopropanol/hexanes, AD-H): Major enantiomer: 39.5 min; Minor enantiomer: 59.8 min; >99% ee; [α]<sub>D</sub><sup>24</sup> = -12.6° (c=.333, CH<sub>3</sub>CN).

**benzyl (2S,3R)-2-fluoro-3-((4-methoxyphenyl)sulfonamido)-3-(4-nitrophenyl)propanoate**  
**(2.51e-OBn)**

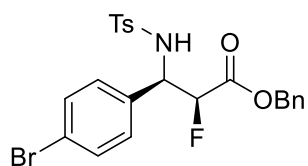


The reaction was conducted at 0 °C for 2 hours. Treated with 1.2 equiv of BnOH. Isolated as a light tan solid (54 mg, 48% combined yield of diastereomers) after chromatography (5→50% EtOAc/hexanes).

Major diastereomer <sup>1</sup>H NMR (500 MHz, CDCl<sub>3</sub>) δ 7.99 (d, J = 9 Hz, 2H), 7.60 (d, J = 9 Hz, 2H), 7.37- 7.32 (m, 3H), 7.31-7.26 (m, 4H), 6.80 (d, J = 9 Hz, 2H), 5.76 (br s, 1 H), 5.18 (d, J = 12 Hz, 1H), 5.10-4.99 (m, 2H), 5.03 (d, J = 12 Hz, 1H), 3.79 (s, 3H); <sup>13</sup>C{<sup>1</sup>H} NMR (125 MHz, CDCl<sub>3</sub>): 166.50 (d, J = 24 Hz), 163.35, 147.90, 142.66,

134.23, 131.58, 129.31, 129.15, 128.97, 128.88, 128.27, 123.79, 114.31, 89.89 (d, J = 196 Hz), 68.35, 57.75 (d, J = 21 Hz), 55.80; IR (cm<sup>-1</sup>): 3249, 1748, 1156; MS: HR-ESI calculated for [C<sub>23</sub>H<sub>21</sub>FN<sub>2</sub>O<sub>7</sub>S+Na]<sup>+</sup> : 511.0946, found: 511.0944; mp: 174-176 °C; HPLC: (30% isopropanol/hexanes, AD-H): Major enantiomer: 27.3 min; Minor enantiomer: 38.8 min; >99% ee; [α]<sub>D</sub><sup>24</sup> = -11.5° (c= 0.200, CH<sub>2</sub>Cl<sub>2</sub>).

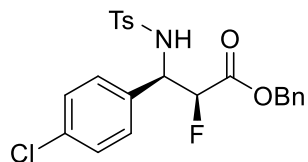
**benzyl (2S,3R)-3-(4-bromophenyl)-2-fluoro-3-((4-methylphenyl)sulfonamido)propanoate (2.51f-OBn)**



The reaction was conducted at 0 °C for 20 hours. Treated with 1.2 equiv of BnOH. Isolated as a white solid (57 mg, 52% yield, single diastereomer) after chromatography (5→20 % EtOAc/hexanes). <sup>1</sup>H

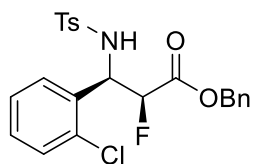
NMR (500 MHz, CDCl<sub>3</sub>) δ 7.53 (d, J = 8 Hz, 2H), 7.40-7.36 (m, 3H), 7.31-7.25 (m, 4H), 7.13 (d, J = 9 Hz, 2H), 6.95 (d, J = 9 Hz, 2H), 5.66 (br s, 1H), 5.18 (d, J = 12 Hz, 1H), 5.07-4.90 (m, 2H), 5.05 (d, J = 12 Hz, 1H), 2.37 (s, 3H); <sup>13</sup>C{<sup>1</sup>H} NMR (125 MHz, CDCl<sub>3</sub>): 166.76 (d, J = 24 Hz), 143.87, 137.31, 134.47, 134.44, 131.80, 129.62, 128.96, 128.90, 128.85, 128.84, 127.15, 122.63, 90.38 (d, J = 194 Hz), 68.14, 57.96 (d, J = 20 Hz), 21.61; IR (cm<sup>-1</sup>): 3301, 1735, 1337, 1158, 816, 666, 549; MS: HR-ESI calculated for [C<sub>23</sub>H<sub>21</sub>BrFNO<sub>4</sub>S+Na]<sup>+</sup> : 528.0251, found: 528.0252; mp: 147-148 °C; HPLC: (7% isopropanol/hexanes, OD-H): Major enantiomer: 33.2 min; Minor enantiomer: 52.2 min; 98% ee; [α]<sub>D</sub><sup>23</sup> = +13.3° (c= 0.400, CH<sub>2</sub>Cl<sub>2</sub>).

**benzyl (2S,3R)-3-(4-chlorophenyl)-2-fluoro-3-((4-methylphenyl)sulfonamido)propanoate**  
**(2.51g-OBn)**



The reaction was conducted at 0 °C for 20 hours. Treated with 1.2 equiv of BnOH. Isolated as a white solid (55 mg, 53% yield, single diastereomer) after chromatography (5→20% EtOAc/hexanes). <sup>1</sup>H NMR (500 MHz, CDCl<sub>3</sub>) δ 7.53 (d, J = 9 Hz, 2H), 7.42-7.36 (m, 3H), 7.33-7.27 (m, 2H), 7.16-7.10 (m, 4H), 7.02 (d, J = 9 Hz, 2H), 5.69 (d, J = 10 Hz, 1H), 5.18 (d, J = 12 Hz, 1H), 5.09-4.93 (m, 2H), 5.04 (d, J = 12 Hz, 1H), 2.36 (s, 3H); <sup>13</sup>C{<sup>1</sup>H} NMR (125 MHz, CDCl<sub>3</sub>): 166.78 (d, J = 24 Hz), 143.83, 137.33, 134.49, 134.45, 133.99, 129.60, 128.95, 128.84, 128.59, 128.58, 127.15, 90.46 (d, J = 194 Hz), 68.12, 57.89 (d, J = 20 Hz), 21.59; IR (cm<sup>-1</sup>): 3303, 2970, 1735, 1338, 1158, 1088, 1062, 815, 666, 549; MS: HR-ESI calculated for [C<sub>23</sub>H<sub>21</sub>ClFO<sub>4</sub>S+Na]<sup>+</sup>: 484.0756, found: 484.0755; mp: 137-140 °C; HPLC: (12 % isopropanol/hexanes, AD-H): Major enantiomer: 36.2 min; Minor enantiomer: 48.2 min; >99% ee; [α]<sub>D</sub><sup>23</sup> = -16.4° (c=.733, CH<sub>2</sub>Cl<sub>2</sub>).

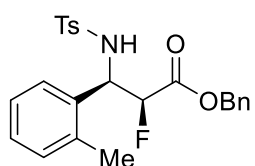
**benzyl (2S,3R)-3-(2-chlorophenyl)-2-fluoro-3-((4-methylphenyl)sulfonamido)propanoate**  
**(2.51h-OBn)**



The reaction was conducted at rt for 2 hours. Treated with 1.2 equiv of BnOH. Isolated as a white solid (35 mg total, 38 % combined yield of diastereomers) after chromatography (5→20% EtOAc/hexanes). Syn diastereomer: <sup>1</sup>H NMR (300 MHz, CDCl<sub>3</sub>) δ 7.57 (d, J = 8 Hz, 2H), 7.39-7.32 (m, 5H), 7.30-7.26 (m, 1H), 7.19-7.13 (m, 2H), 7.11-7.06 (m, 3H), 5.77 (d, J = 10 Hz, 1H), 5.54 (ddd, J = 27 Hz, 10 Hz, 2 Hz, 1H), 5.24 (d, J = 12 Hz, 1 H), 5.10 (dd, J = 47 Hz, 2 Hz, 1H), 4.96 (d, J = 12 Hz, 1H), 2.29 (s, 3H); <sup>13</sup>C{<sup>1</sup>H} NMR (125 MHz, CDCl<sub>3</sub>): 166.51 (d, J = 25 Hz), 143.69, 137.08, 134.71, 133.42, 132.31, 129.78, 129.57, 128.81, 128.76, 128.46, 127.18, 127.15, 89.50 (d, J = 192 Hz),

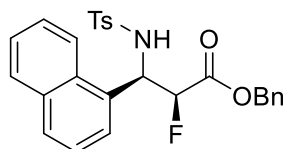
67.97, 55.54 (d,  $J = 19$  Hz), 21.56; IR ( $\text{cm}^{-1}$ ): 3268, 1767, 1336, 1077, 556; MS: HR-ESI calculated for  $[\text{C}_{23}\text{H}_{21}\text{ClFNO}_4\text{S}+\text{Na}]^+$ : 484.0756, found: 484.0753; mp: 124-127 °C; HPLC: (10% isopropanol/hexanes, AD-H): Minor enantiomer: 36.9 min; Major enantiomer: 55.2 min; 99% ee;  $[\alpha]_D^{23} = -0.30^\circ$  ( $c=0.333$ ,  $\text{CH}_2\text{Cl}_2$ ).

**benzyl (2S,3R)-2-fluoro-3-((4-methylphenyl)sulfonamido)-3-(o-tolyl)propanoate (2.51i-OBn)**



The reaction was conducted at rt for 10 hours. Treated with 1.2 equiv of BnOH. Isolated as a white solid (26 mg, 43% combined yield of diastereomers) after chromatography (5→30% EtOAc/hexanes). Major diastereomer:  $^1\text{H}$  NMR (500 MHz,  $\text{CDCl}_3$ )  $\delta$  7.47 (d,  $J = 9$  Hz, 2H), 7.42-7.30 (m, 5 H), 7.11-7.03 (m, 4H), 6.98-6.93 (m, 2H), 5.51 (d,  $J = 10$  Hz, 1H), 5.29 (ddd,  $J = 25$  Hz, 10 Hz, 3 Hz, 1H), 5.20 (d,  $J = 13$  Hz, 1H), 5.07 (d,  $J = 13$  Hz, 1H), 4.95 (dd,  $J = 47$  Hz, 3 Hz, 1H), 2.30 (s, 3H), 2.28 (s, 3H);  $^{13}\text{C}\{^1\text{H}\}$  NMR (125 MHz,  $\text{CDCl}_3$ ): 166.97 (d,  $J = 25$  Hz), 143.46, 137.38, 135.07, 134.71, 133.84, 130.76, 129.41, 128.81, 128.80, 128.65, 128.25, 127.03, 126.86, 126.42, 90.26 (d,  $J = 193$  Hz), 67.99, 54.64 (d,  $J = 20$  Hz), 21.56, 19.34; IR ( $\text{cm}^{-1}$ ): 3275, 1748, 1271, 1161, 546; MS: HR-ESI calculated for  $[\text{C}_{24}\text{H}_{24}\text{FNO}_4\text{S}+\text{Na}]^+$ : 464.1302, found: 464.1288; mp: 120-122 °C; HPLC: (25% isopropanol/hexanes, AS-H): Minor enantiomer: 18.5 min; Major enantiomer: 33.0 min; 99% ee;  $[\alpha]_D^{22} = +0.50^\circ$  ( $c=0.200$ ,  $\text{CH}_2\text{Cl}_2$ ).

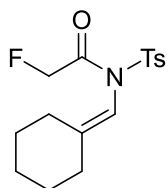
**benzyl (2S,3R)-2-fluoro-3-((4-methylphenyl)sulfonamido)-3-(naphthalen-1-yl)propanoate (2.51j-OBn)**



The reaction was conducted at rt for 9 hours. Treated with 1.2 equiv of BnOH. Isolated as a white solid (37 mg, 39 % combined yield of

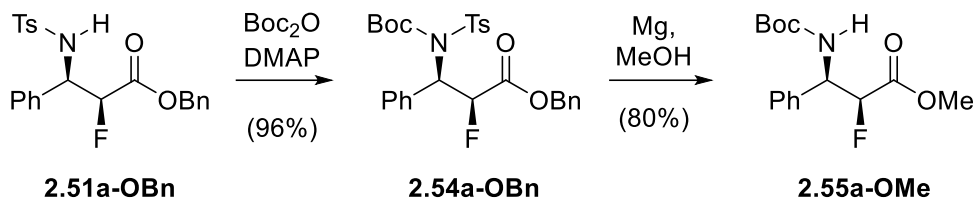
diastereomers) after chromatography (5→20% EtOAc/hexanes). Major diastereomer:  $^1\text{H}$  NMR (500 MHz,  $\text{CDCl}_3$ )  $\delta$  7.94 (d,  $J = 8$  Hz, 1H), 7.84 (d,  $J = 9$  Hz, 1H), 7.74-7.70 (m, 1H), 7.56-7.48 (m, 2H), 7.44 (d,  $J = 8$  Hz, 2H), 7.41-7.35 (m, 5H), 7.26-7.23 (m, 2H), 6.94 (d,  $J = 8$  Hz, 2H), 5.92 (ddd,  $J = 25$  Hz, 10 Hz, 3 Hz, 1H), 5.63 (d,  $J = 9$  Hz, 1H), 5.26 (d,  $J = 12$  Hz, 1H), 5.17 (dd,  $J = 47$  Hz, 3 Hz, 1H), 5.08 (d,  $J = 12$  Hz, 1H), 2.24 (s, 3H);  $^{13}\text{C}\{^1\text{H}\}$  NMR (125 MHz,  $\text{CDCl}_3$ ): 167.06 (d,  $J = 25$  Hz), 143.44, 137.26, 134.74, 133.88, 131.10, 129.99, 129.34, 129.02, 128.86, 128.70, 127.17, 127.10, 126.05, 125.14, 125.05, 121.74, 90.27 (d,  $J = 193$  Hz), 68.15, 54.68 (d,  $J = 19$  Hz), 21.49; IR ( $\text{cm}^{-1}$ ): 3264, 2920, 1772, 1759, 1330, 1158, 1089, 801, 700, 546; MS: HR-ESI calculated for  $[\text{C}_{27}\text{H}_{24}\text{FNO}_4\text{S}+\text{Na}]^+$  : 500.1302, found: 500.1309; mp: 148-150 °C; HPLC: (12% isopropanol/hexanes, AD-H): Minor enantiomer: 32.2 min; Major enantiomer: 45.5 min; 74% ee;  $[\alpha]_D^{23} = +8.00^\circ$  ( $c=0.400$ ,  $\text{CH}_2\text{Cl}_2$ ).

### **N-(cyclohexylidenemethyl)-2-fluoro-N-tosylacetamide (2.63)**



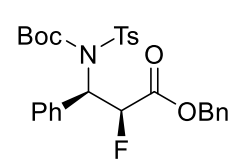
The reaction was conducted at rt for 20 hours, at which time all *N*-tosylimine was consumed. The reaction was worked up as described above. Isolated as a white solid (60 mg, 68% yield) after chromatography (5→20% EtOAc/hexanes).  $^1\text{H}$  NMR (500 MHz,  $\text{CDCl}_3$ )  $\delta$  7.90 (d,  $J = 9$  Hz, 2H), 7.31 (d,  $J = 9$  Hz, 2H), 5.73 (s, 1H), 4.80 (d,  $J = 48$  Hz, 2H), 2.42 (s, 3H), 2.21 (t,  $J = 6$  Hz, 2H), 2.01 (t,  $J = 6$  Hz, 2H), 1.66-1.59 (m, 2H), 1.59-1.53 (m, 2H), 1.52-1.45 (m, 2H);  $^{13}\text{C}\{^1\text{H}\}$  NMR (125 MHz,  $\text{CDCl}_3$ ): 166.59 (d,  $J = 21$  Hz), 153.01, 145.45, 135.34, 129.59, 128.93, 111.50, 78.92 (d,  $J = 182$  Hz), 33.30, 28.40, 27.61, 26.77, 26.05, 21.75; IR ( $\text{cm}^{-1}$ ): 2926, 2857, 1728, 1350, 1169, 1152, 1077, 565; MS: HR-ESI calculated for  $[\text{C}_{16}\text{H}_{20}\text{FNO}_3\text{S}+\text{Na}]^+$ : 348.1040, found 348.1042; mp: 102-106 °C.

### 2.14.3 Protecting group exchange



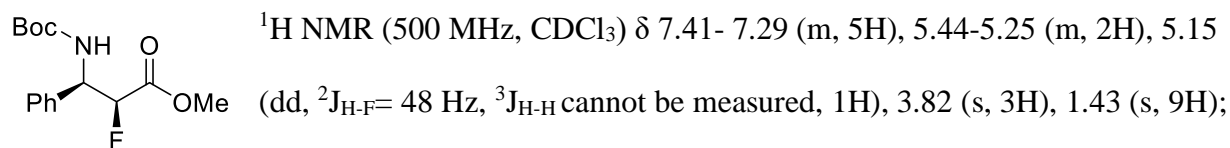
**Intermediate 2.54a-OBn:** To a solution of **2.51a-OBn** (104 mg, 0.24 mmol) in 1.25 mL of freshly distilled CH<sub>2</sub>Cl<sub>2</sub> stirred under inert atmosphere at 0 °C was added dropwise a solution of Boc<sub>2</sub>O (64 mg, 0.29 mmol, 1.2 equiv) and DMAP (2 mg, ca. 5 mol %) in 1.25 mL of CH<sub>2</sub>Cl<sub>2</sub>. The mixture was slowly warmed to rt and monitored by TLC for completion (10% EtOAc/hexanes). After complete consumption of the starting material, the reaction was quenched with saturated aqueous NaHCO<sub>3</sub>. The organic phase was separated, dried with MgSO<sub>4</sub>, and rotary evaporated. After column chromatography (5→10% EtOAc/hexanes), **2.54a-OBn** was obtained as a clear, colorless oil which crystallized on standing (123 mg, 96%).

#### benzyl (2*S*,3*R*)-3-((*N*-(*tert*-butoxycarbonyl)-4-methylphenyl)sulfonamido)-2-fluoro-3-phenylpropanoate (**2.54a-OBn**)

 <sup>1</sup>H NMR (500 MHz, CDCl<sub>3</sub>) δ 7.74 (d, J = 9 Hz, 2H), 7.59-7.55 (m, 2H), 7.35-7.27 (m, 8H), 7.12-7.08 (m, 2H), 6.17-6.02 (m, 2H), 5.11 (d, J = 12 Hz, 1H), 5.04 (d, J = 12 Hz, 1H), 2.44 (s, 3H), 1.29 (s, 9H); <sup>13</sup>C{<sup>1</sup>H} NMR (125 MHz, CDCl<sub>3</sub>): 167.63 (d, J = 22 Hz), 150.61, 144.27, 137.38, 134.64, 134.59, 129.46, 129.21, 128.94, 128.67, 128.63, 128.56, 128.39, 128.37, 87.51 (d, J = 186 Hz), 85.35, 67.64, 61.21 (d, J = 21 Hz), 27.94, 21.73; IR (cm<sup>-1</sup>): 2981, 2929, 1751, 1726, 1353, 1148, 697, 671, 577, 545; MS: HR-ESI calculated for [C<sub>28</sub>H<sub>30</sub>FNO<sub>6</sub>S+Na]<sup>+</sup>: 550.1670, found: 550.1646; mp: 135-137 °C; [α]<sub>D</sub><sup>22</sup> = +2.5° (c=1.133, CH<sub>2</sub>Cl<sub>2</sub>).

**Carbamate 2.55a-OMe:** To a solution of **2.54a-OBn** (54 mg, 0.102 mmol) dissolved in 1.6 mL of anhydrous MeOH and 0.54 mL of anhydrous THF was added powdered magnesium (50 mg, 2.05 mmol, 20 equiv). This solution was sonicated for one hour, at which time TLC (10% EtOAc/hexanes) confirmed complete consumption of the starting material. The mixture was diluted with CH<sub>2</sub>Cl<sub>2</sub> (10 mL) and poured into 10 mL of 0.5 M aqueous HCl. The organic phase was separated, washed with 1 M aqueous NaHCO<sub>3</sub> and brine, dried with MgSO<sub>4</sub> and rotary evaporated to yield a slightly crude crystalline solid. Successive recrystallizations from 15% EtOAc/hexanes gave 24 mg (80% yield) of pure **2.55a-OMe**.

**methyl (2S,3R)-3-((tert-butoxycarbonyl)amino)-2-fluoro-3-phenylpropanoate (2.55a-OMe)**



<sup>13</sup>C{<sup>1</sup>H} NMR (125 MHz, CDCl<sub>3</sub>): 168.15 (d, J = 25 Hz), 155.03, 137.65, 128.95, 128.33, 126.86, 90.58 (d, J = 190 Hz), 80.45, 55.51 (d, J = 19 Hz), 52.85, 28.37; IR (cm<sup>-1</sup>): 1748, 1695, 1510, 1239, 707; MS: HR-ESI calculated for [C<sub>15</sub>H<sub>20</sub>FNO<sub>4</sub>+H]<sup>+</sup> : 298.1449, found: 298.1442; mp: 121-124 °C; [α]<sub>D</sub><sup>22</sup> = +85.5° (c=.600, CH<sub>3</sub>CN).

## 2.15 X-ray crystal structure of 2.51a-OMe

**Table 2.4.** Crystal data and structure refinement for **2.51a-OMe**.

Identification code	v10818t5/lt/x8/MS_03_25
Empirical formula	C <sub>17</sub> H <sub>18</sub> F N O <sub>4</sub> S
Formula weight	351.38
Temperature	100(2) K
Wavelength	0.71073 Å
Crystal system	Monoclinic
Space group	P2 <sub>1</sub>
Unit cell dimensions	a = 11.4126(14) Å      a = 90°. B = 5.3638(6) Å      b = 109.453(8)°. C = 14.3993(19) Å      g = 90°.
Volume	831.14(18) Å <sup>3</sup>
Z	2
Density (calculated)	1.404 Mg/m <sup>3</sup>
Absorption coefficient	0.226 mm <sup>-1</sup>
F(000)	368
Crystal size	0.575 x 0.212 x 0.041 mm <sup>3</sup>
Theta range for data collection	1.500 to 27.541°.
Index ranges	-14 ≤ h ≤ 14, -6 ≤ k ≤ 6, -18 ≤ l ≤ 18
Reflections collected	25583
Independent reflections	25583 [R(int) = 0.037]
Completeness to theta = 25.242°	100.0 %
Absorption correction	Semi-empirical from equivalents
Max. and min. transmission	0.9143 and 0.7949
Refinement method	Full-matrix least-squares on F <sup>2</sup>
Data / restraints / parameters	25583 / 2 / 223
Goodness-of-fit on F <sup>2</sup>	1.023
Final R indices [I > 2σ(I)]	R1 = 0.0496, wR2 = 0.1010
R indices (all data)	R1 = 0.0677, wR2 = 0.1104
Absolute structure parameter	-0.02(4)
Largest diff. peak and hole	0.430 and -0.328 e.Å <sup>-3</sup>



**Table 2.5.** Atomic coordinates ( $\times 10^4$ ) and equivalent isotropic displacement parameters ( $\text{\AA}^2 \times 10^3$ ) for **2.51a-OMe**.  $U(\text{eq})$  is defined as one third of the trace of the orthogonalized  $U^{ij}$  tensor.

	x	y	z	U(eq)
S(1)	847(1)	3621(3)	2282(1)	18(1)
F(1)	3544(3)	8909(6)	4134(2)	22(1)
O(1)	4353(4)	7358(7)	2689(3)	28(1)
O(2)	4894(3)	3673(7)	3454(2)	21(1)
O(3)	989(3)	1268(6)	2788(3)	21(1)
O(4)	-358(3)	4724(7)	1867(3)	26(1)
N(1)	1712(4)	5626(8)	3053(3)	17(1)
C(1)	3831(5)	6369(9)	4137(4)	16(1)
C(2)	4375(5)	5927(10)	3333(4)	17(1)
C(3)	5487(5)	2932(10)	2747(4)	23(1)
C(4)	2641(5)	4868(9)	3977(3)	14(1)
C(5)	2185(5)	5009(10)	4848(4)	15(1)
C(6)	1458(4)	6979(9)	4972(4)	18(1)
C(7)	1044(5)	7013(10)	5774(4)	22(1)
C(8)	1352(5)	5124(11)	6461(4)	22(1)
C(9)	2079(5)	3155(10)	6341(4)	22(1)
C(10)	2490(5)	3097(9)	5539(4)	18(1)
C(11)	1495(5)	3290(11)	1347(4)	19(1)
C(12)	2316(5)	1370(10)	1386(4)	22(1)
C(13)	2848(5)	1155(11)	657(4)	28(1)
C(14)	2586(6)	2865(11)	-108(4)	29(2)
C(15)	1758(6)	4792(12)	-134(4)	33(2)
C(16)	1208(5)	5020(11)	583(4)	23(1)
C(17)	3156(6)	2576(15)	-905(5)	49(2)

**Table 2.6.** Bond lengths [Å] and angles [°] for **2.51a-OMe**.

---

S(1)-O(4)	1.432(4)
S(1)-O(3)	1.439(4)
S(1)-N(1)	1.623(4)
S(1)-C(11)	1.747(5)
F(1)-C(1)	1.401(5)
O(1)-C(2)	1.198(6)
O(2)-C(2)	1.332(6)
O(2)-C(3)	1.452(6)
N(1)-C(4)	1.457(6)
N(1)-H(1N)	0.85(3)
C(1)-C(2)	1.505(7)
C(1)-C(4)	1.528(7)
C(1)-H(1)	1.0000
C(3)-H(3A)	0.9800
C(3)-H(3B)	0.9800
C(3)-H(3C)	0.9800
C(4)-C(5)	1.512(7)
C(4)-H(4)	1.0000
C(5)-C(10)	1.390(7)
C(5)-C(6)	1.391(7)
C(6)-C(7)	1.385(7)
C(6)-H(6)	0.9500
C(7)-C(8)	1.377(8)
C(7)-H(7)	0.9500
C(8)-C(9)	1.389(7)
C(8)-H(8)	0.9500
C(9)-C(10)	1.384(7)
C(9)-H(9)	0.9500
C(10)-H(10)	0.9500
C(11)-C(12)	1.381(7)
C(11)-C(16)	1.393(7)
C(12)-C(13)	1.382(8)
C(12)-H(12)	0.9500
C(13)-C(14)	1.388(8)

C(13)-H(13)	0.9500
C(14)-C(15)	1.392(9)
C(14)-C(17)	1.503(9)
C(15)-C(16)	1.380(8)
C(15)-H(15)	0.9500
C(16)-H(16)	0.9500
C(17)-H(17A)	0.9800
C(17)-H(17B)	0.9800
C(17)-H(17C)	0.9800
O(4)-S(1)-O(3)	120.3(2)
O(4)-S(1)-N(1)	107.0(2)
O(3)-S(1)-N(1)	107.1(2)
O(4)-S(1)-C(11)	108.3(2)
O(3)-S(1)-C(11)	107.2(3)
N(1)-S(1)-C(11)	106.1(2)
C(2)-O(2)-C(3)	116.6(4)
C(4)-N(1)-S(1)	122.2(3)
C(4)-N(1)-H(1N)	118(4)
S(1)-N(1)-H(1N)	117(4)
F(1)-C(1)-C(2)	107.8(4)
F(1)-C(1)-C(4)	108.5(4)
C(2)-C(1)-C(4)	112.0(4)
F(1)-C(1)-H(1)	109.5
C(2)-C(1)-H(1)	109.5
C(4)-C(1)-H(1)	109.5
O(1)-C(2)-O(2)	125.2(5)
O(1)-C(2)-C(1)	126.0(5)
O(2)-C(2)-C(1)	108.8(5)
O(2)-C(3)-H(3A)	109.5
O(2)-C(3)-H(3B)	109.5
H(3A)-C(3)-H(3B)	109.5
O(2)-C(3)-H(3C)	109.5
H(3A)-C(3)-H(3C)	109.5
H(3B)-C(3)-H(3C)	109.5
N(1)-C(4)-C(5)	113.4(4)

N(1)-C(4)-C(1)	109.3(4)
C(5)-C(4)-C(1)	112.5(4)
N(1)-C(4)-H(4)	107.1
C(5)-C(4)-H(4)	107.1
C(1)-C(4)-H(4)	107.1
C(10)-C(5)-C(6)	119.1(5)
C(10)-C(5)-C(4)	118.9(5)
C(6)-C(5)-C(4)	122.0(5)
C(7)-C(6)-C(5)	120.0(5)
C(7)-C(6)-H(6)	120.0
C(5)-C(6)-H(6)	120.0
C(8)-C(7)-C(6)	120.9(5)
C(8)-C(7)-H(7)	119.6
C(6)-C(7)-H(7)	119.6
C(7)-C(8)-C(9)	119.3(5)
C(7)-C(8)-H(8)	120.3
C(9)-C(8)-H(8)	120.3
C(10)-C(9)-C(8)	120.2(5)
C(10)-C(9)-H(9)	119.9
C(8)-C(9)-H(9)	119.9
C(9)-C(10)-C(5)	120.4(5)
C(9)-C(10)-H(10)	119.8
C(5)-C(10)-H(10)	119.8
C(12)-C(11)-C(16)	120.4(5)
C(12)-C(11)-S(1)	120.0(4)
C(16)-C(11)-S(1)	119.5(4)
C(11)-C(12)-C(13)	119.7(5)
C(11)-C(12)-H(12)	120.2
C(13)-C(12)-H(12)	120.2
C(12)-C(13)-C(14)	121.0(6)
C(12)-C(13)-H(13)	119.5
C(14)-C(13)-H(13)	119.5
C(13)-C(14)-C(15)	118.5(6)
C(13)-C(14)-C(17)	120.3(6)
C(15)-C(14)-C(17)	121.2(6)
C(16)-C(15)-C(14)	121.3(6)

C(16)-C(15)-H(15)	119.4
C(14)-C(15)-H(15)	119.4
C(15)-C(16)-C(11)	119.1(6)
C(15)-C(16)-H(16)	120.5
C(11)-C(16)-H(16)	120.5
C(14)-C(17)-H(17A)	109.5
C(14)-C(17)-H(17B)	109.5
H(17A)-C(17)-H(17B)	109.5
C(14)-C(17)-H(17C)	109.5
H(17A)-C(17)-H(17C)	109.5
H(17B)-C(17)-H(17C)	109.5

---

**Table 2.7.** Anisotropic displacement parameters ( $\text{\AA}^2 \times 10^3$ ) for **2.51a-OMe**. The anisotropic displacement factor exponent takes the form:  $-2p^2[ h^2 a^{*2}U^{11} + \dots + 2 h k a^* b^* U^{12} ]$

	U11	U22	U33	U23	U13	U12
S(1)	15(1)	17(1)	19(1)	0(1)	2(1)	-2(1)
F(1)	22(2)	11(2)	32(2)	-3(2)	7(1)	0(1)
O(1)	33(2)	23(2)	29(2)	10(2)	13(2)	7(2)
O(2)	23(2)	15(2)	26(2)	2(2)	12(2)	5(2)
O(3)	25(2)	15(2)	21(2)	1(2)	7(2)	-6(2)
O(4)	14(2)	28(2)	29(2)	-4(2)	1(2)	0(2)
N(1)	19(2)	10(2)	18(2)	-2(2)	0(2)	2(2)
C(1)	18(3)	8(3)	20(3)	1(2)	4(2)	4(2)
C(2)	11(3)	14(3)	23(3)	-1(2)	1(2)	-1(2)
C(3)	23(3)	21(4)	29(3)	-1(2)	12(3)	-2(2)
C(4)	15(3)	11(3)	16(3)	0(2)	3(2)	0(2)
C(5)	11(3)	14(3)	18(3)	-2(2)	2(2)	0(2)
C(6)	16(3)	13(3)	23(3)	0(2)	4(3)	-2(2)
C(7)	16(3)	19(3)	30(3)	-3(3)	7(3)	3(2)
C(8)	19(3)	27(3)	21(3)	-5(3)	9(3)	-2(3)
C(9)	24(3)	21(4)	19(3)	4(3)	6(2)	4(2)
C(10)	18(3)	11(3)	21(3)	-2(2)	2(2)	3(2)
C(11)	19(3)	20(3)	14(3)	-5(3)	1(2)	-5(2)
C(12)	25(3)	19(3)	19(3)	4(3)	3(3)	-1(3)
C(13)	27(3)	31(4)	25(3)	-5(3)	8(3)	2(3)
C(14)	28(3)	41(4)	18(3)	-5(3)	6(3)	-10(3)
C(15)	34(4)	40(4)	20(3)	8(3)	1(3)	-5(3)
C(16)	24(3)	23(3)	19(3)	4(3)	1(3)	0(3)
C(17)	45(4)	79(6)	25(4)	-3(3)	14(4)	-10(4)

**Table 2.8.** Hydrogen coordinates ( $\times 10^4$ ) and isotropic displacement parameters ( $\text{\AA}^2 \times 10^3$ ) for **2.51a-OMe**.

	x	y	z	U(eq)
H(1N)	1460(50)	7130(70)	3000(40)	21
H(1)	4456	5914	4788	19
H(3A)	5036	3660	2103	35
H(3B)	5477	1110	2693	35
H(3C)	6348	3524	2969	35
H(4)	2845	3082	3903	17
H(6)	1244	8301	4507	22
H(7)	542	8357	5851	26
H(8)	1070	5168	7012	26
H(9)	2295	1844	6811	26
H(10)	2984	1741	5460	21
H(12)	2514	202	1912	26
H(13)	3402	-183	680	33
H(15)	1567	5972	-655	40
H(16)	642	6339	555	28
H(17A)	4031	2106	-609	74
H(17B)	3095	4158	-1258	74
H(17C)	2712	1275	-1366	74

**Table 2.9.** Torsion angles [°] for **2.51a-OMe**.

---

O(4)-S(1)-N(1)-C(4)	143.0(4)
O(3)-S(1)-N(1)-C(4)	12.8(5)
C(11)-S(1)-N(1)-C(4)	-101.5(4)
C(3)-O(2)-C(2)-O(1)	0.6(7)
C(3)-O(2)-C(2)-C(1)	-179.2(4)
F(1)-C(1)-C(2)-O(1)	-12.8(7)
C(4)-C(1)-C(2)-O(1)	106.4(6)
F(1)-C(1)-C(2)-O(2)	166.9(4)
C(4)-C(1)-C(2)-O(2)	-73.8(5)
S(1)-N(1)-C(4)-C(5)	-96.7(5)
S(1)-N(1)-C(4)-C(1)	136.9(4)
F(1)-C(1)-C(4)-N(1)	57.8(5)
C(2)-C(1)-C(4)-N(1)	-61.2(5)
F(1)-C(1)-C(4)-C(5)	-69.2(5)
C(2)-C(1)-C(4)-C(5)	171.9(4)
N(1)-C(4)-C(5)-C(10)	138.4(5)
C(1)-C(4)-C(5)-C(10)	-96.9(6)
N(1)-C(4)-C(5)-C(6)	-40.9(7)
C(1)-C(4)-C(5)-C(6)	83.8(6)
C(10)-C(5)-C(6)-C(7)	-0.2(7)
C(4)-C(5)-C(6)-C(7)	179.0(5)
C(5)-C(6)-C(7)-C(8)	0.5(8)
C(6)-C(7)-C(8)-C(9)	-0.5(8)
C(7)-C(8)-C(9)-C(10)	0.1(8)
C(8)-C(9)-C(10)-C(5)	0.3(8)
C(6)-C(5)-C(10)-C(9)	-0.2(7)
C(4)-C(5)-C(10)-C(9)	-179.5(5)
O(4)-S(1)-C(11)-C(12)	-150.0(4)
O(3)-S(1)-C(11)-C(12)	-18.8(5)
N(1)-S(1)-C(11)-C(12)	95.4(4)
O(4)-S(1)-C(11)-C(16)	32.0(5)
O(3)-S(1)-C(11)-C(16)	163.2(4)



N(1)-S(1)-C(11)-C(16)	-82.6(4)
C(16)-C(11)-C(12)-C(13)	-0.5(7)
S(1)-C(11)-C(12)-C(13)	-178.4(4)
C(11)-C(12)-C(13)-C(14)	1.0(8)
C(12)-C(13)-C(14)-C(15)	-0.9(8)
C(12)-C(13)-C(14)-C(17)	-178.9(6)
C(13)-C(14)-C(15)-C(16)	0.2(9)
C(17)-C(14)-C(15)-C(16)	178.2(6)
C(14)-C(15)-C(16)-C(11)	0.3(8)
C(12)-C(11)-C(16)-C(15)	-0.1(8)
S(1)-C(11)-C(16)-C(15)	177.8(4)

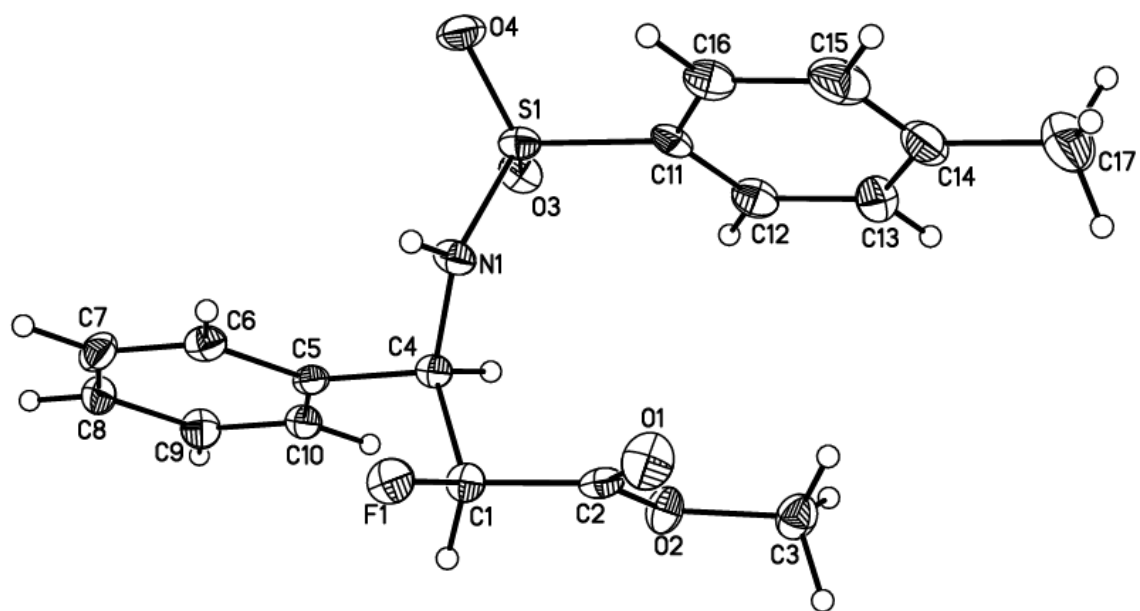
**Table 2.10.** Hydrogen bonds for **2.51a-OMe** [ $\text{\AA}$  and  $^\circ$ ].

D-H...A	d(D-H)	d(H...A)	d(D...A)	$\angle(\text{DHA})$
N(1)-H(1N)...O(3)#1	0.85(3)	2.28(3)	3.127(5)	173(5)
C(1)-H(1)...F(1)#2	1.00	2.53	3.456(6)	153.3
C(3)-H(3B)...O(1)#3	0.98	2.39	3.247(7)	146.5
C(4)-H(4)...F(1)#3	1.00	2.36	3.343(6)	166.5
C(12)-H(12)...O(1)#3	0.95	2.53	3.264(7)	133.7

Symmetry transformations used to generate equivalent atoms:

#1  $x, y+1, z$  #2  $-x+1, y-1/2, -z+1$  #3  $x, y-1, z$

Projection view with 50% probability ellipsoids:



## 2.16 References

1. The results in this chapter were previously published: Straub, M. R.; Birman, V. B. *Org. Lett.* **2018**, *20*, 7550.
2. (a) Gillis, E. P.; Eastman, K. J.; Hill, M. D.; Donnelly, D. J.; Meanwell, N. A. *J. Med. Chem.* **2015**, *58*, 8315. (b) Wang, J.; Sanchez-Rosello, M.; Acena, J. L.; del Pozo, C.; Sorochinsky, A. E.; Fustero, S.; Soloshonok, V. A.; Liu, H. *Chem. Rev.* **2014**, *114*, 2432. (c) Boehm, H.-J.; Banner, D.; Bendels, S.; Kansy, M.; Kuhn, B.; Mueller, K.; Obst-Sander, U.; Stahl, M. *Chembiochem* **2004**, *5*, 637.
3. Harsanyi, A.; Sandford, G. *Green Chem.* **2015**, *17*, 2081.
4. Holmgren, S. K.; Taylor, K. M.; Bretscher, L. E.; Raines, R. T. *Nature* **1998**, *392*, 666.
5. O'Hagan, D. *Chem. Soc. Rev.* **2008**, *37*, 308.
6. For a mini review of fluorine-containing natural products, see: O'Hagan, D.; Harper, D. *B. J. Fluor. Chem.* **1999**, *100*, 127.
7. Buer, B. C.; Marsh, E. Neil G. *Protein Sci.* **2012**, *21*, 453.
8. Gerig, J. T. *Prog Nucl Magn Reson Spectrosc* **1994**, *26*, 293.
9. March, T. L.; Johnston, M. R.; Duggan, P. J.; Gardiner, J. *Chem. Biodivers.* **2012**, *9*, 2410.
10. Mathad, R. I.; Juan, B.; Floegel, O.; Gardiner, J.; Loeweneck, M.; Codée, J. D. C.; Seeberger, P. H.; Seebach, D.; Edmonds, M. K.; Graichen, F. H. M.; Abell, A. D. *Helv. Chim. Acta* **2007**, *90*, 2251.

11. Appayee, C.; Brenner-Moyer, S. E. *Org. Lett.* **2010**, *12*, 3356.
12. Pan, Y.; Zhao, Y.; Ma, T.; Yang, Y.; Liu, H.; Jiang, Z.; Tan, C.-H. *Chem. Eur. J.* **2010**, *16*, 779.
13. Zhang, P.; Wang, C.; Zhou, L.; Sun, J. *Chin. J. Chem.* **2012**, *30*, 2636.
14. Han, Z.; Guan, Y.-Q.; Liu, G.; Wang, R.; Yin, X.; Zhao, Q.; Cong, H.; Dong, X.-Q.; Zhang, X. *Org. Lett.* **2018**, *20*, 6349.
15. Li, X.-G.; Laehitie, M.; Paeivioe, M.; Kanerva, L. T. *Tetrahedron Asymmetry* **2007**, *18*, 1567.
16. Hodous, B. L.; Fu, G. C. *J. Am. Chem. Soc.* **2002**, *124*, 1578.
17. France, S.; Weatherwax, A.; Taggi, A. E.; Lectka, T. *Acc. Chem. Res.* **2004**, *37*, 592.
18. (a) Birman, V. B. *Aldrichimica Acta* **2016**, *49*, 23. (b) Merad, J.; Pons, J.-M.; Chuzel, O.; Bressy, C. *Eur. J. Org. Chem.* **2016**, *2016*, 5589.
19. (a) Leverett, C. A.; Purohit, V. C.; Romo, D. *Angew. Chem. Int. Ed.* **2010**, *49*, 9479. (b) Purohit, V. C. Matla, A. S.; Romo, D. *J. Am. Chem. Soc.* **2008**, *130*, 10478.
20. Leverett, C. A.; Purohit, V. C.; Johnson, A. G.; Davis, R. L.; Tantillo, D. J.; Romo, D. *J. Am. Chem. Soc.* **2012**, *134*, 13348.
21. Liu, G.; Shirley, M. E.; Van, K. N.; McFarlin, R. L.; Romo, D. *Nat. Chem.* **2013**, *5*, 1049.
22. (a) Belmessieri, D.; Joannesse, C.; Woods, P. A.; MacGregor, C.; Jones, C.; Campbell, C. D.; Johnston, C. P.; Duguet, N.; Concellon, C.; Bragg, R. A.; Smith, A. D. *Org. Biomol.*

- Chem.* **2011**, *9*, 559. (b) Joannesse, C.; Johnston, C. P.; Concellon, C.; Simal, C.; Philp, D.; Smith, A. D. *Angew. Chem. Int. Ed.* **2009**, *48*, 8914.
23. Smith, S. R.; Douglas, J.; Prevet, H.; Shapland, P.; Slawin, A. M. Z.; Smith, A. D. *J. Org. Chem.* **2014**, *79*, 1626.
24. Welch, J. T.; Seper, K.; Eswarakrishnan, S.; Samartino, J. *J. Org. Chem.* **1984**, *49*, 4720.
25. Liu, G.; Shirley, M. E.; Romo, D. *J. Org. Chem.* **2012**, *77*, 2496.
26. Kobayashi, M.; Okamoto, S. *Tetrahedron Lett.* **2006**, *47*, 4347.
27. Belmessieri, D.; Morrill, L. C.; Simal, C.; Slawin, A. M. Z.; Smith, A. D. *J. Am. Chem. Soc.* **2011**, *133*, 2714.
28. Inanaga, J.; Hirata, K.; Saeki, H.; Katsuki, T.; Yamaguchi, M. *Bull. Chem. Soc. Jpn.* **1979**, *52*, 1989.
29. Birman, V. B.; Li, X. *Org. Lett.* **2006**, *8*, 1351.
30. Birman, V. B.; Li, X. *Org. Lett.* **2008**, *10*, 1115.
31. Zhang, Y.; Birman, V. B. *Adv. Synth. Catal.* **2009**, *351*, 2525.
32. Flack, H. D.; Bernardinelli, G. *Chirality* **2008**, *20*, 681–690.
33. Epimerization has been observed in a structurally similar case: Kant, J.; Huang, S.; Wong, H.; Fairchild, C.; Vyas, D.; Farina, V. *Bioorg. Med. Chem. Lett.* **1993**, *3*, 2471.
34. Deprot. Of Ts Group: Greene, T. W.; Wuts, P. G. M. *Protective Groups in Organic Synthesis*, 3<sup>rd</sup> ed.; John Wiley & Sons: New York, 1999.
35. Vedejs, E.; Lin, S. *J. Org. Chem.* **1994**, *59*, 1602.

36. McIntosh, J. M.; Matassa, L. C. *J. Org. Chem.* **1988**, *53*, 4452.
37. (a) Haskell, B. E.; Bowlus, S. B. *J. Org. Chem.* **1976**, *41*, 159. (b) Compagnone, R. S.; Rapaport, H. *J. Org. Chem.* **1986**, *51*, 1713. (c) Kudav, D. P.; Samant, S. P.; Hosangadi, B. D. *Synth. Commun.* **1987**, *17*, 1185.
38. Nyasse, B.; Grehn, L.; Ragnarsson, U. *Chem. Commun.* **1997**, 1017–1018.
39. Hammond, G. S. *J. Am. Chem. Soc.* **1955**, *77*, 334.
40. Okamoto, S.; Sakai, Y.; Watanabe, S.; Nishi, S.; Yoneyama, A.; Katsumata, H.; Kosaki, Y.; Sato, R.; Shiratori, M.; Shibuno, M.; Shishido, T. *Tetrahedron Lett.* **2014**, *55*, 1909.
41. Ahlemeyer, N. A.; Streff, E. V.; Muthupandi, P.; Birman, V. B. *Org. Lett.* **2017**, *19*, 6486-6489.
42. (a) Xiao, X.; Zhang, W.; Lu, X.; Deng, Y.; Jiang, H.; Zeng, W. *Adv. Synth. Catal.* **2016**, *358*, 2497-2509. (b) Xiao, L.-J.; Zhao, C.-Y.; Cheng, L.; Feng, B.-Y.; Feng, W.-M.; Xie, J.-H.; Xu, X.-F.; Zhou, Q.-L. *Angew. Chem., Int. Ed.* **2018**, *57*, 3396-3400.
43. Albler, C.; Schmid, W. *Eur. J. Org. Chem.* **2014**, *2014*, 2451-2459.

# Chapter 3: Kinetic resolution of isoxazolidinones<sup>1</sup>

Isoxazolidinones are nitrogen- and oxygen-containing heterocycles that have garnered considerable attention in the synthetic community. One of the more common application of these compounds is to serve as precursors to  $\beta$ -amino acids via hydrogenolytic cleavage of the N-O bond (see Figure 1.5, Eq. 5 for an example). Given their importance, many asymmetric approaches to these compounds exist.<sup>2-8</sup>

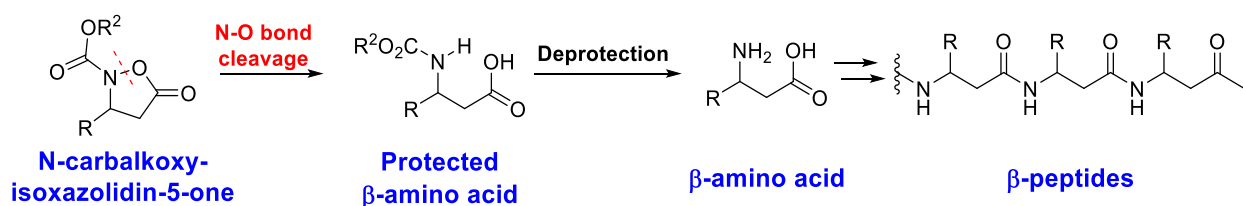


**Figure 3.1:** N-carbalkoxy-isoxazolidin-5-ones as precursors to  $\beta$ -amino acids.

Of all isoxazolidinones, N-carbalkoxy-isoxazolidin-5-ones remain an attractive subset, namely due to the simplicity of deprotecting the nitrogen atom (Figure 3.1). Some asymmetric catalytic approaches to these valuable precursors are illustrated in Figure 3.2; however, more methods exist.<sup>3-6</sup> It is interesting to see the broad range of different modes of catalysis (outlined in red) that have been used to access these compounds in enantioenriched form.

In 2015 Brière et al. published a one pot-multicomponent racemic synthesis of 3-substituted-N-carbalkoxy-isoxazolidin-5-ones.<sup>9</sup> This method involved mixing an aldehyde, an N-hydroxycarbamate, and Meldrum's acid **3.12** using DABCO as a basic catalyst. Unfortunately, attempts at rendering the new methodology enantioselective proved unsuccessful (Figure 3.3).

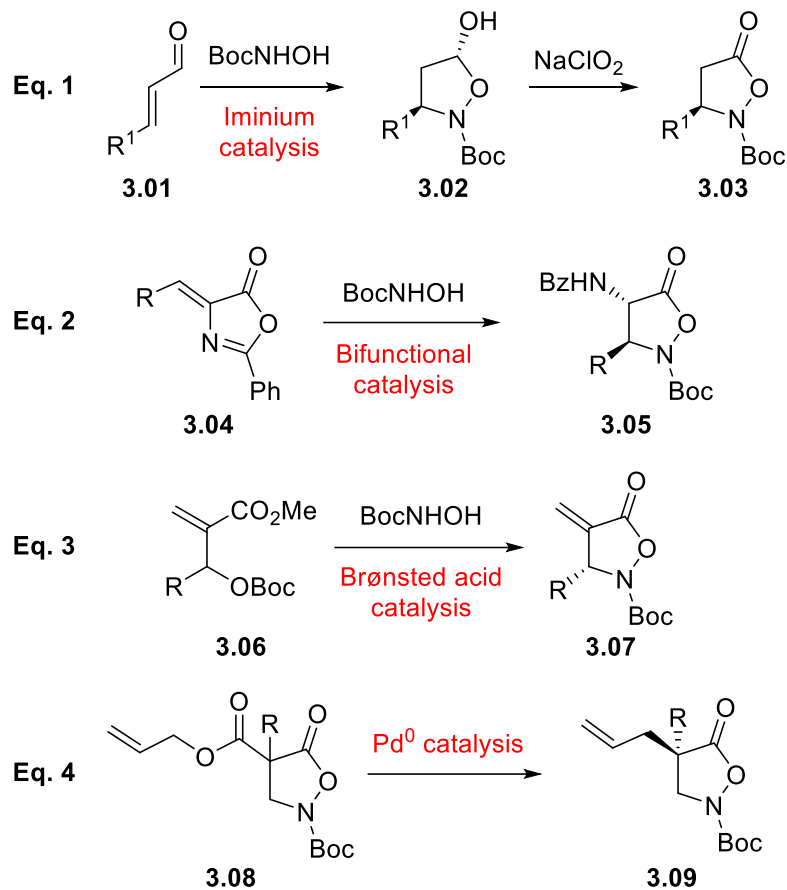
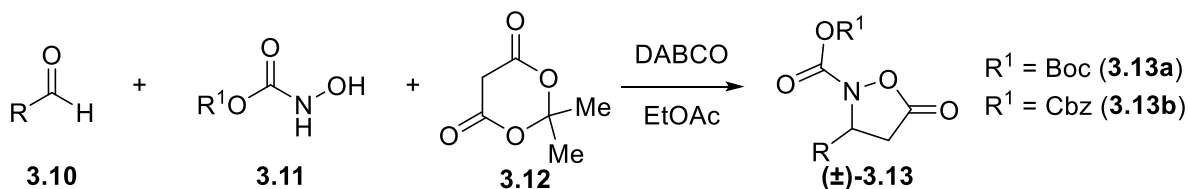


**Figure 3.2.** Asymmetric catalytic approaches to N-Boc-isoxazolidinones.

At first glance this result may be discouraging. However, the simplicity and broad substrate scope (with regard to the aldehyde) of this racemic synthesis offers an opportunity to obtain these compounds in enantioenriched form via resolution into their two enantiomers. Given the vast literature precedent for enantioselective alcoholysis of cyclic acyl donors (see Section 3.2), kinetic resolution seemed to be a viable strategy.



a) Brière's racemic synthesis



b) Attempts at an **enantioselective reaction**

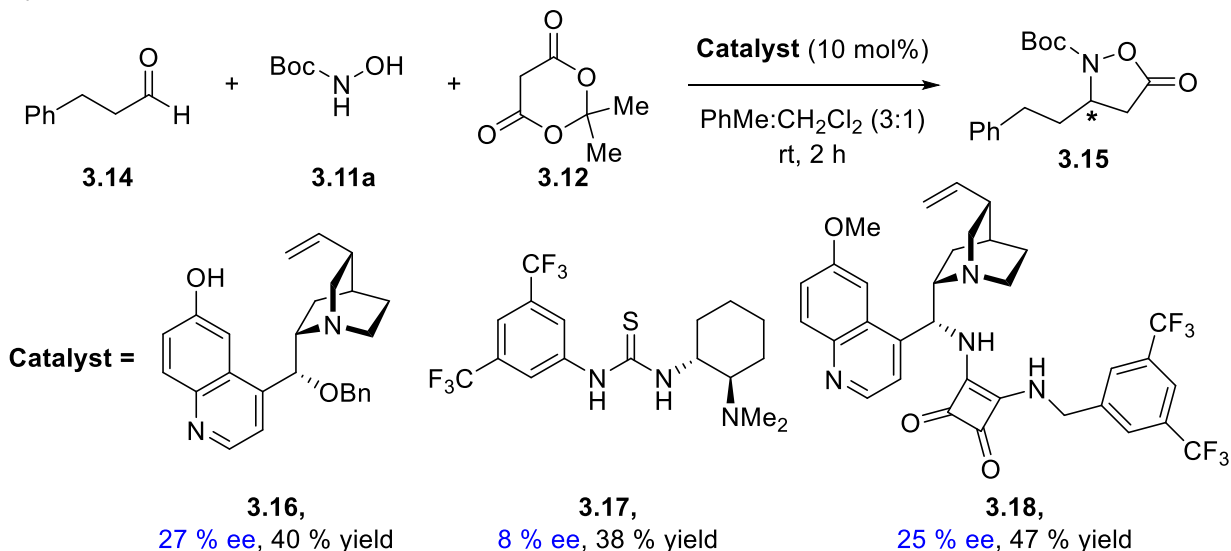


**Figure 3.3:** a) Brière's racemic, one pot-multicomponent synthesis, b) Attempts at rendering this multicomponent reaction enantioselective.<sup>9</sup>

### 3.1 Introduction to kinetic resolution

Kinetic resolution (KR) is one of many available methods in asymmetric catalysis and was discussed very briefly in section 2.2 as one approach to enantioenriched  $\alpha$ -fluoro- $\beta$ -amino acids. Further discussion on this topic has been delayed to this subchapter. In short, KR is one of the oldest means of making enantioenriched compounds from a racemic starting material and relies on both enantiomers reacting with different rates in a chemical process utilizing a chiral catalyst or reagent.<sup>10</sup> Consequently, the enantiomeric excess (*ee*) of the unreacted starting material continually rises as more product is formed. This process can be summarized with the graph and

equations outlined in Figure 3.4, where  $k_R$  (the reaction rate of the (*R*) enantiomer) is larger than  $k_S$  (the reaction rate of the (*S*) enantiomer).

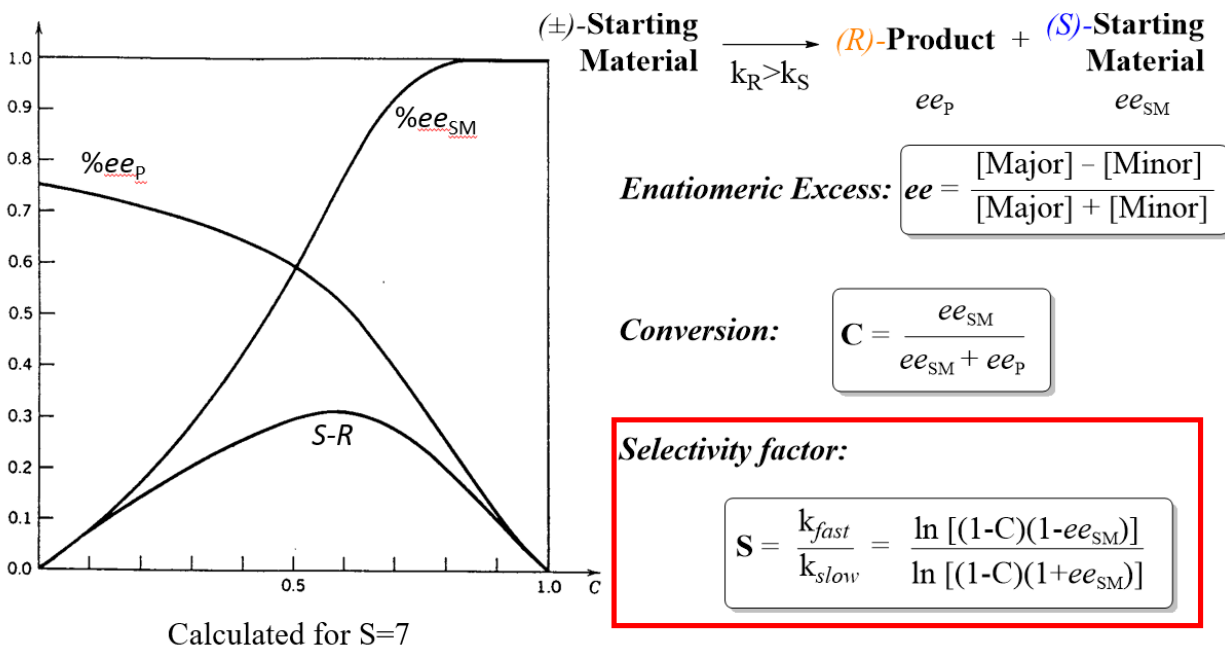


**Figure 3.4:** A graphical representation of KR and the equations used to calculate its efficacy. The maximum height of the curve “*S-R*” represents the conversion that maximizes the enantioenrichment of both starting material and product. Graphic borrowed from Kagan.<sup>10</sup>

The most important variable in determining the efficiency of a kinetic resolution is the selectivity factor<sup>10</sup>, which is the ratio of the reaction rates of the two enantiomers. Thus, when  $s=7$ , one enantiomer is reacting seven times faster than the other. As can be seen from the graph, a selectivity factor of 7 is not useful, especially considering that high levels of conversion are necessary to obtain the starting material with practically useful levels of enantioenrichment. Ideally, the selectivity factor should be as large as possible. As a general rule of thumb, a selectivity factor of 20 or greater is deemed sufficient for practical applications.<sup>11</sup> Assuming perfect selectivity then one enantiomer will react completely and leave the unreacted enantiomer with ~100% *ee* at 50% conversion. One disadvantage of KR is this maximum theoretical yield of 50%,

especially when only one enantiomer is wanted/needed. Conversely, KR is useful when both enantiomers are required.

### **3.2 Kinetic resolution, dynamic kinetic resolution, and desymmetrization of cyclic acyl donors via organocatalytic enantioselective alcoholysis**

Many cyclic compounds structurally related to isoxazolidin-5-ones have been utilized as acyl donors in organocatalytic enantioselective alcoholysis, resulting in their KR, dynamic kinetic resolution (DKR), or desymmetrization. All of these processes are mechanistically similar since they rely on the enantiofacial discrimination of the cyclic acyl donor. In 2001, Deng et al. reported an asymmetric approach to  $\alpha$ -amino acids via a cinchona alkaloid-catalyzed kinetic resolution of carbamate-protected  $\alpha$ -amino acid carboxyanhydrides **3.19** (Figure 3.5a).<sup>12</sup> Prochiral and meso cyclic anhydrides are still very commonly used as precursors in desymmetrizations, a process where chirality is introduced by removing a symmetry element within a molecule.<sup>13</sup> One illustrative example of a desymmetrization involves the cinchona alkaloid-catalyzed alcoholysis of prochiral cyclic anhydride **3.23** (Figure 3.5b).<sup>14</sup> In 2011 our group disclosed the first non-enzymatic KR of  $\beta$ -lactams. ABC-catalyzed alcoholysis delivers the  $\beta$ -amino acid derivatives in highly enantioenriched form (Figure 3.5c).<sup>15</sup> In 2005 Berkessel et. al published a DKR of azlactones via enantioselective alcoholysis using a bifunctional thiourea-amine organocatalyst (Figure 3.5d).<sup>16</sup> Only a single enantiomer of product is isolated because the azlactone can epimerize under the reaction conditions. This equilibration of the two enantiomers of a racemate is the key difference between DKR and KR. In 2010 our group published an analogous DKR via a covalent mode of catalysis using ABC-catalyzed alcoholysis (Figure 3.5d).<sup>17</sup> In 2005 Mukherjee et al. reported an organocatalytic approach to  $\beta$ -amino acid derivatives via a KR of oxazinones,

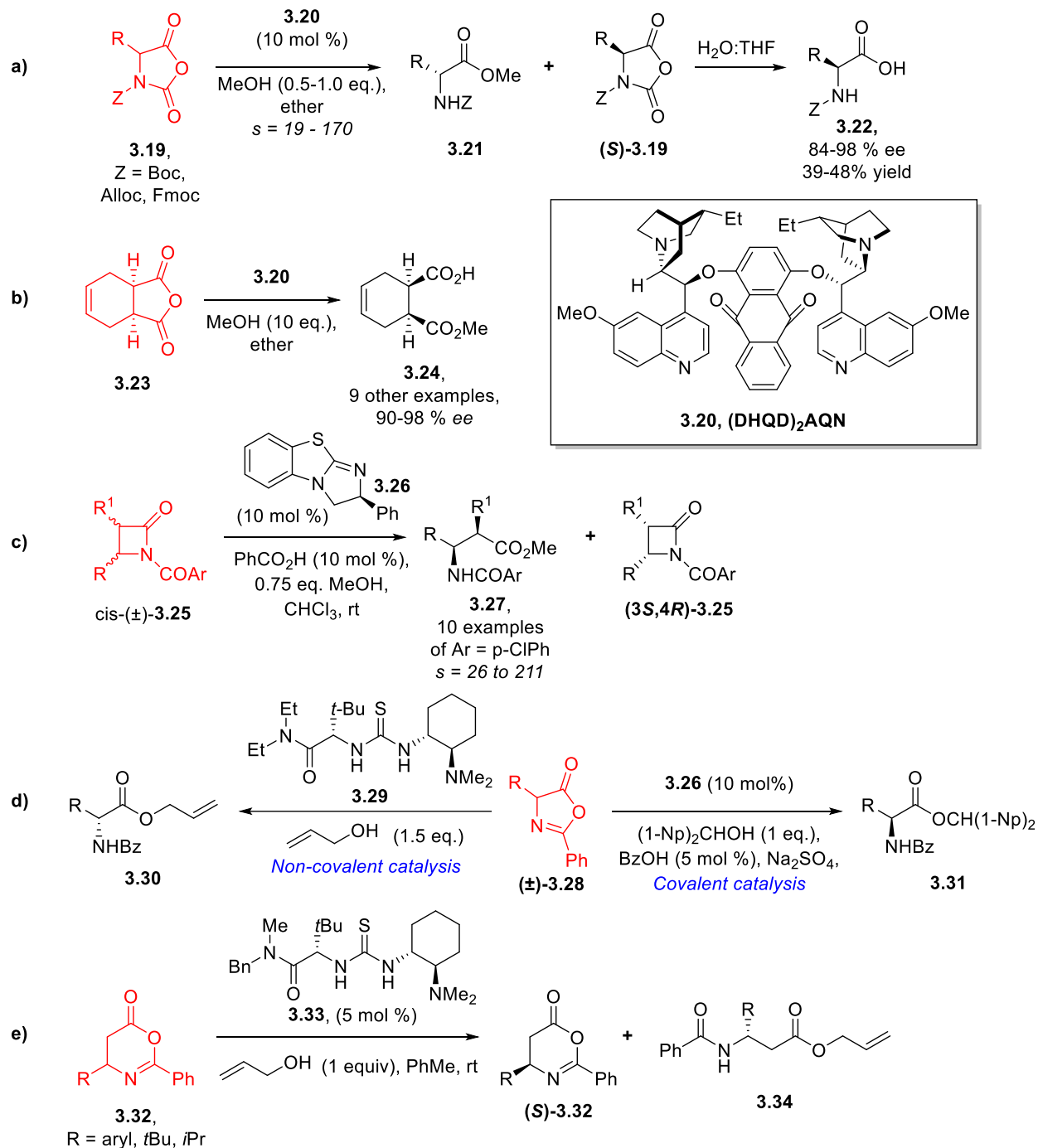


**Figure 3.5.** Examples of enantioselective alcoholysis of **cyclic acyl donors**. a) KR of  $\alpha$ -amino acid carboxyanhydrides, b) desymmetrization of prochiral cyclic anhydrides, c) KR of N-acyl- $\beta$ -lactams, d) DKR of azlactones via non-covalent and covalent modes of catalysis, e) KR of oxazinones.

one carbon homologues of azlactones (Figure 3.5e).<sup>18</sup> A bifunctional thiourea-amine organocatalyst was employed to achieve this resolution.

### 3.3 Introduction to bifunctional organocatalysis

The term bifunctional organocatalyst was used throughout section 3.2 and warrants further discussion. A bifunctional catalyst is a catalyst which complementarily activates two components of a chemical reaction due to having two moieties with separate functionalities. For almost all bifunctional catalysts, these two functional groups work synergistically to activate both the nucleophile (HOMO activation) and electrophile (LUMO activation). In fact, electrophile activation by hydrogen bonding is very common in biological enzymatic pathways, especially hydrolysis of amide bonds.<sup>19</sup> This mode of activation seen in Nature has certainly inspired modern-day chemists, especially considering that at least one hydrogen bond donor is present in virtually all notable bifunctional organocatalysts.<sup>20</sup> Of all these bifunctional organocatalysts, double hydrogen bond donor-amine organocatalysts, especially those containing thiourea/urea/squaramide and tertiary amine functional groups, have arguably received the most attention. The general structure of these catalysts is illustrated in Figure 3.6. The chiral scaffold usually consists of a naturally occurring Cinchona alkaloid or an enantiomerically pure 1,2-cyclohexanediamine, though other chiral scaffolds exist, such as Ricci's chiral thiourea with a 2-indanol scaffold.<sup>21</sup>

In 2003, Takemoto discovered that bifunctional thiourea-amine organocatalyst **3.17** (Figure 3.7) can catalyze the asymmetric Michael addition of various 1,3-dicarbonyls to nitroolefins.<sup>22</sup> This work served as a major foothold in asymmetric bifunctional organocatalysis. While catalytic asymmetric versions of this Michael reaction were known, most required metal

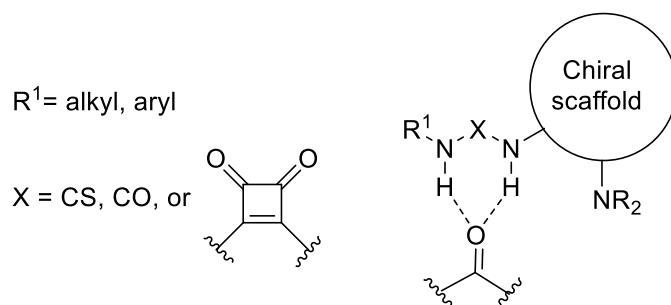


**Figure 3.6.** General structure of the most common bifunctional double hydrogen bond donor-amine organocatalysts. Catalyst is shown H-bonding to a generic carbonyl group.

catalysts or strict reaction conditions. This methodology offered a metal-free and mild approach to these synthetically useful Michael adducts. The transition state Takemoto proposed involved the nitroolefin forming hydrogen bonds to the thiourea moiety, activating the electrophile. The dimethylamino moiety, more than basic enough to deprotonate the 1,3-dicarbonyl, forms a hydrogen bond to the enolic form of the 1,3-dicarbonyl. This places the nucleophile near the nitroolefin, facilitating the Michael addition.

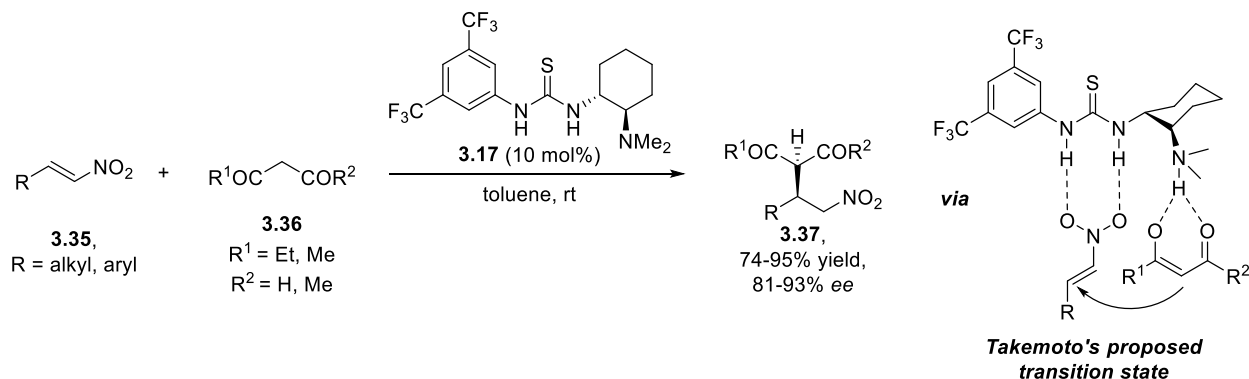
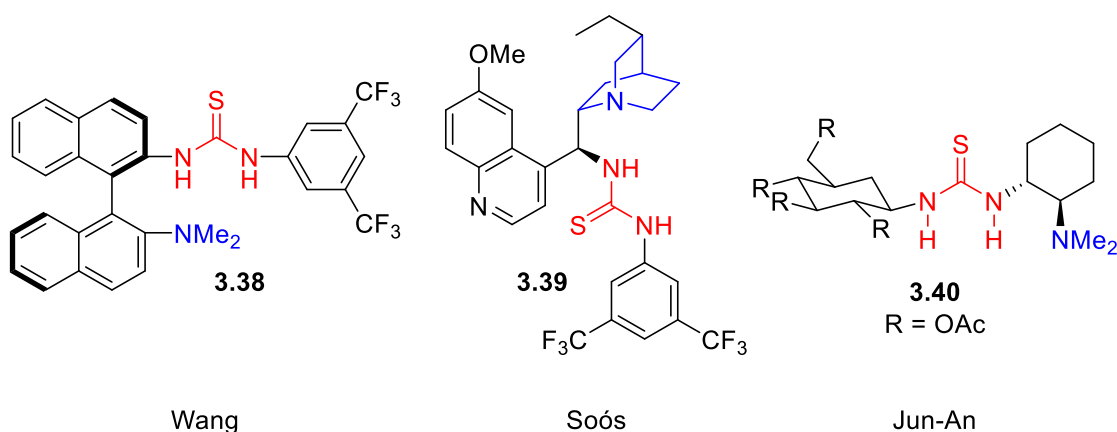


**Figure 3.7.** Asymmetric Michael addition of 1,3-dicarbonyls to nitroolefins.

Despite these synthetic advances at the time, the underlying mechanistic details were still not fully understood. In 2006, Pápai et al. conducted extensive DFT calculations to better elucidate

the dual activation mode of these bifunctional thioureas.<sup>23</sup> These calculations suggested that the actual transition state and the nature of the hydrogen bonding was most likely much more complex than initially proposed by Takemoto. However, dual activation of both substrates is undoubtedly the predominant role of the bifunctional catalyst.

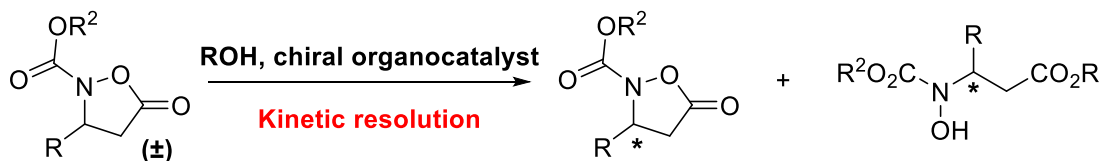
Starting in the mid-2000s, the use of thiourea-tertiary amine organocatalysts in asymmetric synthesis expanded rapidly. Novel catalyst designs and new applications by Wang,<sup>24</sup> Soós,<sup>25</sup> and Jun-An<sup>26</sup> became commonplace (Figure 3.8).



**Figure 3.8.** Novel thiourea-tertiary amine organocatalyst designs.

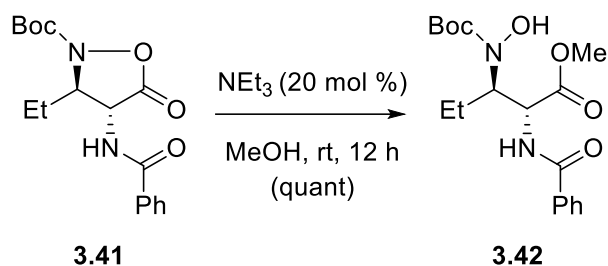
### 3.4 Initial screening of reaction conditions

With the idea of kinetic resolution, it can be easy to envision how resolution of racemic *N*-carbalkoxy-isoxazolin-5-ones can be achieved by enantioselective alcoholysis (Figure 3.9).



**Figure 3.9:** Proposed KR of *N*-carbalkoxy-isoxazolidin-5-ones.

Though this KR has never been pursued, these compounds have been known to be relatively reactive acyl donors, reacting with alcohols under mild conditions (Figure 3.10).<sup>4</sup> However, catalytic acceleration of this process has never been described in the literature for this specific class of acyl donors.

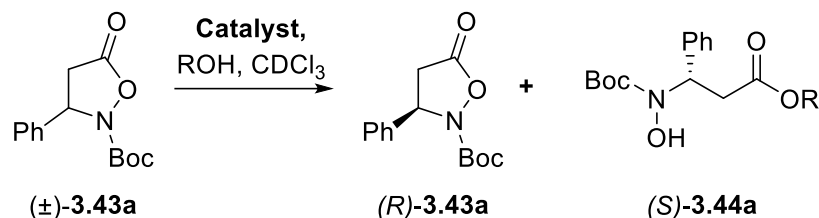


**Figure 3.10:** Ring opening of an N-Boc-isoxazolidinone with MeOH and NEt<sub>3</sub>.

Encouraged by extensive, albeit indirect, literature precedent our group started to explore the asymmetric catalytic ring opening of N-Boc-3-phenylisoxazolidin-5-one **3.43a**, our model substrate (Table 3.1).

First, we wanted to confirm whether methanolysis would occur with the test substrate in the absence of base. As expected, no racemic background reaction occurred, but rapid and quantitative ring opening was observed with addition of stoichiometric NEt<sub>3</sub> (entries 1 and 2). Next, we tested covalent modes of acyl transfer catalysis. Unfortunately, widely used acyl transfer catalysts (*R*)-BTM<sup>27</sup> **3.26** and (*R*)-H-PIP<sup>28</sup> **3.45** (see Figure 3.11) delivered hardly any asymmetric induction (entries 3 and 4). As anticipated by their relative Lewis basicities, H-PIP performed much faster than BTM. We next sought out using non-covalent modes of catalysis. Given the performance displayed by bifunctional thiourea-amine organocatalyst **3.29** in the dynamic kinetic resolution of azlactones (vide supra), we decided to test Takemoto's catalyst **3.17**.<sup>22</sup>



**Table 3.1:** Initial screening of reaction conditions.<sup>a</sup>

entry	Catalyst (mol %)	ROH (equiv)	Time (h)	% conversion	s
1	none	MeOH (10)	24	0 <sup>b</sup>	N/A
2	NEt <sub>3</sub> (100)	MeOH (10)	0.5	100 <sup>b</sup>	N/A
3	<b>3.26</b> (20)	MeOH (1)	192	45 <sup>b</sup>	1.1
4	<b>3.45</b> (20)	MeOH (1)	2.5	63 <sup>b</sup>	1.5
5	<b>3.17</b> (10)	MeOH (1)	5	53	5.2
6 <sup>c</sup>	<b>3.17</b> (10)	MeOH (1)	8	55	5.9
7 <sup>c</sup>	<b>3.17</b> (10)	BnOH (1)	16	46	16.3
8	<b>3.17</b> (10)	Ph <sub>2</sub> CHOH (1)	120	25	7.7
9	<b>3.17</b> (10)	<i>i</i> -PrOH (1)	24	<5	N/A

<sup>a</sup> General conditions: 0.1 mmol of (±)-**3.43a**, 0.1 or 1.0 mmol of ROH, 0.01 mmol of catalyst, 500 μL of CDCl<sub>3</sub>, rt. <sup>b</sup> Determined by <sup>1</sup>H NMR. <sup>c</sup> Carried out at 0 °C.

With this idea we were trying to achieve similar dual modes of activation of the alcohol and isoxazolidinone, which is structurally analogous to the azlactone. The first result was very promising, giving a five-fold increase in selectivity compared to BTM (entry 5). A very slight increase in *s* was observed at 0 °C (entry 6). When testing more sterically bulky alcohols, we discovered that benzyl alcohol further increased the selectivity factor three-fold (entry 7). Secondary alcohols like benzhydrol were very slow and gave lower selectivity factor (entry 8). Finally, isopropyl alcohol was virtually unreactive (entry 9). The difference in reactivity of benzhydrol and isopropyl alcohol is interesting and has been speculated to be the result of an approximately 100 times difference in acidity between the two secondary alcohols.

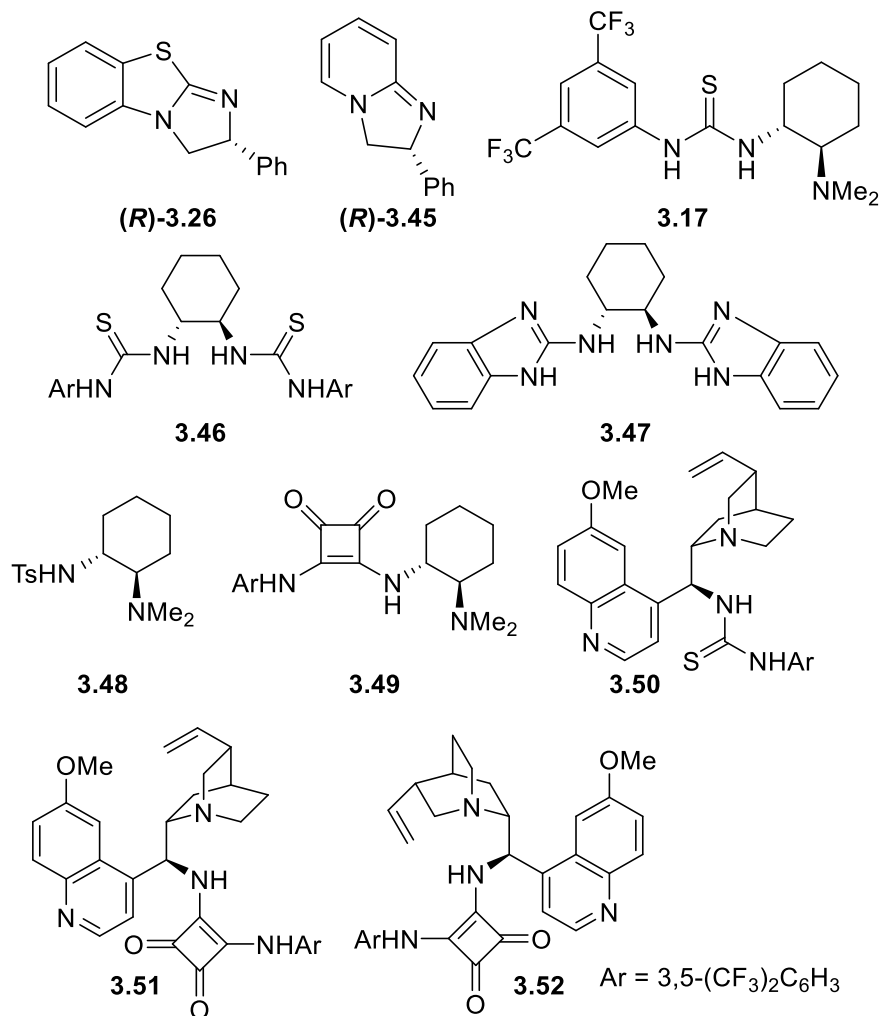


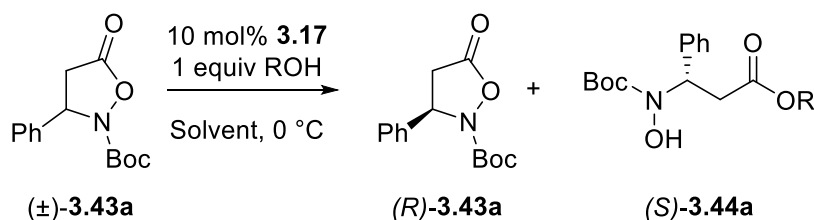
**Figure 3.11:** Catalysts used in this study.

### 3.5 Optimization of solvent and alcohol using Takemoto's catalyst

After the discovery that Takemoto's catalyst gave increased selectivity, we explored a wide variety of solvents (Table 3.2). Most solvents examined gave selectivity factors that were comparable or inferior to chloroform. Of these, the most nonpolar solvents (entries 3-5) were inferior to chloroform and more polar solvents, apart from acetonitrile, gave similar performance to chloroform (entries 6-8). Most interestingly a serendipitous discovery was made with t-amyl

alcohol which delivered the best selectivity factor up to this point (entry 9). This result was surprising considering that the hydrogen bond-donor properties of the solvent can be expected to disrupt hydrogen bonding between the catalyst and the alcohol and/or isoxazolidinone. After re-examining other alcohols, we discovered that allyl alcohol gave yet a better selectivity factor (entry 10). Methanol performed much worse, but still better than with chloroform as solvent (compare Table 3.2, entry 11 to Table 3.1, entry 6). Even better yet, benzhydrol reproducibly delivered a selectivity factor of 199 (entry 12) and demonstrates the drastic effect that solvent can have (compare to Table 3.1, entry 8). Isopropyl alcohol failed to react under these conditions (entry 13).

**Table 3.2:** Solvent study.



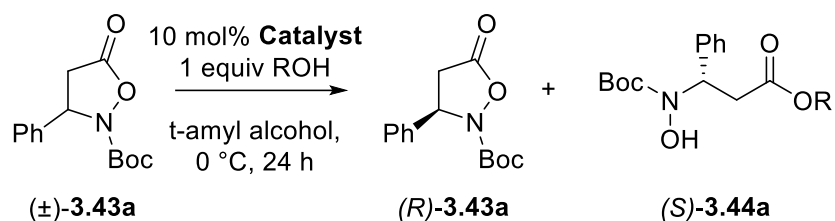
entry	solvent	ROH	Time (h)	% conversion	s
1	CHCl <sub>3</sub>	BnOH	16	46	16.3
2	CH <sub>2</sub> Cl <sub>2</sub>	BnOH	16	43	16.1
3	PhMe	BnOH	7	54	13.0
4	Cyclohexane	BnOH	16	73	6.0
5	THF	BnOH	72	25	21.0
6	EtOAc	BnOH	22	37	18.9
7	Me <sub>2</sub> CO	BnOH	23	24	19.3
8	MeCN	BnOH	23	37	7.4
9	EtCMe <sub>2</sub> OH	BnOH	22	34	25
10	EtCMe <sub>2</sub> OH	allylOH	22	36	45
11	EtCMe <sub>2</sub> OH	MeOH	22	31	14.6
12	EtCMe <sub>2</sub> OH	Ph <sub>2</sub> CHOH	22	39	199
13	EtCMe <sub>2</sub> OH	<i>i</i> -PrOH	22	0	ND

<sup>a</sup>General conditions: 0.10 mmol of (±)-**3.43a**, 0.10 mmol of ROH, 0.01 mmol of **3.17**, 500 μL of solvent.

## 3.6 Bifunctional catalyst survey

Next we explored a diverse range of bifunctional organocatalysts (Table 3.3).

**Table 3.3:** Bifunctional catalyst survey.<sup>a</sup>



entry	catalyst	ROH	% conversion	s
1	<b>3.46</b>	Ph <sub>2</sub> CHOH	0	N/A
2 <sup>b</sup>	<b>3.47</b>	Ph <sub>2</sub> CHOH	35	1.4
3	<b>3.48</b>	Ph <sub>2</sub> CHOH	0	N/A
4	<b>3.49</b>	Ph <sub>2</sub> CHOH	41	33
5 <sup>b</sup>	<b>3.50</b>	Ph <sub>2</sub> CHOH	42	94
6 <sup>b</sup>	<b>3.51</b>	Ph <sub>2</sub> CHOH	38	123
7	<b>3.52</b>	Ph <sub>2</sub> CHOH	42	419
8	<b>3.52</b>	MeOH	47	23
9	<b>3.52</b>	BnOH	47	23
10	<b>3.52</b>	allylOH	43	37

<sup>a</sup> General conditions: 0.10 mmol of (±)-**3.43a**, 0.10 mmol of ROH, 0.01 mmol of catalyst, 500 μL of t-amyl alcohol. <sup>b</sup> The absolute stereochemistry of the product is opposite of that shown.

C<sub>2</sub>-symmetrical bis-thiourea **3.46**<sup>29</sup> gave zero conversion, confirming that a basic moiety must be present in the catalyst (entry 1). Bis-benzimidazole catalyst **3.47**<sup>30</sup> gave decent conversion, but very little enantioselectivity (entry 2). Tosylamide **3.48**<sup>31</sup> was completely ineffective (entry 3). This can be a result of the sulfonamide moiety not being a strong enough hydrogen bond donor, or alternatively, that a double hydrogen bond donor in the catalyst is necessary. Squaramide analogue of Takemoto's catalyst **3.49**<sup>32</sup> gave lower selectivity than Takemoto's catalyst itself; however, this was most likely due to solubility issues in t-amyl alcohol (entry 4). Quinine-derived amino-thiourea **3.50**<sup>25</sup> and amino-squaramide **3.51**<sup>33</sup> gave comparable selectivity factors (entries 5 and 6). Interestingly, the pseudoenantiomeric quinidine-

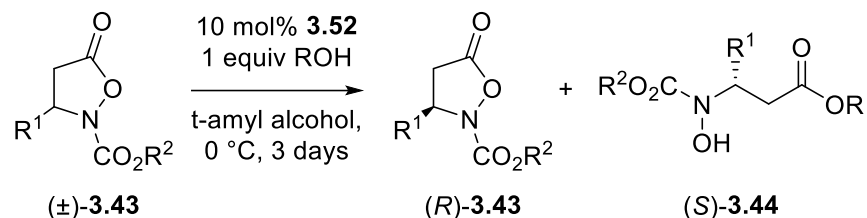
derived amino-squaramide **3.52**<sup>33</sup> gave the superior selectivity factor (entry 7). This difference in performance between these two pseudoenantiomers is surprising; however, there is extensive literature precedent for discrepancies in enantioselectivity (and often reactivity) for asymmetric reactions catalyzed by a pair of pseudoenantiomeric cinchona alkaloid-derived catalysts.<sup>34</sup> Other alcohols were inferior to benzhydrol with this new catalyst (entries 8-10).

### 3.7 Substrate scope of new methodology

Having completed the optimization studies, we next explored the substrate scope of this new methodology (Table 3.4). In some cases, the isoxazolidinone starting materials were insoluble in pure *t*-amyl alcohol, necessitating the use of chloroform/*t*-amyl alcohol mixtures, and in some cases, pure chloroform. The addition of chloroform did not effect the selectivity factor with substrate **3.43a** (compare entries 1 and 2). Substrates with variously substituted aromatic and heteroaromatic groups delivered excellent selectivity factors (entries 1-10). A styryl and primary alkyl group delivered diminished, but still practically useful levels of selectivity (entries 11-12). A secondary alkyl group decreased the reactivity (entry 13); however, less sterically demanding alcohols gave increased conversion without loss of selectivity (entries 14-15). Unfortunately, the *tert*-butyl substrate gave zero conversion with benzhydrol and barely detectable levels of conversion with allyl alcohol (entries 16-17). We also explored the effects of switching from a Boc group to a Cbz group. Surprisingly, this substrate was completely unreactive with benzhydrol (entry 18). Thankfully, just as in the isopropyl substituent case, less sterically hindered alcohols gave increased conversion and practically useful selectivities (entries 19-21). The reaction scale was also increased 10-fold and delivered comparable selectivity factors to the 0.1 mmol scale (compare entries 6 and 22). Finally, we demonstrated that Takemoto's catalyst **3.17** gave practically useful selectivity factors with a 2-naphthyl and isobutyl group (entries 23-24). Even

though the selectivity factors are lower than that obtained with catalyst **3.52**, the commercial availability of Takemoto's catalyst makes it an attractive alternative.

**Table 3.4:** Substrate scope.<sup>a</sup>



entry	R <sup>1</sup>	R <sup>2</sup>	ROH	% conversion	s
1	Ph	<i>t</i> -Bu	Ph <sub>2</sub> CHOH	45	361
2 <sup>b</sup>	Ph	<i>t</i> -Bu	Ph <sub>2</sub> CHOH	45	487
3 <sup>b</sup>	4-ClC <sub>6</sub> H <sub>4</sub>	<i>t</i> -Bu	Ph <sub>2</sub> CHOH	37	344
4 <sup>b</sup>	4-MeOC <sub>6</sub> H <sub>4</sub>	<i>t</i> -Bu	Ph <sub>2</sub> CHOH	41	301
5 <sup>c</sup>	4-NO <sub>2</sub> Ph	<i>t</i> -Bu	Ph <sub>2</sub> CHOH	31	127
6	2-ClC <sub>6</sub> H <sub>4</sub>	<i>t</i> -Bu	Ph <sub>2</sub> CHOH	44	107
7	3-MeOC <sub>6</sub> H <sub>4</sub>	<i>t</i> -Bu	Ph <sub>2</sub> CHOH	45	430
8 <sup>d</sup>	1-naphthyl	<i>t</i> -Bu	Ph <sub>2</sub> CHOH	29	171
9 <sup>d</sup>	2-naphthyl	<i>t</i> -Bu	Ph <sub>2</sub> CHOH	42	334
10	2-thienyl	<i>t</i> -Bu	Ph <sub>2</sub> CHOH	48	352
11	styryl	<i>t</i> -Bu	Ph <sub>2</sub> CHOH	50	80
12	isobutyl	<i>t</i> -Bu	Ph <sub>2</sub> CHOH	40	67
13	isopropyl	<i>t</i> -Bu	Ph <sub>2</sub> CHOH	24	151
14	isopropyl	<i>t</i> -Bu	BnOH	35	144
15	isopropyl	<i>t</i> -Bu	allylOH	37	92
16	<i>tert</i> -butyl	<i>t</i> -Bu	Ph <sub>2</sub> CHOH	N/A	N/A
17	<i>tert</i> -butyl	<i>t</i> -Bu	allylOH	<5%	N/A
18 <sup>c</sup>	Ph	Bn	Ph <sub>2</sub> CHOH	N/A	N/A
19 <sup>c</sup>	Ph	Bn	MeOH	54	27
20 <sup>c</sup>	Ph	Bn	BnOH	50	40
21 <sup>c</sup>	Ph	Bn	allylOH	49	50
22 <sup>e</sup>	2-ClC <sub>6</sub> H <sub>4</sub>	<i>t</i> -Bu	Ph <sub>2</sub> CHOH	44	80
23 <sup>d,f</sup>	2-naphthyl	<i>t</i> -Bu	Ph <sub>2</sub> CHOH	41	118
24 <sup>f</sup>	isobutyl	<i>t</i> -Bu	Ph <sub>2</sub> CHOH	27	21

<sup>a</sup> General conditions: 0.10 mmol of substrate, 0.10 mmol of alcohol, 0.01 mmol of **3.52**, 500  $\mu$ L *tert*-amyl alcohol. <sup>b</sup> A 4:1 *tert*-amyl alcohol/CHCl<sub>3</sub> mixture was used as the solvent. <sup>c</sup> CHCl<sub>3</sub> was used as the solvent. <sup>d</sup> A 3:2 *tert*-amyl alcohol/CHCl<sub>3</sub> mixture was used as the solvent. <sup>e</sup> Performed on a 1.0 mmol of substrate scale. <sup>f</sup> Catalyst **3.17** was used.

All of the resulting ester products underwent transesterification to the methyl ester, a necessary task to analyze these compounds by HPLC (see Appendix A.2). These esters were stable upon long term exposure at 0 °C, even after several months.

### 3.8 Reversible ring closure of *t*-Bu derivative **3.44m-Me**

After obtaining the result with *t*-butyl substrate **3.43m**, we wanted to deduce a logical explanation as to why the KR fails in this one case. It was observed that branching at the  $\alpha$ -position of the alkyl substituent (i.e. the isopropyl group) greatly diminished the reactivity with benzhydrol. While two substituents at this position would be expected to further decrease the reactivity, it was still not clear why <5% conversion was observed in one case and 37% was observed in the other (compare Table 3.4, entry 17 to entry 15). While quantitative methanolysis of **3.43m** occurs under mild conditions, it was quickly discovered that the methyl ester will spontaneously convert back into the ring-closed isoxazolidinone starting material (Figure 3.12). By observing this ring closure by <sup>1</sup>H NMR in CDCl<sub>3</sub>, after 64 hours, 64% of the product had converted back into starting material. Heating this mixture led to quantitative ring closure after a couple of hours.

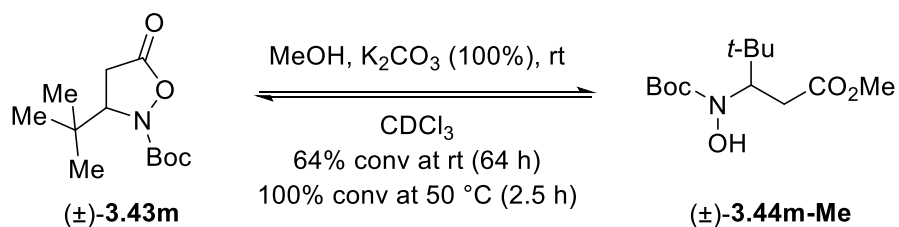


**Figure 3.12:** Reversible ring-closure of *t*-butyl substrate **3.43m**.

According to Baldwin's rules, this 5-exo-trig cyclization is kinetically favorable.<sup>35</sup> However, it should be noted that this was the only substrate that exhibited this behavior. Several other freshly prepared methyl and benzhydryl esters were left in pure chloroform for three days at

rt, and not a single one converted back to the isoxazolidinone. Clearly, this idiosyncratic behavior requires an alternative explanation. Instead, a strong Thorpe-Ingold effect was proposed (see Appendix A.1).<sup>36</sup> It is known that substituents, especially a bulky *t*-butyl group, limit the flexibility of long chains, resulting in restricted rotation relative to the unsubstituted chain. Due to this limited flexibility, there is a much lower entropic penalty for cyclization ( $\Delta S^\ddagger$  is less negative). Consequently,  $\Delta G^\ddagger$  is more negative and the ring forms faster. Under thermodynamic control, as is the case with the long reaction times and heating employed, it is not surprising to detect quantitative ring closure in this specific case.

### 3.9 Additional transformations

Our group demonstrated that the starting materials and products obtained with this KR can partake in useful synthetic transformations. The entire purpose of this project was to demonstrate how these enantioenriched isoxazolidinones can serve as precursors to  $\beta$ -amino acids. Thus, enantioenriched (*R*)-**3.43a** underwent quantitative hydrogenolysis to yield Boc-protected  $\beta$ -phenylalanine (Figure 3.13).<sup>3a</sup>

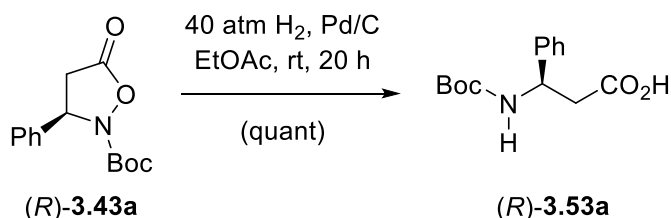


**Figure 3.13:** Quantitative N-O bond cleavage to yield an enantioenriched  $\beta$ -amino acid.

Additionally, we showed that the benzhydryl esters, after being transesterified to the methyl esters, undergo cyclization to the isoxazolidinone with complete retention of enantioenrichment (Figure 3.14).<sup>5</sup> This is a desirable transformation for a couple of reasons. First,



in cases where the isoxazolidinone is not at satisfactory levels of enantioenrichment after the KR, the reacted starting material can be recycled and put forward through another resolution. Furthermore, in cases where conversion is less than optimal (e.g. Table 3.4, entry 8) for a KR, the unreacted starting material may not be as enantioenriched as the reacted product. Thus, in these few cases, the enantioenriched isoxazolidinone can be obtained from the reacted enantiomer at the expense of yield.

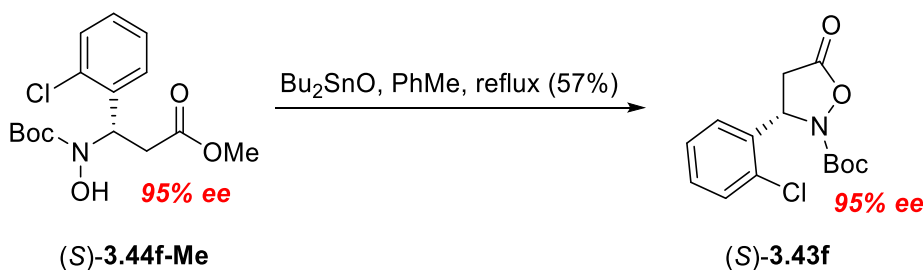


**Figure 3.14:** Recycling of reacted enantiomer.

### 3.10 Conclusions and future directions

This work provides a complementary approach to enantioenriched isoxazolidinones, important precursors to  $\beta$ -amino acids. One practical advantage of this work is that the resolution can be used to further enhance levels of enantiomeric enrichment, even if the isoxazolidinones were obtained from alternative asymmetric methodologies. Though the levels of conversion were less than optimal in certain cases, we demonstrated the efficacy of a two-step transesterification-cyclization procedure that delivered the isoxazolidinone with complete retention of *ee* and assured that the reacted enantiomer does not go to waste. Furthermore, we demonstrated for the first time that N-carbalkoxy-isoxazolidinones are well-tolerated acyl donors amenable to asymmetric acyl transfer catalysis. In addition to these 3-substituted isoxazolidinones, it would be compelling to explore additional substitution patterns such as 4-substituted and 3,4-disubstituted analogues.

While a vast literature precedent indicates the usefulness of acyl donors in asymmetric catalysis, especially in kinetic resolution, this work suggests that there may be other classes of compounds that are worth exploring in kinetic resolutions (Figure 3.15). For example, O-acylated derivatives of N-hydroxysuccinimides **3.54** are expected to be reactive acyl donors. They may even serve as precursors to enantioenriched  $\alpha$ -amino acid derivatives (e.g.  $R^1 = \text{NH}(\text{Boc})$ ). Isoxazolidine-3,5-diones **3.55** and 1,2-oxazinane-3,6-diones **3.56** may also be viable substrates for enantioselective alcoholysis. All these different classes of compounds can be explored with a wide variety of catalysts, investigating both covalent and non-covalent modes (e.g. monofunctional Lewis basic catalysts, bifunctional catalysts, chiral phosphoric acid catalysts, etc.).

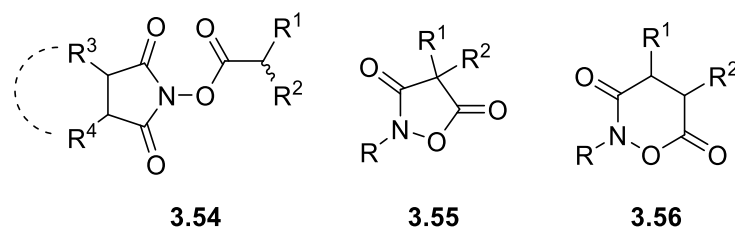


**Figure 3.15.** Other acyl donors that may be amenable to KR via enantioselective alcoholysis.

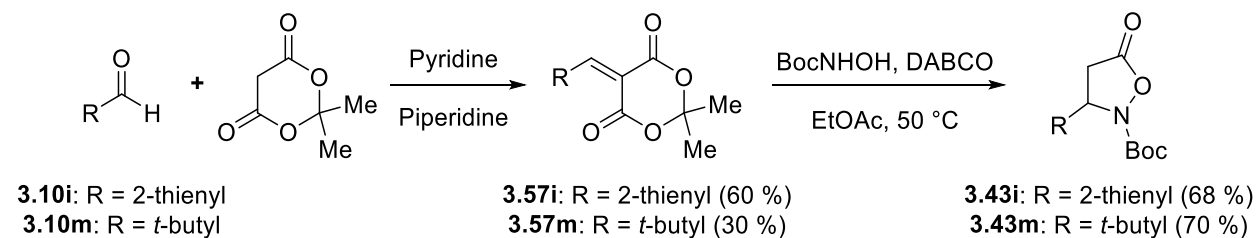
## 3.11 Experimental

All reagents were obtained commercially and used as received unless specified otherwise. Catalysts **3.26**, and **3.45-3.52** were prepared as described in the literature.<sup>25,27,28,29,30,31,32,33</sup> Chloroform used as reaction medium was freshly distilled from calcium hydride. Triethylamine was freshly distilled from potassium hydroxide pellets. Reactions that required heating were carried out in an electrically heated mineral oil bath. Solvents used for chromatography were ACS or HPLC grade. Sorbent Technologies XHL silica gel plates (glass-backed, 250  $\mu\text{m}$ ) were used for TLC analyses. Flash column chromatography was performed over Sorbent Technologies silica gel

(40–63  $\mu\text{m}$ ). HPLC analyses were performed on a Shimadzu LC system using Chiralcel OD-H, Chiralpak AS-H and Chiralpak AD-H analytical chiral stationary phase columns ( $4.6 \times 250$  mm, Chiral Technologies, Inc.) with UV detectors at 254 nm and 204 nm with a flow rate of 1.0 mL/min.  $^1\text{H}$  and  $^{13}\text{C}$  NMR spectra were recorded on Mercury 300 MHz and DD2 500 MHz Agilent spectrometers. The chemical shifts are reported as  $\delta$  values (ppm) relative to TMS using a residual  $\text{CHCl}_3$  peak (7.26 ppm for  $^1\text{H}$  NMR, 77.16 ppm for  $^{13}\text{C}$  NMR) or  $(\text{CH}_3)_2\text{CO}$  (206.26 ppm for  $^{13}\text{C}$  NMR) peak as the reference. Melting points were measured on a Stuart SMP10 melting point apparatus. High resolution mass spectral analyses were performed at Washington University MS Center on a Bruker MaXis QTOF mass spectrometer using electrospray ionization (ESI). Infrared spectra were recorded on a Bruker Alpha Platinum-ATR. Optical rotations were determined on a Rudolph Autopol III polarimeter.

### 3.11.1 Synthesis of new isoxazolidinones

Most isoxazolidinone substrates used in this study were known compounds synthesized according to the published procedure.<sup>9</sup> Isoxazolidinones **3.43e-3.43h**, which have not been previously reported, were synthesized in one step following the same general procedure. Compounds **3.43i** and **3.43m**, which could not be prepared in this manner, were synthesized via the two-step modification shown below.



**Intermediate 3.57i:** A solution of 2-thiophenecarboxaldehyde **3.10i** (234  $\mu\text{L}$ , 2.5 mmol, 1.0 equiv) and Meldrum's acid (360 mg, 2.5 mmol, 1.0 equiv) in 1 mL of pyridine stirring at rt was treated

with one drop of piperidine. After stirring for 1 h, the mixture was quenched by slow addition of 3M aq. HCl until a solid started to form and thicken the reaction mixture. This solid was filtered, washed with copious amounts of water and left to air dry. The product was isolated as a pale orange powder (360 mg, 60% yield). The spectroscopic data matched those reported in the literature.<sup>37</sup>

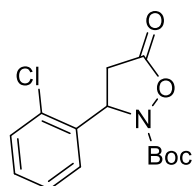
**Isoxazolidinone 3.43i:** A solution of **3.57i** (238 mg, 1.00 mmol, 1 equiv), N-Boc-hydroxylamine (133 mg, 1.00 mmol, 1 equiv) and DABCO (11 mg, 0.10 mmol, 0.1 equiv) in 4 mL of EtOAc was heated at 50 °C for 6 h, at which time TLC (30% EtOAc/hexanes) indicated near complete consumption of the starting material. The reaction mixture was diluted with 10 mL of EtOAc and 10 mL of 10% aq. Na<sub>2</sub>CO<sub>3</sub>. The aqueous layer was further extracted with CH<sub>2</sub>Cl<sub>2</sub> (×2). The organic layer was dried with Na<sub>2</sub>SO<sub>4</sub> and concentrated in vacuo. The product was isolated as a clear, colorless oil (183 mg, 68% yield) after chromatography (5→30% EtOAc/hexane).

**Intermediate 3.57m:** A solution of pivaldehyde **3.10m** (1.0 mL, 9.2 mmol, 1.0 equiv) and Meldrum's acid (1.33 g, 9.2 mmol, 1.0 equiv) in 7.3 mL of pyridine stirring at rt was treated with two drops of piperidine. After stirring at rt overnight, the mixture was diluted with 30 mL of water followed by 10 mL of 3M HCl. The aqueous layer was extracted with CH<sub>2</sub>Cl<sub>2</sub> (×3). The combined organic phase was dried with Na<sub>2</sub>SO<sub>4</sub> and concentrated in vacuo. The crude mixture was subjected to column chromatography (5→20% EtOAc/hexanes) to yield the product as a white powder (580 mg, 30% yield). The spectroscopic data are in accordance with the literature.<sup>38</sup>

**Isoxazolidinone 3.43m:** A solution of **3.57m** (340 mg, 1.60 mmol, 1 equiv), N-Boc-hydroxylamine (320 mg, 2.40 mmol, 1.5 equiv) and DABCO (18 mg, 0.16 mmol, 0.1 equiv) in 6.4 mL of EtOAc was heated at 50 °C for 18 h, at which time TLC (20% EtOAc/hexanes) indicated near complete consumption of the starting material. The reaction mixture was diluted with 10 mL of EtOAc and 10 mL of 10% aq. Na<sub>2</sub>CO<sub>3</sub>. The aqueous layer was further extracted with CH<sub>2</sub>Cl<sub>2</sub>

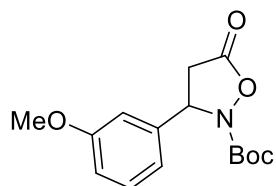
(×2). The organic layer was dried with Na<sub>2</sub>SO<sub>4</sub> and concentrated in vacuo. The product was isolated as a clear, colorless oil (272 mg, 70% yield) after chromatography (5→20% EtOAc/hexane).

**tert-butyl 3-(2-chlorophenyl)-5-oxoisoxazolidine-2-carboxylate (3.43f).**



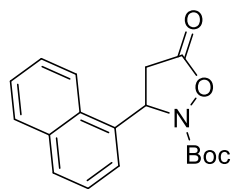
Isolated as a clear, colorless oil which solidified into a colorless, crystalline solid at 0 °C (50% yield) after chromatography (5→20% EtOAc/hexanes). <sup>1</sup>H NMR (500 MHz, CDCl<sub>3</sub>) δ 7.57-7.53 (m, 1H), 7.42-7.38 (m, 1H), 7.35-7.27 (m, 2H), 5.93 (dd, J = 9.5 Hz, 3.5 Hz, 1H), 3.42 (dd, J = 18 Hz, 9.5 Hz, 1H), 2.75 (dd, J = 18 Hz, 3.5 Hz, 1H), 1.49 (s, 9H). <sup>13</sup>C{<sup>1</sup>H} NMR (125 MHz, CDCl<sub>3</sub>): δ 171.9, 155.3, 136.6, 131.8, 130.1, 129.8, 127.7, 126.9, 84.7, 60.7, 36.7, 28.1; IR (cm<sup>-1</sup>): 2982, 1789, 1721, 1347, 1146, 759; HRMS (ESI-TOF) m/z: [M+H]<sup>+</sup> calcd for C<sub>14</sub>H<sub>16</sub>ClNO<sub>4</sub>, 298.0841; found, 298.0845. mp: 53-56 °C. HPLC: (5 % isopropanol/hexanes, AD-H): Minor enantiomer: 7.1 min; Major enantiomer: 23.4 min (77% ee, Table 3.8, entry 6). [α]<sub>D</sub><sup>25</sup> = +48° (c=0.533, CHCl<sub>3</sub>).

**tert-butyl 3-(3-methoxyphenyl)-5-oxoisoxazolidine-2-carboxylate (3.43e).**



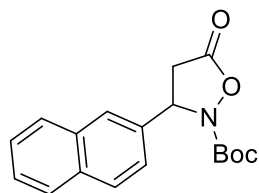
Isolated as a light yellow oil (65% yield) after chromatography (5→20% EtOAc/hexane). <sup>1</sup>H NMR (500 MHz, CDCl<sub>3</sub>) δ 7.32-7.27 (m, 1H), 6.94-6.85 (m, 3H), 5.51 (dd, J = 9.5 Hz, 4 Hz, 1H), 3.81 (s, 3H), 3.32 (dd, J = 18 Hz, 9.5 Hz, 1H), 2.84 (dd, J = 18 Hz, 4 Hz, 1H), 1.46 (s, 9H). <sup>13</sup>C{<sup>1</sup>H} NMR (125 MHz, CDCl<sub>3</sub>): δ 171.8, 160.2, 155.3, 140.6, 130.3, 117.9, 113.9, 111.5, 84.3, 63.0, 55.4, 37.6, 28.1; IR (cm<sup>-1</sup>): 2974, 2938, 1803, 1720, 1143; HRMS (ESI-TOF) m/z: [M+Na]<sup>+</sup> calcd for C<sub>15</sub>H<sub>19</sub>NO<sub>5</sub>, 316.1155; found, 316.1172. HPLC: (5 % isopropanol/hexanes, AD-H): Major enantiomer: 13.6 min; Minor enantiomer: 22.1 min; (81% ee, Table 3.8, entry 8). [α]<sub>D</sub><sup>25</sup> = +30° (c=0.533, CHCl<sub>3</sub>).

**tert-butyl 3-(naphthalen-1-yl)-5-oxoisoxazolidine-2-carboxylate (3.43g).**



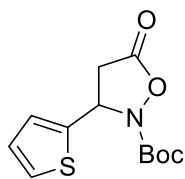
Isolated as a clear, colorless oil which solidified into a white powder at 0 °C (30% yield) after chromatography (5→20% EtOAc/hexane). <sup>1</sup>H NMR (500 MHz, CDCl<sub>3</sub>) δ 7.94-7.90 (m, 1H), 7.88-7.83 (m, 2H), 7.69-7.65 (m, 1H), 7.60-7.47 (m, 3H), 6.37 (dd, J = 9.5 Hz, 3 Hz, 1H), 3.52 (dd, J = 17.5 Hz, 9.5 Hz, 1H), 2.88 (dd, J = 17.5 Hz, 3 Hz, 1H), 1.51 (s, 9H). <sup>13</sup>C{<sup>1</sup>H} NMR (125 MHz, CDCl<sub>3</sub>): δ 172.5, 155.8, 134.1, 133.8, 129.6, 129.4, 129.2, 126.9, 126.1, 125.6, 123.1, 122.3, 84.6, 60.4, 37.0, 28.1; IR (cm<sup>-1</sup>): 2983, 1805, 1720, 1337, 1125; HRMS (ESI-TOF) m/z: [M+H]<sup>+</sup> calcd for C<sub>18</sub>H<sub>19</sub>NO<sub>4</sub>, 314.1387; found, 314.1391. mp: 111-113 °C. [α]<sub>D</sub><sup>25</sup> = +30° (c=1.067, CHCl<sub>3</sub>). (40% ee, Table 3.8, entry 9, measured by HPLC as the corresponding methyl ester).

**tert-butyl 3-(naphthalen-2-yl)-5-oxoisoxazolidine-2-carboxylate (3.43h).**



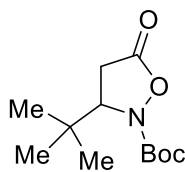
Isolated as a white powder (42% yield) after chromatography (5→20% EtOAc/hexane). <sup>1</sup>H NMR (500 MHz, CDCl<sub>3</sub>) δ 7.90-7.82 (m, 4H), 7.54-7.48 (m, 2H), 7.45-7.41 (m, 1H), 5.71 (dd, J = 9 Hz, 4.5 Hz, 1H), 3.40 (dd, J = 18 Hz, 9 Hz, 1H), 2.94 (dd, J = 18 Hz, 4.5 Hz, 1H), 1.46 (s, 9H). <sup>13</sup>C{<sup>1</sup>H} NMR (125 MHz, CDCl<sub>3</sub>): δ 171.8, 155.5, 136.1, 133.3, 133.2, 129.4, 128.2, 127.8, 126.8, 126.6, 125.0, 123.3, 84.4, 63.2, 37.5, 28.1; IR (cm<sup>-1</sup>): 2971, 1791, 1732, 1148; HRMS (ESI-TOF) m/z: [M+Na]<sup>+</sup> calcd for C<sub>18</sub>H<sub>19</sub>NO<sub>4</sub>Na, 336.1206; found, 336.1217. mp: 133-134 °C. [α]<sub>D</sub><sup>25</sup> = +21° (c=0.733, CHCl<sub>3</sub>) (73% ee, Table 3.8, entry 10, measured by HPLC as the corresponding methyl ester).

**tert-butyl 5-oxo-3-(thiophen-2-yl)isoxazolidine-2-carboxylate (3.43i).**



Isolated as a clear, colorless oil.  $^1\text{H}$  NMR (500 MHz,  $\text{CDCl}_3$ )  $\delta$  7.30 (dd,  $J = 5.3$  Hz, 1.5 Hz, 1H), 7.08-7.06 (m, 1H), 6.99 (dd,  $J = 5.3$  Hz, 3.8 Hz, 1H), 5.80 (dd,  $J = 9$  Hz, 3.5 Hz, 1H), 3.32 (dd,  $J = 18$  Hz, 9 Hz, 1H), 2.95 (dd,  $J = 18$  Hz, 3.5 Hz, 1H), 1.48 (s, 9H).  $^{13}\text{C}\{^1\text{H}\}$  NMR (125 MHz,  $\text{CDCl}_3$ ):  $\delta$  171.6, 154.9, 141.4, 127.2, 125.9, 125.3, 84.6, 59.3, 37.5, 28.0; IR ( $\text{cm}^{-1}$ ): 2980, 1804, 1718, 1142, 705; HRMS (ESI-TOF)  $m/z$ :  $[\text{M}+\text{H}]^+$  calcd for  $\text{C}_{12}\text{H}_{15}\text{NO}_4\text{S}$ , 270.0795; found, 270.0796.  $[\alpha]_D^{25} = +28^\circ$  ( $c=0.200$ ,  $\text{CHCl}_3$ ) for (*R*)- enantiomer (92% ee, Table 3.8, entry 11, measured by HPLC as the corresponding methyl ester).

**tert-butyl 3-(tert-butyl)-5-oxoisoxazolidine-2-carboxylate (3.43m).**



Isolated as a clear, colorless oil.  $^1\text{H}$  NMR (500 MHz,  $\text{CDCl}_3$ )  $\delta$  4.29 (dd,  $J = 10$  Hz, 1.5 Hz, 1H), 2.88 (dd,  $J = 18$  Hz, 10 Hz, 1H), 2.59 (dd,  $J = 18$  Hz, 1.5 Hz, 1H), 1.52 (s, 9H), 0.95 (s, 9H).  $^{13}\text{C}\{^1\text{H}\}$  NMR (125 MHz,  $\text{CDCl}_3$ ):  $\delta$  174.1, 156.8, 84.0, 68.2, 34.8, 29.9, 28.2, 25.4; IR ( $\text{cm}^{-1}$ ): 2968, 2874, 1801, 1742, 1716, 1369, 848; HRMS (ESI-TOF)  $m/z$ :  $[\text{M}+\text{Na}]^+$  calcd for  $\text{C}_{12}\text{H}_{21}\text{NO}_4\text{Na}$ , 266.1363; found, 266.1379.

**Note:** Melting points were determined using racemic samples. HPLC analysis of ester products required prior conversion to the corresponding methyl esters (see Section 3.12.1) or isoxazolidinones (see Section 3.12.2), as indicated.

### 3.11.2 Kinetic resolution experiments: Initial survey of reaction conditions

**Typical procedure:** Unless indicated otherwise, each reaction mixture was prepared by mixing aliquots of the following solutions in an NMR tube: (a) 0.500 M solution of ( $\pm$ )-**3.43a** in  $\text{CDCl}_3$

(200  $\mu\text{L}$ , 0.100 mmol, 1 equiv), (b) 1.00 M solution of the alcohol indicated in  $\text{CDCl}_3$  (100  $\mu\text{L}$ , 0.100 mmol, 1 equiv), (c) 0.100 M solution of Takemoto's catalyst **3.17** (100  $\mu\text{L}$ , 0.0100 mmol, 0.1 equiv). The mixture was brought up to 500  $\mu\text{L}$  total volume with  $\text{CDCl}_3$  (final concentration of the substrate is 0.2 M), the tube capped, sealed off with Parafilm, and kept in an ice bath for the specified amount of time, except to monitor the reaction progress by  $^1\text{H}$  NMR. Deviations from this protocol (nature of catalyst and catalyst loading, amount of alcohol, reaction temperature) are noted in Table 3.1. The reaction mixture was then diluted with 10 mL of  $\text{CH}_2\text{Cl}_2$  and quenched with 5 mL of saturated aqueous ammonium chloride. The aqueous layer was extracted twice with  $\text{CH}_2\text{Cl}_2$ . The combined organic layers were dried with  $\text{Na}_2\text{SO}_4$  and concentrated by rotary evaporation. The crude mixture was pre-adsorbed on silica gel and eluted with 5-30% EtOAc in toluene to separate the ester product from the unreacted isoxazolidinone. The methyl ester (*S*)-**3.44a-Me** and the unreacted starting material (*R*)-**3.43a** were analyzed directly by chiral stationary phase HPLC to determine their enantiomeric excess. Other esters were converted into the methyl ester (see Section 3.12.1) prior to HPLC analysis. When necessary, the unreacted starting material was also converted into the methyl ester to facilitate its analysis. Calculations of conversion ( $C_{\text{HPLC}}$ ) and selectivity factor (*s*) were performed using Kagan's equations<sup>10</sup>:

$$\% C_{\text{HPLC}} = [\text{ee}_{\text{SM}}/(\text{ee}_{\text{SM}}+\text{ee}_{\text{PR}})]\times 100\%$$

$$\text{Selectivity factor } s = \ln[(1-C)(1-\text{ee}_{\text{SM}})]/\ln[(1-C)(1+\text{ee}_{\text{SM}})].$$

In case of racemic or poorly enantioselective reactions (entries 1-4), conversions were estimated from the  $^1\text{H}$  NMR spectra of crude reaction mixtures.



**Table 3.5.** Initial survey of reaction conditions. (corresponds to Table 3.1, section 3.4)

entry	Catalyst (mol %)	ROH (equiv)	Time (h)	Temp, °C	%eesM	%eePR	%CHPLC	S
1	none	MeOH (10)	24	23	N/A	N/A	0 <sup>a</sup>	N/A
2	NEt <sub>3</sub> (100)	MeOH (10)	0.5	23	N/A	N/A	100 <sup>a</sup>	N/A
3	<b>3.26</b> (20)	MeOH (1)	192	23	5.44	2.01	45 <sup>a</sup>	1.1
4	<b>3.45</b> (20)	MeOH (1)	2.5	23	24.0	9.5	62 <sup>a</sup>	1.5
5	<b>3.17</b> (10)	MeOH (1)	5	23	56.4	50.7	52.7	5.2
6	<b>3.17</b> (10)	MeOH (1)	8	0	64.2	51.6	55.4	5.9
7	<b>3.17</b> (10)	BnOH (1)	16	0	58.9	80.0	42.4	16
8	<b>3.17</b> (10)	Ph <sub>2</sub> CHOH (1)	120	23	23.4	72.0	24.6	7.7
9	<b>3.17</b> (10)	<i>i</i> -PrOH (1)	24	23	0	0	N/A	N/A

<sup>a</sup> The conversion shown was estimated by <sup>1</sup>H NMR.

### 3.11.3 Kinetic resolution experiments: Exploring solvents and alcohols with Takemoto's catalyst

General procedure. The reactions were performed analogously to the procedure described above (entries 6-9 in Table 3.5), except that other solvents were used instead of CDCl<sub>3</sub>.

**Table 3.6.** Survey of solvents and alcohols using Takemoto's catalyst **3.17**. (corresponds to Table 3.2, section 3.5)

entry	solvent	ROH	Time (h)	%eesM	%eePR	%CHPLC	s
1	CH <sub>2</sub> Cl <sub>2</sub>	BnOH	16	59.4	79.7	42.7	16
2	PhMe	BnOH	7	79.1	69.3	53.3	13
3	Cyclohexane	BnOH	16	92.8	34.3	73.0	6.0
4	THF	BnOH	72	28.7	88.2	24.6	21
5	EtOAc	BnOH	22	49.4	84.2	37.0	19
6	Me <sub>2</sub> CO	BnOH	23	26.6	87.4	23.3	19
7	MeCN	BnOH	23	39.5	66.5	37.3	7.3
8	<i>t</i> -amyl alcohol	BnOH	22	45.0	88.2	33.8	25
9	<i>t</i> -amyl alcohol	MeOH	22	36.6	82.2	30.8	15
10	<i>t</i> -amyl alcohol	AllylOH	22	51.7	92.9	35.8	45
11 <sup>a</sup>	<i>t</i> -amyl alcohol	Ph <sub>2</sub> CHOH	22	60.4	98.2	38.1	208
12 <sup>a</sup>	<i>t</i> -amyl alcohol	Ph <sub>2</sub> CHOH	22	65.4	97.9	40.0	190

<sup>a</sup>Experiments were performed in duplicate. The values reported for conversion and selectivity factor are averaged over two runs.

### 3.11.4 Kinetic resolution experiments: Bifunctional catalyst survey

General procedure. The reactions were performed analogously to the procedure described above (entries 11 and 12 in Table 3.6), except that other catalysts were used instead of **3.17**. The reactions were run for 22 h in t-amyl alcohol in all cases. The absolute stereochemistry of the unreacted isoxazolidinones **3.43** was determined at this point to be (*R*) by comparing signs of optical rotation of (*R*)-**3.43a** (obtained from Table 3.7, entry 7) to that of the literature value<sup>3a</sup>:  $[\alpha]_D^{25} = +41^\circ$  (c=1.0, CDCl<sub>3</sub>) compared to the literature value of  $[\alpha]_D^{25} = -13^\circ$  (c=1.0, CDCl<sub>3</sub>) reported for (*S*)-X.

**Table 3.7:** Bifunctional catalyst survey. (corresponds to Table 3.3, section 3.6)

entry	catalyst	alcohol	% ee <sub>SM</sub>	% recovery	% ee <sub>PR</sub>	% yield	% CHPLC	s
1	<b>3.46</b>	Ph <sub>2</sub> CHOH	N/A	N/A	N/A	N/A	0 <sup>a</sup>	N/A
2 <sup>b</sup>	<b>3.47</b>	Ph <sub>2</sub> CHOH	-7.3	50	-13.6	29	34.9	1.4 <sup>-1</sup>
3	<b>3.48</b>	Ph <sub>2</sub> CHOH	N/A	N/A	N/A	N/A	0 <sup>a</sup>	N/A
4	<b>3.49</b>	Ph <sub>2</sub> CHOH	61.5	46	89.2	31	40.8	33
5 <sup>b</sup>	<b>3.50</b>	Ph <sub>2</sub> CHOH	-68.9	46	-95.7	36	41.9	94 <sup>-1</sup>
6 <sup>b</sup>	<b>3.51</b>	Ph <sub>2</sub> CHOH	-59.0	50	-97.1	33	37.8	123 <sup>-1</sup>
7 <sup>c</sup>	<b>3.52</b>	Ph <sub>2</sub> CHOH	73.5	46	99.8	38	42.6	441
8 <sup>c</sup>	<b>3.52</b>	Ph <sub>2</sub> CHOH	69.4	46	99.0	33	41.2	397
9	<b>3.52</b>	MeOH	72.3	42	82.5	37	46.7	23
10	<b>3.52</b>	BnOH	72.3	42	82.6	41	46.7	23
11	<b>3.52</b>	AllylOH	67.4	42	89.7	38	42.9	37

<sup>a</sup>No conversion was observed by <sup>1</sup>H NMR. <sup>b</sup>The absolute stereochemistry obtained in these cases was the opposite of other entries. <sup>c</sup>Experiments were performed in duplicate. The values reported for conversion and selectivity factor are averaged over two runs.

### 3.11.5 Kinetic resolution experiments: Substrate scope

General procedure. The reactions were performed analogously to the procedure described above (entries 7-11 in Table 3.7), except that other substrates were used besides (±)-**3.43a**. The reactions were run for 3 days in t-amyl alcohol, except as noted otherwise.

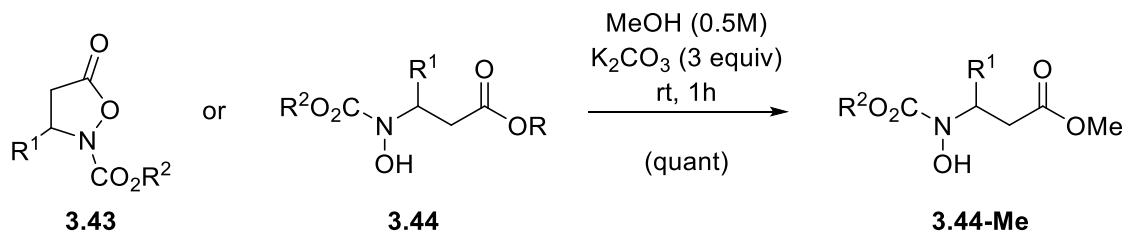
**Table 3.8:** Substrate scope. (corresponds to Table 3.4, section 3.7)

entry	# (3.43)	R <sup>1</sup>	R <sup>2</sup>	ROH	%ee <sub>SM</sub>	% rec	%ee <sub>PR</sub>	% yield	%C <sub>HPLC</sub>	s
1	a	Ph	<i>t</i> -Bu	Ph <sub>2</sub> CHOH	81.6	42	98.6	38	45.3	361
2	a	Ph	<i>t</i> -Bu	Ph <sub>2</sub> CHOH	79.5	46	99.4	38	44.6	487
3	b	4-ClC <sub>6</sub> H <sub>4</sub>	<i>t</i> -Bu	Ph <sub>2</sub> CHOH	57.6	53	99.0	31	36.8	344
4	c	4-MeOC <sub>6</sub> H <sub>4</sub>	<i>t</i> -Bu	Ph <sub>2</sub> CHOH	68.9	45	98.6	35	41.1	301
5	d	4-NO <sub>2</sub> Ph	<i>t</i> -Bu	Ph <sub>2</sub> CHOH	44.3	42	97.6	27	31.2	127
6	f	2-ClC <sub>6</sub> H <sub>4</sub>	<i>t</i> -Bu	Ph <sub>2</sub> CHOH	76.5	43	95.8	38	44.4	107
7	e	3-MeOC <sub>6</sub> H <sub>4</sub>	<i>t</i> -Bu	Ph <sub>2</sub> CHOH	80.9	41	98.8	38	45.0	430
8	g	1-naphthyl	<i>t</i> -Bu	Ph <sub>2</sub> CHOH	39.9	55	98.3	28	28.9	171
9	h	2-naphthyl	<i>t</i> -Bu	Ph <sub>2</sub> CHOH	72.6	45	98.7	36	42.4	334
10	i	2-thienyl	<i>t</i> -Bu	Ph <sub>2</sub> CHOH	91.7	44	98.2	40	48.3	352
11	j	styryl	<i>t</i> -Bu	Ph <sub>2</sub> CHOH	91.3	38	92.3	40	49.7	80
12	k	Isobutyl	<i>t</i> -Bu	Ph <sub>2</sub> CHOH	62.3	50	94.5	37	39.8	67
13	l	Isopropyl	<i>t</i> -Bu	Ph <sub>2</sub> CHOH	31.7	56	98.2	20	24.4	151
14	l	Isopropyl	<i>t</i> -Bu	BnOH	52.9	52	97.7	29	35.1	144
15	l	Isopropyl	<i>t</i> -Bu	AllylOH	57.5	52	96.2	34	37.4	92
16	m	<i>t</i> -butyl	<i>t</i> -Bu	Ph <sub>2</sub> CHOH	N/A	N/A	N/A	N/A	0	N/A
17	m	<i>t</i> -butyl	<i>t</i> -Bu	AllylOH	N/A	N/A	N/A	N/A	0	N/A
18	n	Ph	Bn	Ph <sub>2</sub> CHOH	N/A	N/A	N/A	N/A	0	N/A
19	n	Ph	Bn	MeOH	93.3	33	78.1	42	54.4	27
20	n	Ph	Bn	BnOH	88.1	30	86.5	39	50.4	40
21	n	Ph	Bn	AllylOH	86.7	30	89.4	39	49.3	50
22	e	2-ClC <sub>6</sub> H <sub>4</sub>	<i>t</i> -Bu	Ph <sub>2</sub> CHOH	74.4	43	94.6	32	44.0	80
23	h	2-naphthyl	<i>t</i> -Bu	Ph <sub>2</sub> CHOH	67.8	52	96.6	40	41.2	118
24	k	isobutyl	<i>t</i> -Bu	Ph <sub>2</sub> CHOH	31.9	50	88.0	26	26.6	21.4

<sup>a</sup> 4:1 *t*-amyl alcohol/CHCl<sub>3</sub> was used as solvent. <sup>b</sup> CHCl<sub>3</sub> was used as solvent. <sup>c</sup> 3:2 *t*-amyl alcohol/CHCl<sub>3</sub> was used as solvent. <sup>d</sup> No conversion was detected by <sup>1</sup>H NMR. <sup>e</sup> Performed on 1.0 mmol of substrate. <sup>f</sup> Catalyst **3.17** was used instead of **3.52**.

## 3.12 Interconversion of kinetic resolution products

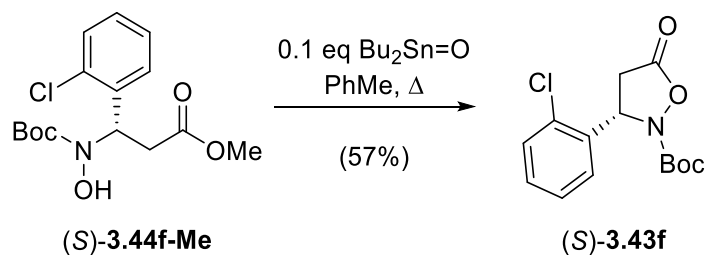
### 3.12.1 Methanolysis of isoxazolidinones or esters



*Typical procedure.* A solution of an isoxazolidinone (**3.43**) or a benzhydryl, benzyl or allyl ester (**3.44**) in MeOH (0.5M) was stirred with 3 equiv of potassium carbonate at rt for 1 h or until TLC

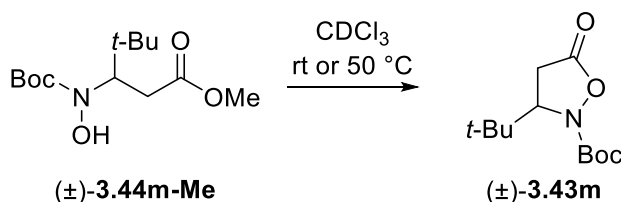
indicated complete consumption of the starting material. The reaction mixture was quenched with 10 mL of saturated aqueous ammonium chloride and the methyl ester was extracted with CH<sub>2</sub>Cl<sub>2</sub> (×3). The organic extract was dried with Na<sub>2</sub>SO<sub>4</sub> and concentrated by rotary evaporation. The product methyl esters **3.44-Me** were purified by chromatography (10→30% EtOAc/toluene) and isolated in essentially quantitative yields.

### 3.12.2 Recyclization of methyl ester **3.44f-Me** into isoxazolidinone **3.43f**



A published procedure was followed.<sup>5</sup> A solution of methyl ester (*S*)-**3.44f-Me** obtained as described above (33 mg, 0.10 mmol) and dibutyltin oxide (3 mg, 0.01 mmol, 0.1 equiv) in 2 mL of dry toluene (0.05 M) was gently refluxed for 4 h, at which time TLC (30% ethyl acetate/hexanes) revealed complete consumption of the starting material. The toluene was removed by rotary evaporation and the crude mixture pre-adsorbed onto silica gel. Elution with EtOAc/toluene (5→20%) gave (*S*)-**3.43f** in 57% yield (17 mg).

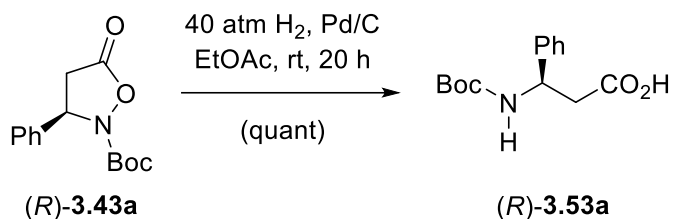
### 3.12.3. Recyclization of methyl ester **3.44m-Me** into **3.43m**



Methyl ester ( $\pm$ )-**3.44-Me** obtained as described above from ( $\pm$ )-**3.43m** (28 mg, 0.10 mmol) was dissolved in 500  $\mu$ L of CDCl<sub>3</sub> and its conversion to **3.43m** was monitored by <sup>1</sup>H NMR. After 64 h

at rt, the conversion was estimated at 64%. The solution was heated at 50 °C for 2.5 h at which time NMR showed complete conversion to isoxazolidinone.

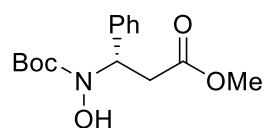
### 3.13 Hydrogenolysis of 3.43a into $\beta$ -phenylalanine



A slightly modified literature procedure was followed.<sup>3a</sup> To a solution of isoxazolidinone (**(R)-3.43a**) (54 mg, 0.21 mmol) in 2 mL of EtOAc was added 5.3 mg of 10% Pd/C. The resulting mixture was placed in a steel bomb and stirred under 40 atm of hydrogen for 20 h, at which time TLC (30% EtOAc/ hexanes) indicated complete consumption of starting material. The crude mixture was filtered through a plug of Celite and concentrated by rotary evaporation to yield pure (**(R)-3.53a**) as a clear, colorless oil which quickly solidified into a white powder under vacuum (54 mg, quantitative yield). The spectroscopic and optical rotation data are in accordance with the literature.<sup>39</sup> <sup>1</sup>H NMR (300 MHz, CDCl<sub>3</sub>)  $\delta$  7.37-7.27 (m, 5H), 5.08 (br, 1H), 2.86 (br, 2H), 1.40 (br s, 9H). HRMS (ESI-TOF) m/z: [M+Na]<sup>+</sup> calcd for C<sub>14</sub>H<sub>19</sub>NO<sub>4</sub>, 288.1206; found 288.1203.  $[\alpha]_D^{25} = +10^\circ$  (c=1.067, MeOH).

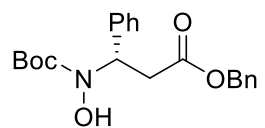
### 3.14 Characterization of ester products

#### methyl (S)-3-((tert-butoxycarbonyl)(hydroxy)amino)-3-phenylpropanoate (3.44a-Me).



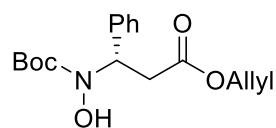
Clear, colorless oil.  $^1\text{H}$  NMR (500 MHz,  $\text{CDCl}_3$ )  $\delta$  7.41-7.37 (m, 2H), 7.35-7.27 (m, 3H), 6.55 (br s, 1H), 5.51 (dd,  $J = 9.5$  Hz, 6 Hz, 1H), 3.68 (s, 3H), 3.20 (dd,  $J = 15.3$  Hz, 9.5 Hz, 1H), 2.89 (dd,  $J = 15.3$  Hz, 6 Hz, 1H), 1.43 (s, 9H).  $^{13}\text{C}\{^1\text{H}\}$  NMR (125 MHz,  $\text{CDCl}_3$ ):  $\delta$  171.7, 156.6, 138.9, 128.6, 128.1, 127.4, 82.5, 59.4, 52.1, 37.1, 28.4; IR ( $\text{cm}^{-1}$ ): 3209 (br), 2978, 1737, 1684, 1161, 1103, 699; HRMS (ESI-TOF)  $m/z$ :  $[\text{M}+\text{H}]^+$  calcd for  $\text{C}_{15}\text{H}_{22}\text{NO}_5$ , 296.1492; found, 296.1494. HPLC: (7 % isopropanol/hexanes, AS-H): Major enantiomer: 7.0 min; Minor enantiomer: 9.9 min; 82% ee (Table 3.6, entry 9).  $[\alpha]_D^{25} = -15^\circ$  ( $c=0.350$ ,  $\text{CHCl}_3$ ).

#### benzyl (S)-3-((tert-butoxycarbonyl)(hydroxy)amino)-3-phenylpropanoate (3.44a-Bn)



Clear, colorless oil.  $^1\text{H}$  NMR (500 MHz,  $\text{CDCl}_3$ )  $\delta$  7.41-7.27 (m, 10H), 6.10 (s, 1H), 5.53 (dd,  $J = 9.5$  Hz, 6 Hz, 1H), 5.12 (s, 2H), 3.23 (dd,  $J = 15$  Hz, 9.5 Hz, 1H), 2.96 (dd,  $J = 15$  Hz, 6 Hz, 1H), 1.43 (s, 9H).  $^{13}\text{C}\{^1\text{H}\}$  NMR (125 MHz,  $\text{CDCl}_3$ ):  $\delta$  171.0, 156.5, 138.6, 135.8, 128.72, 128.65, 128.4, 128.3, 128.2, 127.5, 82.6, 66.8, 59.5, 37.4, 28.4; IR ( $\text{cm}^{-1}$ ): 3200 (br), 2976, 1735, 1685, 1159, 1103, 696; HRMS (ESI-TOF)  $m/z$ :  $[\text{M}+\text{Na}]^+$  calcd for  $\text{C}_{21}\text{H}_{25}\text{NO}_5\text{Na}$ , 394.1625; found, 394.1630.  $[\alpha]_D^{25} = -14^\circ$  ( $c=0.550$ ,  $\text{CHCl}_3$ ); 88% ee (Table 3.6, entry 8, measured by HPLC as the corresponding methyl ester).

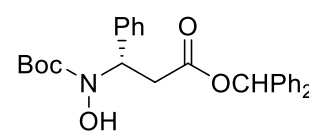
#### allyl (S)-3-((tert-butoxycarbonyl)(hydroxy)amino)-3-phenylpropanoate (3.44a-Allyl).



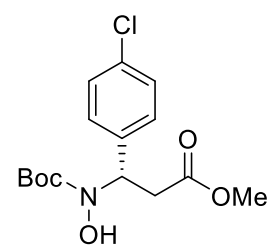
Clear, colorless oil.  $^1\text{H}$  NMR (500 MHz,  $\text{CDCl}_3$ )  $\delta$  7.42-7.38 (m, 2H), 7.36-7.27 (m, 3H), 6.02 (s, 1H), 5.93-5.84 (m, 1H), 5.52 (dd,  $J = 9.5$  Hz,

6 Hz, 1H), 5.32-5.21 (m, 2H), 4.61-4.58 (m, 2H), 3.22 (dd, J = 15 Hz, 9.5 Hz, 1H), 2.93 (dd, J = 15 Hz, 6 Hz, 1H), 1.44 (s, 9H).  $^{13}\text{C}\{^1\text{H}\}$  NMR (125 MHz,  $\text{CDCl}_3$ ):  $\delta$  170.9, 156.5, 138.7, 132.0, 128.7, 128.2, 127.5, 118.6, 82.6, 65.7, 59.4, 37.3, 28.4; IR ( $\text{cm}^{-1}$ ): 3203 (br), 2978, 2932, 1736, 1686, 1161, 1103, 699; HRMS (ESI-TOF) m/z:  $[\text{M}+\text{Na}]^+$  calcd for  $\text{C}_{17}\text{H}_{23}\text{NO}_5\text{Na}$ , 344.1468; found, 344.1456.  $[\alpha]_D^{25} = -17^\circ$  (c=0.550,  $\text{CHCl}_3$ ); 93% ee (Table 3.6, entry 10, measured by HPLC as the corresponding methyl ester).

**benzhydryl (S)-3-((tert-butoxycarbonyl)(hydroxy)amino)-3-phenylpropanoate (3.44a-Bzh).**

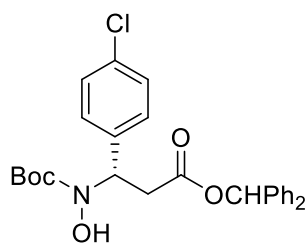
 Clear, colorless oil.  $^1\text{H}$  NMR (500 MHz,  $\text{CDCl}_3$ )  $\delta$  7.42-7.39 (m, 2H), 7.35-7.25 (m, 13H), 6.87 (s, 1H), 6.46 (s, 1H), 5.56 (dd, J = 9 Hz, 7 Hz, 1H), 3.29 (dd, J = 15 Hz, 9 Hz, 1H), 3.09 (dd, J = 15 Hz, 7 Hz, 1H), 1.40 (s, 9H).  $^{13}\text{C}\{^1\text{H}\}$  NMR (125 MHz,  $\text{CDCl}_3$ ):  $\delta$  170.2, 156.5, 139.99, 139.97, 138.6, 128.64, 128.61, 128.12, 128.08, 128.0, 127.6, 127.2, 127.1, 82.5, 77.6, 59.5, 37.8, 28.3; IR ( $\text{cm}^{-1}$ ): 2922, 2852, 1737, 1692, 1284, 1102, 697; HRMS (ESI-TOF) m/z:  $[\text{M}+\text{Na}]^+$  calcd for  $\text{C}_{27}\text{H}_{29}\text{NO}_5\text{Na}$ , 470.1938; found, 470.1929.  $[\alpha]_D^{25} = -11^\circ$  (c=0.700,  $\text{CHCl}_3$ ); 98% ee (Table 3.6, entry 11, measured by HPLC as the corresponding methyl ester).

**methyl (S)-3-((tert-butoxycarbonyl)(hydroxy)amino)-3-(4-chlorophenyl)propanoate (3.44b-Me)**

 Clear, colorless oil.  $^1\text{H}$  NMR (500 MHz,  $\text{CDCl}_3$ )  $\delta$  7.33 (d, J = 8.5 Hz, 2H), 7.29 (d, J = 8.5 Hz, 2H), 6.88 (br s, 1H), 5.46 (dd, J = 9 Hz, 6.5 Hz, 1H), 3.67 (s, 3H), 3.15 (dd, J = 16 Hz, 9 Hz, 1H), 2.87 (dd, J = 16 Hz, 6.5 Hz, 1H), 1.42 (s, 9H).  $^{13}\text{C}\{^1\text{H}\}$  NMR (125 MHz,  $\text{CDCl}_3$ ):  $\delta$  171.4, 156.5, 137.4, 134.0, 128.9, 128.8, 82.8, 58.7, 52.2, 37.1, 28.3; IR ( $\text{cm}^{-1}$ ): 3205 (br), 2978, 2930, 1738,

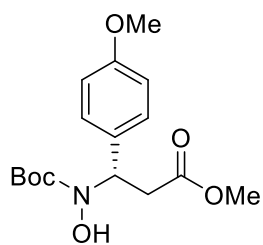
1686, 1163, 1109, 1091; HRMS (ESI-TOF)  $m/z$ :  $[M+Na]^+$  calcd for  $C_{15}H_{20}NO_5ClNa$ , 352.0922; found, 352.0923. HPLC: (7 % isopropanol/hexanes, AS-H): Major enantiomer: 6.4 min; Minor enantiomer: 9.9 min; 99% ee.  $[\alpha]_D^{25} = -19^\circ$  ( $c=0.400$ ,  $CHCl_3$ ).

**benzhydryl (S)-3-((tert-butoxycarbonyl)(hydroxy)amino)-3-(4-chlorophenyl)propanoate (3.44b-Bzh)**



Clear, colorless oil.  $^1H$  NMR (500 MHz,  $CDCl_3$ )  $\delta$  7.35-7.25 (m, 12H), 7.25-7.21 (m, 2H), 6.85 (s, 1H), 6.51 (br s, 1H), 5.49 (dd,  $J = 8$  Hz, 7 Hz, 1H), 3.23 (dd,  $J = 15$  Hz, 8 Hz, 1H), 3.06 (dd,  $J = 15$  Hz, 7 Hz, 1H), 1.39 (s, 9H).  $^{13}C\{^1H\}$  NMR (125 MHz,  $CDCl_3$ ):  $\delta$  169.9, 156.4, 139.84, 139.81, 137.0, 134.0, 129.1, 128.8, 128.7, 128.6, 128.2, 128.1, 127.2, 127.1, 82.8, 77.7, 58.8, 37.8, 28.3; IR ( $cm^{-1}$ ): 3197 (br s), 2925, 2362, 1736, 1686, 1160, 1108; HRMS (ESI-TOF)  $m/z$ :  $[M+Na]^+$  calcd for  $C_{27}H_{28}ClNO_5Na$ , 504.1548; found, 504.1523.  $[\alpha]_D^{25} = -13^\circ$  ( $c=0.993$ ,  $CHCl_3$ ); 99% ee (Table 3.8, entry 3, measured by HPLC as the corresponding methyl ester).

**methyl (S)-3-((tert-butoxycarbonyl)(hydroxy)amino)-3-(4-methoxyphenyl)propanoate (3.44c-Me)**

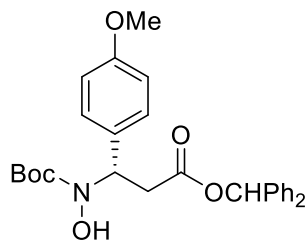


Clear, colorless oil.  $^1H$  NMR (500 MHz,  $CDCl_3$ )  $\delta$  7.32 (d,  $J = 9$  Hz, 2H), 6.85 (d,  $J = 9$  Hz, 2H), 6.25 (br s, 1H), 5.46 (dd,  $J = 9$  Hz, 6.5 Hz, 1H), 3.79 (s, 3H), 3.67 (s, 3H), 3.16 (dd,  $J = 15.3$  Hz, 9 Hz, 1H), 2.87 (dd,  $J = 15.3$  Hz, 6.5 Hz, 1H), 1.44 (s, 9H).  $^{13}C\{^1H\}$  NMR (125 MHz,  $CDCl_3$ ):  $\delta$  171.7, 159.4, 156.6, 130.7, 128.8, 114.0, 82.5, 58.9, 55.4, 52.1, 37.2, 28.4; IR ( $cm^{-1}$ ): 3205 (br s), 2929, 1737, 1684, 1513, 1247, 1162, 1103, 780; HRMS (ESI-TOF)  $m/z$ :  $[M+H]^+$  calcd for



C<sub>16</sub>H<sub>24</sub>NO<sub>6</sub>, 326.1598; found, 326.1595.  $[\alpha]_D^{25} = -24^\circ$  (c=0.450, CHCl<sub>3</sub>); 99% ee (measured by HPLC as the corresponding isoxazolidinone).

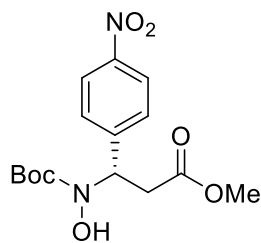
**benzhydryl (S)-3-((tert-butoxycarbonyl)(hydroxy)amino)-3-(4-methoxyphenyl)propanoate (3.44c-Bzh)**



Clear, colorless oil. <sup>1</sup>H NMR (500 MHz, CDCl<sub>3</sub>) δ 7.34-7.21 (m, 11H), 6.86-6.81 (m, 3H), 6.52 (br s, 1H), 5.50 (dd, J = 8.5 Hz, 7.5 Hz, 1H), 3.79 (s, 3H), 3.24 (dd, J = 16 Hz, 8.5 Hz, 1H), 3.07 (dd, J = 16 Hz, 7.5 Hz, 1H), 1.39 (s, 9H). <sup>13</sup>C{<sup>1</sup>H} NMR (125 MHz, CDCl<sub>3</sub>): δ 170.2, 159.4, 156.6, 140.0, 139.98, 130.5, 128.9, 128.61, 128.56, 128.1, 128.0, 127.2, 127.1, 113.9, 82.5, 77.5, 58.9, 55.3, 37.9, 28.3; IR (cm<sup>-1</sup>): 2977, 2933, 1735, 1686, 1248, 1158, 1108, 735, 697; HRMS (ESI-TOF) m/z: [M+Na]<sup>+</sup> calcd for C<sub>28</sub>H<sub>31</sub>NO<sub>6</sub>Na, 500.2044; found, 500.2059.

$[\alpha]_D^{25} = -11^\circ$  (c=1.067, CHCl<sub>3</sub>); 99% ee (Table 3.8, entry 4, measured by HPLC as the corresponding isoxazolidinone).

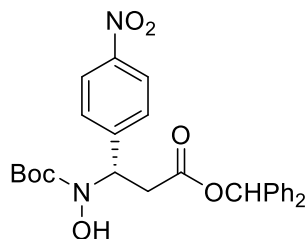
**methyl (S)-3-((tert-butoxycarbonyl)(hydroxy)amino)-3-(4-nitrophenyl)propanoate (3.44d-Me)**



Clear, colorless oil. <sup>1</sup>H NMR (500 MHz, CDCl<sub>3</sub>) δ 8.19 (d, J = 9 Hz, 2H), 7.58 (d, J = 9 Hz, 2H), 6.99 (br s, 1H), 5.57 (dd, J = 9 Hz, 7 Hz, 1H), 3.69 (s, 3H), 3.18 (dd, J = 16 Hz, 9 Hz, 1H), 2.92 (dd, J = 16 Hz, 7 Hz, 1H), 1.42 (s, 9H). <sup>13</sup>C{<sup>1</sup>H} NMR (125 MHz, CDCl<sub>3</sub>): δ 171.1, 156.4, 147.7, 146.2, 128.4, 123.9, 83.2, 58.7, 52.3, 37.0, 28.3; IR (cm<sup>-1</sup>): 3211 (br), 2928, 1740, 1691, 1523, 1347, 1166, 1110; HRMS (ESI-TOF) m/z: [M+H]<sup>+</sup> calcd for C<sub>15</sub>H<sub>21</sub>N<sub>2</sub>O<sub>7</sub>, 341.1343; found,

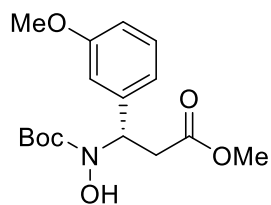
341.1342. HPLC: (7 % isopropanol/hexanes, AD-H): Major enantiomer: 21.7 min; Minor enantiomer: 27.7 min; 96% ee.  $[\alpha]_D^{25} = -12^\circ$  (c=0.550, CHCl<sub>3</sub>).

**benzhydryl (S)-3-((tert-butoxycarbonyl)(hydroxy)amino)-3-(4-nitrophenyl)propanoate (3.44d-Bzh)**



Clear, colorless oil. <sup>1</sup>H NMR (500 MHz, CDCl<sub>3</sub>) δ 8.12 (d, J = 9 Hz, 2H), 7.54 (d, J = 9 Hz, 2H), 7.35-7.22 (m, 10H), 6.85 (s, 1H), 6.52 (br s, 1H), 5.58 (dd, J = 8.5 Hz, 7.5 Hz, 1H), 3.25 (dd, J = 15.5 Hz, 8.5 Hz, 1H), 3.08 (dd, J = 15.5 Hz, 7.5 Hz, 1H), 1.38 (s, 9H). <sup>13</sup>C{<sup>1</sup>H} NMR (125 MHz, CDCl<sub>3</sub>): δ 169.6, 156.3, 147.7, 145.8, 139.7, 139.6, 128.72, 128.66, 128.5, 128.3, 128.2, 127.2, 127.1, 123.8, 83.3, 77.9, 58.8, 37.6, 28.3; IR (cm<sup>-1</sup>): 3194 (br), 2926, 1737, 1688, 1522, 1346, 1163, 1110; HRMS (ESI-TOF) m/z: [M+Na]<sup>+</sup> calcd for C<sub>27</sub>H<sub>28</sub>N<sub>2</sub>O<sub>7</sub>Na, 515.1789; found, 515.1790.  $[\alpha]_D^{25} = -8^\circ$  (c=0.600, CHCl<sub>3</sub>); 96% ee (Table 3.8, entry 5, measured by HPLC as the corresponding methyl ester).

**methyl (S)-3-((tert-butoxycarbonyl)(hydroxy)amino)-3-(3-methoxyphenyl)propanoate (3.44e-Me).**

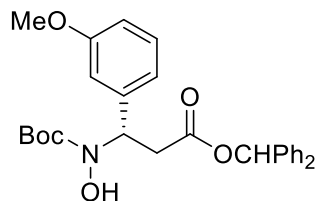


Clear, colorless oil which slowly solidified into a white powder. <sup>1</sup>H NMR (500 MHz, CDCl<sub>3</sub>) δ 7.24-7.21 (m, 1H), 6.97-6.93 (m, 2H), 6.83-6.79 (m, 1H), 5.48 (dd, J = 9 Hz, 6 Hz, 1H), 3.78 (s, 3H), 3.67 (s, 3H), 3.18 (dd, J = 16 Hz, 9 Hz, 1H), 2.86 (dd, J = 16 Hz, 6 Hz, 1H), 1.42 (s, 9H). <sup>13</sup>C{<sup>1</sup>H} NMR (125 MHz, CDCl<sub>3</sub>): δ 171.7, 159.7, 156.5, 140.5, 129.6, 119.7, 113.5, 113.1, 82.4, 59.2, 55.3, 52.1, 37.1, 28.4; IR (cm<sup>-1</sup>): 3215 (br), 2976, 1737, 1685, 1255, 1160, 1104; HRMS (ESI-TOF) m/z: [M+Na]<sup>+</sup> calcd for C<sub>16</sub>H<sub>23</sub>NO<sub>6</sub>Na, 348.1418; found, 348.1413. mp: 66- 67 °C. HPLC: (7 %

isopropanol/hexanes, AS-H): Major enantiomer: 10.0 min; Minor enantiomer: 13.5 min; 99% ee.

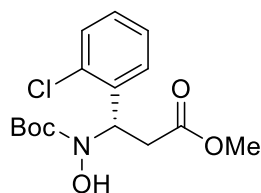
$[\alpha]_D^{25} = -11^\circ$  (c=0.600, CHCl<sub>3</sub>).

**benzhydryl (S)-3-((tert-butoxycarbonyl)(hydroxy)amino)-3-(3-methoxyphenyl)propanoate (3.44e-Bzh)**



Clear, colorless oil. <sup>1</sup>H NMR (500 MHz, CDCl<sub>3</sub>) δ 7.35-7.21 (m, 11H), 7.01-6.95 (m, 2H), 6.87 (s, 1H), 6.85-6.82 (m, 1H), 5.54 (dd, J = 8.5 Hz, 7 Hz, 1H), 3.77 (s, 3H), 3.28 (dd, J = 16 Hz, 8.5 Hz, 1H), 3.08 (dd, J = 16 Hz, 7 Hz, 1H), 1.39 (s, 9H). <sup>13</sup>C{<sup>1</sup>H} NMR (125 MHz, CDCl<sub>3</sub>): δ 170.1, 159.7, 156.5, 140.1, 140.0, 129.6, 128.60, 128.57, 128.03, 127.97, 127.2, 127.1, 119.9, 113.7, 113.1, 82.4, 77.5, 59.3, 55.3, 37.7, 28.3; IR (cm<sup>-1</sup>): 3209 (br), 2975, 2931, 1736, 1685, 1156, 1104, 696; HRMS (ESI-TOF) m/z: [M+Na]<sup>+</sup> calcd for C<sub>28</sub>H<sub>31</sub>NO<sub>6</sub>Na, 500.2044; found, 500.2043.  $[\alpha]_D^{25} = -9^\circ$  (c=1.133, CHCl<sub>3</sub>); 99% ee (Table 3.8, entry 7, measured by HPLC as the corresponding methyl ester).

**methyl (S)-3-((tert-butoxycarbonyl)(hydroxy)amino)-3-(2-chlorophenyl)propanoate (3.44f-Me).**

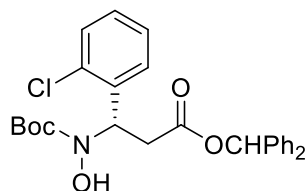


Clear, colorless oil. <sup>1</sup>H NMR (500 MHz, CDCl<sub>3</sub>) δ 7.69-7.65 (m, 1H), 7.36-7.33 (m, 1H), 7.28-7.20 (m, 2H), 6.69 (br s, 1H), 5.93 (dd, J = 11 Hz, 5 Hz, 1H), 3.72 (s, 3H), 3.08 (dd, J = 15 Hz, 11 Hz, 1H), 2.85 (dd, J = 15 Hz, 5 Hz, 1H), 1.40 (s, 9H). <sup>13</sup>C{<sup>1</sup>H} NMR (125 MHz, CDCl<sub>3</sub>): δ 171.5, 156.4, 137.9, 132.5, 129.6, 129.1, 128.3, 127.4, 82.6, 56.5, 52.2, 36.4, 28.3; IR (cm<sup>-1</sup>): 3199 (br), 2928, 1742, 1688, 1168, 1112; HRMS (ESI-TOF) m/z: [M+Na]<sup>+</sup> calcd for C<sub>15</sub>H<sub>20</sub>ClNO<sub>5</sub>Na, 352.0922; found,

352.0936. HPLC: (7 % isopropanol/hexanes, AD-H): Minor enantiomer: 13.4 min; Major enantiomer: 17.0 min; 96% ee.  $[\alpha]_D^{25} = +6^\circ$  (c=0.533, CHCl<sub>3</sub>).

**benzhydryl (S)-3-((tert-butoxycarbonyl)(hydroxy)amino)-3-(2-chlorophenyl)propanoate**

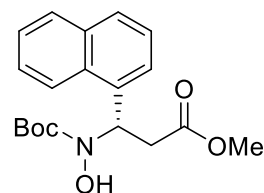
**(3.44f-Bzh)**



Clear, colorless oil. <sup>1</sup>H NMR (500 MHz, CDCl<sub>3</sub>) δ 7.70-7.67 (m, 1H), 7.36-7.17 (m, 13H), 6.88 (s, 1H), 6.03 (dd, J = 9.5 Hz, 6 Hz, 1H), 3.18 (dd, J = 15.5 Hz, 9.5 Hz, 1H), 3.05 (dd, J = 15.5 Hz, 6 Hz, 1H), 1.33 (s, 9H). <sup>13</sup>C{<sup>1</sup>H} NMR (125 MHz, CDCl<sub>3</sub>): δ 169.8, 156.2, 140.01, 139.99, 137.6, 132.7, 129.6, 129.0, 128.6, 128.5, 128.0, 127.3, 127.12, 127.09, 82.5, 77.5, 56.3, 36.9, 28.2; IR (cm<sup>-1</sup>): 3193 (br), 2978, 2930, 1739, 1686, 1159, 1109, 744, 697; HRMS (ESI-TOF) m/z: [M+Na]<sup>+</sup> calcd for C<sub>27</sub>H<sub>28</sub>ClNO<sub>5</sub>Na, 504.1548; found, 504.1534.  $[\alpha]_D^{25} = +2^\circ$  (c=1.067, CHCl<sub>3</sub>); 96% ee (Table 3.8, entry 6, measured by HPLC as the corresponding methyl ester).

**methyl (S)-3-((tert-butoxycarbonyl)(hydroxy)amino)-3-(naphthalen-1-yl)propanoate**

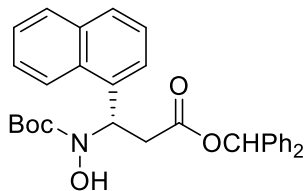
**(3.44g-Me)**



Clear, colorless oil. <sup>1</sup>H NMR (500 MHz, CDCl<sub>3</sub>) δ 8.21-8.17 (m, 1H), 7.87-7.84 (m, 1H), 7.81-7.77 (m, 1H), 7.71-7.67 (m, 1H), 7.56-7.52 (m, 1H), 7.51-7.42 (m, 2H), 6.70 (br s, 1H), 6.38 (dd, J = 9.5 Hz, 5.5 Hz, 1H), 3.69 (s, 3H), 3.33 (dd, J = 15.5 Hz, 9.5 Hz, 1H), 3.01 (dd, J = 15.5 Hz, 5.5 Hz, 1H), 1.36 (s, 9H). <sup>13</sup>C{<sup>1</sup>H} NMR (125 MHz, CDCl<sub>3</sub>): δ 171.8, 156.0, 134.9, 133.9, 130.9, 129.0, 128.7, 126.5, 125.8, 125.4, 124.7, 123.1, 82.4, 54.9, 52.2, 36.6, 28.3; IR (cm<sup>-1</sup>): 3201 (br), 2976, 2928, 1737, 1685, 1165, 1107, 778; HRMS (ESI-TOF) m/z: [M+Na]<sup>+</sup> calcd for C<sub>19</sub>H<sub>23</sub>NO<sub>5</sub>Na, 368.1468;

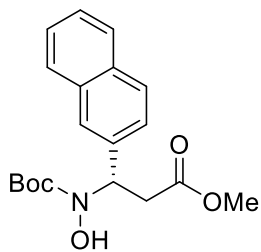
found, 368.1446. HPLC: (7 % isopropanol/hexanes, OD-H): Minor enantiomer: 8.1 min; Major enantiomer: 10.0 min; 98% ee.  $[\alpha]_D^{25} = +7^\circ$  (c=0.467, CHCl<sub>3</sub>).

**benzhydryl (S)-3-((tert-butoxycarbonyl)(hydroxy)amino)-3-(naphthalen-1-yl)propanoate**  
**(3.44g-Bzh)**



Clear, colorless oil. <sup>1</sup>H NMR (500 MHz, CDCl<sub>3</sub>) δ 8.24-8.20 (m, 1H), 7.89-7.86 (m, 1H), 7.82-7.78 (m, 1H), 7.75-7.72 (m, 1H), 7.56-7.48 (m, 2H), 7.45-7.41 (m, 1H), 7.33-7.15 (m, 10H), 7.03 (br s, 1H), 6.85 (s, 1H), 6.47 (dd, J = 8.5 Hz, 7 Hz, 1H), 3.38 (dd, J = 16 Hz, 8.5 Hz, 1H), 3.29 (dd, J = 16 Hz, 7 Hz, 1H), 1.30 (s, 9H). <sup>13</sup>C{<sup>1</sup>H} NMR (125 MHz, CDCl<sub>3</sub>): δ 170.0, 155.8, 140.0, 139.9, 134.5, 134.0, 131.1, 129.0, 128.7, 128.6, 128.5, 128.0, 127.9, 127.1, 127.0, 126.5, 125.7, 125.4, 125.0, 123.2, 82.4, 77.5, 54.5, 37.2, 28.2; IR (cm<sup>-1</sup>): 2975, 2928, 1736, 1684, 1158, 1104, 696; HRMS (ESI-TOF) m/z: [M+Na]<sup>+</sup> calcd for C<sub>31</sub>H<sub>31</sub>NO<sub>5</sub>Na, 520.2094; found, 520.2075.  $[\alpha]_D^{25} = -5^\circ$  (c=0.933, CHCl<sub>3</sub>); 98% ee (Table 3.8, entry 8, measured by HPLC as the corresponding methyl ester).

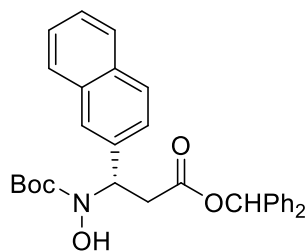
**methyl (S)-3-((tert-butoxycarbonyl)(hydroxy)amino)-3-(naphthalen-2-yl)propanoate**  
**(3.44h-Me)**



Clear, colorless oil. <sup>1</sup>H NMR (500 MHz, CDCl<sub>3</sub>) δ 7.86-7.78 (m, 4H), 7.55-7.51 (m, 1H), 7.50-7.44 (m, 2H), 7.19 (br s, 1H), 5.68 (dd, J = 9 Hz, 6 Hz, 1H), 3.68 (s, 3H), 3.29 (dd, J = 16 Hz, 9 Hz, 1H), 3.01 (dd, J = 16 Hz, 6 Hz, 1H), 1.39 (s, 9H). <sup>13</sup>C{<sup>1</sup>H} NMR (125 MHz, CDCl<sub>3</sub>): δ 171.7, 156.6, 136.4, 133.3, 133.1, 128.3, 128.2, 127.7, 126.4, 126.24, 126.17, 125.6, 82.5, 59.4, 52.1, 37.1, 28.; IR (cm<sup>-1</sup>): 3206 (br), 3058, 2977, 1736, 1683, 1162, 1103; HRMS (ESI-TOF) m/z: [M+Na]<sup>+</sup>

calcd for C<sub>19</sub>H<sub>23</sub>NO<sub>5</sub>Na, 368.1468; found, 368.1444. HPLC: (7 % isopropanol/hexanes, AS-H): Major enantiomer: 8.1 min; Minor enantiomer: 13.4 min; 99% ee.  $[\alpha]_D^{25} = -16^\circ$  (c=0.600, CHCl<sub>3</sub>).

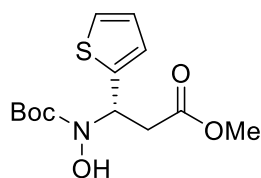
**benzhydryl (S)-3-((tert-butoxycarbonyl)(hydroxy)amino)-3-(naphthalen-2-yl)propanoate (3.44h-Bzh)**



Clear, colorless oil. <sup>1</sup>H NMR (500 MHz, CDCl<sub>3</sub>) δ 7.84-7.76 (m, 4H), 7.56-7.53 (m, 1H), 7.51-7.46 (m, 2H), 7.30-7.18 (m, 10H), 6.85 (s, 1H), 6.78 (br s, 1H), 5.72 (dd, J = 8 Hz, 7.5 Hz, 1H), 3.36 (dd, J = 15.5 Hz, 8 Hz, 1H), 3.22 (dd, J = 15.5 Hz, 7.5 Hz, 1H), 1.36 (s, 9H).

<sup>13</sup>C{<sup>1</sup>H} NMR (125 MHz, CDCl<sub>3</sub>): δ 170.2, 156.5, 139.91, 139.88, 136.0, 133.3, 133.2, 128.6, 128.5, 128.4, 128.3, 128.1, 128.0, 127.7, 127.2, 127.0, 126.6, 126.24, 126.22, 125.7, 82.6, 77.6, 59.5, 37.8, 28.3; IR (cm<sup>-1</sup>): 2975, 1735, 1685, 1159, 1103; HRMS (ESI-TOF) m/z: [M+Na]<sup>+</sup> calcd for C<sub>31</sub>H<sub>31</sub>NO<sub>5</sub>Na, 520.2094; found, 520.2103.  $[\alpha]_D^{25} = -9^\circ$  (c=1.200, CHCl<sub>3</sub>); 99% ee (Table 3.8, entry 9, measured by HPLC as the corresponding methyl ester).

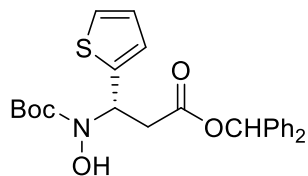
**methyl (S)-3-((tert-butoxycarbonyl)(hydroxy)amino)-3-(thiophen-2-yl)propanoate (3.44i-Me)**



Clear, colorless oil. <sup>1</sup>H NMR (500 MHz, CDCl<sub>3</sub>) δ 7.23 (dd, J = 5 Hz, 1 Hz, 1H), 7.05-7.02 (m, 1H), 6.95 (dd, J = 5 Hz, 4 Hz, 1H), 6.13 (br s, 1H), 5.76 (dd, J = 9 Hz, 6.5 Hz, 1H), 3.69 (s, 3H), 3.19 (dd, J = 15 Hz, 9 Hz, 1H), 2.96 (dd, J = 15 Hz, 6.5 Hz, 1H), 1.48 (s, 9H). <sup>13</sup>C{<sup>1</sup>H} NMR (125 MHz, CDCl<sub>3</sub>): δ 171.1, 156.7, 140.5, 126.6, 125.9, 125.3, 83.1, 55.5, 52.2, 38.3, 28.4; IR (cm<sup>-1</sup>): 3236 (br), 2928, 1738, 1693, 1163, 1102; HRMS (ESI-TOF) m/z: [M+Na]<sup>+</sup> calcd for C<sub>13</sub>H<sub>19</sub>NO<sub>5</sub>SNa, 324.0876; found,

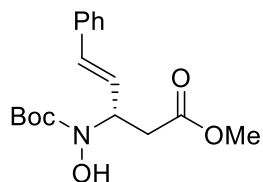
324.0885. HPLC: (7 % isopropanol/hexanes, AS-H): Major enantiomer: 8.4 min; Minor enantiomer: 11.9 min; 98% ee.  $[\alpha]_D^{25} = -15^\circ$  (c=0.400, CHCl<sub>3</sub>).

**benzhydryl (S)-3-((tert-butoxycarbonyl)(hydroxy)amino)-3-(thiophen-2-yl)propanoate (3.44i-Bzh)**



Clear, colorless oil which slowly solidified into a white powder. <sup>1</sup>H NMR (500 MHz, CDCl<sub>3</sub>) δ 7.35-7.25 (m, 10H), 7.22 (dd, J = 5 Hz, 1 Hz, 1H), 7.04-7.02 (m, 1H), 6.93 (dd, J = 5 Hz, 4 Hz, 1H), 6.87 (s, 1H), 6.70 (br s, 1H), 5.82 (dd, J = 8 Hz, 7 Hz, 1H), 3.28 (dd, J = 16 Hz, 8 Hz, 1H), 3.13 (dd, J = 16 Hz, 7 Hz, 1H), 1.44 (s, 9H). <sup>13</sup>C{<sup>1</sup>H} NMR (125 MHz, CDCl<sub>3</sub>): δ 169.6, 156.7, 140.1, 139.9, 128.61, 128.57, 128.1, 128.0, 127.2, 127.1, 126.6, 126.0, 125.3, 83.0, 77.6, 55.4, 38.9, 28.3; IR (cm<sup>-1</sup>): 3186 (br), 2914, 1744, 1690, 1366, 1101, 699; HRMS (ESI-TOF) m/z: [M+H]<sup>+</sup> calcd for C<sub>25</sub>H<sub>28</sub>NO<sub>5</sub>S, 454.1683; found, 454.1675. mp: 103-105 °C.  $[\alpha]_D^{25} = -14^\circ$  (c=1.067, CHCl<sub>3</sub>); 98% ee (Table 3.8, entry 10, measured by HPLC as the corresponding methyl ester).

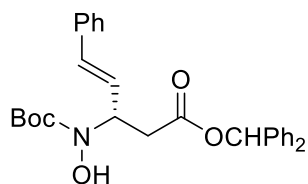
**methyl (S,E)-3-((tert-butoxycarbonyl)(hydroxy)amino)-5-phenylpent-4-enoate (3.44j-Me)**



Clear, colorless oil. <sup>1</sup>H NMR (500 MHz, CDCl<sub>3</sub>) δ 7.40-7.36 (m, 2H), 7.35-7.29 (m, 2H), 7.28-7.23 (m, 1H), 6.61 (d, J = 16 Hz, 1H), 6.49 (br s, 1H), 6.29 (dd, J = 16 Hz, 7 Hz, 1H), 5.10-5.03 (m, 1H), 3.72 (s, 3H), 2.96 (dd, J = 15 Hz, 8.5 Hz, 1H), 2.75 (dd, J = 15 Hz, 6.5 Hz, 1H), 1.50 (s, 9H). <sup>13</sup>C{<sup>1</sup>H} NMR (125 MHz, CDCl<sub>3</sub>): δ 171.7, 157.0, 136.4, 132.9, 128.7, 128.1, 126.7, 125.5, 82.6, 58.5, 52.1, 37.2, 28.4; IR (cm<sup>-1</sup>): 3224 (br), 2977, 1737, 1685, 1161, 1103, 966, 750, 694; HRMS (ESI-TOF) m/z: [M+Na]<sup>+</sup> calcd for C<sub>17</sub>H<sub>23</sub>NO<sub>5</sub>Na, 344.1468; found, 344.1480. HPLC: (7 % isopropanol/hexanes,

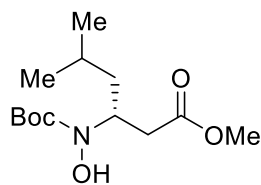
OD-H): Minor enantiomer: 8.0 min; Major enantiomer: 17.2 min; 92% ee.  $[\alpha]_D^{25} = -5^\circ$  (c=0.600, CHCl<sub>3</sub>).

**benzhydryl (S,E)-3-((tert-butoxycarbonyl)(hydroxy)amino)-5-phenylpent-4-enoate (3.44j-Bzh)**



Clear, colorless oil. <sup>1</sup>H NMR (500 MHz, CDCl<sub>3</sub>) δ 7.37-7.23 (m, 15H), 6.90 (s, 1H), 6.58-6.53 (m, 1H), 6.38 (br s, 1H), 6.31-6.26 (m, 1H), 5.13-5.07 (m, 1H), 3.07-3.01 (m, 1H), 2.93-2.87 (m, 1H), 1.46 (s, 9H). <sup>13</sup>C{<sup>1</sup>H} NMR (125 MHz, CDCl<sub>3</sub>): δ 170.1, 157.1, 140.01, 139.97, 136.4, 133.1, 128.7, 128.62, 128.59, 128.1, 128.01, 128.00, 127.3, 127.1, 126.7, 125.2, 82.6, 77.6, 58.7, 37.9, 28.4; IR (cm<sup>-1</sup>): 2977, 1735, 1686, 1157, 1103, 694; HRMS (ESITOF) m/z: [M+Na]<sup>+</sup> calcd for C<sub>29</sub>H<sub>31</sub>NO<sub>5</sub>Na, 496.2094; found, 496.2091.  $[\alpha]_D^{25} = +2^\circ$  (c=0.933, CHCl<sub>3</sub>); 92% ee (Table 3.8, entry 11, measured by HPLC as the corresponding methyl ester).

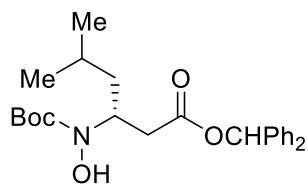
**methyl (R)-3-((tert-butoxycarbonyl)(hydroxy)amino)-5-methylhexanoate (3.44k-Me)**



Clear, colorless oil. <sup>1</sup>H NMR (500 MHz, CDCl<sub>3</sub>) δ 6.45 (br s, 1H), 4.52-4.45 (m, 1H), 3.67 (s, 3H), 2.69 (dd, J = 15 Hz, 8.5 Hz, 1H), 2.43 (dd, J = 15 Hz, 5.5 Hz, 1H), 1.77-1.71 (m, 1H), 1.65-1.58 (m, 1H), 1.48 (s, 9H), 1.19-1.12 (m, 1H), 0.94-0.90 (m, 6H). <sup>13</sup>C{<sup>1</sup>H} NMR (125 MHz, CDCl<sub>3</sub>): δ 172.3, 156.3, 81.9, 53.9, 51.9, 41.1, 37.4, 28.4, 24.8, 23.3, 21.8; IR (cm<sup>-1</sup>): 3207 (br), 2955, 2929, 1740, 1683, 1365, 1168, 1120, 1097; HRMS (ESI-TOF) m/z: [M+Na]<sup>+</sup> calcd for C<sub>13</sub>H<sub>25</sub>NO<sub>5</sub>Na, 298.1625; found, 298.1639. HPLC: (5 % isopropanol/hexanes, AD-H): Minor enantiomer: 7.5 min; Major enantiomer: 9.9 min; 95% ee.  $[\alpha]_D^{25} = +11^\circ$  (c=0.350, CHCl<sub>3</sub>).

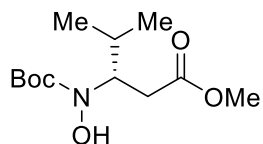


**benzhydryl (R)-3-((tert-butoxycarbonyl)(hydroxy)amino)-5-methylhexanoate (3.44k-Bzh)**



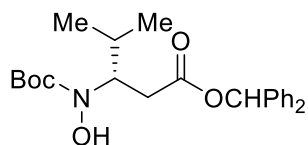
Clear, colorless oil.  $^1\text{H}$  NMR (500 MHz,  $\text{CDCl}_3$ )  $\delta$  7.37-7.24 (m, 10H), 6.88 (s, 1H), 4.57-4.49 (m, 1H), 2.79 (dd,  $J = 15$  Hz, 8 Hz, 1H), 2.61 (dd,  $J = 15$  Hz, 7 Hz, 1H), 1.78-1.71 (m, 1H), 1.63-1.56 (m, 1H), 1.42 (s, 9H), 1.16-1.10 (m, 1H), 0.88 (d,  $J = 7$  Hz, 6H).  $^{13}\text{C}\{^1\text{H}\}$  NMR (125 MHz,  $\text{CDCl}_3$ ):  $\delta$  170.8, 156.4, 140.2, 128.7, 128.6, 128.1, 127.23, 127.18, 82.0, 77.4, 53.9, 40.8, 38.1, 28.3, 24.7, 23.3, 21.8; IR ( $\text{cm}^{-1}$ ): 3199 (br), 2956, 1738 1684, 1165, 1118; HRMS (ESI-TOF)  $m/z$ :  $[\text{M}+\text{Na}]^+$  calcd for  $\text{C}_{25}\text{H}_{33}\text{NO}_5\text{Na}$ , 450.2251; found, 450.2269.  $[\alpha]_D^{25} = +1^\circ$  ( $c=1.000$ ,  $\text{CHCl}_3$ ); 95% ee (Table 3.8, entry 12, measured by HPLC as the corresponding methyl ester).

**methyl (S)-3-((tert-butoxycarbonyl)(hydroxy)amino)-4-methylpentanoate (3.44l-Me)**



Clear, colorless oil.  $^1\text{H}$  NMR (500 MHz,  $\text{CDCl}_3$ )  $\delta$  6.27 (br s, 1H), 4.13-4.07 (m, 1H), 3.67 (s, 3H), 2.73 (dd,  $J = 15$  Hz, 10 Hz, 1H), 2.55 (dd,  $J = 15$  Hz, 4 Hz, 1H), 1.98-1.89 (m, 1H), 1.48 (s, 9H), 0.95 (dd,  $J = 6.5$  Hz, 2Hz, 6H).  $^{13}\text{C}\{^1\text{H}\}$  NMR (125 MHz,  $\text{CDCl}_3$ ):  $\delta$  172.8, 156.5, 81.6, 61.4, 51.9, 34.8, 31.1, 28.4, 19.8, 19.5; IR ( $\text{cm}^{-1}$ ): 3209 (br), 2964, 1742, 1683, 1169, 1129; HRMS (ESI-TOF)  $m/z$ :  $[\text{M}+\text{Na}]^+$  calcd for  $\text{C}_{12}\text{H}_{23}\text{NO}_5\text{Na}$ , 284.1468; found 284.1480. HPLC: (5 % isopropanol/hexanes, AD-H): Minor enantiomer: 9.5 min; Major enantiomer: 12.9 min; 98% ee.  $[\alpha]_D^{25} = -1^\circ$  ( $c=0.600$ ,  $\text{CHCl}_3$ ).

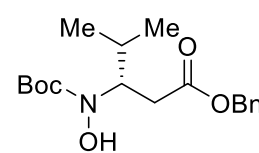
**benzhydryl (S)-3-((tert-butoxycarbonyl)(hydroxy)amino)-4-methylpentanoate (3.44l-Bzh)**



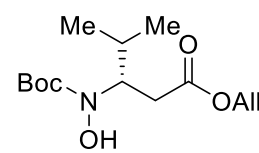
Clear, colorless oil.  $^1\text{H}$  NMR (500 MHz,  $\text{CDCl}_3$ )  $\delta$  7.34-7.27 (m, 10H), 6.87 (s, 1H), 6.06 (br s, 1H), 4.19-4.12 (m, 1H), 2.84 (dd,  $J = 15$  Hz, 10 Hz, 1H), 2.67 (dd,  $J = 15$  Hz, 5 Hz, 1H), 2.00-1.90 (m, 1H), 1.41 (s,

9H), 0.94 (d,  $J = 7$  Hz, 6H).  $^{13}\text{C}\{^1\text{H}\}$  NMR (125 MHz,  $\text{CDCl}_3$ ):  $\delta$  171.4, 156.3, 140.12, 140.05, 128.67, 128.65, 128.1, 127.3, 127.2, 81.8, 77.5, 61.3, 35.5, 31.3, 28.4, 19.8, 19.5; IR ( $\text{cm}^{-1}$ ): 3207 (br), 2968, 1737, 1681, 1162, 1117, 743, 697; HRMS (ESI-TOF)  $m/z$ :  $[\text{M}+\text{Na}]^+$  calcd for  $\text{C}_{24}\text{H}_{31}\text{NO}_5\text{Na}$ , 436.2094; found, 436.2090.  $[\alpha]_D^{25} = -1^\circ$  ( $c=0.467$ ,  $\text{CHCl}_3$ ); 98% ee (Table 3.8, entry 13, measured by HPLC as the corresponding methyl ester).

**benzyl (S)-3-((tert-butoxycarbonyl)(hydroxy)amino)-4-methylpentanoate (3.44I-Bn)**

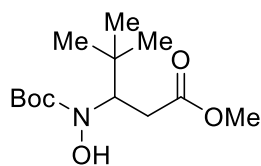
 Clear, colorless oil.  $^1\text{H}$  NMR (500 MHz,  $\text{CDCl}_3$ )  $\delta$  7.38-7.30 (m, 5H), 5.10 (s, 2H), 4.17-4.11 (m, 1H), 2.79 (dd,  $J = 15$  Hz, 10 Hz, 1H), 2.60 (dd,  $J = 15$  Hz, 5 Hz, 1H), 1.99-1.90 (m, 1H), 1.46 (s, 9H), 0.95 (dd,  $J = 6.5$  Hz, 2 Hz, 6H).  $^{13}\text{C}\{^1\text{H}\}$  NMR (125 MHz,  $\text{CDCl}_3$ ):  $\delta$  172.1, 156.6, 135.8, 128.6, 128.29, 128.25, 81.6, 66.6, 61.3, 35.1, 31.1, 28.4, 19.8, 19.4; IR ( $\text{cm}^{-1}$ ): 3206 (br), 2966, 1737, 1681, 1164, 1118; HRMS (ESI-TOF)  $m/z$ :  $[\text{M}+\text{Na}]^+$  calcd for  $\text{C}_{18}\text{H}_{27}\text{NO}_5\text{Na}$ , 360.1781; found 360.1782.  $[\alpha]_D^{25} = -4^\circ$  ( $c=0.667$ ,  $\text{CHCl}_3$ ); 98% ee (Table 3.8, entry 14, measured by HPLC as the corresponding methyl ester).

**allyl (S)-3-((tert-butoxycarbonyl)(hydroxy)amino)-4-methylpentanoate (3.44I-Allyl)**

 Clear, colorless oil.  $^1\text{H}$  NMR (500 MHz,  $\text{CDCl}_3$ )  $\delta$  6.16 (br s, 1H), 5.95-5.85 (m, 1H), 5.34-5.29 (m, 1H), 5.25-5.22 (m, 1H), 4.59-4.55 (m, 2H), 4.15-4.08 (m, 1H), 2.75 (dd,  $J = 15$  Hz, 10 Hz, 1H), 2.58 (dd,  $J = 15$  Hz, 4 Hz, 1H), 1.99-1.91 (m, 1H), 1.48 (s, 9H), 0.95 (dd,  $J = 7$  Hz, 3 Hz, 6H).  $^{13}\text{C}\{^1\text{H}\}$  NMR (125 MHz,  $\text{CDCl}_3$ ):  $\delta$  171.9, 156.6, 132.1, 118.4, 81.5, 65.4, 61.3, 35.1, 31.0, 28.4, 19.8, 19.4; IR ( $\text{cm}^{-1}$ ): 3197 (br), 2966, 1738, 1682, 1166, 1120; HRMS (ESI-TOF)  $m/z$ :  $[\text{M}+\text{Na}]^+$  calcd for

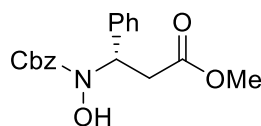
C<sub>14</sub>H<sub>25</sub>NO<sub>5</sub>Na, 310.1625; found 310.1616. [ $\alpha$ ]<sub>D</sub><sup>25</sup> = -2° (c=0.667, CHCl<sub>3</sub>); 96% ee (Table 3.8, entry 15, measured by HPLC as the corresponding methyl ester).

**methyl 3-((tert-butoxycarbonyl)(hydroxy)amino)-4,4-dimethylpentanoate (3.44m-Me)**



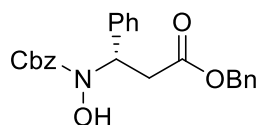
<sup>1</sup>H NMR (500 MHz, CDCl<sub>3</sub>)  $\delta$  6.82 (br s, 1H), 4.18 (br dd, 1H), 3.65 (s, 3H), 2.88 (br dd, 1H), 2.45 (br dd, 1H), 1.48 (s, 9H), 0.97 (s, 9H). <sup>13</sup>C{<sup>1</sup>H} NMR (125 MHz, (CD<sub>3</sub>)<sub>2</sub>CO):  $\delta$  172.9, 157.2, 80.8, 63.6, 51.8, 36.0, 31.8, 28.7, 27.6; IR (cm<sup>-1</sup>): 3188 (br), 2957, 1741, 1680, 1163, 1108; HRMS (ESI-TOF) m/z: [M+Na]<sup>+</sup> calcd for C<sub>13</sub>H<sub>25</sub>NO<sub>5</sub>Na, 298.1625; found 298.1635.

**methyl (S)-3-(((benzyloxy)carbonyl)(hydroxy)amino)-3-phenylpropanoate (3.44n-Me)**



Clear, colorless oil. <sup>1</sup>H NMR (500 MHz, CDCl<sub>3</sub>)  $\delta$  7.38-7.27 (m, 10H), 6.52 (br s, 1H), 5.60 (dd, J = 10 Hz, 5.5 Hz, 1H), 5.19 (d, J = 12 Hz, 1H), 5.14 (d, J = 12 Hz, 1H), 3.65 (s, 3H), 3.21 (dd, J = 15.5 Hz, 10 Hz, 1H), 2.89 (dd, J = 15.5 Hz, 5.5 Hz, 1H). <sup>13</sup>C{<sup>1</sup>H} NMR (125 MHz, CDCl<sub>3</sub>):  $\delta$  171.7, 157.1, 138.4, 135.9, 128.7, 128.6, 128.4, 128.19, 128.17, 127.4, 68.3, 59.3, 52.2, 36.8; IR (cm<sup>-1</sup>): 3276 (br), 2952, 1695, 1271, 1098, 696; HRMS (ESI-TOF) m/z: [M+Na]<sup>+</sup> calcd for C<sub>18</sub>H<sub>19</sub>NO<sub>5</sub>Na, 352.1155; found, 352.1157. HPLC: (10 % isopropanol/hexanes, AD-H): Major enantiomer: 16.8 min; Minor enantiomer: 24.1 min; 78% ee (Table 3.8, entry 19). [ $\alpha$ ]<sub>D</sub><sup>25</sup> = -24° (c=0.800, CHCl<sub>3</sub>).

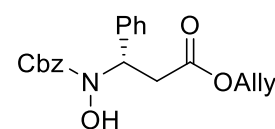
**benzyl (S)-3-(((benzyloxy)carbonyl)(hydroxy)amino)-3-phenylpropanoate (3.44n-Bn)**



Clear, colorless oil. <sup>1</sup>H NMR (500 MHz, CDCl<sub>3</sub>)  $\delta$  7.38-7.26 (m, 15H), 6.74 (br s, 1H), 5.63 (dd, J = 10 Hz, 6 Hz, 1H), 5.18-5.14 (m, 1H), 5.11-5.06 (m, 3H), 3.25 (dd, J = 16 Hz, 10 Hz, 1H), 2.96 (dd, J = 16 Hz, 6 Hz, 1H). <sup>13</sup>C{<sup>1</sup>H} NMR (125 MHz, CDCl<sub>3</sub>):  $\delta$  171.0, 157.1, 138.3, 135.8, 135.6, 128.63, 128.56, 128.4, 128.3, 128.13,

128.09, 127.5, 68.2, 66.8, 59.2, 37.1; IR (cm<sup>-1</sup>): 3261 (br), 2950, 1731, 1695, 694; HRMS (ESI-TOF) m/z: [M+Na]<sup>+</sup> calcd for C<sub>24</sub>H<sub>23</sub>NO<sub>5</sub>Na, 428.1458; found, 428.1468.  $[\alpha]_D^{25} = -26^\circ$  (c=0.800, CHCl<sub>3</sub>); 87% ee (Table 3.8, entry 20, measured by HPLC as the corresponding methyl ester).

**allyl (S)-3-(((benzyloxy)carbonyl)(hydroxy)amino)-3-phenylpropanoate (3.44n-Allyl)**

 Clear, colorless oil. <sup>1</sup>H NMR (500 MHz, CDCl<sub>3</sub>) δ 7.39-7.27 (m, 10H), 6.73 (br s, 1H), 5.89-5.80 (m, 1H), 5.62 (dd, J = 10 Hz, 6 Hz, 1H), 5.29-5.24 (m, 1H), 5.22-5.15 (m, 2H), 5.15-5.10 (m, 1H), 4.57-4.55 (m, 2H), 3.23 (dd, J = 15 Hz, 10 Hz, 1H), 2.92 (dd, J = 15 Hz, 6 Hz, 1H). <sup>13</sup>C{<sup>1</sup>H} NMR (125 MHz, CDCl<sub>3</sub>): δ 170.8, 157.1, 138.4, 135.9, 131.8, 128.61, 128.55, 128.3, 128.11, 128.09, 127.5, 118.6, 68.2, 65.6, 59.2, 37.0; IR (cm<sup>-1</sup>): 3267 (br), 2947, 1732, 1696, 1271, 1098, 696; HRMS (ESI-TOF) m/z: [M+Na]<sup>+</sup> calcd for C<sub>20</sub>H<sub>21</sub>NO<sub>5</sub>Na, 378.1312; found, 378.1308.  $[\alpha]_D^{25} = -26^\circ$  (c=0.667, CHCl<sub>3</sub>); 89% ee (Table 3.8, entry 21, measured by HPLC as the corresponding methyl ester).

## 3.15 References

1. The results in this chapter were previously published: Straub, M. R.; Birman, V. B. *Org. Lett.* **2021**, *23*, 984.
2. For a comprehensive review of catalytic enantioselective syntheses of isoxazolidine-5-ones, see: Annibaleto, J.; Oudeyer, S.; Levacher, V.; Briere, J.-F. *Synthesis* **2017**, *49*, 2117.
3. (a) Ibrahim, I.; Rios, R.; Vesely, J.; Zhao, G.-L.; Cordova, A. *Chem. Commun.* **2007**, 849. (b) Ibrahim, I.; Rios, R.; Vesely, J.; Zhao, G.-L.; Cordova, A. *Synthesis* **2008**, *2008*, 1153.
4. Izumi, S.; Kobayashi, Y.; Takemoto, Y. *Org. Lett.* **2016**, *18*, 696.
5. Kamlar, M.; Cisarova, I.; Hybelbauerova, S.; Vesely, J. *Eur. J. Org. Chem.* **2017**, *2017*, 1926.
6. (a) Yu, J.-S.; Noda, H.; Shibasaki, M. *Angew. Chem., Int. Ed.* **2018**, *57*, 818. See also: (b) Cadart, T.; Berthonneau, C.; Levacher, V.; Perrio, S.; Briere, J.-F. *Chem. – Eur. J.* **2016**, *22*, 15261. (c) Tite, T.; Sabbah, M.; Levacher, V.; Briere, J.-F. *Chem. Commun.* **2013**, *49*, 11569. (d) Capaccio, V.; Zielke, K.; Eitzinger, A.; Massa, A.; Palombi, L.; Faust, K.; Waser, M. *Org. Chem. Front.* **2018**, *5*, 3336. (e) Eitzinger, A.; Winter, M.; Schoergenheimer, J.; Waser, M. *Chem. Commun.* **2020**, *56*, 579–582. (f) Capaccio, V.; Sicignano, M.; Rodriguez, R. I.; Della Sala, G.; Aleman, J. *Org. Lett.* **2020**, *22*, 219.

7. For asymmetric catalytic approaches to N-alkylisoxazolidinones, see: (a) Sibi, M. P.; Liu, M. *Org. Lett.* **2001**, *3*, 4181. (b) Sibi, M. P.; Prabakaran, N.; Ghorpade, S. G.; Jasperse, C. P. *J. Am. Chem. Soc.* **2003**, *125*, 11796.
8. For select noncatalytic approaches to enantioenriched isoxazolidinones, see: (a) Ishikawa, T.; Nagai, K.; Kudoh, T.; Saito, S. *Synlett* **1995**, *1995*, 1171. (b) Juarez-Garcia, M.; Yu, S.; Bode, J. W. *Tetrahedron* **2010**, *66*, 4841 (c) Frazier, C. P.; Engelking, J. R.; Read de Alaniz, J. *J. Am. Chem. Soc.* **2011**, *133*, 10430.
9. (a) Berini, C.; Sebban, M.; Oulyadi, H.; Sanselme, M.; Levacher, V.; Briere, J.-F. *Org. Lett.* **2015**, *17*, 5408. See also: (b) Le Foll Devaux, A.; Deau, E.; Corrot, E.; Bischoff, L.; Levacher, V.; Briere, J.-F. *Eur. J. Org. Chem.* **2017**, *2017*, 3265. See also: (c) Martzel, T.; Annibaleto, J.; Millet, P.; Pair, E.; Sanselme, M.; Oudeyer, S.; Levacher, V.; Briere, J.-F. *Chem. – Eur. J.* **2020**, *26*, 8541.
10. Kagan, H. B.; Fiaud, J. C. “Kinetic Resolution” *Top. Stereochem.* **1988**, *18*, 249.
11. Vedejs, E.; Jure, M. *Angew. Chem. Int. Ed.* **2005**, *44*, 3974.
12. Hang, J.; Tian, S.-K.; Tang, L.; Deng, L. *J. Am. Chem. Soc.* **2001**, *123*, 12696.
13. Willis, M. C. *J. Chem. Soc., Perkin Trans. 1* **1999**, 1765.
14. Chen, Y.; Tian, S.-K.; Deng, L. *J. Am. Chem. Soc.* **2000**, *122*, 9542.
15. Bumbu, V.; Birman, V. B. *J. Am. Chem. Soc.* **2011**, *133*, 13902.
16. Berkessel, A.; Cleemann, F.; Mukherjee, S.; Mueller, T. N.; Lex, J. *Angew. Chem. Int. Ed.* **2005**, *44*, 807.
17. Yang, X.; Lu, G.; Birman, V. B. *Org. Lett.* **2010**, *12*, 892.

18. Berkessel, A.; Cleemann, F.; Mukherjee, S. *Angew. Chem. Int. Ed.* **2005**, *44*, 7466.
19. White, A. J.; Wharton, C. W. *Biochem.* **1990**, *270*, 627.
20. (a) Connon, S. J. *Chem. Commun.* **2008**, 2499. (b) Bhadury, P. S.; Song, B.-A.; Yang, S.; Hu, D.-Y.; Xue, W. *Curr. Org. Synth.* **2009**, *6*, 380. (c) Aleman, J.; Parra, A.; Jiang, H.; Jorgensen, K. A. *Chem. Eur. J.* **2011**, *17*, 6890. (d) Serdyuk, O. V.; Heckel, C. M.; Tsogoeva, S. B. *Org. Biomol. Chem.* **2013**, *11*, 7051. (e) Fang, X.; Wang, C.-J. *Chem. Commun.* **2015**, *51*, 1185.
21. Herrera, R. P.; Sgarzani, V.; Bernardi, L.; Ricci, A. *Angew. Chem. Int. Ed.* **2005**, *44*, 6576.
22. Okino, T.; Hoashi, Y.; Takemoto, Y. *J. Am. Chem. Soc.* **2003**, *125*, 12672.
23. Hamza, A.; Schubert, G.; Soós, T.; Pápai, I. *J. Am. Chem. Soc.* **2006**, *128*, 13151.
24. Wang, J.; Li, H.; Yu, X.; Zu, L.; Wang, W. *Org. Lett.* **2005**, *7*, 4293.
25. Vakulya, B.; Varga, S.; Csampai, A.; Soós, T. *Org. Lett.* **2005**, *7*, 1967.
26. Liu, K.; Han-Feng, C.; Jing, N.; Ke-Yan, D.; Xiao-Juan, L.; Jun-An, M. *Org. Lett.* **2007**, *9*, 923.
27. Birman, V. B.; Li, X. *Org. Lett.* **2006**, *8*, 1351.
28. Birman, V. B.; Uffman, E. W.; Jiang, H.; Li, X.; Kilbane, C. J. *J. Am. Chem. Soc.* **2004**, *126*, 12226.
29. Sohtome, Y.; Tanatani, A.; Hashimoto, Y.; Nagasawa, K. *Tetrahedron Lett.* **2004**, *45*, 5589.

30. Gomez-Torres, E.; Alonso, D. A.; Gomez-Bengoa, E.; Najera, C. *Org. Lett.* **2011**, *13*, 6106.
31. Azuma, T.; Murata, A.; Kobayashi, Y.; Inokuma, T.; Takemoto, Y. *Org. Lett.* **2014**, *16*, 4256.
32. Konishi, H.; Lam, T. Y.; Malerich, J. P.; Rawal, V. H. *Org. Lett.* **2010**, *12*, 2028.
33. Yang, W.; Du, D.-M. *Org. Lett.* **2010**, *12*, 5450.
34. Hu, B.; Bezpalko, M. W.; Fei, C.; Dickie, D. A.; Foxman, B. M.; Deng, L. *J. Am. Chem. Soc.* **2018**, *140*, 13913.
35. Baldwin, J. E. *J. Chem. Soc., Chem. Commun.* **1976**, 734.
36. Thorpe-Ingold effect: Beesley, R. M.; Ingold, C. K.; Thorpe, J. F. *J. Chem. Soc., Trans.* **1915**, *107*, 1080.
37. Drennhaus, T.; Oehler, L.; Djalali, S.; Hoefmann, S.; Mueller, C.; Pietruszka, J.; Worgull, D. *Adv. Synth. Catal.* **2020**, *362*, 2385-2396.
38. Kummer, D. A.; Chain, W. J.; Morales, M. R.; Quiroga, O.; Myers, A. G. *J. Am. Chem. Soc.* **2008**, *130*, 13231.
39. Diosdado, S.; Lopez, R.; Palomo, C. *Chem. Eur. J.* **2014**, *20*, 6526.



# Chapter 4: Organocatalyzed rearrangements of thioesters<sup>1</sup>

## 4.1 General introduction to asymmetric acyl transfer catalysis

Asymmetric acyl transfer catalysis is an indispensable tool in enantioselective synthesis. As was evidenced in Chapters 2 and 3, new discoveries are still being made in this area of research, but a lot of areas are yet to be explored. Acyl transfer catalysis operates via three general reaction pathways outlined in Figure 4.1. Pathway 3a, starting with an activated carboxylic acid derivative **4.10**, was outlined in Chapter 2.

In pathway 1, a generic acyl donor **4.01** reacts with a Lewis basic acyl transfer catalyst (Cat) to generate reactive ion pair **4.02**. A nucleophile H-Nu then displaces the catalyst and generates the final product. A classic example of this reaction pathway would be an esterification of an alcohol catalyzed by 4-(dimethylamino)pyridine (DMAP).<sup>2</sup> In pathway 2, an  $\alpha,\beta$ -unsaturated acyl donor **4.04** reacts with the catalyst to form reactive ion pair **4.05** which can react with a Michael donor (Pathway 2a). Alternatively, the unsaturated acyl ammonium cation may react with a diene in a [4+2] cycloaddition fashion to deliver Diels-Alder adduct **4.08** (Pathway 2b). Regardless of which pathway operates, another nucleophile is introduced to turn over the catalyst. In pathway 3, an acyl donor with an acidic  $\alpha$  proton reacts with a catalyst and undergoes deprotonation to form zwitterion **4.13**. This zwitterionic species can also be made from the corresponding ketene **4.12**. This zwitterion can react with a pi-electrophile, delivering a product resulting from a formal [2+2] cycloaddition (Pathway 3a). Alternatively, the zwitterion can react with an electrophile in an S<sub>N</sub>2 fashion. The displaced nucleofuge can then replace the catalyst, generating the final product **4.17** (Pathway 3b).

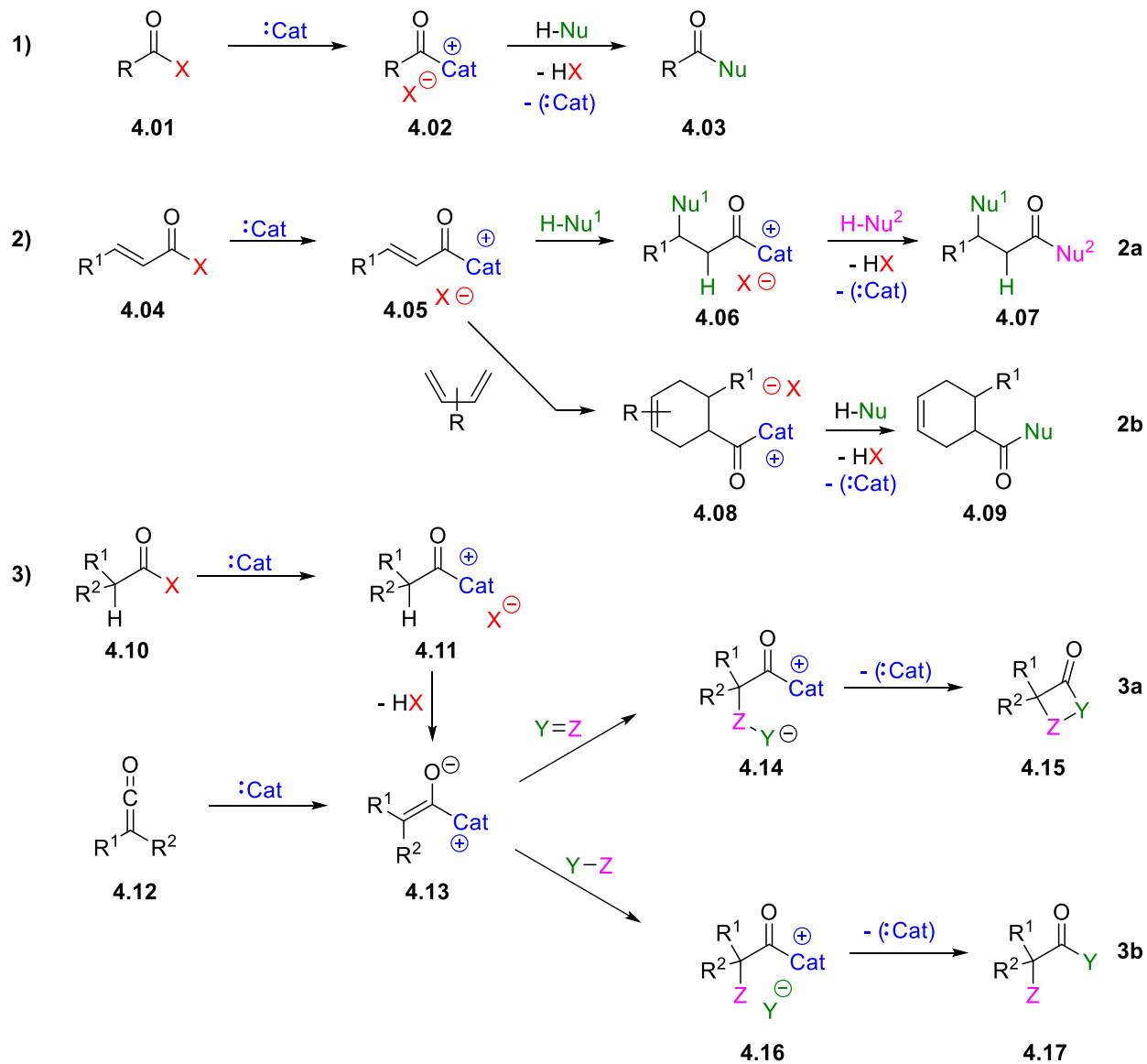


**Figure 4.1.** Three mechanistically distinct pathways involving catalytic acyl transfer.

Several structurally distinct groups of Lewis basic catalysts have been used as acyl transfer catalysts (Figure 4.2). 4-aminopyridines such as DMAP and 4-pyrrolidinopyridine (PPY), phosphines, N-alkylimidazoles, and N-heterocyclic carbenes (NHCs) are among the most common.

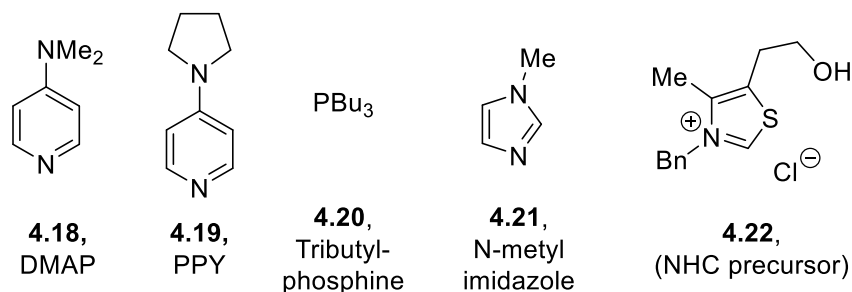


**Figure 4.2.** Some examples from the most common classes of achiral acyl transfer catalysts.

While all the catalysts listed in Figure 4.2 are achiral, significant progress has been made since the 1990s to synthesize chiral variants of these catalysts and render their catalyzed processes enantioselective.<sup>3</sup> Some of the most illustrative chiral catalysts in this regard are given in Figure 4.3.<sup>4</sup>

Prior to these works, lipase and esterase families of enzymes, in addition to naturally occurring alkaloids, were most used for enantioselective acyl transfer. In 2004 our group designed and introduced an alternative class of chiral acyl transfer catalysts that we called amidine-based catalysts (ABCs) (see Figure 2.5, section 2.4 where they were first introduced). With this new class of catalysts, our goal was to i) make these catalysts from cheap and commercially available starting materials, ii) synthesize them with a minimal number of steps, and iii) allow for easy incorporation of a chiral center adjacent to the Lewis basic nitrogen without destroying its catalytic activity.<sup>5</sup> Continually inspired by the broad synthetic uses of ABCs by our group and others, we became interested in yet another unexplored application: their ability to activate thioesters via nucleophilic acyl substitution.

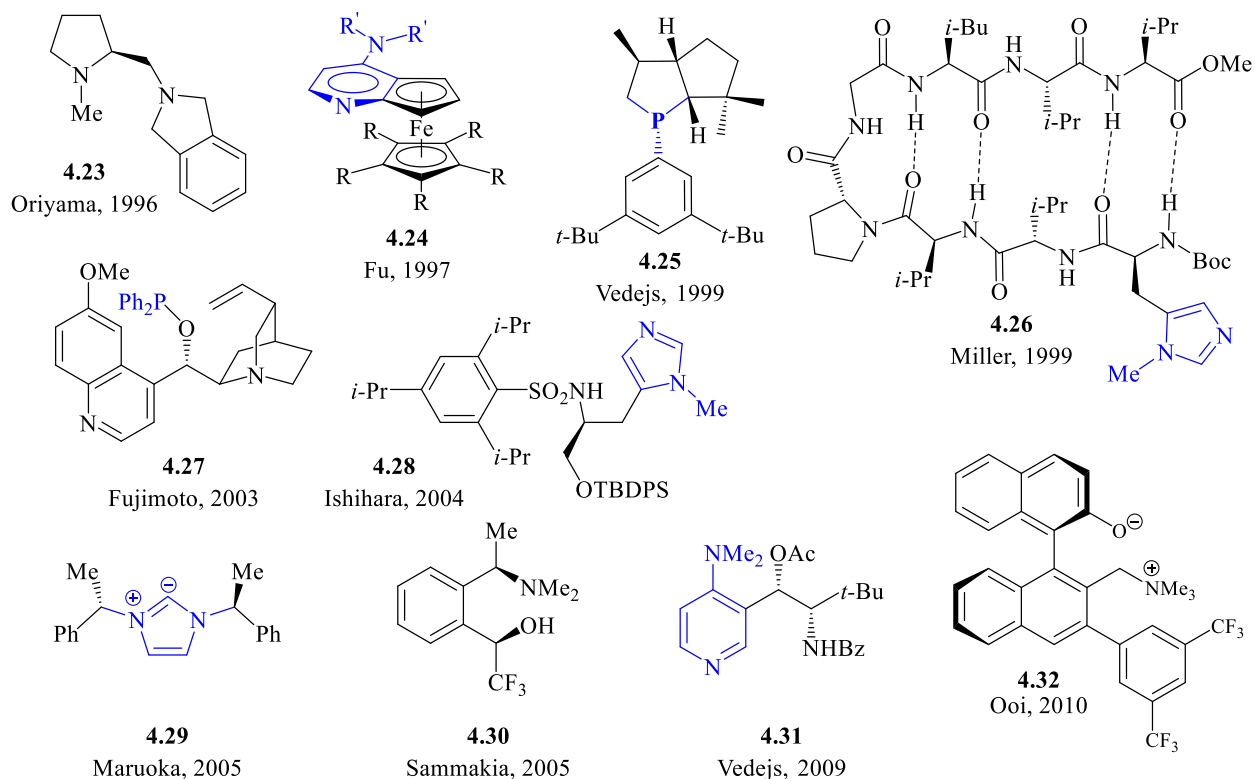


**Figure 4.3.** Chiral acyl transfer catalysts developed by other groups.

## 4.2 Introduction to thioesters as acyl donors

The most conventional acyl donors (Figure 4.4) such as acid chlorides, mixed and symmetrical acid anhydrides, and highly activated esters are all easily activated by Lewis base catalysts. However, less reactive acyl donors such as thioesters had remained underexplored in this context of acyl transfer catalysis until recently.

Despite their relatively low reactivity thioesters offer some distinct advantages as acyl donors. As shown in Figure 4.4, acyl donors generate stoichiometric amounts of byproduct, the leaving group, or nucleofuge. This often requires stoichiometric amounts of base or another

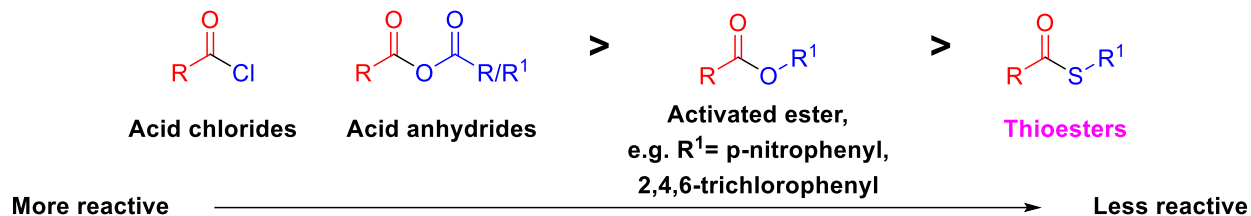


**Figure 4.4:** Conventional acyl donors and thioesters. The acyl group is highlighted in *red* and the leaving group (nucleofuge) is highlighted in *blue*.

additive to quench the byproduct over the course of the reaction. Thioesters are unique in that the displaced nucleofuge, the thiolate anion, is an inherently soft and highly nucleophilic species. If the structure of the acyl donor allows it, the resulting thiolate anion can essentially be repurposed in the next step of the catalytic cycle as a nucleophile, allowing the sulfur-containing leaving group to be incorporated into the final product. This obviates the need for additional stoichiometric reagents and allows the acyl donor to rearrange into a new product, possibly without generating additional byproducts. Furthermore, this rearrangement mode allows for an unconventional approach to  $\text{C}_1$  ammonium zwitterionic enolates, key intermediates in many pathways involving catalytic acyl transfer (Figure 4.5). This can exclude the need for up to two procedural steps, activation of a carboxylic acid and an externally introduced nucleophile (NuH), translating to greater operational simplicity.

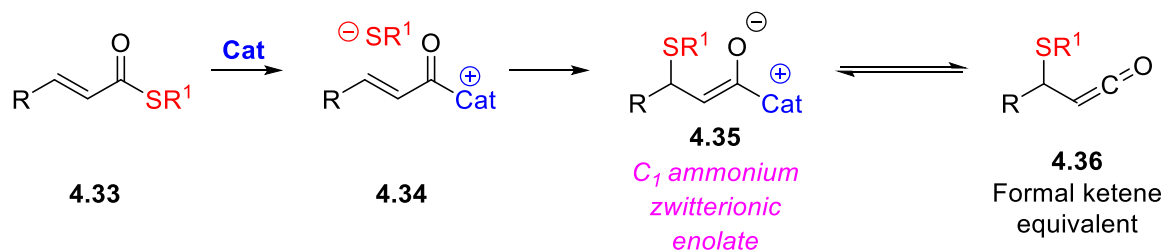


**Figure 4.5:** Thioesters: An alternative approach to  $\text{C}_1$  ammonium zwitterionic enolates.

Interestingly, prior to our involvement, few examples of an acyl donor amenable to this rearrangement mode were reported in the literature. An example by the Lupton group in 2009 demonstrated that enol ester **4.37** reacted with NHC catalyst **4.38**. The displaced enolate reacted via a Michael addition to generate zwitterionic ammonium enolate **4.40**. Tautomerization and lactonization led to the final product **4.42**. (Figure 4.6).<sup>6</sup>

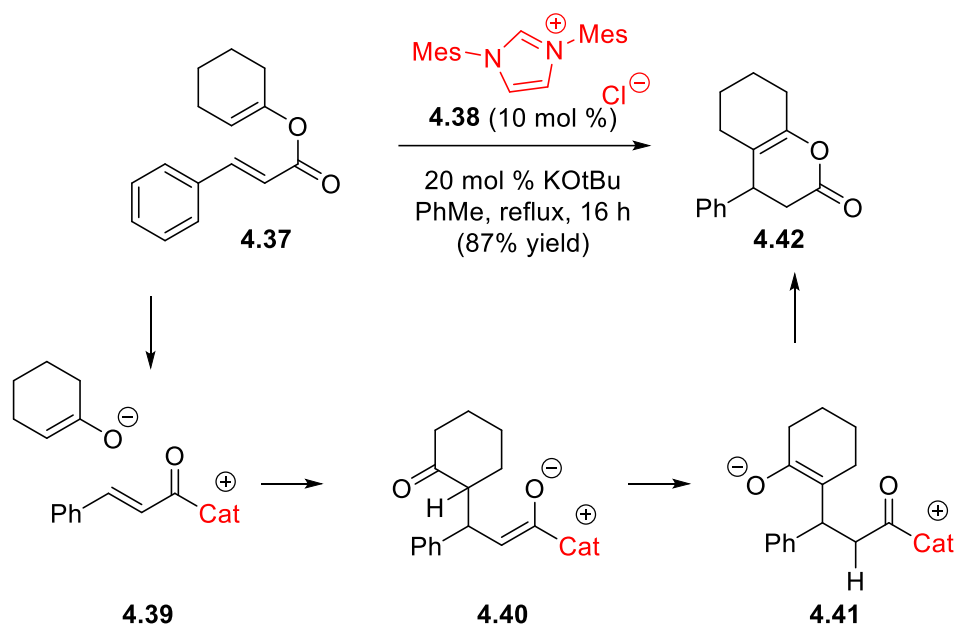


**Figure 4.6:** Organocatalyzed rearrangement of an enol ester.

Another example of an asymmetric organocatalyzed rearrangement was disclosed in 2014 by Matsubara.<sup>7</sup>  $\gamma$ -hydroxy- $\alpha,\beta$ -unsaturated thioesters **4.43** were subjected to rearrangement into  $\beta$ -mercaptolactones **4.45** using Takemoto's catalyst **4.44** (see Chapter 3.3); however, further studies are needed to fully elucidate the reaction mechanism (Figure 4.7).

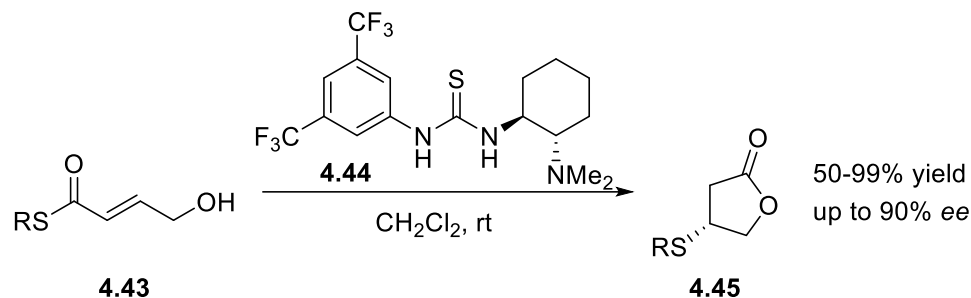


**Figure 4.7.** Organocatalyzed rearrangement of  $\omega$ -hydroxy- $\alpha,\beta$ -unsaturated thioesters.

## 4.3 Our previous work on rearrangements of thioesters

Despite the scarcity of literature precedent our group aimed to verify the use of thioesters as acyl donors operating in a rearrangement mode.

### 4.3.1 Asymmetric synthesis of thiochromenes

With this newly conceived idea in hand, our group set out to explore the catalytic rearrangement of  $\alpha,\beta$ -unsaturated thioester **4.46a** (Figure 4.8, R = H, R<sup>1</sup> = Ph, X=CH).

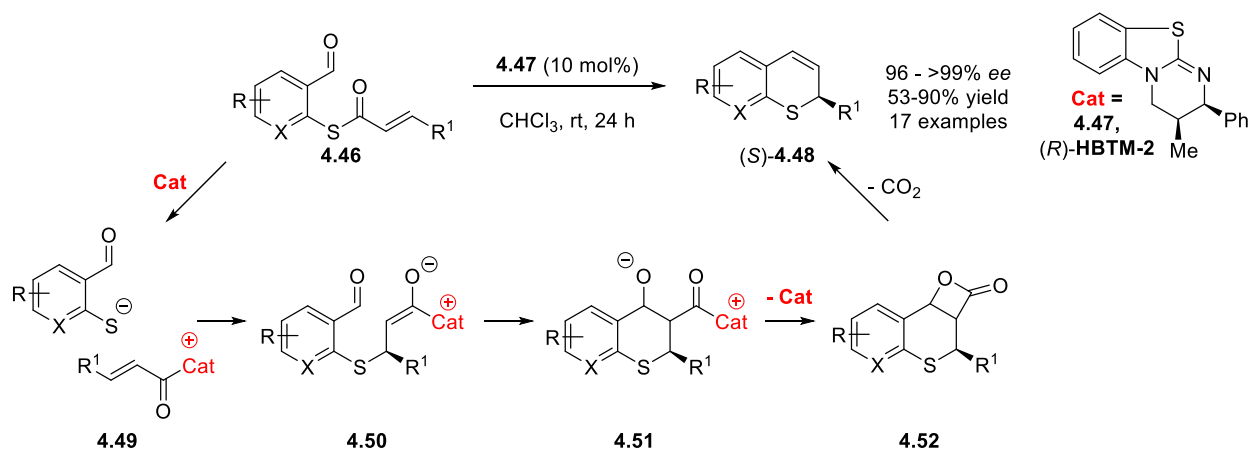


**Figure 4.8:** Organocatalyzed enantioselective rearrangements of ortho-formylthioesters using HBTM-2.

The key to this test substrate is the pi-electrophilic aldehyde moiety that is tethered in the molecule. In addition to activating the thioacyl moiety, this serves as a trap for the zwitterionic ammonium enolate intermediate. A member of our group, Dr. Nick Ahlemeyer, discovered that not only does this reaction work in the envisioned rearrangement mode, but that the process can be rendered enantioselective with chiral acyl transfer catalyst (*R*)-HBTM-2<sup>8</sup> **4.47**.<sup>9</sup>

### 4.3.2 Asymmetric synthesis of thiochromanes

After revealing this proof of concept, our group quickly began exploring an analogous [4+2] cycloaddition<sup>10</sup> utilizing enone-containing S-aryl thioesters **4.53** (Figure 4.9). The mechanism is conceptually analogous to the thiochromene synthesis, with the main difference being an intramolecular Michael addition replacing the intramolecular aldehyde addition.

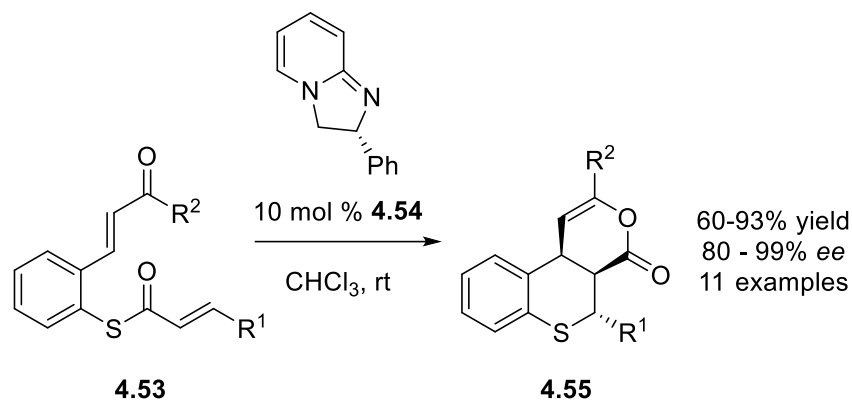


**Figure 4.9:** Organocatalyzed enantioselective rearrangement of S-aryl thioesters into tricyclic ene-lactones using H-PIP.

While this reaction did work with catalyst DHPB<sup>11</sup> **4.56a**, the reaction was very sluggish, reaching about 35% conversion after 5 days. This was in stark contrast to DHPB's activity with ortho-formylthioester **4.46a**, where clean conversion to the thiochromene was observed after 15

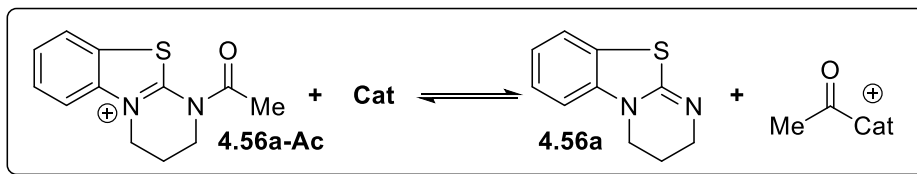


hours. Unfortunately, the reaction did not occur even after one week with chiral derivative HBTM-2, which worked optimally in the enantioselective thiochromene synthesis.

It was hypothesized that more Lewis basic catalysts would overcome the issue of lower reactivity of this structure of thioesters. As a result, a computational study was performed to calculate the isodesmic acyl transfer enthalpy between N-acetyl DHPB cation **4.56a-Ac** and various other achiral amidine-based catalysts (Figure 4.10, see reference 10 for more specific details). With the acylation enthalpy of DHPB being set to zero, a negative acylation enthalpy implies that the catalyst is more Lewis basic than DHPB.

The results of this study suggested that all catalysts for which the calculation was conducted would display higher Lewis basicity than DHPB. This correlated well with reality, with DHIP<sup>12</sup> **4.59a**, for example, giving 430 times increase in reaction rate compared to DHPB (relative rate) for the tandem reaction outlined in Figure 4.9. Consequently, the chiral derivative of DHIP, H-PIP<sup>12</sup> **4.54**, was chosen for the substrate scope (Figure 4.9). It should also be noted that during studies by our group, Xu et al. disclosed the same transformation enabled by a chiral NHC catalyst.<sup>13</sup>

The results of this study were vital. The data suggested that more Lewis basic acyl transfer catalysts were necessary for reacting with these less reactive acyl donors and that the standard “go-to” acyl transfer catalysts like DMAP are insufficient in this context. While intuition will naturally lead to this conclusion, simple computational results correlated well with experimental reality. In fact, all catalysts listed in Figure 4.10 catalyzed the tandem transformation faster than DHPB. Of all catalysts listed in Figure 4.10, the modification of one core structure remained uninvestigated: the DHIP structure. Considering that DHIP gave one of the largest accelerations of the tandem reaction outlined in Figure 4.9, it was anticipated that more electron rich derivatives would



#	X	$\Delta H_{Ac}$ (Kcal/mol)	Relative rate	#	X	$\Delta H_{Ac}$ (Kcal/mol)	Relative rate
4.56a	H	0	1	4.57a	H	-4.53	210
4.56b	OMe	-1.73	3.20	4.57b	OMe	-5.20	308
4.56c	NMe <sub>2</sub>	-3.65	22.6	4.57c	NMe <sub>2</sub>	-6.23	574
4.56d	N-pyrrolidino	-4.36	31.3	4.57d	N-pyrrolidino	-6.38	537
	4.56e			#	X	$\Delta H_{Ac}$ (Kcal/mol)	Relative rate
		$\Delta H_{Ac} = -7.36$ (Kcal/mol)		4.58a	H	-4.10	98
		Rel. rate = 221		4.58b	OMe	-4.79	180
				4.58c	NMe <sub>2</sub>	-6.10	392
				4.58d	N-pyrrolidino	-6.19	509
	4.59a						
		$\Delta H_{Ac} = -8.70$ (Kcal/mol)					
		Rel. rate = 430					

**Figure 4.10.** Relative acylation enthalpies and relative rates of various achiral ABCs.

lead to even larger relative rates. Furthermore, these highly nucleophilic catalysts were expected to react well with even less reactive acyl donors.

## 4.4 Synthesis and exploration of 5-aryl-DHIP derivatives

Computational results from the isodesmic acyl transfer equation revealed that DHIP with electron-donating substituents, particularly aryl groups, at the 5-position display even more negative acylation enthalpies (see **4.59b** and **4.59c** in Figure 4.13). Simple resonance considerations would place greater negative charge on the reacting nitrogen (Figure 4.11). While 7-substitution would also increase electron density on the nitrogen, the 5-substituted derivatives are arguably easier to prepare. Additionally, our calculations predicted little difference in how 5- and 7-substitution would affect the reactivity of the catalyst. Placing an electron donating group such as methoxy or dialkylamino on the DHIP core is also expected to increase its Lewis basicity; however, these compounds were predicted to be unstable during catalyst preparation.

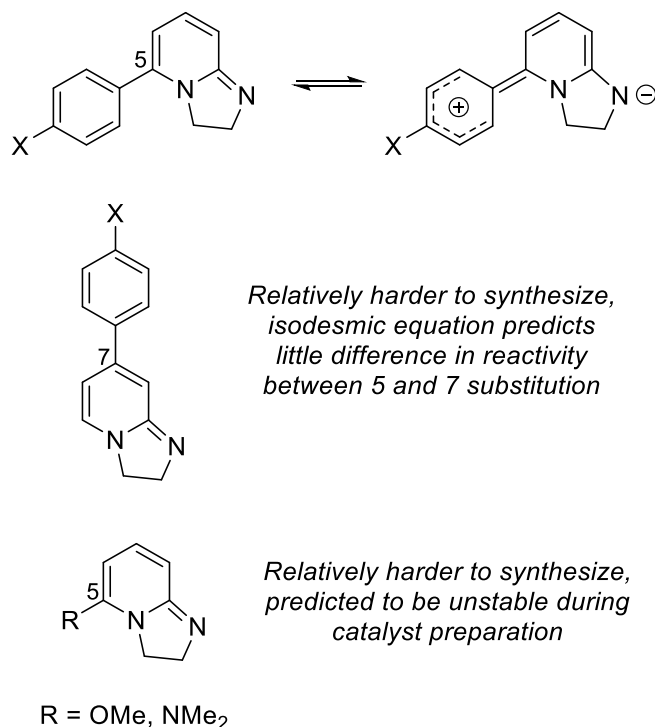


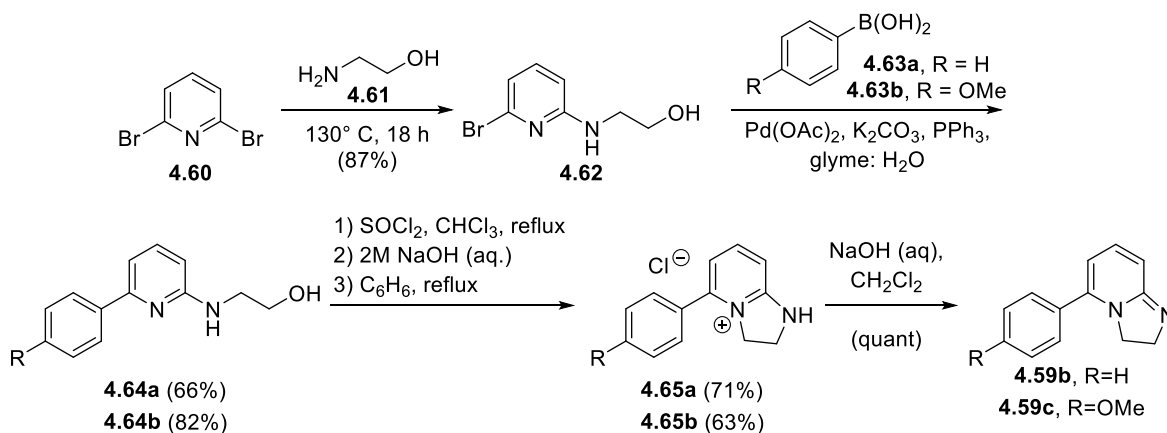
**Figure 4.11.** 5- and 7-substituted DHIP derivatives.

An optimized synthetic sequence to catalysts **4.59b** and **4.59c** was devised (Figure 4.12a). Heating 2,6-dibromopyridine with ethanolamine gives monosubstituted aminoalcohol **4.62** cleanly and in high yield. Then, a Suzuki coupling installs the aromatic ring, tailoring the electron donating properties through the choice of boronic acid. This order of reactions turned out to be the most effective. If the Suzuki reaction is conducted on 2,6-dibromopyridine, then a hard-to-separate mixture of unreacted starting material, 2-arylated, and 2,6-diarylated compounds is obtained. Conversion of the hydroxyl group in **4.64** into the chloride and subsequent cyclization delivers the hydrochloride salts **4.65** which can be stored long term. To obtain the active catalysts, the salt is treated with aq. NaOH and the free bases **4.59b** and **4.59c** are extracted into dichloromethane. Chiral PIP analogues (5-substituted H-PIPs) can be synthesized in the exact same manner, with (*R*)-2-phenylglycinol **4.66** replacing ethanolamine in the first step (Figure 4.12b).

These two achiral catalysts, **4.59b** and **4.59c**, were tested in the rearrangement of thioester **4.53a** (Figure 4.13). As a result of these two derivatives catalyzing the reaction very rapidly, there was too much error associated with the calculation of the relative rate. However, the time at which the reaction reached 50% completion ( $t_{1/2}$ ) was reliably and reproducibly calculated (see Appendix A.1 for specifics).

Clearly, the Ph derivative **4.59b** outperforms DHIP itself. As expected, the p-MeOPh derivative **4.59c** is yet more reactive than **4.59b**, as indicated by the slightly lower value of  $t_{1/2}$ . The efficacy of the designed synthetic route allows for a quick and facile approach to many arylated DHIP derivatives whose electronics (reactivity) may be tailored for a specific application. These two achiral catalysts, in addition to one chiral analogue **4.69**, are the most Lewis basic ABCs reported to date and were quickly explored in other rearrangements of even less reactive thioesters (see e.g. sections 4.5.2, 4.5.3, and 4.6.1).

a) Synthesis of achiral 5-aryl DHIP derivaives



b) Synthesis of a chiral 5-aryl-PIP derivative

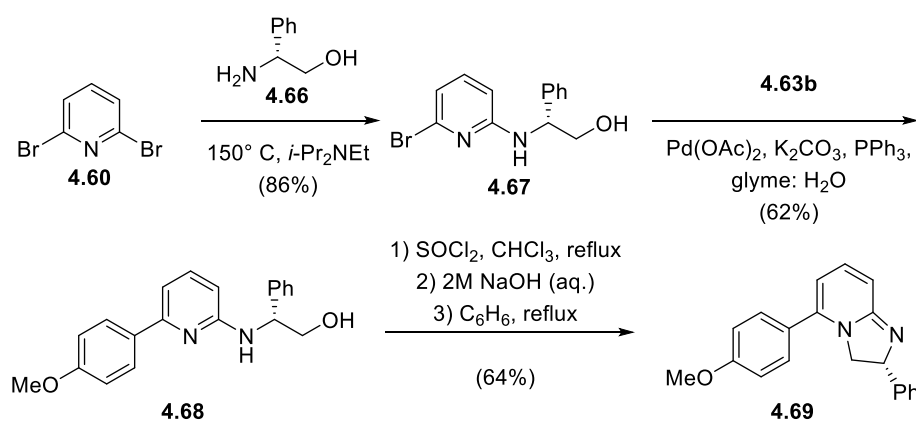


Figure 4.12. Synthesis of achiral 5-aryl-DHIP and chiral 5-aryl-PIP derivatives.

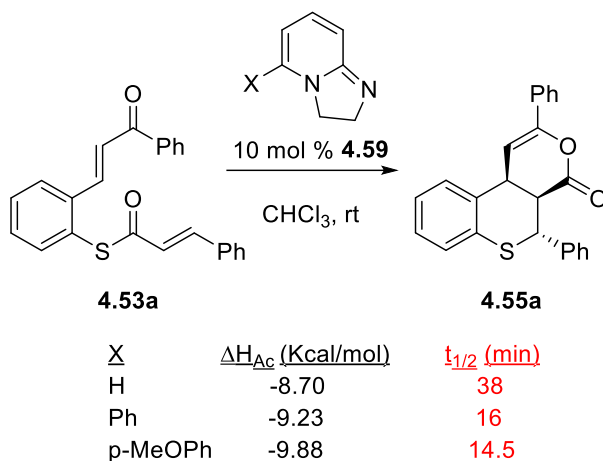


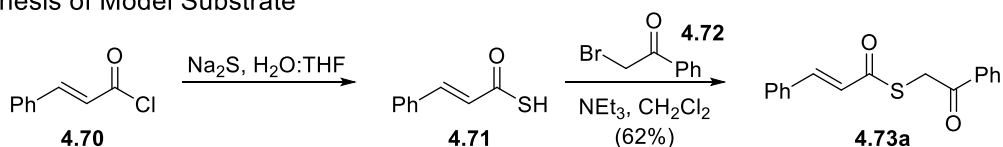
Figure 4.13. Testing 5-aryl DHIP derivatives.

## 4.5 Organocatalyzed rearrangement of S-(2-oxoalkyl)-thioenates

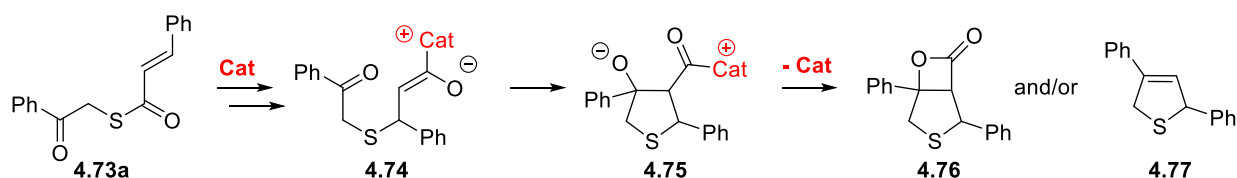
### 4.5.1 Mechanistically different rearrangement

With more electron rich ABCs on hand, our group set out to explore the rearrangement of an even less reactive class of acyl donor, an S-alkyl thioester. It was envisaged that S-alkyl thioesters may rearrange in a manner similar to the two previous S-aryl thioester cases that our group reported (cf. Figures 4.8 and 4.9). The test substrate, S-phenacyl thiocinnamate **4.73a**, was easily prepared via alkylation of crude thiocinnamic acid **4.71** (Figure 4.16a).

#### a) Synthesis of Model Substrate



#### b) Expected mechanism and product(s)



#### c) Experimentally observed mechanism and product

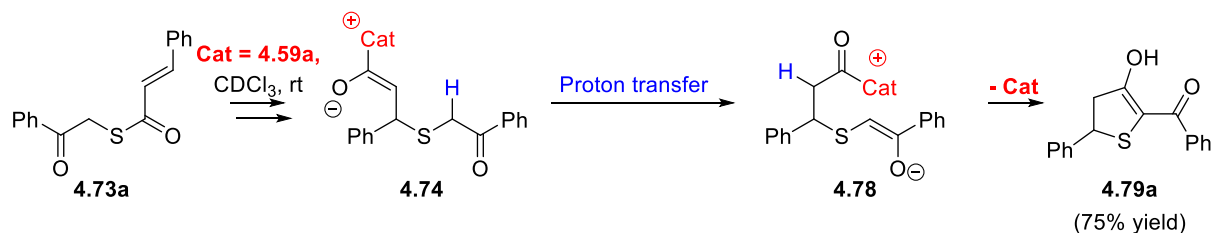


**Figure 4.14:** a) Synthesis of S-phenacyl thiocinnamate, b) The expected catalyzed rearrangement pathway, c) The experimentally observed rearrangement pathway.

Analogously to the S-aryl thioester cases, **4.73a** was expected to react to form zwitterionic enolate **4.74**. Cyclization onto the aryl ketone followed by displacement of the catalyst will give beta-lactone fused tetrahydrothiophene **4.76**. This may or may not lose carbon dioxide to give **4.77**

(Figure 4.14b). However, when this test substrate was mixed with 20 mol% of DHIP **4.59a**, the formation of neither **4.76** nor **4.79** were observed by  $^1\text{H}$  NMR. While surprising at first, a clean singlet at around 14 ppm in the  $^1\text{H}$  NMR spectra, characteristic of a chelated proton, confirmed that an unexpected, yet easily identifiable product formed (Figure 4.14c). Instead of cyclizing onto the aryl ketone carbonyl, zwitterionic enolate **4.74** undergoes a proton transfer. The resulting enolate reacts with the acyl ammonium moiety to deliver a 1,3-diketone which exists exclusively as its enol tautomer **4.79a**. Although unexpected at first glance, this Dieckmann-like cyclization is well reported in the literature.<sup>14</sup>

## 4.5.2 Optimization of solvent and achiral catalyst

After the initial discovery that DHIP catalyzes this rearrangement, we sought to optimize this new process by first exploring achiral catalysts (Figure 4.15) and solvent (Table 4.1).

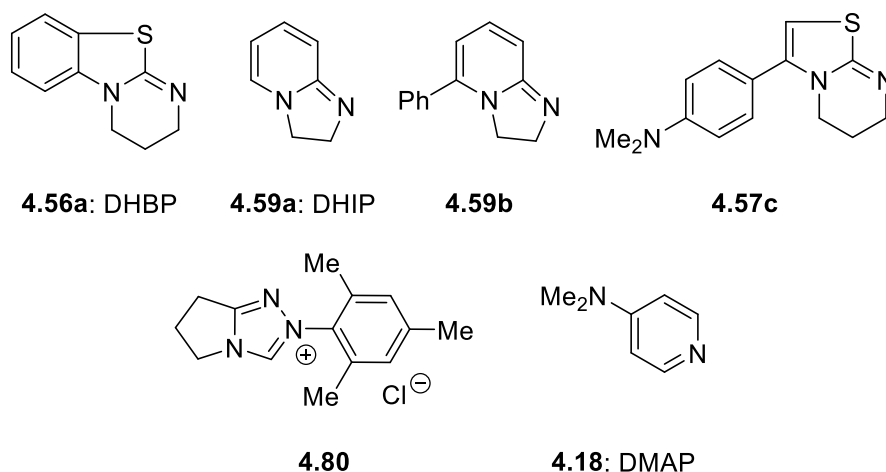
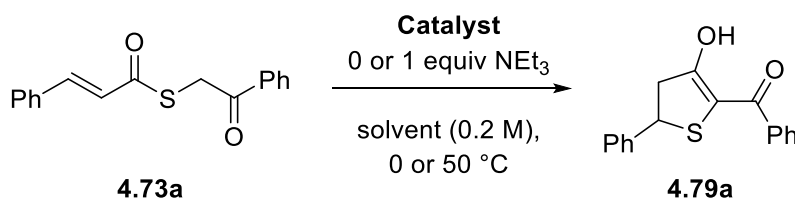


**Figure 4.15:** Achiral catalysts used in this study.

We first confirmed that stoichiometric triethylamine does not promote the reaction in the absence of a Lewis basic catalyst (compare Table 4.1, entry 1 vs entry 2). Catalysts **4.59b**<sup>1a</sup> and **4.57c**<sup>10</sup> displayed comparable reactivity to DHIP (entries 3 and 4). DHPB **4.56a**, though active

enough to react with S-aryl thioesters **4.46a** and **4.53a** (see Figures 4.8 and 4.9), failed to react with an S-alkyl thioester (entry 5). N-heterocyclic carbene precursor **4.80** did catalyze the rearrangement, but required extended heating (entry 6). DMAP **4.18** was completely ineffective, even with heating (entry 7). With DHIP clearly being the optimal catalyst, a brief solvent survey was conducted. Both toluene and THF gave lower isolated yields of the product (entries 8 and 9). While the reaction is slower with triethylamine absent or with a lower catalyst loading, comparable yields are eventually obtained in both cases with prolonged reaction time (entries 10 and 11). Finally, heating the reaction increases the reaction rate but does not deliver a higher yield (entry 12).

**Table 4.1:** Optimization of achiral catalyst and solvent.<sup>a</sup>



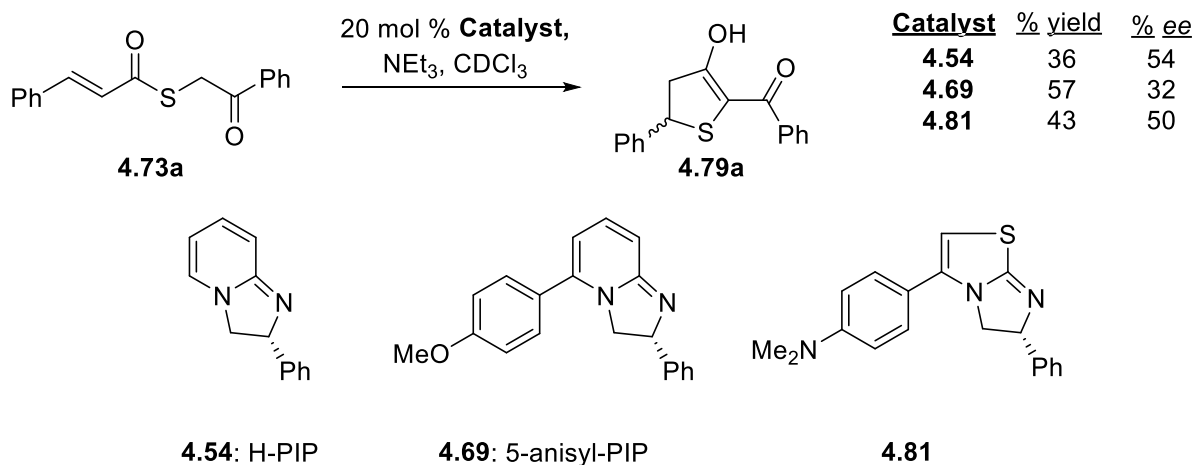
entry	Catalyst (mol %)	solvent	Time (h)	Yield (%)
1	<b>4.59a</b> (20)	CDCl <sub>3</sub>	12.5	75
2	none	CDCl <sub>3</sub>	48	0
3	<b>4.59b</b> (20)	CDCl <sub>3</sub>	12	75
4	<b>4.57c</b> (20)	CDCl <sub>3</sub>	12.5	75
5	<b>4.56a</b> (20)	CDCl <sub>3</sub>	47	0
6 <sup>b</sup>	<b>4.80</b> (20)	CDCl <sub>3</sub>	120	46
7 <sup>b</sup>	<b>4.18</b> (20)	CDCl <sub>3</sub>	48	0
8	<b>4.59a</b> (20)	PhMe	24	43
9	<b>4.59a</b> (20)	THF	24	54
10 <sup>c</sup>	<b>4.59a</b> (20)	CDCl <sub>3</sub>	25	75
11	<b>4.59a</b> (10)	CDCl <sub>3</sub>	25	71
12 <sup>b</sup>	<b>4.59a</b> (20)	CDCl <sub>3</sub>	4	68

<sup>a</sup> General conditions: 0.1 mmol of **4.73a**, 0.1 mmol of NEt<sub>3</sub>, 0.02 mmol of catalyst, 0.5 mL of CDCl<sub>3</sub>. <sup>b</sup> The reaction mixture was heated at 50 °C. <sup>c</sup> No base was added.



### 4.5.3 Initial attempts at an enantioselective variant

We next briefly examined an enantioselective variant of this reaction. H-PIP **4.54** gave the product in 54% *ee*. Unfortunately, other chiral catalysts such as **4.69**<sup>1a</sup> and **4.81**<sup>15</sup> yielded lower or comparable levels of enantioenrichment (Figure 4.16).

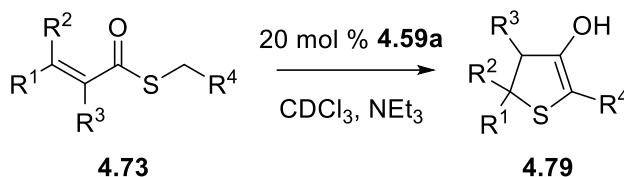


**Figure 4.16.** Attempts at an enantioselective variant.

While initially surprising there is a good explanation for this low enantioselectivity (Figure 4.18, *vide infra* in Section 4.5.6).

### 4.5.4 Racemic substrate scope

After fruitless efforts to render this reaction enantioselective, it was decided that we would analyze the substrate scope as a racemic synthesis using DHIP **4.59a** (Table 4.2). All thioester substrates tested were synthesized as outline in Figure 4.14a.

**Table 4.2:** Racemic substrate scope.<sup>a</sup>

entry	R <sup>1</sup>	R <sup>2</sup>	R <sup>3</sup>	R <sup>4</sup>	Yield (%)
1	Ph	H	H	Bz	75 <sup>b</sup>
2	4-MeOC <sub>6</sub> H <sub>4</sub>	H	H	Bz	77
3	4-CF <sub>3</sub> C <sub>6</sub> H <sub>4</sub>	H	H	Bz	63
4	2-MeC <sub>6</sub> H <sub>4</sub>	H	H	Bz	82
5	2-thienyl	H	H	Bz	56
6 <sup>c</sup>	Me	Me	H	Bz	65
7 <sup>c</sup>	Ph	H	Me	Bz	NR <sup>d</sup>
8	Ph	H	H	4-MeOBz	81
9	Ph	H	H	4-ClBz	69
10	Ph	H	H	4-NO <sub>2</sub> Bz	53
11	Ph	H	H	2-furoyl	71
12	Ph	H	H	Ac	41
13 <sup>c</sup>	Ph	H	H	CO <sub>2</sub> Et	NR <sup>d</sup>
14	Ph	H	H	CN	0 <sup>e</sup>

<sup>a</sup>General conditions: 0.1 mmol of **4.73**, 0.1 mmol of NEt<sub>3</sub>, 0.02 mmol of **4.59a**, 0.5 mL of CDCl<sub>3</sub>, rt, 16–24 h. <sup>b</sup> 60% yield was obtained on a 2.5 mmol scale. <sup>c</sup> The mixture was heated at 50 °C. <sup>d</sup> No reaction was observed. <sup>e</sup> A complex mixture formed.

Aryl substituents with electron-donating and -withdrawing groups, as well as a heteroaryl, were well tolerated at position R<sup>1</sup> (entries 2-5). While two methyl groups at the β-position also worked, heating was required (entry 6). Unfortunately, the introduction of a methyl group at the α-position R<sup>3</sup> rendered the thioester unreactive to rearrangement (entry 7). A variety of aryls and a furoyl group were also tolerated at R<sup>4</sup> (entries 8-11). In contrast to aryl ketones, the methyl ketone rearranged, but gave additional side reactions that resulted in a lower isolated yield (entry 12). When the ketone was replaced with an ester moiety the rearrangement did not occur, not even with prolonged heating (entry 13). The cyanomethyl thioester did react, but it did not produce the desired product (entry 14).

### 4.5.5 Alternative two-component approach to the same products

Early in this project it was discovered that some thioester substrates **4.73** were difficult to prepare following the method outlined in Figure 4.14a. In some cases, contamination due to an undesired side product resulting from a thio-Michael of the thiocinnamic acid onto the thioester was observed. To overcome this obstacle an alternative two-component approach was designed that would prevent this problematic side reaction (Figure 4.17).<sup>16</sup>

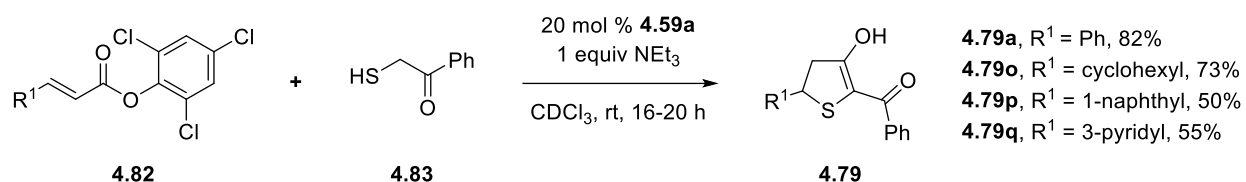


**Figure 4.17:** Alternative two-component approach the dihydrothiophenes **4.79**.

Instead of starting from the thioester, easy to synthesize trichlorophenyl esters **4.82** were used in conjunction with phenacyl mercaptan **4.83**.<sup>17</sup> Not only did this method produce comparable yields (e.g. compare Table 4.1 entry 1 to Figure 4.17), but the substrate scope was increased to include cyclohexyl, 1-naphthyl, and 3-pyridyl substituents at position  $\text{R}^1$ .

### 4.5.6 Origins of low enantioselectivity

One explanation for the low enantioselectivity of this rearrangement can be explained by the mechanism given in Figure 4.18. It was discovered that when *S*-phenacyl thiocinnamate **4.73a** is reacted with phenacyl mercaptan in the presence of triethylamine, the expected product can be obtained in 57% yield. Because phenacyl mercaptan is regenerated in the last step, only a catalytic amount is necessary for this racemic background reaction to occur, diverting the reaction from the asymmetric pathway. Interestingly, when 2,4,6-trichlorophenyl cinnamate **4.82a** is used in lieu of thioester **4.73a**, only 4% of **4.79a** is isolated. In this case, the formation of 2,4,6-trichlorophenol

and thioester starting material explains what is happening. Evidently the trichlorophenyl ester is much less reactive as a thio-Michael acceptor and undergoes acyl substitution instead. The one equivalent of thiolate is quickly consumed and cannot be used in the pathway leading to the dihydrothiophene product. The alternative two component approach outlined in Figure 4.19 still delivers the dihydrothiophene products since DHIP is capable of reacting with the thioester that forms, regenerating the thiolate anion. As expected, low enantioselectivities were also observed when catalysts **4.54**, **4.69**, and **4.81** were employed in this two-component method using the trichlorophenyl ester in lieu of thioester.

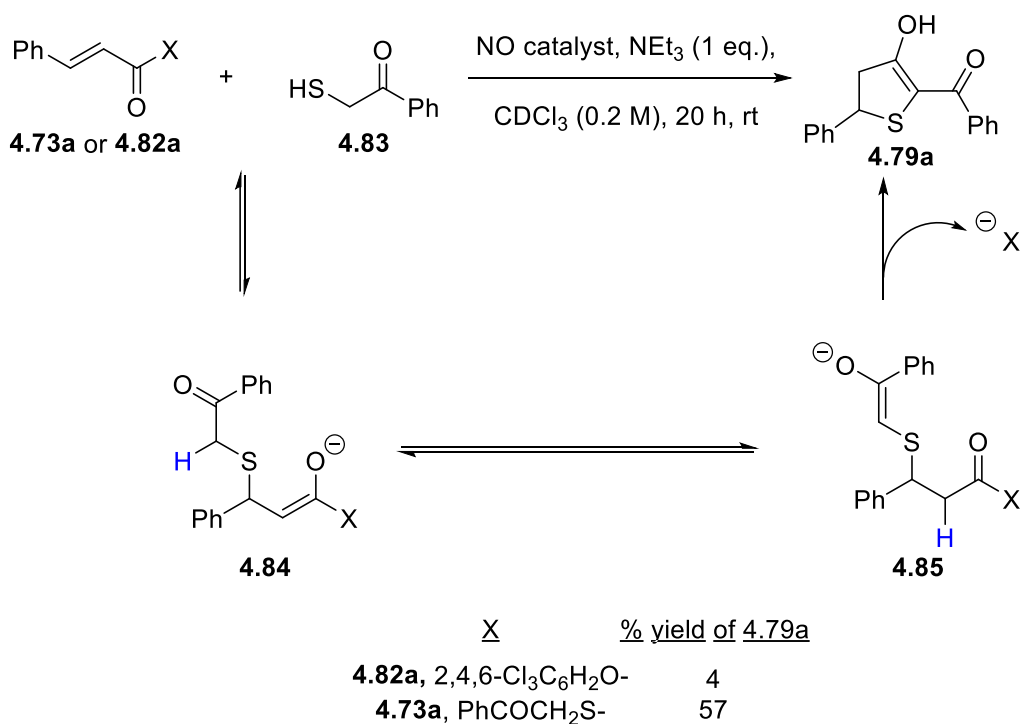


**Figure 4.18:** Origins of low enantioselectivity.

Though only becoming an issue with this class of thioester substrates, this alternative mode of catalysis, a chain reaction initiated by a free thiolate, was discovered by Dr. Nick Ahlemeyer while studying rearrangements of thioesters into thiochromenes (Figure 4.19).

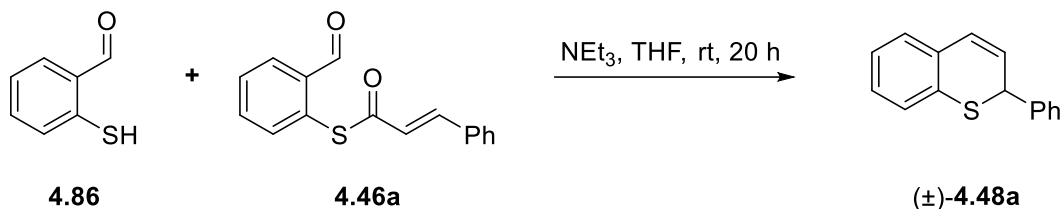


**Figure 4.19:** Alternative mode of catalysis used to make racemic thiochromenes.

It was observed that when thioester **4.46a** was reacted with 2-mercaptobenzaldehyde **4.86** in the presence of triethylamine, the racemic thiochromene was isolated in 45% yield. Interestingly this racemic background reaction is a negligible pathway when a chiral catalyst is introduced and allowed an asymmetric version of this reaction to be developed. However, in the case of the S-alkyl thioesters, the more reactive S-alkyl thiolate leaving group is probably nucleophilic and abundant enough to slowly react with the thioester, leading to a racemic background reaction, in addition to the more reactive  $\alpha,\beta$ -unsaturated acyl ammonium cation **4.88** formed in the first step of the catalytic pathway (see Figure 4.20).

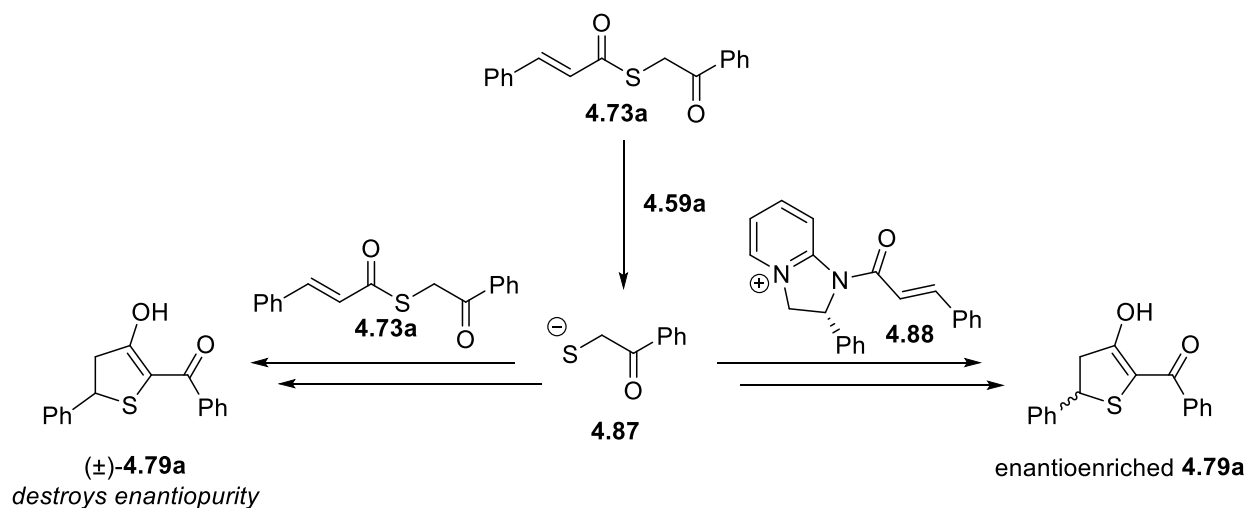


**Figure 4.20.** S-alkyl thiolate capable of reacting with thioester in addition to ammonium cation: one possible explanation for the origin of low enantioselectivity.

## 4.6 Additional organocatalyzed rearrangements of S-aryl thioesters

When our group first explored this area of thioester rearrangements there were two notable variations of the S-aryl thioester core that proved troublesome with DHPB (Figure 4.21).

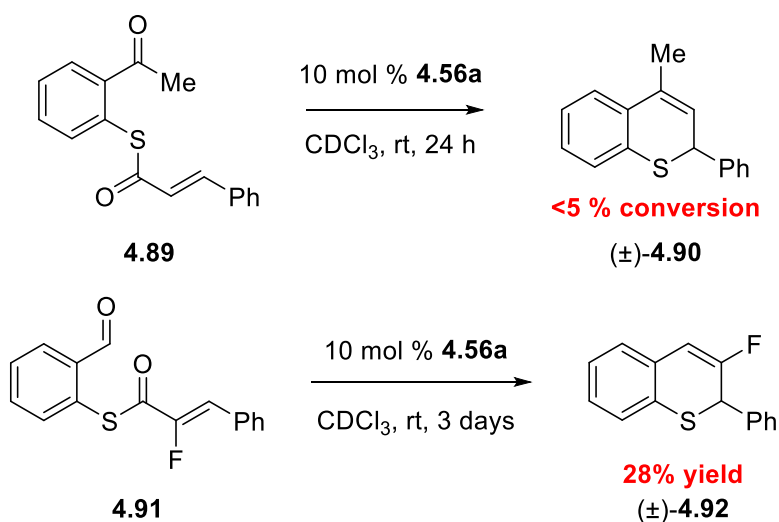


**Figure 4.21.** Troublesome substrates in the thiochromene synthesis.

When the aldehyde moiety is replaced with a methyl ketone, like in **4.89**, the less electrophilic moiety drastically slowed down the reaction. Additionally, the fluorinated thioester **4.91** was also less reactive to rearrangement. After publishing our results concerning the rearrangements of S-alkyl thioesters<sup>1a</sup>, we sought to re-explore these tricky substrates with a greater understanding of the importance of Lewis basicity of the catalyst.

### 4.6.1 Asymmetric synthesis of a 4-substituted thiochromene

Knowing that DHIP and its chiral analogue H-PIP proved superior in the synthesis of thiochromanes and dihydrothiophenes we attempted to use these catalysts to induce the rearrangement of methyl ketone-containing thioester **4.89**. It was hypothesized that the enhanced Lewis basicity of these catalysts would bode well in the case with the less electrophilic ketone

moiety. As predicted, 5-anisyl-PIP **4.69**, which delivered low enantioinduction in the rearrangement of S-phenacyl thiocinnamate (see Figure 4.16), gave the thiochromene in 79% yield and 96% *ee* after 18 hours (Figure 4.22).

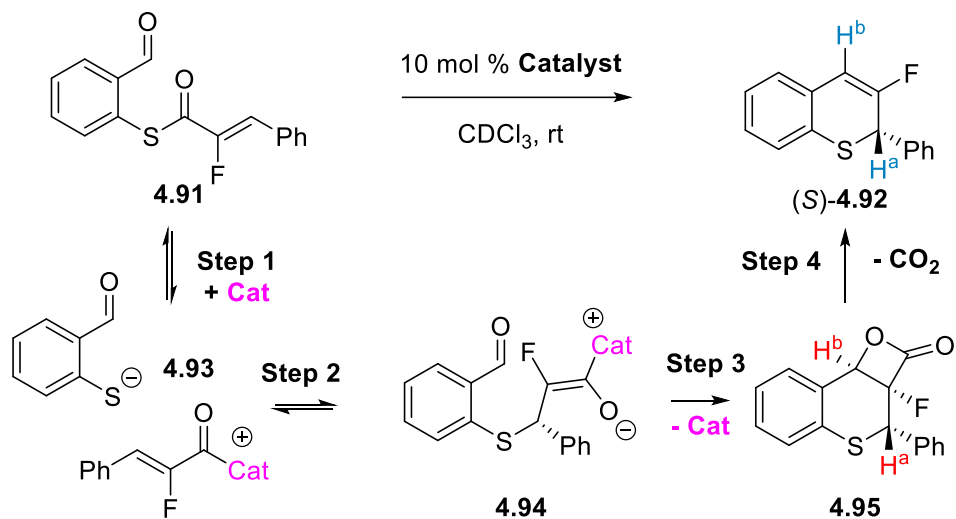


**Figure 4.22:** Synthesis of a 4-substituted thiochromene.

#### 4.6.2 Asymmetric synthesis of a 3-fluoro thiochromene

With these more Lewis basic ABCs on hand we reinvestigated the rearrangement of thioester **4.91** (Table 4.3). As aforementioned DHPB **4.56a** (Figure 4.21) gave **4.92** in 28% yield after 3 days (entry 1). Its chiral analogue HBTM-2.1<sup>18</sup> **4.96** gave both low yield and negligible enantioselectivity (entry 2). This is a very surprising result considering how well this catalyst performed with analogous non-fluorinated compounds.<sup>9</sup> H-PIP catalyzes the rearrangement well, but gives low enantioselectivities (entry 3). Bicyclic isothioureia **4.81**<sup>15</sup> performed better than H-PIP, giving higher yield and enantioselectivity (entry 4). With these results in hand, we predicted that a possible reason for low enantioinduction in certain cases arose from a reversible Step 2. Because enolate intermediate **4.94** is stabilized by the fluorine, Step 3 may be considerably slower than for the non-fluorinated analogue. Additionally, fluorine's slightly larger size than hydrogen may also help to impede this intramolecular cyclization. That being said experimental evidence suggested that the 5,5-fused bicyclic core, such as that seen in catalyst **4.81**, leads to higher

**Table 4.3:** Synthesis of a 3-fluorothiochromene.<sup>a</sup>



Entry	catalyst	time	% yield	% ee
1	<b>4.56a</b>	3 days	28	N/A
2	<b>4.96</b>	8 days	25	4
3	<b>4.54</b>	46 h	50	54
4	<b>4.81</b>	18 h	75	88
5	<b>4.97</b>	8 days	54	94
6 <sup>b</sup>	<b>4.57c</b>	14 h	56	N/A

<sup>a</sup>Conditions: 0.1 mmol of **4.91**, 0.01 mmol of catalyst, 0.5 mL of CDCl<sub>3</sub>, rt. <sup>b</sup>1.0 mL of CDCl<sub>3</sub> was used.

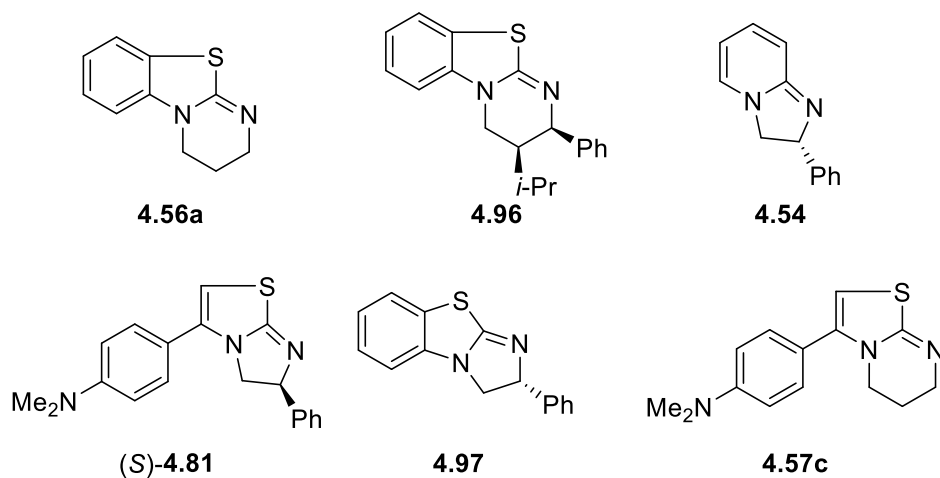


**Figure 4.23.** Catalysts used in the fluorothiochromene study.



conversions and enantioselectivities than catalysts with fused 5,6-bicyclic cores (e.g. DHIP and H-PIP). Keeping that possible geometrical constraint in mind we next tested (*R*)-BTM<sup>19</sup> **4.97** (entry 5). As expected from its inherently lower Lewis basicity the reaction was much slower than with catalyst **4.81**, but BTM provided the highest levels of enantioselectivity observed up to this point. Finally, using achiral isothiourea **4.57c**<sup>10</sup>, we were able to monitor the reaction's progress by <sup>1</sup>H NMR and observe the formation and disappearance of the putative fluorinated  $\beta$ -lactone **4.95** (Figure 4.24).

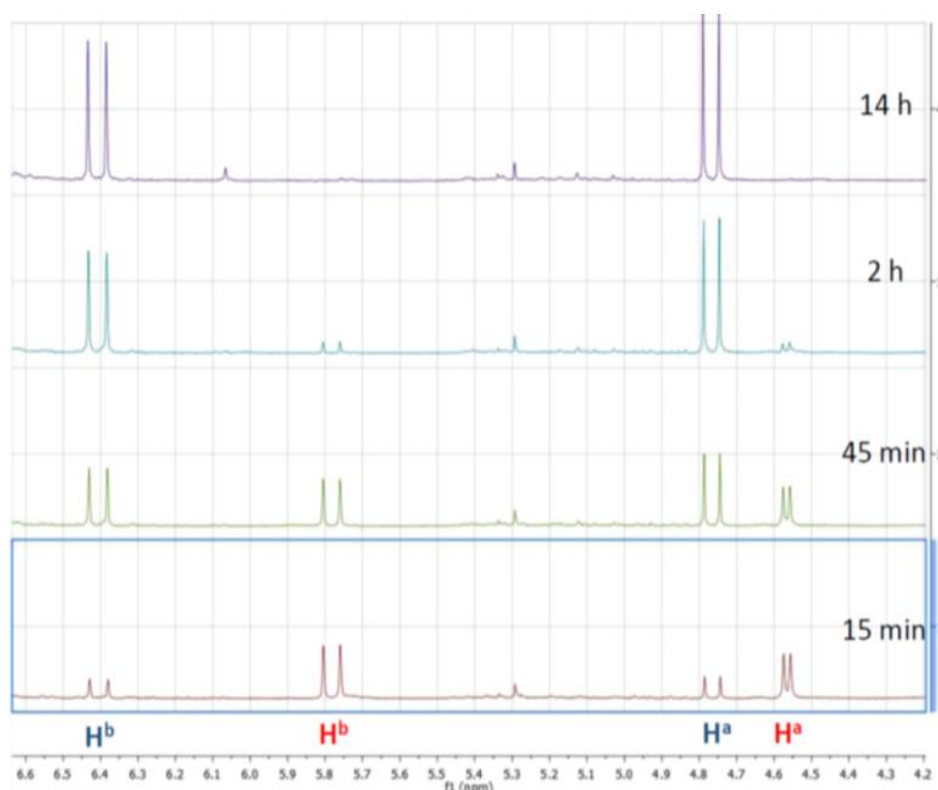


**Figure 4.24:** <sup>1</sup>H NMR spectra showing formation and disappearance of **4.95**.

Interestingly, this same observation cannot be made for the non-fluorinated analogue. It is quite possible that the rate of decarboxylation is greatly decreased because of the electron-withdrawing effects of fluorine destabilizing the benzylic cation that forms (Figure 4.25). This

energetic hurdle may explain why a true  $\beta$ -lactone fused thiochromane intermediate is discerned in this specific case.

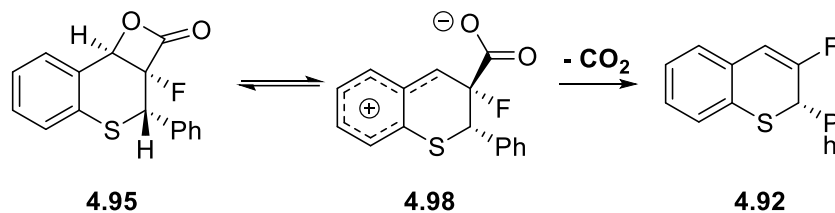


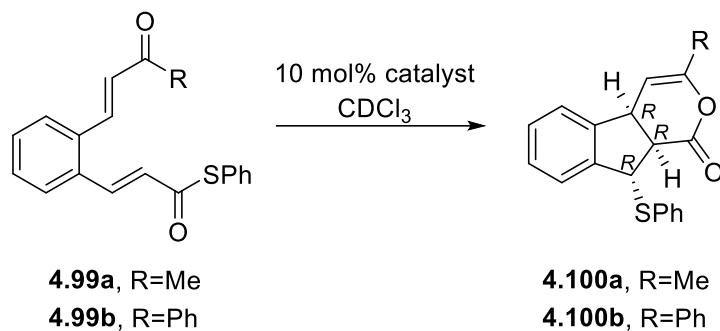
**Figure 4.25.** Decarboxylation of fluorinated  $\beta$ -lactone intermediate.

### 4.6.3 Synthesis of fused indanes

As described in chapters 4.3.1, 4.3.2, and 4.6.1, the precursor thioesters contained the terminal electrophile (aldehyde, ketone, or enone) tethered to the thioester moiety through the sulfur atom. This guaranteed that the sulfur atom would be incorporated inside of the ring of the product heterocycle. However, there is one structural variation of thioesters that our group wanted to explore, one in which the thiolate anion would end up outside of the rearranged carbocyclic skeleton as a thioether moiety. To investigate this possibility, we constructed thioester substrates **4.99a** and **4.99b**, which were expected to give the tricyclic indane-fused dihydropyranones **4.100a** and **4.100b** (Table 4.4).

Both thioesters underwent rearrangement with DHPB **4.56a** at room temperature (Table 4.4, entries 1-2). Moderate yields of a single diastereomer were obtained. This relative stereochemistry was assigned in analogy to the thiochromane syntheses (see Figure 4.9).

To test the enantioselective version, chiral catalysts (*R*)-BTM **4.97** and (*R*)-HBTM-2.1 **4.96** were used, but required prolonged heating for a week before all of the starting material was consumed (entries 3-6). The enantioselectivities were low to moderate in all cases. H-PIP **4.54**, a

**Table 4.4.** Synthesis of fused indanes **4.100a** and **4.100b**.<sup>a</sup>

entry	catalyst	R	Temp (°C)	Time (h)	% yield	% <i>ee</i>
1	<b>4.56a</b>	Me	23	48	50	NA
2	<b>4.56a</b>	Ph	23	21	51	NA
3	<b>4.97</b>	Me	60	168	35	67 ( <i>R</i> )
4	<b>4.97</b>	Ph	60	168	32	16 ( <i>S</i> )
5	<b>4.96</b>	Me	60	168	29	23 ( <i>S</i> )
6	<b>4.96</b>	Ph	60	168	41	69 ( <i>R</i> )
7	<b>4.54</b>	Me	0	72	45	88 ( <i>R</i> )
8	<b>4.54</b>	Ph	0	72	30	35 ( <i>R</i> )

<sup>a</sup> Conditions: 0.1 mmol of thioester, 0.01 mmol of catalyst, 0.5 mL of CDCl<sub>3</sub>.

more Lewis basic catalyst, promoted the rearrangement even at 0 °C (entries 7-8). The *ee* for the methyl enone substrate **4.99a** was good, but lower *ee* was obtained with the phenyl enone **4.99b**. All these enantioselectivities are poor in comparison to those obtained in our previous works with analogous thiochromene and thiochromane syntheses.<sup>9,10</sup> Furthermore, X-ray analysis of the two products (see Figures 4.27 and 4.28) indicated that, in some cases (for clarity, these cases are highlighted in red in Table 4.4), the absolute stereochemistry of the products was opposite from what we expected based on the facial selectivity of the sulfa-Michael addition step in our previous publications. To further exacerbate this issue, the two substrates responded differently to all three chiral catalysts utilized.

The results with **4.99a** are consistent with the opposite absolute configuration of (*R*)-HBTM-2.1 vs. (*R*)-BTM and (*R*)-H-PIP (entries 3 and 7 give the opposite enantiomer of entry 5); though only thioester **4.99b** reacts with the expected sulfa-Michael controlled enantioselectivity

with catalysts (*R*)-BTM and (*R*)-HBTM-2.1 (entries 4 and 6). However, with **4.99b**, the opposite expected absolute stereochemistry is obtained with (*R*)-H-PIP (entry 8). To explain this drastic inversion of enantioselectivity, we hypothesized that conjugate addition within ion pairs **4.101a** and **4.101b** occurs reversibly (Figure 4.26).

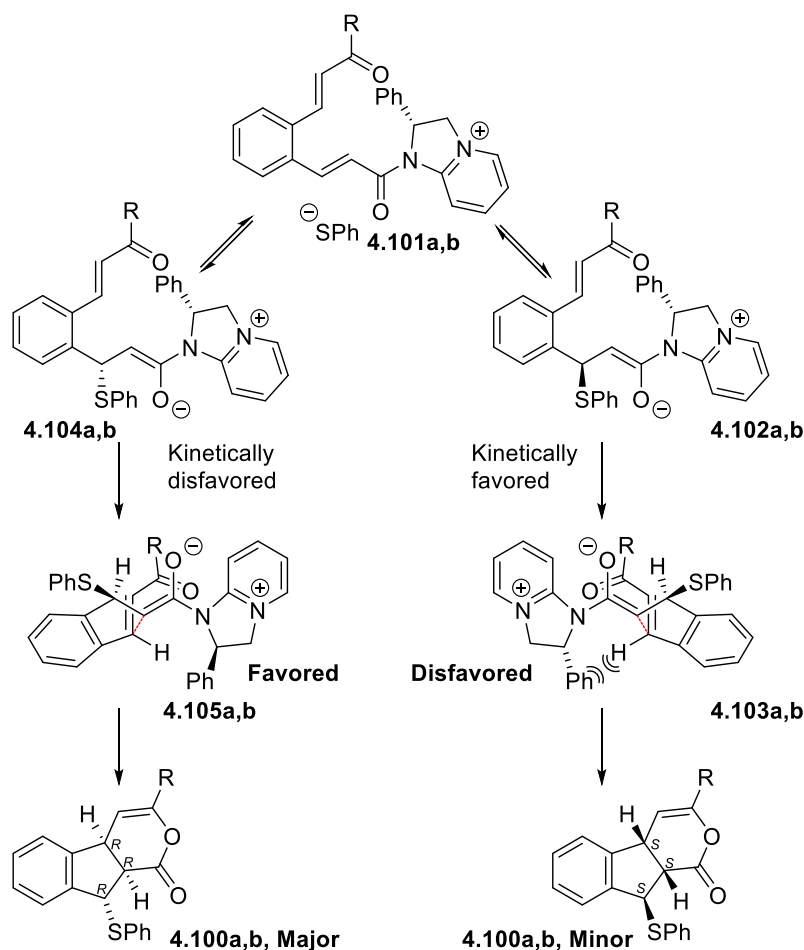


**Figure 4.26.** Proposed explanation for inversion of enantioselectivity.

Although the sulfa-Michael addition step favors diastereomers **4.102a** and **b**, on account that the thiolate adds to the face of the cation unblocked by the phenyl group of the catalyst, the subsequent intramolecular Michael addition is hampered by the mismatch between the substrate control (the phenylthio group hinders the approach of the enone moiety to the  $\beta$ -face of the enolate)

and the catalyst control (the phenyl group of the catalyst blocks the  $\alpha$ -face) (cf. **4.103a** and **b**). On the other hand, the same factors are matched in the kinetically disfavored diastereomer **4.104a** and **b** (cf. **4.105a** and **b**: the  $\alpha$ -face remains open). The high level of enantioenrichment of **4.100a** in entry 7 suggests that asymmetric induction in this case is completely controlled by the second step (i.e., the Curtin-Hammett scenario). By contrast, the low ee in entry 8 reflects the residual influence of the sulfa-Michael step, which is consistent with the higher electrophilicity of the phenylenone moiety in **4.103b** relative to the methylenone in **4.103a**. Comparison of the ee values obtained with three chiral catalysts and both substrates reveals another interesting trend: H-PIP **4.54** leads to the highest proportion of the Curtin-Hammett-favored enantiomer, HBTM-2.1 **4.96** favors the opposite outcome, while BTM **4.97** falls somewhere in between. In summary, while Curtin-Hammett operates in all cases, it does so to different degrees. With the methyl enone **4.99a**, this predominates with all catalysts; however, with the phenyl enone **4.99b**, the ee is either eroded or reversed as a result of the Curtin-Hammett scenario. It should be noted that structurally similar substrates have been subjected to tandem double Michael additions of enolate nucleophiles. However, in the reported cases, the absolute stereochemistry of the products was set during the irreversible intermolecular Michael addition step and was not affected by the mismatch in the subsequent cyclization.<sup>16,20</sup>

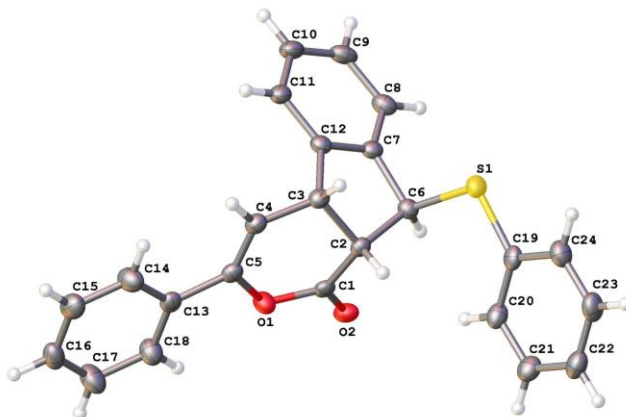


**Figure 4.27.** X-ray crystal structure of **4.100b**. This crystal structure was obtained from Table 4.4, entry 6.

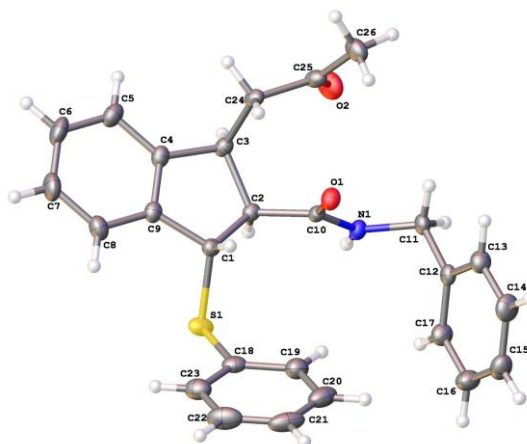


**Figure 4.28.** X-ray crystal structure of **4.100a**, analyzed as the ring-opened benzyl amide (**4.100a-BnNH<sub>2</sub>**). This crystal structure was obtained from Table 4.4, entry 7.

## 4.7 Conclusions and future directions

In conclusion, we have developed a new racemic synthesis of highly substituted dihydrothiophene derivatives via an organocatalyzed rearrangement of S-phenyl thiocinnamate

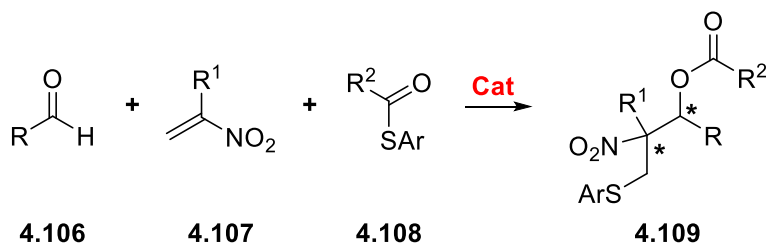
and its derivatives. In addition to starting from a thioester, an alternative two-component approach was devised to overcome limitations in the synthesis of certain thioesters. Even though an enantioselective version of this process could not be developed, the importance of synthesizing more Lewis basic chiral ABCs in the context of this project cannot be understated. For example, thanks to our efforts in catalyst development, a newly designed chiral PIP derivative proved to be the best catalyst of choice in catalyzing the rearrangement of methyl ketone **4.89** into a 4-substituted thiochromene, the first of its kind using our methodology. Though not being currently investigated by our group, these chiral PIP derivatives with enhanced Lewis basicity may have broad application elsewhere in the field of asymmetric catalysis.

Equally important was the discovery that BTM could catalyze the rearrangement of fluorine-containing thioester **4.91** into 3-fluorothiochromene **4.92**. Not only did this show the first synthesis of a 2,3-disubstituted thiochromene using our methodology, but this one example also expanded upon the use of fluoroenolates in asymmetric catalysis.

Since 2015 our group greatly increased the utility of thioesters in asymmetric catalysis, namely through their rearrangements into useful sulfur-containing heterocycles. However, it is still possible to find additional uses for thioesters as acyl donors that have remained unexplored in the literature. One example is given in Figure 4.29.

An aldehyde and activated olefin like an  $\alpha$ -substituted nitroethylene are not expected to react on their own, but the addition of a phosphine or amine catalyst like DABCO will allow the Morita-Baylis-Hillman (MBH) reaction to occur. Surprisingly, employing a thiolate as a nucleophile has never been explored. Using a more nucleophilic thiolate may drastically cut down on long reaction times, an infamous characteristic of the MBH reaction. Furthermore, the more reactive thiolate may allow for the use of  $\beta$ -substituted activated olefins, which are hardly ever

used in MBH reactions. Products **4.109** may be obtained with high diastereoselectivity; however, an enantioselective process may prove difficult.



**Mechanism:**

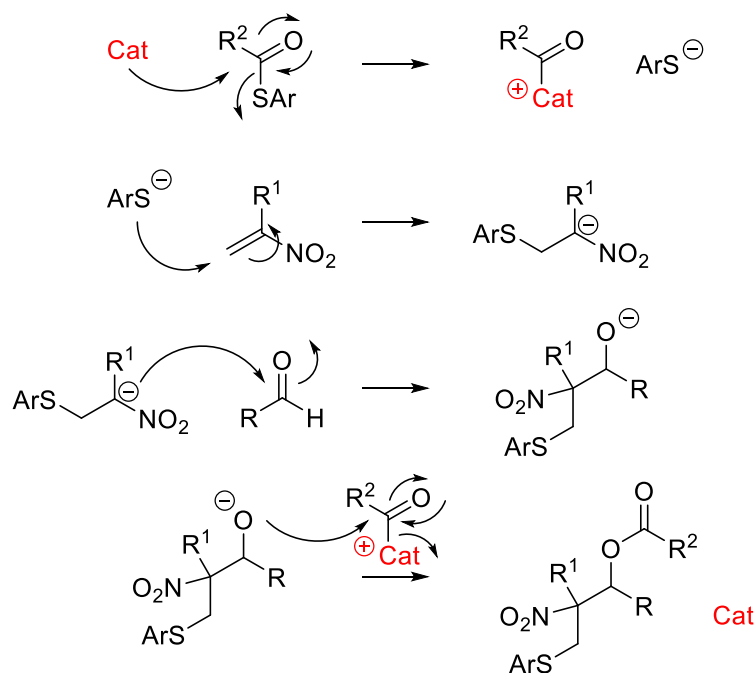


**Figure 4.29:** Possible additional application for thioesters as acyl donors.

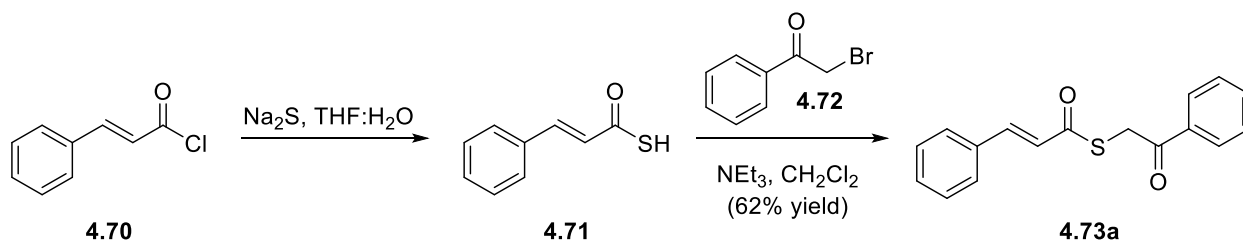
## 4.8 Experimental

All reagents were obtained commercially and used as received unless specified otherwise. Catalysts **4.54**, **4.56a**, **4.57c**, **4.59a-c**, **4.69**, **4.81**, **4.96**, and **4.97** were prepared as previously described.<sup>1a,10,11,12,15,18,19</sup> Reactions that required heating were carried out in an electrically heated mineral oil bath. Dichloromethane and deuterated chloroform used as reaction media were freshly



distilled from calcium hydride. Triethylamine was freshly distilled from potassium hydroxide. Solvents used for chromatography were ACS or HPLC grade. Sorbent Technologies XHL silica gel plates (glass-backed, 250  $\mu\text{m}$ ) were used for TLC analyses. Flash column chromatography was performed over Sorbent Technologies silica gel (40–63  $\mu\text{m}$ ). HPLC analyses were performed on a Shimadzu LC system using a Chiralcel OD-H or Chiralpak AD-H analytical chiral stationary phase columns (4.6  $\times$  250 mm, Chiral Technologies, Inc.) with a UV detector at 254 or 204 nm with a flow rate of 0.7 mL/min (**4.79a**) or 1.0 mL/min (**4.90**, **4.92**, and **4.100a,b**).  $^1\text{H}$  and  $^{13}\text{C}$  NMR spectra were recorded on Mercury 300 MHz and DD2 500 MHz Agilent spectrometers. The chemical shifts are reported as  $\delta$  values (ppm) relative to TMS using a residual  $\text{CHCl}_3$  peak (7.26 ppm for  $^1\text{H}$  NMR, 77.16 ppm for  $^{13}\text{C}$  NMR) or  $(\text{CH}_3)_2\text{CO}$  (29.84 ppm for  $^{13}\text{C}$  NMR) peaks as the reference. Melting points were measured on a Stuart SMP10 melting point apparatus. High-resolution mass spectral analyses were performed at Washington University MS Center on a Bruker MaXis QTOF mass spectrometer using electrospray ionization (ESI). Infrared spectra were recorded on a Bruker Alpha Platinum-ATR. Optical rotations were measured on a Rudolph Autopol III polarimeter.

#### 4.8.1 Synthesis of S-phenacyl thiocinnamate derivatives 4.73



### General procedure for the synthesis of thioesters **4.73**.

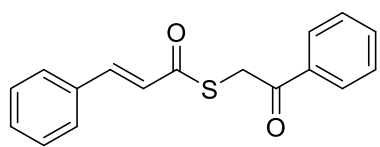
#### *Thiocinnamic acid* **4.71**

A solution of cinnamoyl chloride **4.70** (1.00 g, 6.00 mmol) in 10 mL of THF was added to a rapidly stirring solution of Na<sub>2</sub>S (2.00 g, 25.6 mmol, 4.27 equiv) in 5 mL of H<sub>2</sub>O. After 30 min, the organic phase was separated and the aqueous phase extracted with THF (3 × 5 mL). The resulting bright-orange solution of sodium thiocinnamate in THF was diluted with 50 mL of H<sub>2</sub>O, acidified with 20 mL of 1 M HCl, and extracted with EtOAc (3 × 10 mL). The organic extract was dried over MgSO<sub>4</sub> and rotary evaporated to give crude thiocinnamic acid **4.71**, which was used immediately without further purification.

#### *S-phenacyl thiocinnamate* **4.73a**

A stirring solution of the crude thiocinnamic acid **4.71** and 2-bromoacetophenone **4.72** (1.20 g, 6.03 mmol) in 20 mL of freshly distilled CH<sub>2</sub>Cl<sub>2</sub> was treated with NEt<sub>3</sub> (1.00 mL, 0.726 g, 7.19 mmol) dropwise at 0 °C. After completion, the mixture was stirred at 0 °C for an additional 10 min and at rt for 50 min, then washed with 1 M HCl (×2) and saturated aqueous NaHCO<sub>3</sub> (×2), then dried over MgSO<sub>4</sub>. After rotary evaporation and flash chromatography (hexanes/CH<sub>2</sub>Cl<sub>2</sub> 2:1 → 1:1), 1.05 g of thioester **4.73a** was obtained as a white crystalline powder (62% yield). Unless indicated otherwise, all thioester substrates listed below were obtained analogously from the corresponding acids<sup>21</sup> and bromoketones<sup>22</sup> and purified by chromatography under conditions indicated below. Note that, due to their limited solubility in hexane/ ethyl acetate mixtures, preadsorption on silica gel is recommended.

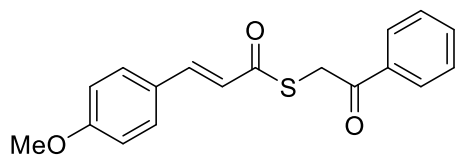
**S-(2-oxo-2-phenylethyl) (E)-3-phenylprop-2-enethioate (4.73a).**



$^1\text{H}$  NMR (500 MHz,  $\text{CDCl}_3$ ):  $\delta$  8.04 (d,  $J = 8$  Hz, 2H), 7.67 (d,  $J = 16$  Hz, 1H), 7.63–7.58 (m, 1H), 7.57–7.52 (m, 2H), 7.52–7.47 (m, 2H), 7.42–7.36 (m, 3H), 6.77 (d,  $J = 16$  Hz, 1H), 4.54 (s, 2H).

$^{13}\text{C}\{^1\text{H}\}$  NMR (125 MHz,  $\text{CDCl}_3$ ):  $\delta$  193.5, 188.2, 141.9, 135.7, 134.0, 133.8, 130.9, 129.1, 128.9, 128.7, 128.6, 124.2, 36.5. IR ( $\text{cm}^{-1}$ ): 1695, 1656, 1612, 1197, 1038. HRMS (ESI-TOF)  $m/z$ :  $[\text{M} + \text{Na}]^+$  calcd for  $\text{C}_{17}\text{H}_{14}\text{O}_2\text{S}$ , 305.0607; found, 305.0614. Mp: 117–119 °C.

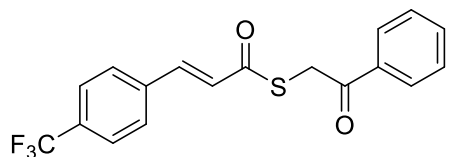
**S-(2-oxo-2-phenylethyl) (E)-3-(4-methoxyphenyl)prop-2-enethioate (4.73b).**



Isolated as a fine light tan powder (137 mg, 42% yield) after chromatography (5 → 15% EtOAc/hexane).  $^1\text{H}$  NMR (500 MHz,  $\text{CDCl}_3$ ):  $\delta$  8.04 (d,  $J = 9$  Hz, 2H), 7.64 (d,  $J = 16$

Hz, 1H), 7.61–7.58 (m, 1H), 7.52–7.47 (m, 4H), 6.91 (d,  $J = 9$  Hz, 2H), 6.65 (d,  $J = 16$  Hz, 1H), 4.52 (s, 2H), 3.85 (s, 3H).  $^{13}\text{C}\{^1\text{H}\}$  NMR (125 MHz,  $\text{CDCl}_3$ ):  $\delta$  193.7, 188.1, 162.0, 141.7, 135.8, 133.8, 130.4, 128.9, 128.7, 126.7, 121.9, 114.6, 55.5, 36.4. IR ( $\text{cm}^{-1}$ ): 1697, 1658, 1597, 1508, 1243, 1037, 995, 809. HRMS (ESI-TOF)  $m/z$ :  $[\text{M} + \text{Na}]^+$  calcd for  $\text{C}_{18}\text{H}_{16}\text{O}_3\text{S}$ , 335.0712; found, 335.0710. Mp: 118–122 °C.

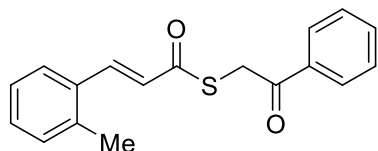
**S-(2-oxo-2-phenylethyl) (E)-3-(4-(trifluoromethyl)phenyl)prop-2-enethioate (4.73c).**



Isolated as a faint yellow powder (379 mg, 58% yield) after chromatography (5 → 15% EtOAc/ hexane).  $^1\text{H}$  NMR (500 MHz,  $\text{CDCl}_3$ ):  $\delta$  8.04 (d,  $J = 7$  Hz, 2H), 7.69–7.59 (m, 6H), 7.53–7.48 (m, 2H), 6.83 (d,  $J = 16$  Hz, 1H), 4.56 (s, 2H).  $^{13}\text{C}\{^1\text{H}\}$  NMR (125 MHz,  $\text{CDCl}_3$ ):  $\delta$  193.2, 188.1, 139.8, 137.4, 135.7, 133.9, 132.3 (q,  $^2J_{\text{C-F}} = 33$  Hz), 129.0, 128.7, 128.7, 126.5, 126.1 (q,  $^3J_{\text{C-F}} = 4$  Hz), 123.9 (q,  $^1J_{\text{C-F}}$

= 271 Hz), 36.8. IR (cm<sup>-1</sup>): 1693, 1661, 1619, 1322, 826, 745, 686. HRMS (ESI-TOF) m/z: [M + Na]<sup>+</sup> calcd for C<sub>18</sub>H<sub>13</sub>F<sub>3</sub>O<sub>2</sub>S, 373.0480; found, 373.0483. Mp: 156–159 °C.

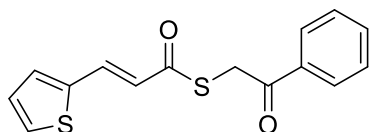
**S-(2-oxo-2-phenylethyl) (E)-3-(o-tolyl)prop-2-enethioate (4.73d).**



Isolated as a light tan powder (102 mg, 49% yield) after chromatography (2 → 5% EtOAc/ hexanes). <sup>1</sup>H NMR (500 MHz, CDCl<sub>3</sub>): δ 8.07–8.03 (m, 2H), 7.97 (d, J = 16 Hz, 1H), 7.64–7.55

(m, 2H), 7.53–7.48 (m, 2H), 7.32–7.28 (m, 1H), 7.25–7.19 (m, 2H), 6.70 (d, J = 16 Hz, 1H), 4.54 (s, 2H), 2.44 (s, 3H). <sup>13</sup>C{<sup>1</sup>H} NMR (125 MHz, CDCl<sub>3</sub>): δ 193.6, 188.4, 139.5, 138.6, 135.8, 133.8, 132.9, 131.1, 130.7, 128.9, 128.7, 126.6, 126.6, 125.2, 36.6, 19.9. IR (cm<sup>-1</sup>): 2971, 2912, 1692, 1656, 1202, 1038, 973. HRMS (ESI-TOF) m/z: [M + H]<sup>+</sup> calcd for C<sub>18</sub>H<sub>16</sub>O<sub>2</sub>S, 297.0944; found, 297.0938. Mp: 78–80 °C.

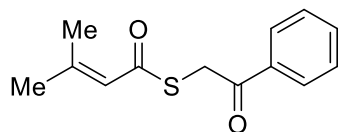
**S-(2-oxo-2-phenylethyl) (E)-3-(thiophen-2-yl)prop-2-enethioate (4.73e).**



Isolated as a faint yellow powder (110 mg, 48% yield) after chromatography (2 → 10% EtOAc/ hexanes). <sup>1</sup>H NMR (500

MHz, CDCl<sub>3</sub>): δ 8.03 (d, J = 7 Hz, 2H), 7.78 (d, J = 16 Hz, 1H), 7.61 (t, J = 7 Hz, 1H), 7.50 (t, J = 7 Hz, 2H), 7.43 (d, J = 5 Hz, 1H), 7.32 (d, J = 4 Hz, 1H), 7.07 (dd, J = 5 Hz, 4 Hz, 1H), 6.57 (d, J = 16 Hz, 1H), 4.53 (s, 2H). <sup>13</sup>C{<sup>1</sup>H} NMR (125 MHz, CDCl<sub>3</sub>): δ 193.5, 187.6, 139.2, 135.7, 134.2, 133.8, 132.4, 129.5, 128.9, 128.6, 128.5, 122.8, 36.5. IR (cm<sup>-1</sup>): 1692, 1661, 1592, 1196, 1034, 980. HRMS (ESI-TOF) m/z: [M + H]<sup>+</sup> calcd for C<sub>15</sub>H<sub>12</sub>O<sub>2</sub>S<sub>2</sub>, 289.0352; found, 289.0345. Mp: 133–137 °C.

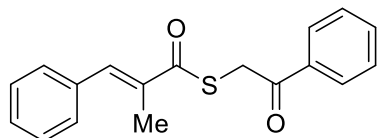
**S-(2-oxo-2-phenylethyl) 3-methylbut-2-enethioate (4.73f).**



Preparation according to the standard procedure was not successful.

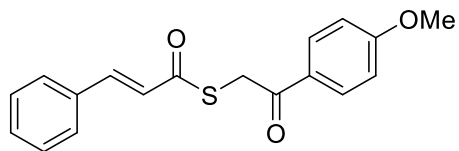
The compound was synthesized as follows: Phenacyl mercaptan (800  $\mu\text{L}$  of 0.62 M stock in  $\text{CH}_2\text{Cl}_2$ , 0.50 mmol) was added at 0  $^\circ\text{C}$  to 3,3-dimethylacryloyl chloride (55  $\mu\text{L}$ , 0.5 mmol) in 2.5 mL of freshly distilled  $\text{CH}_2\text{Cl}_2$ . Triethylamine (83  $\mu\text{L}$ , 0.60 mmol) was added dropwise. The reaction mixture was slowly warmed to rt, stirred for an additional 2 h, and quenched by adding 1 M aq HCl. The organic layer was separated, washed with 1 M aq  $\text{NaHCO}_3$ , dried with  $\text{Na}_2\text{SO}_4$ , and concentrated by rotary evaporation. The residue was purified by column chromatography (3  $\rightarrow$  7% EtOAc/hexanes) to afford the thioester as a clear, light yellow oil (110 mg, 94% yield).  $^1\text{H}$  NMR (500 MHz,  $\text{CDCl}_3$ ):  $\delta$  8.03–8.00 (m, 2H), 7.61–7.57 (m, 1H), 7.50–7.46 (m, 2H), 6.06–6.04 (m, 1H), 4.41 (s, 2H), 2.17 (d,  $J = 1$  Hz, 3H), 1.90 (d,  $J = 1$  Hz, 3H).  $^{13}\text{C}\{^1\text{H}\}$  NMR (125 MHz,  $\text{CDCl}_3$ ):  $\delta$  193.8, 187.1, 155.5, 135.7, 133.6, 128.8, 128.6, 122.5, 36.2, 27.3, 21.4. IR ( $\text{cm}^{-1}$ ): 2911, 1673, 1625, 1447, 1276, 1199, 1010. HRMS (ESI-TOF)  $m/z$ :  $[\text{M} + \text{Na}]^+$  calcd for  $\text{C}_{13}\text{H}_{14}\text{O}_2\text{S}$ , 257.0607; found, 257.0601.

**S-(2-oxo-2-phenylethyl) (E)-2-methyl-3-phenylprop-2-enethioate (4.73g).**



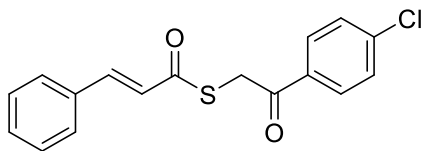
Isolated as a clear, colorless oil (185 mg, 72% yield) after chromatography (2  $\rightarrow$  6% EtOAc/hexane).  $^1\text{H}$  NMR (500 MHz,  $\text{CDCl}_3$ ):  $\delta$  8.07–8.03 (m, 2H), 7.73 (d,  $J = 1$  Hz, 1H), 7.64–7.59 (m, 1H), 7.53–7.48 (m, 2H), 7.43–7.39 (m, 4H), 7.37–7.33 (m, 1H), 4.50 (s, 2H), 2.19 (d,  $J = 1$  Hz, 3H).  $^{13}\text{C}\{^1\text{H}\}$  NMR (125 MHz,  $\text{CDCl}_3$ ):  $\delta$  193.8, 192.8, 138.4, 135.9, 135.6, 135.3, 133.8, 130.0, 129.0, 128.9, 128.7, 128.6, 36.9, 14.4. IR ( $\text{cm}^{-1}$ ): 3058, 2915, 1685, 1650, 1447, 1179, 1019, 988, 908, 747, 687. HRMS (ESI-TOF)  $m/z$ :  $[\text{M} + \text{Na}]^+$  calcd for  $\text{C}_{18}\text{H}_{16}\text{O}_2\text{S}$ , 319.0763; found, 319.0758.

**S-(2-(4-methoxyphenyl)-2-oxoethyl) (E)-3-phenylprop-2-enethioate (4.73h).**



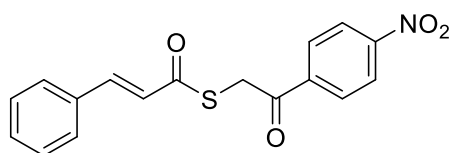
Isolated as a fine white powder (123 mg, 57% yield) after chromatography (5 → 15% EtOAc/ hexanes).  $^1\text{H}$  NMR (500 MHz,  $\text{CDCl}_3$ ):  $\delta$  8.02 (d,  $J$  = 9 Hz, 2H), 7.67 (d,  $J$  = 16 Hz, 1H), 7.57–7.51 (m, 2H), 7.43–7.36 (m, 3H), 6.96 (d,  $J$  = 9 Hz, 2H), 6.76 (d,  $J$  = 16 Hz, 1H), 4.49 (s, 2H), 3.87 (s, 3H).  $^{13}\text{C}\{^1\text{H}\}$  NMR (125 MHz,  $\text{CDCl}_3$ ):  $\delta$  192.0, 188.4, 164.1, 141.7, 134.0, 131.0, 130.9, 129.1, 128.7, 128.6, 124.3, 114.1, 55.6, 36.2. IR ( $\text{cm}^{-1}$ ): 1687, 1598, 1257, 1033, 982, 757. HRMS (ESI-TOF)  $m/z$ :  $[\text{M} + \text{Na}]^+$  calcd for  $\text{C}_{18}\text{H}_{16}\text{O}_3\text{S}$ , 335.0712; found, 335.0715. Mp: 116–118 °C.

**S-(2-(4-chlorophenyl)-2-oxoethyl) (E)-3-phenylprop-2-enethioate (4.73i).**



Isolated as a fine white powder (967 mg, 57% yield) after chromatography (5 → 15% EtOAc/ hexane).  $^1\text{H}$  NMR (500 MHz,  $\text{CDCl}_3$ ):  $\delta$  7.98 (d,  $J$  = 9 Hz, 2H), 7.67 (d,  $J$  = 16 Hz, 1H), 7.57–7.51 (m, 2H), 7.47 (d,  $J$  = 9 Hz, 2H), 7.43–7.36 (m, 3H), 6.76 (d,  $J$  = 16 Hz, 1H), 4.48 (s, 2H).  $^{13}\text{C}\{^1\text{H}\}$  NMR (125 MHz,  $\text{CDCl}_3$ ):  $\delta$  192.5, 188.1, 142.1, 140.4, 134.0, 133.9, 131.0, 130.1, 129.2, 129.1, 128.6, 124.0, 36.3. IR ( $\text{cm}^{-1}$ ): 1693, 1655, 1614, 1039, 754. HRMS (ESI-TOF)  $m/z$ :  $[\text{M} + \text{Na}]^+$  calcd for  $\text{C}_{17}\text{H}_{13}\text{ClO}_2\text{S}$ , 339.0217; found, 339.0218. Mp: 127–129 °C.

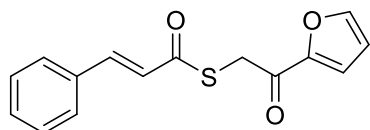
**S-(2-(4-nitrophenyl)-2-oxoethyl) (E)-3-phenylprop-2-enethioate (4.73j).**



Isolated as a faint yellow powder (320 mg, 25% yield) after chromatography (5 → 20% EtOAc/ hexane).  $^1\text{H}$  NMR (500 MHz,  $\text{CDCl}_3$ ):  $\delta$  8.35 (d,  $J$  = 9 Hz, 2H), 8.20 (d,  $J$  = 9 Hz,

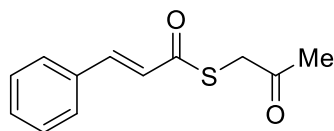
2H), 7.68 (d,  $J = 16$  Hz, 1H), 7.57–7.54 (m, 2H), 7.44–7.38 (m, 3H), 6.76 (d,  $J = 16$  Hz, 1H), 4.51 (s, 2H).  $^{13}\text{C}\{^1\text{H}\}$  NMR (125 MHz,  $\text{CDCl}_3$ ):  $\delta$  192.6, 187.8, 150.8, 142.6, 140.3, 133.8, 131.2, 129.8, 129.2, 128.7, 124.1, 123.8, 36.4. IR ( $\text{cm}^{-1}$ ): 1698, 1675, 1514, 973, 762. HRMS (ESI-TOF)  $m/z$ :  $[\text{M} + \text{Na}]^+$  calcd for  $\text{C}_{17}\text{H}_{13}\text{NO}_4\text{S}$ , 350.0457; found, 350.0450. Mp: 157–160 °C.

**S-(2-(furan-2-yl)-2-oxoethyl) (E)-3-phenylprop-2-enethioate (4.73k).**



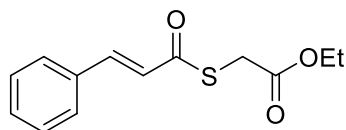
Isolated as a yellow crystalline solid (171 mg, 66% yield) after chromatography (2  $\rightarrow$  10% EtOAc/ hexanes).  $^1\text{H}$  NMR (500 MHz,  $\text{CDCl}_3$ ):  $\delta$  7.68–7.63 (m, 2H), 7.55–7.51 (m, 2H), 7.41–7.34 (m, 4H), 6.75 (d,  $J = 16$  Hz, 1H), 6.59–6.55 (m, 1H), 4.36 (s, 2H).  $^{13}\text{C}\{^1\text{H}\}$  NMR (125 MHz,  $\text{CDCl}_3$ ):  $\delta$  188.0, 182.3, 151.6, 147.3, 142.0, 133.9, 131.0, 129.1, 128.6, 124.1, 118.7, 112.7, 35.5. IR ( $\text{cm}^{-1}$ ): 2925, 1669, 1615, 1465, 1392, 1236, 1036. HRMS (ESI-TOF)  $m/z$ :  $[\text{M} + \text{Na}]^+$  calcd for  $\text{C}_{15}\text{H}_{12}\text{O}_3\text{S}$ , 295.0399; found, 295.0397. Mp: 102–104 °C.

**S-(2-oxopropyl) (E)-3-phenylprop-2-enethioate (4.73l).**



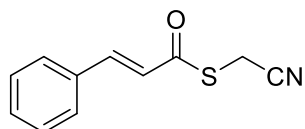
Isolated as a light yellow oil (210 mg, 76% yield), which crystallized upon standing, after chromatography (2  $\rightarrow$  6% EtOAc/hexane).  $^1\text{H}$  NMR (500 MHz,  $\text{CDCl}_3$ ):  $\delta$  7.66 (d,  $J = 16$  Hz, 1H), 7.58–7.52 (m, 2H), 7.44–7.37 (m, 3H), 6.76 (d,  $J = 16$  Hz, 1H), 3.88 (s, 2H), 2.32 (s, 3H).  $^{13}\text{C}\{^1\text{H}\}$  NMR (125 MHz,  $\text{CDCl}_3$ ):  $\delta$  201.9, 188.1, 141.9, 133.8, 130.9, 129.0, 128.5, 124.0, 39.4, 28.8. IR ( $\text{cm}^{-1}$ ): 2920, 1712, 1611, 1046, 772. HRMS (ESI-TOF)  $m/z$ :  $[\text{M} + \text{Na}]^+$  calcd for  $\text{C}_{12}\text{H}_{12}\text{O}_2\text{S}$ , 243.0450; found, 243.0442. Mp: 55–57 °C.

### ethyl 2-(cinnamoylthio)acetate (4.73m).



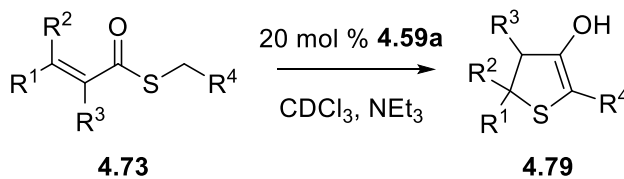
Isolated as a clear oil (124 mg, 70% yield) after chromatography (2 → 6% EtOAc/hexane). <sup>1</sup>H NMR (500 MHz, CDCl<sub>3</sub>): δ 7.66 (d, J = 16 Hz, 1H), 7.57–7.53 (m, 2H), 7.43–7.38 (m, 3H), 6.75 (d, J = 16 Hz, 1H), 4.22 (q, J = 7 Hz, 2H), 3.83 (s, 2H), 1.30 (t, J = 7 Hz, 3H). <sup>13</sup>C{<sup>1</sup>H} NMR (125 MHz, CDCl<sub>3</sub>): δ 187.9, 168.9, 141.9, 134.0, 131.0, 129.1, 128.6, 124.1, 62.0, 31.5, 14.3. IR (cm<sup>-1</sup>): 2982, 1733, 1656, 1613, 1449, 1293, 1262, 1133, 1022, 752. HRMS (ESI-TOF) m/z: [M + H]<sup>+</sup> calcd for C<sub>13</sub>H<sub>14</sub>O<sub>3</sub>S, 251.0737; found, 251.0736.

### S-(cyanomethyl) (E)-3-phenylprop-2-enthioate (4.73n).



Isolated as a white powder (483 mg, 79% yield) after chromatography (2 → 10% EtOAc/hexane). <sup>1</sup>H NMR (500 MHz, CDCl<sub>3</sub>): δ 7.70 (d, J = 16 Hz, 1H), 7.58–7.54 (m, 2H), 7.47–7.39 (m, 3H), 6.72 (d, J = 16 Hz, 1H), 3.81 (s, 2H). <sup>13</sup>C{<sup>1</sup>H} NMR (125 MHz, CDCl<sub>3</sub>): δ 185.7, 143.7, 133.5, 131.5, 129.2, 128.8, 122.9, 116.0, 14.3. IR (cm<sup>-1</sup>): 3059, 2970, 2927, 1672, 1607, 1038, 997, 752, 688. HRMS (ESI-TOF) m/z: [M + Na]<sup>+</sup> calcd for C<sub>11</sub>H<sub>9</sub>NOS, 226.0297; found, 226.0289. Mp: 82–83 °C.

## 4.8.2 Rearrangements of thioesters 4.73





## General procedure for the rearrangements (0.1 mmol scale)

### *Synthesis of 4.79a*

Thioester **4.73a** (0.1 mmol) was dissolved in freshly distilled CDCl<sub>3</sub> (450 μL) and transferred to an NMR tube. To this solution was added 20 mol % of DHIP **4.59a** (50 μL of 0.4 M solution in CDCl<sub>3</sub>) followed by triethylamine (14 μL, 0.10 mmol). The contents were mixed, and the reaction progress was monitored by <sup>1</sup>H NMR. After complete consumption of the thioester (16–24 h), the reaction was quenched with 1 M aqueous HCl. The aqueous layer was extracted twice with CH<sub>2</sub>Cl<sub>2</sub>. The combined organic layers were dried with Na<sub>2</sub>SO<sub>4</sub> and concentrated by rotary evaporation. The crude product was adsorbed on silica gel and purified by flash chromatography (1 → 3% EtOAc/hexane). The product **4.79a** was isolated as an orange oil (21 mg, 75%), which solidified upon standing. Other thioester substrates were rearranged on a 0.1 mmol scale as described above for **4.73a** to give the products listed below.

### Large scale (2.5 mmol) rearrangement

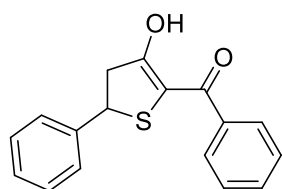
The reaction was conducted analogously to the small scale procedure using the following quantities: 706 mg of substrate **4.73a** (2.50 mmol), 1.08 mL of 0.463 M DHIP **4.59a** (0.5 mmol) in CDCl<sub>3</sub>, 349 μL of triethylamine (2.50 mmol), 11.5 mL of CDCl<sub>3</sub>. The product was obtained in 60% yield (426 mg).

### Enantioselective rearrangement

The reaction was conducted analogously to the small-scale procedure described above using chiral catalysts **4.54**, **4.69**, and **4.81**. Reaction times were extended appropriately. Product **4.79a** was obtained in 36% yield (10 mg) using catalyst **4.54**. HPLC (0.5% isopropanol/hexanes):

minor enantiomer, 37.3 min; major enantiomer, 42.2 min; 54% ee;  $[\alpha]_D^{23} = -7.5^\circ$  (c 0.133,  $\text{CH}_2\text{Cl}_2$ ).

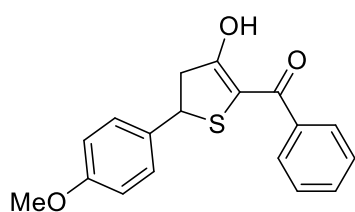
**(3-hydroxy-5-phenyl-4,5-dihydrothiophen-2-yl)(phenyl)methanone (4.79a).**



$^1\text{H}$  NMR (500 MHz,  $\text{CDCl}_3$ ):  $\delta$  13.96 (s, 1H), 7.89–7.85 (m, 2H), 7.48–7.40 (m, 5H), 7.38–7.33 (m, 2H), 7.32–7.28 (m, 1H), 4.78 (t,  $J = 8$  Hz, 1H), 3.23 (dd,  $J = 17$  Hz, 8 Hz, 1H), 3.14 (dd,  $J = 17$  Hz, 8 Hz, 1H).

$^{13}\text{C}\{^1\text{H}\}$  NMR (125 MHz,  $\text{CDCl}_3$ ):  $\delta$  206.1, 163.4, 140.0, 134.1, 131.3, 129.1, 128.5, 128.3, 128.1, 127.2, 106.4, 47.5, 46.6. IR ( $\text{cm}^{-1}$ ): 1560, 1489, 1446, 1236, 1095, 690. HRMS (ESI-TOF)  $m/z$ :  $[\text{M} + \text{Na}]^+$  calcd for  $\text{C}_{17}\text{H}_{14}\text{O}_2\text{S}$ , 305.0607; found, 305.0597. Mp: 81–83  $^\circ\text{C}$ .

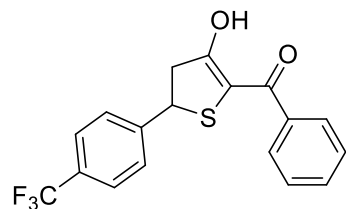
**(3-hydroxy-5-(4-methoxyphenyl)-4,5-dihydrothiophen-2-yl)(phenyl)methanone (4.79b).**



Isolated as a yellow oil (24 mg, 77% yield) after chromatography (2.5  $\rightarrow$  5% EtOAc/ hexane).  $^1\text{H}$  NMR (500 MHz,  $\text{CDCl}_3$ ):  $\delta$  13.95 (s, 1H), 7.88–7.84 (m, 2H), 7.47–7.42 (m, 3H), 7.34 (d,  $J = 9$  Hz, 2H), 6.88 (d,  $J = 9$  Hz, 2H), 4.75 (t,  $J = 8$  Hz, 1H), 3.80 (s, 3H), 3.19 (dd,  $J = 17$  Hz, 8 Hz, 1H), 3.11 (dd,  $J = 17$  Hz, 8 Hz, 1H).

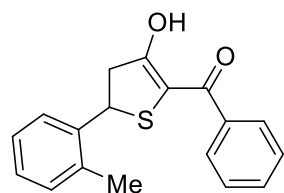
$^{13}\text{C}\{^1\text{H}\}$  NMR (125 MHz,  $\text{CDCl}_3$ ):  $\delta$  206.3, 163.3, 159.6, 134.1, 131.8, 131.3, 128.5, 128.4, 128.1, 114.4, 106.6, 55.5, 47.7, 46.3. IR ( $\text{cm}^{-1}$ ): 1609, 1561, 1512, 1339, 1250, 1178, 1102. HRMS (ESI-TOF)  $m/z$ :  $[\text{M} + \text{Na}]^+$  calcd for  $\text{C}_{18}\text{H}_{16}\text{O}_3\text{S}$ , 335.0712; found, 335.0718.

**(3-hydroxy-5-(4-(trifluoromethyl)phenyl)-4,5-dihydrothiophen-2-yl)(phenyl)methanone (4.79c).**



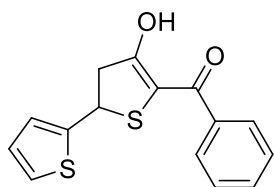
Isolated as a yellow oil (22 mg, 63% yield) after chromatography (1 → 6% EtOAc/ hexane).  $^1\text{H}$  NMR (500 MHz,  $\text{CDCl}_3$ ):  $\delta$  13.97 (s, 1H), 7.88–7.84 (m, 2H), 7.61 (d,  $J = 9$  Hz, 2H), 7.53 (d,  $J = 9$  Hz, 2H), 7.49–7.44 (m, 3H), 4.79 (t,  $J = 8$  Hz, 1H), 3.28 (dd,  $J = 18$  Hz, 8 Hz, 1H), 3.10 (dd,  $J = 18$  Hz, 8 Hz, 1H).  $^{13}\text{C}\{^1\text{H}\}$  NMR (125 MHz,  $\text{CDCl}_3$ ):  $\delta$  205.3, 164.1, 144.4, 134.0, 131.6, 130.5 (q,  $^2J_{\text{C-F}} = 33$  Hz), 128.6, 128.1, 127.7, 127.3, 126.1 (q,  $^3J_{\text{C-F}} = 4$  Hz), 124.0 (q,  $^1J_{\text{C-F}} = 270$  Hz), 47.2, 45.8. IR ( $\text{cm}^{-1}$ ): 2925, 1619, 1589, 1561, 1324, 1112, 1069. HRMS (ESI-TOF)  $m/z$ :  $[\text{M} + \text{Na}]^+$  calcd for  $\text{C}_{18}\text{H}_{13}\text{F}_3\text{O}_2\text{S}$ , 373.0480; found, 373.0471.

**(3-hydroxy-5-(o-tolyl)-4,5-dihydrothiophen-2-yl)(phenyl)methanone (4.79d).**



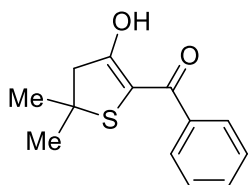
Isolated as a yellow oil (23 mg, 82%), which solidified upon standing, after chromatography (2 → 6% EtOAc/hexane).  $^1\text{H}$  NMR (500 MHz,  $\text{CDCl}_3$ ):  $\delta$  14.01 (s, 1H), 7.89–7.83 (m, 2H), 7.50 (d,  $J = 8$  Hz, 1H), 7.47–7.41 (m, 3H), 7.25–7.15 (m, 3H), 4.98 (t,  $J = 8$  Hz, 1H), 3.22 (dd,  $J = 17$  Hz, 8 Hz, 1H), 3.15 (dd,  $J = 17$  Hz, 8 Hz, 1H), 2.40 (s, 3H).  $^{13}\text{C}\{^1\text{H}\}$  NMR (125 MHz,  $\text{CDCl}_3$ ):  $\delta$  206.4, 163.8, 138.0, 136.1, 134.1, 131.3, 130.9, 128.5, 128.1, 128.0, 126.9, 125.8, 106.0, 46.4, 42.6, 19.7. IR ( $\text{cm}^{-1}$ ): 1556, 1488, 1443, 1341, 1242, 1095, 832, 779, 687. HRMS (ESI-TOF)  $m/z$ :  $[\text{M} + \text{Na}]^+$  calcd for  $\text{C}_{18}\text{H}_{16}\text{O}_2\text{S}$ , 319.0763; found, 319.0754. Mp: 100–103 °C.

**(4-hydroxy-2,3-dihydro-[2,2'-bithiophen]-5-yl)(phenyl)methanone (4.79e).**



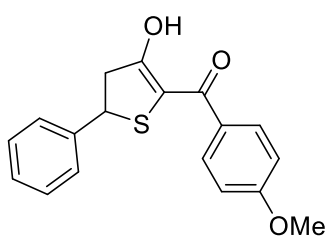
Isolated as a yellow oil (15 mg, 56% yield) after chromatography (2 → 10% EtOAc/ hexane).  $^1\text{H}$  NMR (500 MHz,  $\text{CDCl}_3$ ):  $\delta$  13.96 (s, 1H), 7.87–7.83 (m, 2H), 7.48–7.44 (m, 3H), 7.26–7.23 (m, 1H), 7.06–7.03 (m, 1H), 6.96–6.94 (m, 1H), 5.02 (t,  $J = 8$  Hz, 1H), 3.28 (dd,  $J = 17$  Hz, 8 Hz, 1H), 3.15 (dd,  $J = 17$  Hz, 8 Hz, 1H).  $^{13}\text{C}\{^1\text{H}\}$  NMR (125 MHz,  $\text{CDCl}_3$ ):  $\delta$  205.2, 164.0, 144.0, 134.0, 131.4, 128.5, 128.1, 127.1, 125.6, 125.4, 106.0, 48.6, 42.0. IR ( $\text{cm}^{-1}$ ): 3066, 1630, 1586, 1557, 1338, 1237, 1097, 690. HRMS (ESI-TOF)  $m/z$ :  $[\text{M} + \text{Na}]^+$  calcd for  $\text{C}_{15}\text{H}_{12}\text{O}_2\text{S}_2$ , 311.0171; found, 311.0159.

**(3-hydroxy-5,5-dimethyl-4,5-dihydrothiophen-2-yl)(phenyl)methanone (4.79f).**



The rearrangement was carried out for 24 h at 50 °C. Isolated as a yellow crystalline solid (15 mg, 65% yield) after chromatography (1 → 3% EtOAc/hexane).  $^1\text{H}$  NMR (500 MHz,  $\text{CDCl}_3$ ):  $\delta$  13.92 (s, 1H), 7.86–7.82 (m, 2H), 7.48–7.44 (m, 3H), 2.76 (s, 2H), 1.53 (s, 6H).  $^{13}\text{C}\{^1\text{H}\}$  NMR (125 MHz,  $\text{CDCl}_3$ ):  $\delta$  206.9, 163.5, 134.2, 131.2, 128.4, 128.1, 107.5, 55.1, 48.8, 30.1. IR ( $\text{cm}^{-1}$ ): 2957, 2925, 1633, 1589, 1562, 1338, 1249. HRMS (ESI-TOF)  $m/z$ :  $[\text{M} + \text{H}]^+$  calcd for  $\text{C}_{13}\text{H}_{14}\text{O}_2\text{S}$ , 235.0787; found, 235.0782. Mp: 64–65 °C.

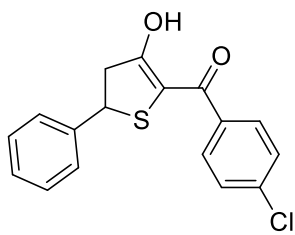
**(3-hydroxy-5-phenyl-4,5-dihydrothiophen-2-yl)(4-methoxyphenyl)methanone (4.79h).**



Isolated as a yellow oil (25 mg, 81% yield) after chromatography (2.5 → 5% EtOAc/ hexane).  $^1\text{H}$  NMR (500 MHz,  $\text{CDCl}_3$ ):  $\delta$  14.19 (s, 1H), 7.87 (d,  $J = 9$  Hz, 2H), 7.44–7.40 (m, 2H), 7.38–7.33 (m, 2H), 7.32–7.28 (m, 1H), 6.96 (d,  $J = 9$  Hz, 2H), 4.77 (t,  $J = 8$  Hz, 1H), 3.85 (s, 3H), 3.21 (dd,  $J = 17$  Hz, 8 Hz, 1H), 3.12 (dd,  $J = 17$  Hz, 8 Hz, 1H).  $^{13}\text{C}\{^1\text{H}\}$  NMR (125

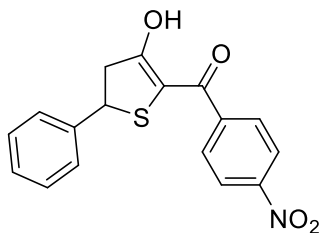
MHz, CDCl<sub>3</sub>):  $\delta$  205.2, 164.1, 162.1, 140.2, 130.1, 129.1, 128.2, 127.3, 126.3, 114.0, 104.8, 55.6, 47.4, 46.6. IR (cm<sup>-1</sup>): 2930, 2839, 1599, 1506, 1253, 1175, 1102, 1026, 837, 697. HRMS (ESI-TOF) m/z: [M + Na]<sup>+</sup> calcd for C<sub>18</sub>H<sub>16</sub>O<sub>3</sub>S, 335.0712; found, 335.0708.

**(4-chlorophenyl)(3-hydroxy-5-phenyl-4,5-dihydrothiophen-2-yl)methanone (4.79i).**



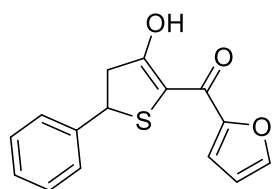
Isolated as an orange oil (22 mg, 69%), which solidified upon standing, after chromatography (2 → 5% EtOAc/hexane). <sup>1</sup>H NMR (500 MHz, CDCl<sub>3</sub>):  $\delta$  13.92 (s, 1H), 7.83 (d, J = 9 Hz, 2H), 7.44–7.39 (m, 4H), 7.39–7.34 (m, 2H), 7.34–7.29 (m, 1H), 4.78 (t, J = 8 Hz, 1H), 3.23 (dd, J = 17 Hz, 8 Hz, 1H), 3.13 (dd, J = 17 Hz, 8 Hz, 1H). <sup>13</sup>C{<sup>1</sup>H} NMR (125 MHz, CDCl<sub>3</sub>):  $\delta$  206.3, 161.8, 139.8, 137.3, 132.5, 129.4, 129.1, 128.8, 128.4, 127.2, 106.7, 47.4, 46.6. IR (cm<sup>-1</sup>): 1578, 1485, 1230, 1088, 830. HRMS (ESI-TOF) m/z: [M + H]<sup>+</sup> calcd for C<sub>17</sub>H<sub>13</sub>ClO<sub>2</sub>S, 317.0398; found, 317.0376. Mp: 72–75 °C.

**(3-hydroxy-5-phenyl-4,5-dihydrothiophen-2-yl)(4-nitrophenyl)methanone (4.79j).**



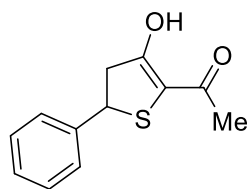
Isolated as a red oil (17 mg, 53% yield) after chromatography (1 → 4% EtOAc/hexane). Note that the solution may need to be heated to fully dissolve thioester **4.76j** prior to the addition of the catalyst. <sup>1</sup>H NMR (500 MHz, CDCl<sub>3</sub>):  $\delta$  13.68 (s, 1H), 8.29 (d, J = 9 Hz, 2H), 8.04 (d, J = 9 Hz, 2H), 7.43–7.30 (m, 5H), 4.83 (t, J = 8 Hz, 1H), 3.28 (dd, J = 18 Hz, 8 Hz, 1H), 3.16 (dd, J = 18 Hz, 8 Hz, 1H). <sup>13</sup>C{<sup>1</sup>H} NMR (125 MHz, CDCl<sub>3</sub>):  $\delta$  207.2, 159.1, 148.7, 140.1, 139.4, 129.2, 129.0, 128.6, 127.2, 123.7, 109.2, 47.4, 46.6. IR (cm<sup>-1</sup>): 1640, 1566, 1519, 1344, 1231, 1098, 698. HRMS (ESI-TOF) m/z: [M + Na]<sup>+</sup> calcd for C<sub>17</sub>H<sub>13</sub>NO<sub>4</sub>S, 350.0457; found, 350.0450.

### furan-2-yl(3-hydroxy-5-phenyl-4,5-dihydrothiophen-2-yl)methanone (4.79k).



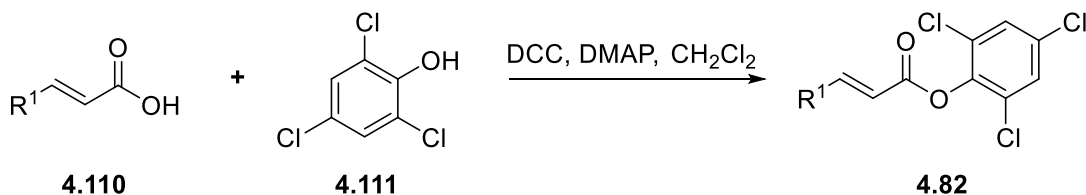
Isolated as an orange oil (20 mg, 71%), which solidified upon standing, after chromatography (2 → 10% EtOAc/hexane).  $^1\text{H}$  NMR (500 MHz,  $\text{CDCl}_3$ ):  $\delta$  13.48 (s, 1H), 7.65–7.62 (m, 1H), 7.42 (d,  $J = 8$  Hz, 2H), 7.38–7.33 (m, 2H), 7.33–7.28 (m, 1H), 7.09 (d,  $J = 4$  Hz, 1H), 6.59–6.56 (m, 1H), 4.80 (t,  $J = 8$  Hz, 1H), 3.22 (dd,  $J = 17$  Hz, 8 Hz, 1H), 3.09 (dd,  $J = 17$  Hz, 8 Hz, 1H).  $^{13}\text{C}\{^1\text{H}\}$  NMR (125 MHz,  $\text{CDCl}_3$ ):  $\delta$  205.9, 153.0, 147.8, 145.9, 140.3, 129.1, 128.2, 127.2, 116.3, 112.7, 104.8, 47.6, 46.3. IR ( $\text{cm}^{-1}$ ): 1604, 1455, 1255, 1242, 1164, 1113, 1009, 745, 694. HRMS (ESI-TOF)  $m/z$ :  $[\text{M} + \text{Na}]^+$  calcd for  $\text{C}_{15}\text{H}_{12}\text{O}_3\text{S}$ , 295.0399; found, 295.0389. Mp: 79–82 °C.

### 1-(3-hydroxy-5-phenyl-4,5-dihydrothiophen-2-yl)ethan-1-one (4.79l).



Isolated as a yellow oil (9 mg, 41%, ca. 90% pure by  $^1\text{H}$  NMR) after chromatography (0.5 → 1.5% EtOAc/hexane).  $^1\text{H}$  NMR (500 MHz,  $\text{CDCl}_3$ ):  $\delta$  13.00 (s, 1H), 7.44–7.33 (m, 4H), 7.32–7.28 (m, 1H), 4.73 (t,  $J = 8$  Hz, 1H), 3.12 (dd,  $J = 17$  Hz, 8 Hz, 1H), 3.01 (dd,  $J = 17$  Hz, 8 Hz, 1H), 2.01 (s, 3H).  $^{13}\text{C}\{^1\text{H}\}$  NMR (125 MHz,  $\text{CDCl}_3$ ):  $\delta$  203.1, 167.8, 140.4, 129.0, 128.2, 127.2, 107.2, 47.7, 46.2, 21.8. IR ( $\text{cm}^{-1}$ ): 2922, 1646, 1598, 1332, 1219, 698. HRMS (ESI-TOF)  $m/z$ :  $[\text{M} + \text{Na}]^+$  calcd for  $\text{C}_{12}\text{H}_{12}\text{O}_2\text{S}$ , 243.0450; found, 243.0442.

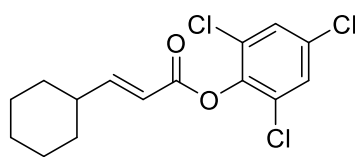
## 4.8.3 Synthesis of trichlorophenyl esters 4.82



*2,4,6-trichlorophenyl cinnamate* **4.82a** ( $R^1=Ph$ )

Following a published procedure<sup>16</sup>, to a solution of cinnamic acid (1.00 g, 6.75 mmol) in 10 mL of CH<sub>2</sub>Cl<sub>2</sub> stirring at 0 °C was added a solution of DCC (1.67 g, 8.10 mmol, 1.2 equiv) and DMAP (17 mg, 0.14 mmol, 2 mol %) in 5 mL of CH<sub>2</sub>Cl<sub>2</sub> under an inert atmosphere. After 20 min, a solution of 2,4,6-trichlorophenol (1.33 g, 6.75 mmol, 1.0 equiv) in 5 mL of CH<sub>2</sub>Cl<sub>2</sub> was added dropwise. In 1 h, the mixture was allowed to warm to rt and the stirring continued until complete consumption of the phenol by TLC (10% EtOAc/hexane). The reaction mixture was filtered, and the precipitated N,N'-dicyclohexylurea was washed on the filter with CH<sub>2</sub>Cl<sub>2</sub>. The filtrate was concentrated by rotary evaporation, and the crude product was purified by column chromatography (2 → 10% EtOAc/hexane) to afford the product as a white crystalline solid (2.10 g, 95% yield, mp 79–80 °C). Its spectroscopic data matched those reported in the literature.<sup>23</sup> Other trichlorophenyl esters listed below were obtained analogously from the corresponding carboxylic acids<sup>21</sup> and purified by chromatography using the same eluent as above.

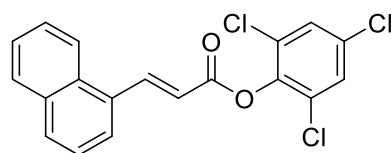
**2,4,6-trichlorophenyl (E)-3-cyclohexylacrylate (4.82o).**



White crystalline solid (619 mg, 89% yield). <sup>1</sup>H NMR (500 MHz, CDCl<sub>3</sub>): δ 7.38 (s, 2H), 7.23 (dd, J = 16 Hz, 7 Hz, 1H), 6.02 (dd, J = 16 Hz, 2 Hz, 1H), 2.30–2.20 (m, 1H), 1.89–1.76 (m, 4H),

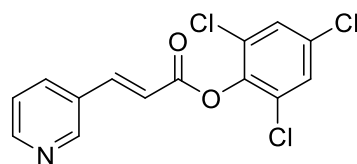
1.75–1.67 (m, 1H), 1.40–1.16 (m, 5H). <sup>13</sup>C{<sup>1</sup>H} NMR (125 MHz, CDCl<sub>3</sub>): δ 162.9, 158.8, 143.2, 131.8, 129.8, 128.6, 116.4, 40.9, 31.5, 26.0, 25.8. IR (cm<sup>-1</sup>): 2933, 2851, 1746, 1645, 1564, 1445, 1096, 854. HRMS (ESI-TOF) m/z: [M + Na]<sup>+</sup> calcd for C<sub>15</sub>H<sub>15</sub>Cl<sub>3</sub>O<sub>2</sub>, 355.0030; found, 355.0025. Mp: 70–72 °C.

### 2,4,6-trichlorophenyl (E)-3-(naphthalen-1-yl)acrylate (4.82p).



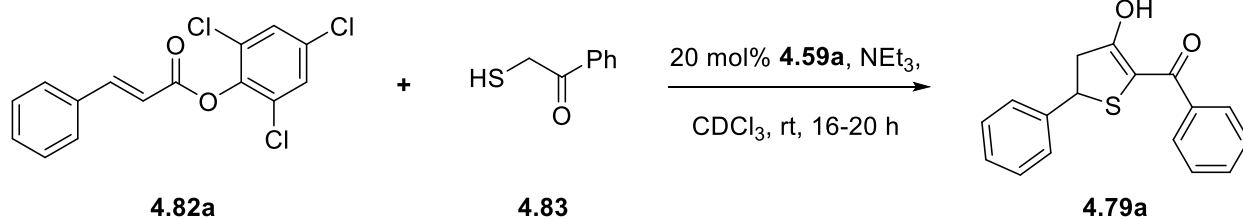
Colorless crystalline solid (265 mg, 88% yield).  $^1\text{H}$  NMR (500 MHz,  $\text{CDCl}_3$ ):  $\delta$  8.12 (d,  $J = 16$  Hz, 1H), 8.04–8.00 (m, 1H), 7.92–7.84 (m, 3H), 7.77–7.73 (m, 1H), 7.58–7.51 (m, 2H), 7.42 (s, 2H), 6.80 (d,  $J = 16$  Hz, 1H).  $^{13}\text{C}\{^1\text{H}\}$  NMR (125 MHz,  $\text{CDCl}_3$ ):  $\delta$  163.2, 148.6, 143.3, 134.8, 133.4, 132.1, 131.5, 131.1, 130.0, 129.1, 128.9, 128.8, 128.0, 127.9, 127.1, 123.6, 115.5. IR ( $\text{cm}^{-1}$ ): 3059, 2927, 2853, 1736, 1626, 1562, 1444, 1110, 814. HRMS (ESI-TOF)  $m/z$ :  $[\text{M} + \text{Na}]^+$  calcd for  $\text{C}_{19}\text{H}_{11}\text{Cl}_3\text{O}_2$ , 398.9723; found, 398.9705. Mp: 144–146  $^\circ\text{C}$ .

### 2,4,6-trichlorophenyl (E)-3-(pyridin-3-yl)acrylate (4.82q).



Light tan crystalline solid (596 mg, 80% yield).  $^1\text{H}$  NMR (500 MHz,  $\text{CDCl}_3$ ):  $\delta$  8.81 (s, 1H), 8.66–8.62 (m, 1H), 7.92 (d,  $J = 16$  Hz, 1H), 7.92–7.87 (m, 1H), 7.40–7.32 (m, 3H), 6.74 (d,  $J = 16$  Hz, 1H).  $^{13}\text{C}\{^1\text{H}\}$  NMR (125 MHz,  $\text{CDCl}_3$ ):  $\delta$  162.4, 151.8, 150.2, 144.7, 142.9, 134.6, 132.2, 129.7, 129.6, 128.7, 123.9, 117.5. IR ( $\text{cm}^{-1}$ ): 3079, 2928, 1736, 1447, 1412, 1204, 801. HRMS (ESI-TOF)  $m/z$ :  $[\text{M} + \text{H}]^+$  calcd for  $\text{C}_{14}\text{H}_8\text{Cl}_3\text{NO}_2$ , 327.9701; found, 327.9686. Mp: 133–135  $^\circ\text{C}$ .

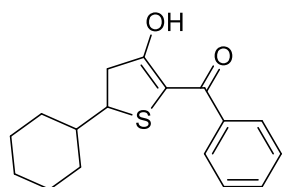
## 4.8.4 Two component synthesis of dihydrothiophene 4.79a





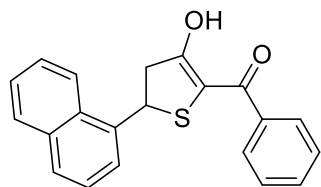
A solution of trichlorophenyl cinnamate **4.82a** (33 mg, 0.1 mmol) and phenacylmercaptan **4.83** (15 mg, 0.1 mmol) in 450  $\mu\text{L}$  of  $\text{CDCl}_3$  was placed into an NMR tube and treated with a stock solution of DHIP (50  $\mu\text{L}$  of 0.4 M in  $\text{CDCl}_3$ ) followed by triethylamine (14  $\mu\text{L}$ , 0.1 mmol). The contents were mixed, and the reaction progress was monitored by  $^1\text{H}$  NMR. After complete consumption of the ester (16–20 h), the reaction was quenched by pouring into 1 M HCl. The aqueous layer was extracted twice with  $\text{CH}_2\text{Cl}_2$ . The combined organic extracts were dried with  $\text{Na}_2\text{SO}_4$  and concentrated by rotary evaporation. The crude product was adsorbed on silica gel and purified by flash chromatography (1  $\rightarrow$  3% EtOAc/hexane). The product **4.82a** was isolated as an orange oil (27 mg, 82% yield), which solidified upon standing. Other dihydrothiophene products listed below were obtained analogously.

**(5-cyclohexyl-3-hydroxy-4,5-dihydrothiophen-2-yl)(phenyl)methanone (4.79o).**



Isolated as a yellow oil (24 mg, 73% yield), which solidified upon standing, after chromatography (1  $\rightarrow$  3% ether/hexane).  $^1\text{H}$  NMR (500 MHz,  $\text{CDCl}_3$ ):  $\delta$  13.93 (s, 1H), 7.92–7.87 (m, 2H), 7.49–7.44 (m, 3H), 3.47–3.40 (m, 1H), 2.94 (dd,  $J = 17$  Hz, 8 Hz, 1H), 2.71 (dd,  $J = 17$  Hz, 8 Hz, 1H), 1.86–1.72 (m, 4H), 1.71–1.64 (m, 1H), 1.62–1.50 (m, 3H), 1.32–1.00 (m, 3H).  $^{13}\text{C}\{^1\text{H}\}$  NMR (125 MHz,  $\text{CDCl}_3$ ):  $\delta$  207.3, 162.9, 134.3, 131.1, 128.5, 128.1, 106.5, 49.5, 44.3, 43.6, 31.1, 30.9, 26.3, 26.1, 26.0. IR ( $\text{cm}^{-1}$ ): 2922, 2852, 1629, 1583, 1555, 1335, 1241, 685. HRMS (ESI-TOF)  $m/z$ :  $[\text{M} + \text{Na}]^+$  calcd for  $\text{C}_{17}\text{H}_{20}\text{O}_2\text{S}$ , 311.1076; found, 311.1065. Mp: 68–71  $^\circ\text{C}$ .

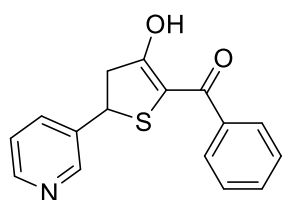
**(3-hydroxy-5-(naphthalen-1-yl)-4,5-dihydrothiophen-2-yl)(phenyl)methanone (4.79p).**



Isolated as a yellow solid (19 mg, 50% yield) after chromatography (2  $\rightarrow$  6% EtOAc/ hexane).  $^1\text{H}$  NMR (500 MHz,  $\text{CDCl}_3$ ):  $\delta$  14.01 (s, 1H), 7.91–7.80 (m, 6H), 7.57–7.44 (m, 6H), 4.95 (t,  $J = 8$  Hz, 1H),

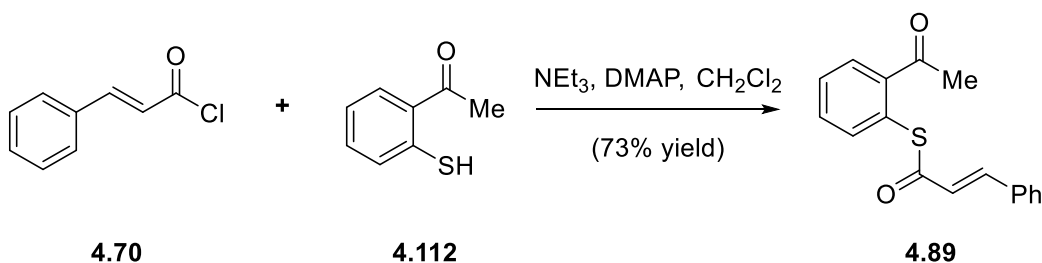
3.31 (dd,  $J = 18$  Hz, 8 Hz, 1H), 3.25 (dd,  $J = 18$  Hz, 8 Hz, 1H).  $^{13}\text{C}\{^1\text{H}\}$  NMR (125 MHz,  $\text{CDCl}_3$ ):  $\delta$  206.1, 163.6, 137.3, 134.1, 133.4, 133.2, 131.4, 129.1, 128.5, 128.1, 128.0, 127.9, 126.7, 126.5, 126.1, 125.0, 106.4, 47.4, 46.7. IR ( $\text{cm}^{-1}$ ): 3058, 2923, 1631, 1554, 1335, 1235, 1098, 825. HRMS (ESI-TOF)  $m/z$ :  $[\text{M} + \text{Na}]^+$  calcd for  $\text{C}_{21}\text{H}_{16}\text{O}_2\text{S}$ , 355.0763; found, 355.0761. Mp: 94–96 °C.

**(3-hydroxy-5-(pyridin-3-yl)-4,5-dihydrothiophen-2-yl)(phenyl)methanone (4.79q).**



Isolated as a light brown oil (18 mg, 55% yield) after chromatography using a short silica gel column (approximately 3 g of silica gel/50 mg of crude material loaded) (10% EtOAc/hexane  $\rightarrow$  pure EtOAc).  $^1\text{H}$  NMR (500 MHz,  $\text{CDCl}_3$ ):  $\delta$  13.97 (s, 1H), 8.64 (s, 1H), 8.57–8.53 (m, 1H), 7.88–7.83 (m, 2H), 7.80–7.75 (m, 1H), 7.49–7.43 (m, 3H), 7.32–7.27 (m, 1H), 4.76 (t,  $J = 8$  Hz, 1H), 3.28 (dd,  $J = 18$  Hz, 8 Hz, 1H), 3.09 (dd,  $J = 18$  Hz, 8 Hz, 1H).  $^{13}\text{C}\{^1\text{H}\}$  NMR (125 MHz,  $\text{CDCl}_3$ ):  $\delta$  205.1, 164.2, 149.7, 148.9, 136.1, 134.6, 133.9, 131.6, 128.6, 128.1, 123.9, 105.6, 47.2, 43.8. IR ( $\text{cm}^{-1}$ ): 2921, 1677, 1629, 1586, 1237, 1099, 688. HRMS (ESI-TOF)  $m/z$ :  $[\text{M} + \text{H}]^+$  calcd for  $\text{C}_{16}\text{H}_{13}\text{NO}_2\text{S}$ , 284.0740; found, 284.0737.

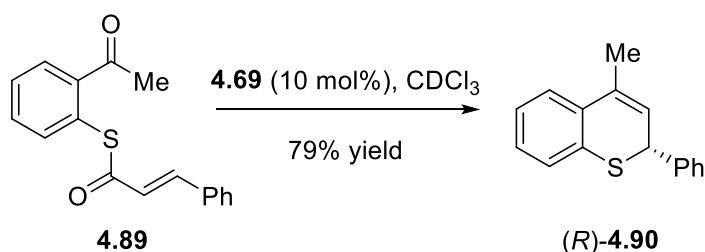
**4.8.5 Synthesis of a 4-substituted thiochromene**



*Synthesis of thioester 4.89.*

Cinnamoyl chloride (366 mg, 2.2 mmol, 1.16 equiv), 4-dimethylaminopyridine (23 mg, 0.189 mmol, 0.1 equiv), and triethylamine (300  $\mu$ L, 2.2 mmol, 1.16 equiv) were dissolved in 4 mL of freshly distilled  $\text{CH}_2\text{Cl}_2$  under an inert atmosphere. A solution of o-mercaptoacetophenone **4.112** (288 mg, 1.89 mmol, 1.0 equiv) in 3 mL of  $\text{CH}_2\text{Cl}_2$  (final concentration of  $\sim 0.3$  M in thiol) was added dropwise at 0  $^\circ\text{C}$  over 30 min. The solution was allowed to slowly warm to rt and stirred overnight. The mixture was concentrated by rotovap and subjected to column chromatography (5  $\rightarrow$  20% EtOAc/ hexanes). **4.89** was isolated as a very fine white powder (346 mg, 73%).  $^1\text{H}$  NMR (500 MHz,  $\text{CDCl}_3$ ):  $\delta$  7.71–7.68 (m, 1H), 7.68 (d,  $J = 16$  Hz, 1H), 7.64–7.61 (m, 1H), 7.58–7.53 (m, 2H), 7.53–7.48 (m, 2H), 7.43–7.38 (m, 3H), 6.79 (d,  $J = 16$  Hz, 1H), 2.61 (s, 3H).  $^{13}\text{C}\{^1\text{H}\}$  NMR (125 MHz,  $\text{CDCl}_3$ ):  $\delta$  200.9, 187.3, 143.2, 142.0, 136.7, 134.0, 131.3, 131.0, 129.5, 129.1, 128.6, 128.6, 125.9, 124.2, 29.4. IR ( $\text{cm}^{-1}$ ): 2922, 1693, 1673, 1573, 1249, 1033, 973, 761, 693. HRMS (ESI-TOF)  $m/z$ :  $[\text{M} + \text{Na}]^+$  calcd for  $\text{C}_{17}\text{H}_{14}\text{O}_2\text{SNa}$ , 305.0612; found, 305.0595. mp: 117–121  $^\circ\text{C}$ .

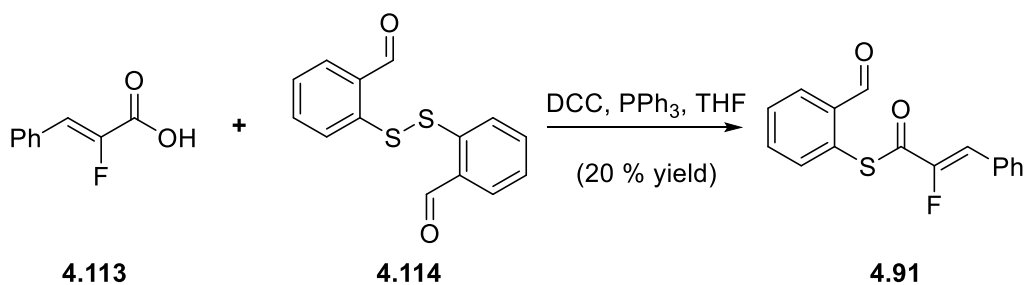
*Enantioselective rearrangement of thioester 4.89*



An NMR tube was charged with thiocinnamate ester **4.89** (28 mg, 0.10 mmol, 1 equiv), catalyst **4.69** (100  $\mu$ L of 0.10 M in  $\text{CDCl}_3$ , 0.010 mmol, 0.1 equiv), and an additional 400  $\mu$ L of  $\text{CDCl}_3$ , shaken, and left at rt. The reaction progress was monitored by  $^1\text{H}$  NMR. After 18 h ( $>95\%$  conversion), the mixture was rotary evaporated and subjected to column chromatography (0.5%

EtOAc/hexanes). The product was isolated as a clear colorless oil (19 mg, 79% yield).  $^1\text{H}$  NMR (500 MHz,  $\text{CDCl}_3$ ):  $\delta$  7.39–7.36 (m, 1H), 7.35–7.33 (m, 2H), 7.31–7.27 (m, 2H), 7.26–7.21 (m, 2H), 7.17–7.10 (m, 2H), 5.95 (d,  $J = 6$  Hz, 1H), 4.80 (d,  $J = 6$  Hz, 1H), 2.20 (s, 3H).  $^{13}\text{C}\{^1\text{H}\}$  NMR (125 MHz,  $\text{CDCl}_3$ ):  $\delta$  141.9, 133.9, 133.6, 131.8, 128.8, 128.0, 127.8, 127.7, 127.3, 125.6, 125.1, 123.8, 42.7, 21.1. IR ( $\text{cm}^{-1}$ ): 3057, 3026, 2919, 1451, 1431, 1033, 752, 695. HRMS (ESI-TOF)  $m/z$ :  $[\text{M} + \text{Na}]^+$  calcd for  $\text{C}_{16}\text{H}_{14}\text{SNa}$ , 261.0714; found, 261.0685. HPLC: (0.25% isopropanol/hexane, AD-H): minor enantiomer: 6.9 min; major enantiomer: 7.8 min, 96% ee.  $[\alpha]_D^{22} = -63.1^\circ$  ( $c = 0.867$ ,  $\text{CH}_2\text{Cl}_2$ ).

#### 4.8.6 Synthesis of a 3-fluorothiochromene

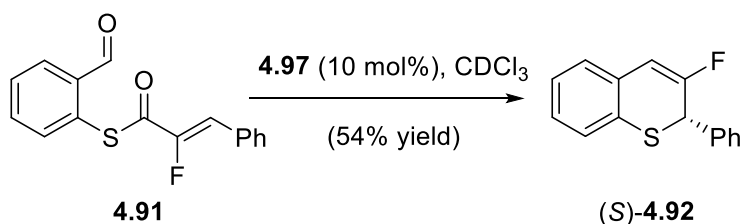


##### *Synthesis of thioester 4.91*

**4.91** was synthesized following a published procedure.<sup>9</sup> To a solution of  $\alpha$ -fluorocinnamic acid<sup>24</sup> (1.284 g, 7.73 mmol, 1.0 equiv) dissolved in 39 mL of freshly distilled THF (0.2 M) was added DCC (0.796 g, 3.87 mmol, 0.5 equiv). This mixture was cooled to 0 °C and stirred for 20 min. Then, triphenylphosphine (1.22 g, 4.64 mmol, 0.6 equiv) and 2,2'-dithiobisbenzaldehyde **4.114**<sup>25</sup> (1.06 g, 3.87 mmol, 0.5 equiv) were added in one portion and allowed to slowly warm to rt. After the mixture was stirred at rt for 24 h, it was filtered and concentrated under reduced pressure. The product **4.91** was isolated as a tan powder (434 mg, 1.51 mmol, 20% yield) after chromatography (2  $\rightarrow$  8% EtOAc/hexanes).  $^1\text{H}$  NMR (500 MHz,  $\text{CDCl}_3$ ):  $\delta$  10.27 (s, 1H), 8.10

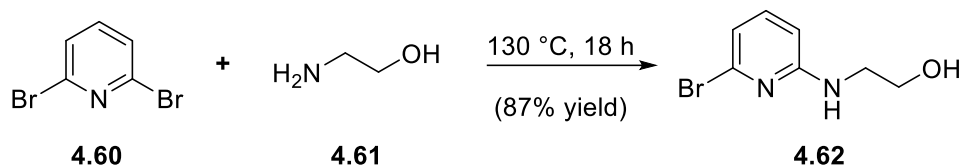
(dd,  $J = 8$  Hz, 2 Hz, 1H), 7.71–7.62 (m, 4H), 7.59–7.56 (m, 1H), 7.45–7.41 (m, 3H), 6.88 (d,  $J = 37$  Hz, 1H).  $^{13}\text{C}\{^1\text{H}\}$  NMR (125 MHz,  $\text{CDCl}_3$ ):  $\delta$  190.5, 183.8 (d,  $J = 39$  Hz), 151.5 (d,  $J = 269$  Hz), 137.6, 137.0, 134.5, 131.2 (d,  $J = 8$  Hz), 130.9, 130.6 (d,  $J = 3$  Hz), 130.6 (d,  $J = 4$  Hz), 129.5, 129.3 (d,  $J = 5$  Hz), 129.2, 115.2 (d,  $J = 4$  Hz). IR ( $\text{cm}^{-1}$ ): 2924, 2871, 1692, 1675, 1637, 1156, 942, 746. HRMS (ESI-TOF)  $m/z$ :  $[\text{M} + \text{Na}]^+$  calcd for  $\text{C}_{16}\text{H}_{11}\text{FO}_2\text{SNa}$ , 309.0361; found, 309.0347. mp: 95–99 °C.

#### Enantioselective rearrangement of thioester **4.91**



**4.92** was prepared as described above (see synthesis of **4.90**) using thioester **4.91** (29 mg, 0.10 mmol, 1 equiv) and (*R*)-BTM **4.97** (100  $\mu\text{L}$  of 0.10 M in  $\text{CDCl}_3$ , 0.010 mmol, 0.1 equiv). After 1 week (>90% conversion), the mixture was rotary evaporated and subjected to column chromatography (1% EtOAc/hexanes). The product was isolated as a colorless oil (13 mg, 54% yield).  $^1\text{H}$  NMR (500 MHz,  $\text{CDCl}_3$ ):  $\delta$  7.33–7.24 (m, 5H), 7.20–7.17 (m, 1H), 7.14–7.09 (m, 3H), 6.42 (d,  $J = 15$  Hz, 1H), 4.77 (d,  $J = 13$  Hz, 1H).  $^{13}\text{C}\{^1\text{H}\}$  NMR (125 MHz,  $\text{CDCl}_3$ ):  $\delta$  157.7 (d,  $J = 271$  Hz), 139.8 (d,  $J = 3$  Hz), 130.6 (d,  $J = 8$  Hz), 129.0, 128.4, 127.9 (d,  $J = 9$  Hz), 127.88, 126.9, 126.8, 126.5, 126.1, 107.5 (d,  $J = 23$  Hz), 43.1 (d,  $J = 29$  Hz). IR ( $\text{cm}^{-1}$ ): 3061, 2923, 2852, 1678, 1471, 1105, 749. HRMS (ESI-TOF)  $m/z$ :  $[\text{M} + \text{Na}]^+$  calcd for  $\text{C}_{15}\text{H}_{11}\text{FSNa}$ , 265.0463; found, 265.0431. HPLC: (0.25% isopropanol/hexane, OD-H): major enantiomer: 12.0 min; minor enantiomer: 14.9 min, 94% ee.  $[\alpha]_D^{26} = -80.3^\circ$  ( $c = 0.467$ ,  $\text{CH}_2\text{Cl}_2$ ).

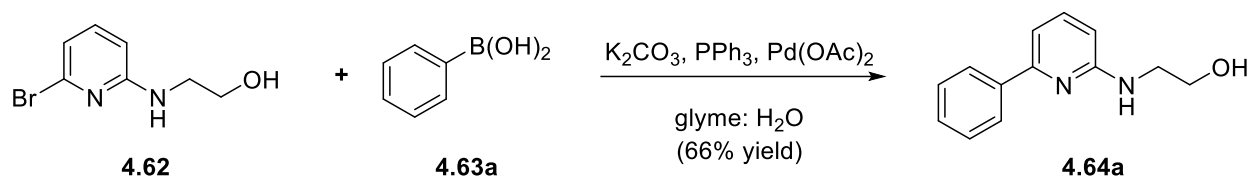
### 4.8.7 Synthesis of new catalysts



#### *Synthesis of Aminoalcohol 4.62*

A mixture of 2,6-dibromopyridine (2.00 g, 8.45 mmol) and ethanolamine (2.55 mL, 38.36 mmol, 4.0 equiv) was heated at 130 °C for 18 h, at which time TLC (5% MeOH/CH<sub>2</sub>Cl<sub>2</sub>) indicated complete consumption of the starting material. This crude reaction mixture was dissolved in a minimum amount of water and extracted three times with EtOAc. The combined organic layers were washed with brine, dried over Na<sub>2</sub>SO<sub>4</sub>, and concentrated in vacuo. Flash chromatography (1 → 5% MeOH/CH<sub>2</sub>Cl<sub>2</sub>) afforded the product as a clear, colorless oil (1.60 g, 87% yield). <sup>1</sup>H NMR (500 MHz, CDCl<sub>3</sub>): δ 7.22 (dd, J = 9 Hz, 8 Hz, 1H), 6.72 (d, J = 8 Hz, 1H), 6.34 (d, J = 9 Hz, 1H), 5.08 (br s, 1H), 3.81 (t, J = 5 Hz, 2H), 3.48–3.44 (m, 2H), 3.34 (br s, 1H). <sup>13</sup>C{<sup>1</sup>H} NMR (125 MHz, CDCl<sub>3</sub>): δ 159.1, 140.0, 139.6, 116.1, 106.0, 62.5, 44.9. IR (cm<sup>-1</sup>): 3311 (broad), 2926, 2867, 1591, 1555, 1497, 1431, 1388, 1325, 1160, 1102, 1048, 973, 768. HRMS (ESI-TOF) m/z: [M + H]<sup>+</sup> calcd for C<sub>7</sub>H<sub>9</sub>BrN<sub>2</sub>O, 216.9971; found, 216.9985.

#### *Synthesis of Aminoalcohol 4.64a*

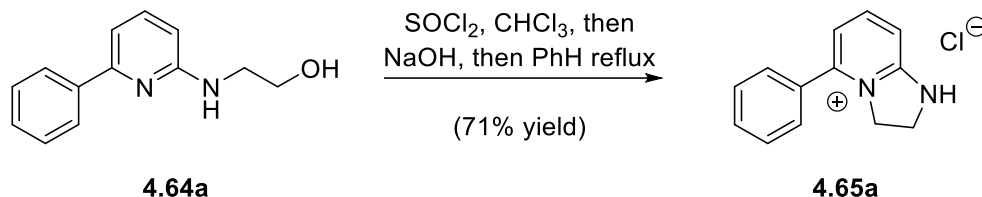


To a solution of **4.62** (454 mg, 2.09 mmol), phenylboronic acid (510 mg, 4.18 mmol, 2.0 equiv), and triphenylphosphine (93 mg, 0.355 mmol, 0.17 equiv) in 10 mL of 1,2-dimethoxyethane

were added 10 mL of water and  $K_2CO_3$  (1.94 g, 14 mmol, 6.7 equiv). The mixture was degassed three times using the freeze–pump–thaw technique.  $Pd(OAc)_2$  (19 mg, 0.084 mmol, 4 mol %) was added under argon, and the solution was gently refluxed for 20 h, at which time TLC (1% MeOH/ $CH_2Cl_2$ ) indicated near complete consumption of the starting material. The reaction mixture was diluted with 5 mL of EtOAc and 5 mL of water. The aqueous layer was extracted twice with EtOAc. The combined organic layers were dried over  $Na_2SO_4$  and concentrated by rotary evaporation. The crude mixture was subjected to column chromatography (1 → 5% MeOH/ $CH_2Cl_2$ ) to afford the product as a clear, colorless oil (296 mg, contaminated with ca. 10% triphenylphosphine oxide, 66% corrected yield).  $^1H$  NMR (300 MHz,  $CDCl_3$ ):  $\delta$  7.91 (d,  $J$  = 8 Hz, 2H), 7.53–7.33 (m, 4H), 7.04 (d,  $J$  = 8 Hz, 1H), 6.43 (d,  $J$  = 8 Hz, 1H), 4.95 (br s, 1H), 3.86 (br t,  $J$  = 5 Hz, 2H), 3.67–3.59 (m, 2H).  $^{13}C\{^1H\}$  NMR (125 MHz,  $CDCl_3$ ):  $\delta$  158.9, 155.7, 139.5, 138.4, 128.9, 128.8, 126.9, 110.5, 107.4, 64.5, 45.7. IR ( $cm^{-1}$ ): 3344 (br), 2922, 2857, 1598, 1574, 1509, 1492, 1442, 1337, 1265, 1161, 1047, 760. HRMS (ESI-TOF)  $m/z$ :  $[M + H]^+$  calcd for  $C_{13}H_{14}N_2O$ , 215.1179; found, 215.1188.

Aminoalcohol **4.64b** was prepared analogously to **4.64a** using the following quantities: 537 mg (2.47 mmol) of **4.62**, 752 mg (4.95 mmol) of 4-methoxyphenylboronic acid, 12 mL of glyme, 12 mL of water, 110 mg (0.42 mmol) of triphenylphosphine, 2.28 g (16.5 mmol) of  $K_2CO_3$ , and 22 mg (0.099 mmol) of  $Pd(OAc)_2$ . **4.64b** was isolated as a clear light brown oil (497 mg, 82%) after chromatography (pure  $CH_2Cl_2$  → 2% MeOH/ $CH_2Cl_2$ ).  $^1H$  NMR (500 MHz,  $CDCl_3$ )  $\delta$  7.86 (d,  $J$  = 9 Hz, 2H), 7.44 (t,  $J$  = 8 Hz, 1H), 6.97 (d,  $J$  = 9 Hz, 2H), 6.99–6.95 (m, 1H), 6.36 (d,  $J$  = 8 Hz, 1H), 4.87 (br s, 1H), 3.86–3.83 (m, 2H), 3.84 (s, 3H), 3.61 (q,  $J$  = 5 Hz, 2H).  $^{13}C$  NMR (125 MHz,  $CDCl_3$ ):  $\delta$  160.34, 158.82, 155.37, 138.33, 132.24, 128.14, 114.16, 109.65, 106.61, 64.54, 55.46, 45.64; MS: HR-ESI calculated for  $[C_{14}H_{16}N_2O_2 + Na]^+$ : 267.1104, found 267.1083.

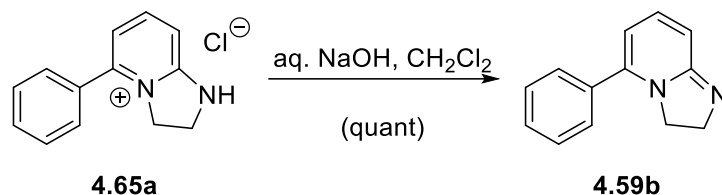
Synthesis of **4.65a** (Hydrochloride salt)



To a solution of **4.64a** (92 mg, containing ca. 10% Ph<sub>3</sub>PO, see above) in freshly distilled chloroform (1.2 mL) was added SOCl<sub>2</sub> (93 μL, 1.28 mmol, ca. 3 equiv) dropwise at 0 °C. The mixture was refluxed for 2 h, cooled to rt, and quenched by adding 100 μL of methanol. The solvent was removed by rotary evaporation. The resulting oil was suspended in 2 mL of water and heated to 60 °C. The aqueous phase was passed through a cotton plug to remove the gummy residue. The filtrate was basified with 2 M aqueous NaOH and extracted repeatedly with benzene until the aqueous phase was only pale yellow. The combined benzene extracts were dried briefly over Na<sub>2</sub>SO<sub>4</sub>, decanted into a round-bottom flask, and refluxed overnight. The mixture was cooled to 0 °C, and the precipitated product (**4.65a**) was filtered off and washed several times with benzene to remove the Ph<sub>3</sub>PO impurity carried forward from the previous step. Compound **4.65a** was isolated as a light orange solid (60 mg, 71% yield). <sup>1</sup>H NMR (500 MHz, D<sub>2</sub>O; HOD used as a reference peak at δ 4.79 ppm): δ 7.96 (t, J = 9 Hz, 1H), 7.70–7.57 (m, 5H), 7.04 (d, J = 9 Hz, 1H), 6.89 (d, J = 9 Hz, 1H), 4.55 (t, J = 10 Hz, 2H), 3.70 (t, J = 10 Hz, 2H). <sup>13</sup>C{<sup>1</sup>H} NMR (125 MHz, D<sub>2</sub>O, (CH<sub>3</sub>)<sub>2</sub>CO added and used as a reference peak at δ 29.84 ppm): δ 157.1, 149.0, 144.8, 132.2, 131.1, 129.4, 128.7, 114.8, 108.3, 50.8, 42.9. IR (cm<sup>-1</sup>): 3409, 2954, 1647, 1571, 1550, 1298, 1145, 778, 706. HRMS (ESI-TOF) m/z: [M]<sup>+</sup> calcd for C<sub>13</sub>H<sub>13</sub>N<sub>2</sub>, 197.1073; found, 197.1086. Mp: 234–235 °C.



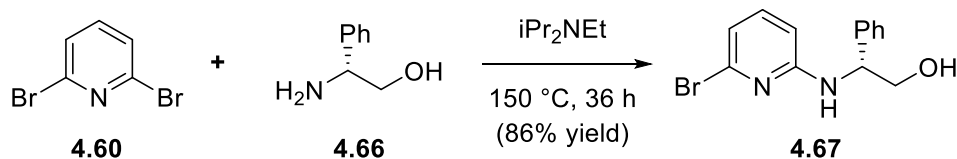
Synthesis of **4.61b** (free base)



The hydrochloride salt of **4.65a** (18 mg, 0.078 mmol) was dissolved in 1 mL of water and treated with 2 mL of 33 wt % aqueous NaOH. The resulting yellow oil was extracted with CH<sub>2</sub>Cl<sub>2</sub> several times until the aqueous phase was only faint yellow. The organic extract was dried over NaOH pellets and rotary evaporated to afford the product as a dark yellow oil (15 mg, quantitative yield). <sup>1</sup>H NMR (500 MHz, CDCl<sub>3</sub>): δ 7.44–7.40 (m, 3H), 7.40–7.36 (m, 2H), 6.83 (dd, J = 10 Hz, 7 Hz, 1H), 6.32 (d, J = 10 Hz, 1H), 5.52 (d, J = 7 Hz, 1H), 3.90–3.80 (m, 4H). <sup>13</sup>C{<sup>1</sup>H} NMR (125 MHz, CDCl<sub>3</sub>): δ 159.4, 147.5, 136.4, 135.4, 129.2, 128.6, 127.8, 113.8, 103.4, 52.3, 49.4.

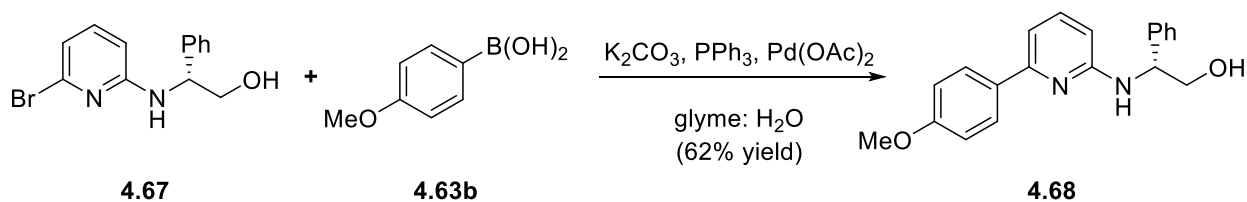
The hydrochloride salt **4.65b** and free base **4.59c** were prepared analogously to **4.65a** and **4.59b** as above using the following quantities: 157 mg (0.643 mmol) of **4.64b**, 140 μL (1.93 mmol) of SOCl<sub>2</sub>, and 1.8 mL of CHCl<sub>3</sub>. Characterization of free base **4.59c**: <sup>1</sup>H NMR (500 MHz, CDCl<sub>3</sub>) δ 7.30 (d, J = 9 Hz, 2H), 6.93 (d, J = 9 Hz, 2H), 6.81 (dd, J = 10 Hz, 7 Hz, 1H), 6.29 (d, J = 10 Hz, 1H), 5.49 (d, J = 7 Hz, 1H), 3.86–3.83 (m, 7H). <sup>13</sup>C NMR (125 MHz, CDCl<sub>3</sub>): δ 160.34, 159.66, 147.48, 136.54, 129.26, 127.96, 114.06, 113.39, 103.30, 55.52, 52.31, 49.56.

Synthesis of chiral aminoalcohol **4.67**



2,6-Dibromopyridine (3.45 g, 14.5 mmol), (*R*)-2-phenylglycinol (2.00 g, 14.5 mmol), and *N,N*-diisopropylethylamine (3.8 mL, 22 mmol) were added to a high pressure flask and heated at 150 °C for 36 h. After cooling to room temperature, the crude mixture was dissolved in CH<sub>2</sub>Cl<sub>2</sub> and loaded directly onto the column. Flash chromatography (CH<sub>2</sub>Cl<sub>2</sub> → 4% MeOH/CH<sub>2</sub>Cl<sub>2</sub>) afforded the product as a white powder (3.67 g, 86% yield). <sup>1</sup>H NMR (500 MHz, CDCl<sub>3</sub>): δ 7.38–7.34 (m, 4H), 7.33–7.28 (m, 1H), 7.16 (t, *J* = 8 Hz, 1H), 6.73 (d, *J* = 8 Hz, 1H), 6.15 (d, *J* = 8 Hz, 1H), 5.48 (br s, 1H), 4.77–4.72 (m, 1H), 4.00–3.94 (m, 1H), 3.90–3.83 (m, 1H), 2.63 (br s, 1H). <sup>13</sup>C{<sup>1</sup>H} NMR (125 MHz, CDCl<sub>3</sub>): δ 158.6, 139.9, 139.8, 139.5, 129.1, 128.1, 126.8, 116.6, 105.5, 67.4, 58.8. IR (cm<sup>-1</sup>): 3287 (br), 1594, 1441, 1166, 1108, 1068, 977, 755, 700. HRMS (ESI-TOF) *m/z*: [M + H]<sup>+</sup> calcd for C<sub>13</sub>H<sub>13</sub>BrN<sub>2</sub>O, 293.0284; found, 293.0284. Mp: 137–138 °C. [α]<sub>D</sub><sup>21</sup> = -32.8° (c 0.400, CH<sub>3</sub>CN).

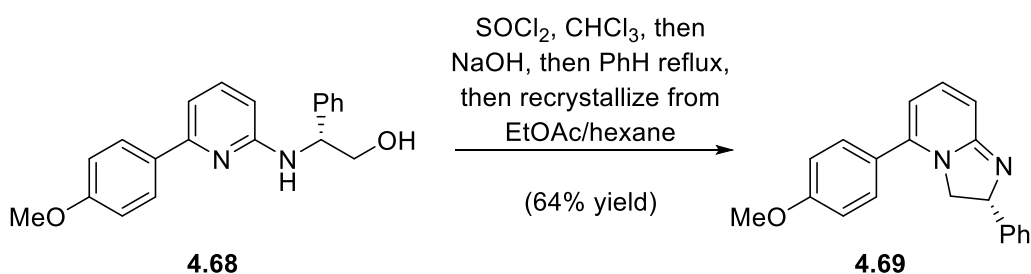
#### Chiral aminoalcohol **4.68**



The compound was prepared analogously to **4.64a** using the following quantities: 504 mg of **4.67** (1.72 mmol), 523 mg of 4-methoxyphenylboronic acid (3.44 mmol), 77 mg of triphenylphosphine (0.29 mmol), 1.59 g of K<sub>2</sub>CO<sub>3</sub> (11.5 mmol), 15 mg of Pd(OAc)<sub>2</sub> (0.69 mmol), 10 mL of water, and 10 mL of 1,2-dimethoxyethane. The product was isolated as a light gray powder (343 mg, 62% yield) after chromatography (CH<sub>2</sub>Cl<sub>2</sub> → 4% MeOH/CH<sub>2</sub>Cl<sub>2</sub>). <sup>1</sup>H NMR (500 MHz, CDCl<sub>3</sub>): δ 7.87–7.83 (m, 2H), 7.43–7.35 (m, 5H), 7.33–7.29 (m, 1H), 7.00–6.95 (m, 3H), 6.26 (d, *J* = 8 Hz, 1H), 5.12 (br d, *J* = 5 Hz, 1H), 4.96 (dd, *J* = 11 Hz, 6 Hz,

1H), 4.46 (br s, 1H), 3.98–3.93 (m, 2H), 3.85 (s, 3H).  $^{13}\text{C}\{^1\text{H}\}$  NMR (125 MHz,  $\text{CDCl}_3$ ):  $\delta$  160.4, 158.4, 155.4, 140.5, 138.5, 132.3, 129.0, 128.3, 127.8, 126.9, 114.2, 110.1, 106.1, 68.5, 59.8, 55.5. IR ( $\text{cm}^{-1}$ ): 3254 (br), 1595, 1572, 1460, 1449, 1245, 1171, 1029, 786, 699. HRMS (ESI-TOF)  $m/z$ :  $[\text{M} + \text{H}]^+$  calcd for  $\text{C}_{20}\text{H}_{20}\text{N}_2\text{O}_2$ , 321.1598; found, 321.1606. Mp: 134–136 °C.  $[\alpha]_D^{21} = -72.6^\circ$  (c 0.333,  $\text{CH}_3\text{CN}$ ).

#### Synthesis of catalyst **4.69**

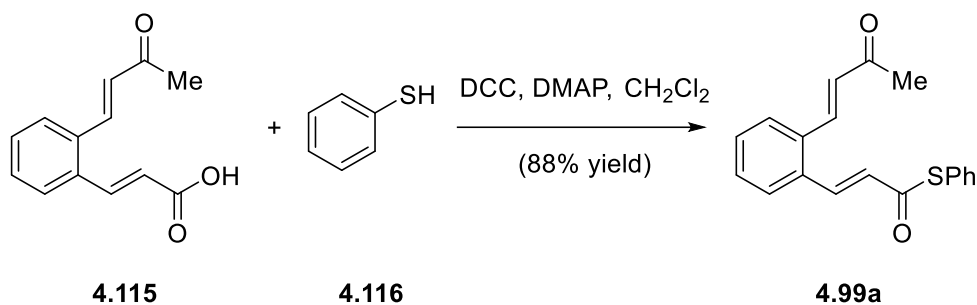


The compound was prepared analogously to **4.65a** following a slightly modified procedure. To a solution of **4.68** (206 mg, 0.64 mmol) in freshly distilled chloroform (1.8 mL) was added  $\text{SOCl}_2$  (140  $\mu\text{L}$ , 1.93 mmol, 3 equiv) dropwise at 0 °C. The mixture was refluxed for 4 h, cooled to rt, and quenched by adding 100  $\mu\text{L}$  of methanol. The solvent was removed by rotary evaporation. The resulting oil was suspended in 2 mL of water and heated to 60 °C. The aqueous phase was passed through a cotton plug to remove the gummy residue. The filtrate was basified with 2 M aqueous  $\text{NaOH}$  and extracted repeatedly with benzene until the aqueous phase was only pale yellow. The combined benzene extracts were dried briefly over  $\text{Na}_2\text{SO}_4$ , decanted into a round-bottom flask, and refluxed overnight. After cooling to room temperature, the benzene was removed by rotary evaporation. The yellow flaky solid was dissolved in a minimal 10% ethyl acetate/hexane mixture and cooled to 0 °C until a yellow solid precipitated out of the solution. The yellow solid, determined to be free base **4.69**, was filtered off and left to dry (140 mg, 64%

yield).  $^1\text{H}$  NMR (500 MHz,  $\text{CDCl}_3$ ):  $\delta$  7.36–7.27 (m, 6H), 7.26–7.25 (m, 1H), 7.25–7.21 (m, 1H), 6.93–6.89 (m, 3H), 6.43 (d,  $J = 10$  Hz, 1H), 5.59 (d,  $J = 7$  Hz, 1H), 5.19 (dd,  $J = 11$  Hz, 10 Hz, 1H), 4.26 (t,  $J = 11$  Hz, 1H), 3.83 (s, 3H), 3.73 (dd,  $J = 11$  Hz, 10 Hz, 1H).  $^{13}\text{C}\{^1\text{H}\}$  NMR (125 MHz,  $\text{CDCl}_3$ ):  $\delta$  160.4, 159.3, 147.2, 145.0, 137.0, 129.3, 128.7, 127.6, 127.2, 126.7, 114.1, 113.2, 103.9, 66.9, 57.3, 55.5. IR ( $\text{cm}^{-1}$ ): 2933, 1640, 1608, 1553, 1505, 1248, 1176, 1029, 907, 724, 698. HRMS (ESI-TOF)  $m/z$ :  $[\text{M} + \text{H}]^+$  calcd for  $\text{C}_{20}\text{H}_{18}\text{N}_2\text{O}$ , 303.1492; found, 303.1498. Mp: 122–124 °C.  $[\alpha]_D^{21} = +203.6^\circ$  (c 0.333,  $\text{CH}_2\text{Cl}_2$ ).

#### 4.8.8 Synthesis of fused indanes 4.100a,b

##### Synthesis of thioesters 4.99a,b

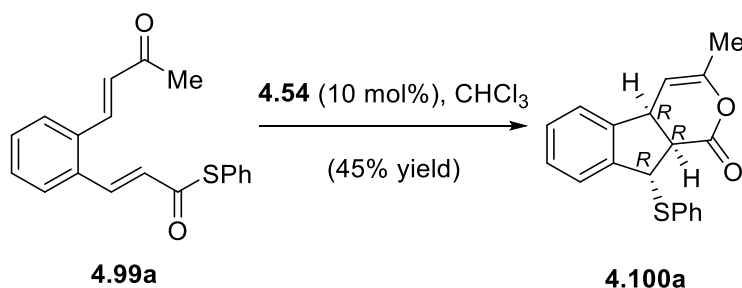


A stirring solution of **4.115**<sup>16</sup> (490 mg, 2.25 mmol, 1.0 equiv) in 15 mL of freshly distilled  $\text{CH}_2\text{Cl}_2$  stirred was treated with a solution of DMAP (6 mg, 0.045 mmol, 0.02 equiv) and DCC (557 mg, 2.7 mmol, 1.2 equiv) in 7 mL of  $\text{CH}_2\text{Cl}_2$  added dropwise at 0 °C. This was stirred for 20 min. Then, thiophenol (185  $\mu\text{L}$ , 1.8 mmol, 0.8 equiv) dissolved in 6 mL of  $\text{CH}_2\text{Cl}_2$  was added dropwise over 30 min. The reaction was left to slowly warm to rt and stirred overnight. The mixture was then filtered, concentrated under reduced pressure, and subjected to column chromatography (10  $\rightarrow$  20% EtOAc/hexanes). **4.99a** was isolated as a light tan solid (487 mg, 88% yield).  $^1\text{H}$  NMR (500 MHz,  $\text{CDCl}_3$ ):  $\delta$  8.03 (d,  $J = 16$  Hz, 1H), 7.86 (d,  $J = 16$  Hz, 1H),

7.64–7.58 (m, 2H), 7.52–7.48 (m, 2H), 7.47–7.42 (m, 5H), 6.71 (d,  $J = 16$  Hz, 1H), 6.62 (d,  $J = 16$  Hz, 1H), 2.40 (s, 3H).  $^{13}\text{C}\{^1\text{H}\}$  NMR (125 MHz,  $\text{CDCl}_3$ ):  $\delta$  197.9, 187.8, 139.8, 138.0, 135.1, 134.6, 134.1, 131.0, 130.7, 130.4, 129.7, 129.4, 128.0, 127.9, 127.6, 127.4, 27.8. IR ( $\text{cm}^{-1}$ ): 1662, 1258, 1127, 956, 749. HRMS (ESI-TOF)  $m/z$ :  $[\text{M} + \text{Na}]^+$  calcd for  $\text{C}_{19}\text{H}_{16}\text{O}_2\text{SNa}$ , 331.0769; found, 331.0760. mp: 88–89 °C.

Thioester **4.99b** was prepared analogously to the methyl derivative **4.99a** (see above) using the following quantities: *o*-(3-oxo-3-phenylpropenyl)-cinnamic acid<sup>16</sup> (626 mg, 2.25 mmol, 1.0 equiv), DCC (557 mg, 2.7 mmol, 1.2 equiv), DMAP (6 mg, 0.045 mmol, 0.02 equiv), thiophenol (185  $\mu\text{L}$ , 1.8 mmol, 0.8 equiv), and 28 mL of  $\text{CH}_2\text{Cl}_2$ . **4.99b** was isolated as a yellow solid (517 mg, 78%) after chromatography (5  $\rightarrow$  15% EtOAc/hexanes).  $^1\text{H}$  NMR (500 MHz,  $\text{CDCl}_3$ ):  $\delta$  8.13 (d,  $J = 16$  Hz, 1H), 8.10 (d,  $J = 16$  Hz, 1H), 8.05–8.02 (m, 2H), 7.72–7.68 (m, 1H), 7.65–7.62 (m, 1H), 7.61–7.57 (m, 1H), 7.53–7.48 (m, 4H), 7.48–7.43 (m, 5H), 7.41 (d,  $J = 16$  Hz, 1H), 6.72 (d,  $J = 16$  Hz, 1H).  $^{13}\text{C}\{^1\text{H}\}$  NMR (125 MHz,  $\text{CDCl}_3$ ):  $\delta$  190.1, 187.7, 141.4, 138.6, 138.0, 135.6, 134.7, 134.4, 133.1, 130.6, 130.3, 129.6, 129.4, 128.8, 128.7, 128.4, 128.0, 127.7, 127.5, 126.5. IR ( $\text{cm}^{-1}$ ): 1669, 1656, 1593, 1292, 1216. HRMS (ESI-TOF)  $m/z$ :  $[\text{M} + \text{Na}]^+$  calcd for  $\text{C}_{24}\text{H}_{18}\text{O}_2\text{SNa}$ , 393.0925; found, 393.0902. mp: 61–65 °C.

#### Rearrangement of thioester **4.99a**

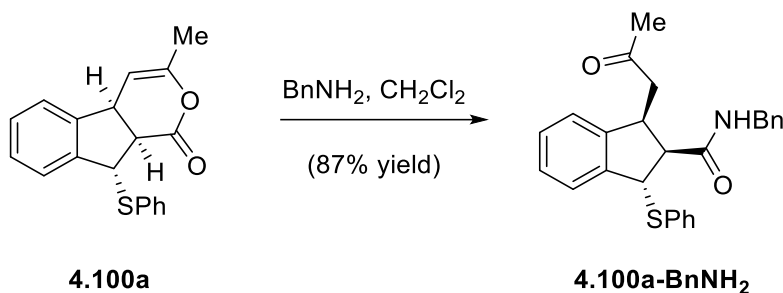


**4.100a** was prepared by mixing thioester **4.99a** (31 mg, 0.10 mmol, 1 equiv) and (*R*)-H-PIP **4.54** (100  $\mu$ L of 0.10 M in CDCl<sub>3</sub>, 0.010 mmol, 0.1 equiv). After 3 days at 0 °C (complete consumption of the starting material by <sup>1</sup>H NMR), the mixture was rotary evaporated, and the crude product was preadsorbed onto silica gel. The pure product (14 mg, 45% yield) was obtained as a clear, colorless oil after column chromatography (1  $\rightarrow$  2% EtOAc/hexanes). <sup>1</sup>H NMR (500 MHz, CDCl<sub>3</sub>):  $\delta$  7.48–7.45 (m, 2H), 7.37–7.35 (m, 1H), 7.34–7.24 (m, 5H), 7.18–7.16 (m, 1H), 5.42 (d, *J* = 2 Hz, 1H), 5.32 (dd, *J* = 6 Hz, 1 Hz, 1H), 4.11–4.06 (m, 1H), 3.33 (dd, *J* = 9 Hz, 2 Hz, 1H), 1.91–1.89 (m, 3H). <sup>13</sup>C{<sup>1</sup>H} NMR (125 MHz, CDCl<sub>3</sub>):  $\delta$  169.0, 148.7, 143.7, 139.9, 135.0, 131.1, 129.3, 129.0, 128.0, 127.4, 125.7, 123.8, 99.4, 53.6, 48.8, 39.5, 19.1. IR (cm<sup>-1</sup>): 3069, 2921, 1748, 1706, 1169, 1150, 1090. HRMS (ESI-TOF) *m/z*: [M + H]<sup>+</sup> calcd for C<sub>19</sub>H<sub>17</sub>O<sub>2</sub>S, 309.0949; found, 309.0945. HPLC: (2% isopropanol/hexane, AD-H): minor enantiomer: 12.1 min; major enantiomer: 19.0 min, 88% ee (Table 4.4, entry 7). [ $\alpha$ ]<sub>D</sub><sup>26</sup> = +63.1° (*c* = 0.800, CHCl<sub>3</sub>).

**4.100b** was prepared analogously as described above using thioester **4.99b** (37 mg, 0.10 mmol, 1 equiv) and (*R*)-H-PIP **4.54** (100  $\mu$ L of 0.10 M in CDCl<sub>3</sub>, 0.010 mmol, 0.1 equiv). After 3 days at 0 °C, the mixture was rotary evaporated and purified by chromatography (1  $\rightarrow$  2% EtOAc/hexanes). The pure product (11 mg, 30% yield) was obtained as a clear, colorless oil that crystallized on standing. <sup>1</sup>H NMR (500 MHz, CDCl<sub>3</sub>):  $\delta$  7.63–7.60 (m, 2H), 7.50–7.47 (m, 2H), 7.40–7.22 (m, 10H), 6.09 (d, *J* = 6 Hz, 1H), 5.48 (d, *J* = 2 Hz, 1H), 4.33–4.29 (m, 1H), 3.45 (dd, *J* = 9 Hz, 2 Hz, 1H). <sup>13</sup>C{<sup>1</sup>H} NMR (125 MHz, CDCl<sub>3</sub>):  $\delta$  168.5, 149.4, 143.3, 140.0, 134.9, 132.3, 131.3, 129.4, 129.3, 129.2, 128.7, 128.1, 127.5, 125.8, 124.9, 123.9, 99.3, 53.7, 49.0, 39.9. IR (cm<sup>-1</sup>): 3059, 2922, 1752, 1332, 1164, 753, 735. HRMS (ESI-TOF) *m/z*: [M + Na]<sup>+</sup> calcd for C<sub>24</sub>H<sub>18</sub>O<sub>2</sub>SNa, 393.0925; found, 393.0910. HPLC: (1% isopropanol/hexane, OD-H): major enantiomer: 30.0 min; minor enantiomer: 34.9 min, 35% ee (Table 4.4, entry 8). Specific optical

rotation was measured using a sample with 69% ee (see entry 6 in Table 4.4):  $[\alpha]_D^{26} = +12.1^\circ$  ( $c = 0.667$ ,  $\text{CHCl}_3$ ).

#### Aminolysis of **4.100a**



In order to determine its absolute configuration, tricycle **4.100a** (56 mg, 0.182 mmol, 1.0 equiv) was subjected to aminolysis with benzylamine (30  $\mu\text{L}$ , 0.27 mmol, 1.5 equiv) in 900  $\mu\text{L}$  of  $\text{CH}_2\text{Cl}_2$  (20 h at rt). The reaction mixture was washed successively with 1 M aqueous HCl, water, and brine. The organic phase was dried over  $\text{Na}_2\text{SO}_4$  and concentrated under reduced pressure to yield almost pure product, which was recrystallized from a 1:1  $\text{CH}_2\text{Cl}_2$ /hexanes mixture. The product was isolated as a colorless, crystalline solid (66 mg, 0.16 mmol, 87% yield).  $^1\text{H}$  NMR (500 MHz,  $\text{CDCl}_3$ ):  $\delta$  7.45–7.21 (m, 13H), 7.11–7.07 (m, 1H), 5.90 (br s, 1H), 5.10 (d,  $J = 7$  Hz, 1H), 4.35 (dd,  $J = 15$  Hz, 6 Hz, 1H), 4.24 (dd,  $J = 15$  Hz, 5 Hz, 1H), 4.01–3.95 (m, 1H), 3.23 (dd,  $J = 8$  Hz, 7 Hz, 1H), 3.01 (dd,  $J = 19$  Hz, 10 Hz, 1H), 2.63 (dd,  $J = 19$  Hz, 5 Hz, 1H), 2.01 (s, 3H).  $^{13}\text{C}\{^1\text{H}\}$  NMR (125 MHz,  $\text{CDCl}_3$ ):  $\delta$  207.9, 171.7, 144.3, 141.8, 138.1, 134.6, 132.0, 129.1, 128.8, 128.4, 128.1, 127.8, 127.7, 127.4, 125.2, 123.7, 56.5, 54.0, 45.7, 43.9, 41.3, 30.3. IR ( $\text{cm}^{-1}$ ): 3306, 3023, 2924, 1703, 1641, 1525, 1360, 1234, 1211, 748, 738, 693. HRMS (ESI-TOF)  $m/z$ :  $[\text{M} + \text{H}]^+$  calcd for  $\text{C}_{26}\text{H}_{26}\text{NO}_2\text{S}$ , 416.1684; found, 416.1691. mp: 99–101  $^\circ\text{C}$ .

## 4.9 X-ray crystal structure of 4.100a-BnNH<sub>2</sub>

**Table 4.5.** Crystal data and structure refinement for 4.100a-BnNH<sub>2</sub>.

Identification code	v22219t5/lt/venture/Straub-Birman	
Empirical formula	C <sub>26</sub> H <sub>25</sub> N O <sub>2</sub> S	
Formula weight	415.53	
Temperature	100(2) K	
Wavelength	1.54178 Å	
Crystal system	Triclinic	
Space group	P1	
Unit cell dimensions	a = 5.0234(2) Å	a = 82.3574(16)°.
	b = 9.9548(4) Å	b = 83.6826(18)°.
	c = 10.9540(5) Å	g = 83.417(2)°.
Volume	536.83(4) Å <sup>3</sup>	
Z	1	
Density (calculated)	1.285 Mg/m <sup>3</sup>	
Absorption coefficient	1.510 mm <sup>-1</sup>	
F(000)	220	
Crystal size	0.298 x 0.124 x 0.091 mm <sup>3</sup>	
Theta range for data collection	4.505 to 72.223°.	
Index ranges	-6 ≤ h ≤ 6, -12 ≤ k ≤ 12, -13 ≤ l ≤ 13	
Reflections collected	19886	
Independent reflections	6011 [R(int) = 0.043]	
Completeness to theta = 67.679°	99.1 %	
Absorption correction	Semi-empirical from equivalents	
Max. and min. transmission	0.7536 and 0.6038	
Refinement method	Full-matrix least-squares on F <sup>2</sup>	
Data / restraints / parameters	6011 / 3 / 273	
Goodness-of-fit on F <sup>2</sup>	1.078	
Final R indices [I > 2σ(I)]	R1 = 0.0320, wR2 = 0.0862	
R indices (all data)	R1 = 0.0322, wR2 = 0.0864	
Absolute structure parameter	-0.016(10)	
Largest diff. peak and hole	0.207 and -0.249 e.Å <sup>-3</sup>	



**Table 4.6.** Atomic coordinates ( $\times 10^4$ ) and equivalent isotropic displacement parameters ( $\text{\AA}^2 \times 10^3$ ) for **4.100a-BnNH<sub>2</sub>**. U(eq) is defined as one third of the trace of the orthogonalized  $U^{ij}$  tensor.

	x	y	z	U(eq)
S(1)	4014(1)	2587(1)	4483(1)	26(1)
O(1)	5214(5)	6308(2)	5621(2)	20(1)
O(2)	1208(4)	6582(2)	8477(2)	35(1)
N(1)	751(5)	6404(2)	5522(2)	17(1)
C(1)	5320(5)	3345(3)	5705(2)	18(1)
C(2)	3122(5)	4269(2)	6395(2)	17(1)
C(3)	3739(5)	4044(3)	7790(2)	18(1)
C(4)	5470(6)	2692(3)	7871(3)	20(1)
C(5)	6335(6)	1910(3)	8937(3)	28(1)
C(6)	8087(7)	746(3)	8814(3)	33(1)
C(7)	8977(7)	357(3)	7650(3)	34(1)
C(8)	8127(6)	1130(3)	6593(3)	27(1)
C(9)	6364(5)	2306(3)	6716(2)	20(1)
C(10)	3108(5)	5744(2)	5804(2)	16(1)
C(11)	509(5)	7869(3)	5111(2)	20(1)
C(12)	1433(5)	8254(3)	3762(3)	19(1)
C(13)	3287(6)	9209(3)	3430(3)	26(1)
C(14)	4041(7)	9624(3)	2187(3)	33(1)
C(15)	2978(7)	9087(3)	1273(3)	31(1)
C(16)	1165(8)	8117(3)	1600(3)	32(1)
C(17)	375(6)	7713(3)	2837(3)	26(1)
C(18)	5960(6)	3297(3)	3143(3)	23(1)
C(19)	5292(7)	4635(3)	2631(3)	29(1)
C(20)	6833(8)	5190(4)	1606(3)	38(1)
C(21)	9034(8)	4417(4)	1075(3)	41(1)
C(22)	9673(8)	3086(4)	1579(3)	42(1)
C(23)	8145(7)	2516(3)	2621(3)	31(1)
C(24)	5263(5)	5118(3)	8221(2)	20(1)
C(25)	3642(6)	6484(3)	8329(3)	22(1)

C(26)

5194(7)

7685(3)

8275(3)

31(1)

---

**Table 4.7.** Bond lengths [ $\text{\AA}$ ] and angles [ $^\circ$ ] for **4.100a-BnNH<sub>2</sub>**.

---

S(1)-C(18)	1.782(3)
S(1)-C(1)	1.835(3)
O(1)-C(10)	1.239(4)
O(2)-C(25)	1.210(4)
N(1)-C(10)	1.333(4)
N(1)-C(11)	1.464(3)
N(1)-H(1)	0.8800
C(1)-C(9)	1.506(4)
C(1)-C(2)	1.550(4)
C(1)-H(1A)	1.0000
C(2)-C(10)	1.524(3)
C(2)-C(3)	1.574(4)
C(2)-H(2)	1.0000
C(3)-C(4)	1.514(4)
C(3)-C(24)	1.535(4)
C(3)-H(3)	1.0000
C(4)-C(9)	1.384(4)
C(4)-C(5)	1.397(4)
C(5)-C(6)	1.385(4)
C(5)-H(5)	0.9500
C(6)-C(7)	1.394(5)
C(6)-H(6)	0.9500
C(7)-C(8)	1.383(5)
C(7)-H(7)	0.9500
C(8)-C(9)	1.397(4)
C(8)-H(8)	0.9500
C(11)-C(12)	1.511(4)
C(11)-H(11A)	0.9900
C(11)-H(11B)	0.9900
C(12)-C(17)	1.389(4)
C(12)-C(13)	1.393(4)
C(13)-C(14)	1.394(4)
C(13)-H(13)	0.9500
C(14)-C(15)	1.377(5)

C(14)-H(14)	0.9500
C(15)-C(16)	1.388(5)
C(15)-H(15)	0.9500
C(16)-C(17)	1.389(4)
C(16)-H(16)	0.9500
C(17)-H(17)	0.9500
C(18)-C(23)	1.386(4)
C(18)-C(19)	1.394(4)
C(19)-C(20)	1.381(5)
C(19)-H(19)	0.9500
C(20)-C(21)	1.392(6)
C(20)-H(20)	0.9500
C(21)-C(22)	1.382(6)
C(21)-H(21)	0.9500
C(22)-C(23)	1.396(5)
C(22)-H(22)	0.9500
C(23)-H(23)	0.9500
C(24)-C(25)	1.514(4)
C(24)-H(24A)	0.9900
C(24)-H(24B)	0.9900
C(25)-C(26)	1.492(4)
C(26)-H(26A)	0.9800
C(26)-H(26B)	0.9800
C(26)-H(26C)	0.9800
C(18)-S(1)-C(1)	101.19(12)
C(10)-N(1)-C(11)	120.7(2)
C(10)-N(1)-H(1)	119.6
C(11)-N(1)-H(1)	119.6
C(9)-C(1)-C(2)	104.0(2)
C(9)-C(1)-S(1)	113.40(18)
C(2)-C(1)-S(1)	112.44(18)
C(9)-C(1)-H(1A)	108.9
C(2)-C(1)-H(1A)	108.9
S(1)-C(1)-H(1A)	108.9
C(10)-C(2)-C(1)	110.6(2)

C(10)-C(2)-C(3)	113.9(2)
C(1)-C(2)-C(3)	106.0(2)
C(10)-C(2)-H(2)	108.7
C(1)-C(2)-H(2)	108.7
C(3)-C(2)-H(2)	108.7
C(4)-C(3)-C(24)	109.1(2)
C(4)-C(3)-C(2)	102.4(2)
C(24)-C(3)-C(2)	116.7(2)
C(4)-C(3)-H(3)	109.4
C(24)-C(3)-H(3)	109.4
C(2)-C(3)-H(3)	109.4
C(9)-C(4)-C(5)	120.2(3)
C(9)-C(4)-C(3)	112.2(2)
C(5)-C(4)-C(3)	127.3(3)
C(6)-C(5)-C(4)	118.8(3)
C(6)-C(5)-H(5)	120.6
C(4)-C(5)-H(5)	120.6
C(5)-C(6)-C(7)	120.8(3)
C(5)-C(6)-H(6)	119.6
C(7)-C(6)-H(6)	119.6
C(8)-C(7)-C(6)	120.5(3)
C(8)-C(7)-H(7)	119.7
C(6)-C(7)-H(7)	119.7
C(7)-C(8)-C(9)	118.7(3)
C(7)-C(8)-H(8)	120.7
C(9)-C(8)-H(8)	120.7
C(4)-C(9)-C(8)	120.9(3)
C(4)-C(9)-C(1)	110.9(2)
C(8)-C(9)-C(1)	128.0(3)
O(1)-C(10)-N(1)	121.8(2)
O(1)-C(10)-C(2)	120.6(2)
N(1)-C(10)-C(2)	117.6(2)
N(1)-C(11)-C(12)	114.8(2)
N(1)-C(11)-H(11A)	108.6
C(12)-C(11)-H(11A)	108.6
N(1)-C(11)-H(11B)	108.6

C(12)-C(11)-H(11B)	108.6
H(11A)-C(11)-H(11B)	107.6
C(17)-C(12)-C(13)	119.0(3)
C(17)-C(12)-C(11)	121.0(2)
C(13)-C(12)-C(11)	119.9(3)
C(12)-C(13)-C(14)	120.3(3)
C(12)-C(13)-H(13)	119.9
C(14)-C(13)-H(13)	119.9
C(15)-C(14)-C(13)	120.4(3)
C(15)-C(14)-H(14)	119.8
C(13)-C(14)-H(14)	119.8
C(14)-C(15)-C(16)	119.5(3)
C(14)-C(15)-H(15)	120.3
C(16)-C(15)-H(15)	120.3
C(15)-C(16)-C(17)	120.4(3)
C(15)-C(16)-H(16)	119.8
C(17)-C(16)-H(16)	119.8
C(16)-C(17)-C(12)	120.3(3)
C(16)-C(17)-H(17)	119.8
C(12)-C(17)-H(17)	119.8
C(23)-C(18)-C(19)	120.3(3)
C(23)-C(18)-S(1)	119.7(2)
C(19)-C(18)-S(1)	120.0(2)
C(20)-C(19)-C(18)	119.8(3)
C(20)-C(19)-H(19)	120.1
C(18)-C(19)-H(19)	120.1
C(19)-C(20)-C(21)	120.4(3)
C(19)-C(20)-H(20)	119.8
C(21)-C(20)-H(20)	119.8
C(22)-C(21)-C(20)	119.6(3)
C(22)-C(21)-H(21)	120.2
C(20)-C(21)-H(21)	120.2
C(21)-C(22)-C(23)	120.6(3)
C(21)-C(22)-H(22)	119.7
C(23)-C(22)-H(22)	119.7
C(18)-C(23)-C(22)	119.3(3)

C(18)-C(23)-H(23)	120.4
C(22)-C(23)-H(23)	120.4
C(25)-C(24)-C(3)	114.8(2)
C(25)-C(24)-H(24A)	108.6
C(3)-C(24)-H(24A)	108.6
C(25)-C(24)-H(24B)	108.6
C(3)-C(24)-H(24B)	108.6
H(24A)-C(24)-H(24B)	107.5
O(2)-C(25)-C(26)	122.1(3)
O(2)-C(25)-C(24)	121.2(3)
C(26)-C(25)-C(24)	116.8(2)
C(25)-C(26)-H(26A)	109.5
C(25)-C(26)-H(26B)	109.5
H(26A)-C(26)-H(26B)	109.5
C(25)-C(26)-H(26C)	109.5
H(26A)-C(26)-H(26C)	109.5
H(26B)-C(26)-H(26C)	109.5

---

**Table 4.8.** Anisotropic displacement parameters ( $\text{\AA}^2 \times 10^3$ ) for **4.100a-BnNH<sub>2</sub>**. The anisotropic displacement factor exponent takes the form:  $-2p^2 [ h^2 a^{*2} U^{11} + \dots + 2 h k a^* b^* U^{12} ]$

	U11	U22	U33	U23	U13	U12
S(1)	31(1)	29(1)	22(1)	-6(1)	-1(1)	-14(1)
O(1)	13(1)	21(1)	26(1)	1(1)	-3(1)	-3(1)
O(2)	18(1)	36(1)	50(1)	-13(1)	-2(1)	6(1)
N(1)	13(1)	18(1)	20(1)	1(1)	-2(1)	-2(1)
C(1)	18(1)	18(1)	18(1)	-2(1)	-3(1)	-3(1)
C(2)	14(1)	18(1)	17(1)	0(1)	-2(1)	-3(1)
C(3)	15(1)	22(1)	17(1)	1(1)	-1(1)	-1(1)
C(4)	17(1)	19(1)	24(1)	2(1)	-2(1)	-3(1)
C(5)	29(2)	27(1)	25(1)	6(1)	-6(1)	-5(1)
C(6)	32(2)	27(2)	37(2)	12(1)	-12(2)	-1(1)
C(7)	32(2)	21(1)	46(2)	0(1)	-9(2)	6(1)
C(8)	26(2)	19(1)	34(2)	-4(1)	-1(1)	0(1)
C(9)	18(1)	18(1)	23(1)	1(1)	-2(1)	-4(1)
C(10)	15(1)	17(1)	15(1)	-1(1)	-3(1)	0(1)
C(11)	19(1)	15(1)	24(1)	-2(1)	-2(1)	3(1)
C(12)	16(1)	16(1)	23(1)	-1(1)	-2(1)	2(1)
C(13)	26(2)	23(1)	30(2)	-1(1)	-5(1)	-5(1)
C(14)	34(2)	28(2)	36(2)	6(1)	-1(1)	-12(1)
C(15)	35(2)	30(1)	26(2)	3(1)	2(1)	-1(1)
C(16)	40(2)	33(2)	25(1)	-3(1)	-8(1)	-6(1)
C(17)	28(1)	24(1)	27(1)	0(1)	-4(1)	-8(1)
C(18)	22(1)	31(2)	18(1)	-6(1)	-3(1)	-8(1)
C(19)	33(2)	29(2)	25(1)	-4(1)	-4(1)	-5(1)
C(20)	49(2)	42(2)	25(2)	2(1)	-11(2)	-20(2)
C(21)	40(2)	68(2)	20(2)	-6(2)	-2(2)	-26(2)
C(22)	26(2)	69(3)	32(2)	-20(2)	2(2)	-3(2)
C(23)	27(2)	39(2)	29(2)	-10(1)	-5(1)	0(1)
C(24)	16(1)	24(1)	18(1)	-3(1)	-4(1)	2(1)
C(25)	20(1)	29(1)	19(1)	-7(1)	-5(1)	4(1)
C(26)	26(2)	26(1)	40(2)	-13(1)	-7(1)	5(1)



**Table 4.9.** Hydrogen coordinates ( $\times 10^4$ ) and isotropic displacement parameters ( $\text{\AA}^2 \times 10^3$ ) for **4.100a-BnNH<sub>2</sub>**.

	x	y	z	U(eq)
H(1)	-676	5953	5584	21
H(1A)	6806	3900	5327	22
H(2)	1326	3952	6339	20
H(3)	2022	3947	8335	22
H(5)	5732	2172	9732	33
H(6)	8689	206	9532	40
H(7)	10176	-446	7582	41
H(8)	8731	867	5798	32
H(11A)	1574	8315	5620	24
H(11B)	-1399	8235	5265	24
H(13)	4041	9579	4054	31
H(14)	5296	10281	1968	40
H(15)	3482	9378	426	38
H(16)	461	7727	974	38
H(17)	-897	7064	3051	31
H(19)	3781	5164	2986	35
H(20)	6388	6106	1262	45
H(21)	10091	4801	370	49
H(22)	11166	2555	1213	50
H(23)	8598	1602	2968	37
H(24A)	5892	4757	9038	24
H(24B)	6877	5260	7632	24
H(26A)	6111	7872	7442	46
H(26B)	6531	7491	8879	46
H(26C)	3960	8482	8467	46

**Table 4.10.** Torsion angles [°] for **4.100a-BnNH<sub>2</sub>**.

---

C(18)-S(1)-C(1)-C(9)	-124.5(2)
C(18)-S(1)-C(1)-C(2)	117.79(19)
C(9)-C(1)-C(2)-C(10)	144.0(2)
S(1)-C(1)-C(2)-C(10)	-92.9(2)
C(9)-C(1)-C(2)-C(3)	20.1(3)
S(1)-C(1)-C(2)-C(3)	143.20(18)
C(10)-C(2)-C(3)-C(4)	-141.9(2)
C(1)-C(2)-C(3)-C(4)	-20.1(2)
C(10)-C(2)-C(3)-C(24)	-22.8(3)
C(1)-C(2)-C(3)-C(24)	99.0(2)
C(24)-C(3)-C(4)-C(9)	-111.1(3)
C(2)-C(3)-C(4)-C(9)	13.2(3)
C(24)-C(3)-C(4)-C(5)	64.2(4)
C(2)-C(3)-C(4)-C(5)	-171.5(3)
C(9)-C(4)-C(5)-C(6)	-0.2(4)
C(3)-C(4)-C(5)-C(6)	-175.1(3)
C(4)-C(5)-C(6)-C(7)	0.0(5)
C(5)-C(6)-C(7)-C(8)	0.1(5)
C(6)-C(7)-C(8)-C(9)	0.0(5)
C(5)-C(4)-C(9)-C(8)	0.3(4)
C(3)-C(4)-C(9)-C(8)	176.0(2)
C(5)-C(4)-C(9)-C(1)	-176.3(3)
C(3)-C(4)-C(9)-C(1)	-0.6(3)
C(7)-C(8)-C(9)-C(4)	-0.2(4)
C(7)-C(8)-C(9)-C(1)	175.7(3)
C(2)-C(1)-C(9)-C(4)	-12.5(3)
S(1)-C(1)-C(9)-C(4)	-135.0(2)
C(2)-C(1)-C(9)-C(8)	171.2(3)
S(1)-C(1)-C(9)-C(8)	48.7(4)
C(11)-N(1)-C(10)-O(1)	-6.9(4)
C(11)-N(1)-C(10)-C(2)	171.6(2)
C(1)-C(2)-C(10)-O(1)	-51.6(3)
C(3)-C(2)-C(10)-O(1)	67.7(3)
C(1)-C(2)-C(10)-N(1)	129.9(2)

C(3)-C(2)-C(10)-N(1)	-110.8(3)
C(10)-N(1)-C(11)-C(12)	80.5(3)
N(1)-C(11)-C(12)-C(17)	54.9(3)
N(1)-C(11)-C(12)-C(13)	-127.9(3)
C(17)-C(12)-C(13)-C(14)	0.7(4)
C(11)-C(12)-C(13)-C(14)	-176.5(3)
C(12)-C(13)-C(14)-C(15)	-0.5(5)
C(13)-C(14)-C(15)-C(16)	-0.6(5)
C(14)-C(15)-C(16)-C(17)	1.6(5)
C(15)-C(16)-C(17)-C(12)	-1.4(5)
C(13)-C(12)-C(17)-C(16)	0.3(4)
C(11)-C(12)-C(17)-C(16)	177.4(3)
C(1)-S(1)-C(18)-C(23)	101.4(2)
C(1)-S(1)-C(18)-C(19)	-78.2(2)
C(23)-C(18)-C(19)-C(20)	-0.7(4)
S(1)-C(18)-C(19)-C(20)	178.9(3)
C(18)-C(19)-C(20)-C(21)	0.6(5)
C(19)-C(20)-C(21)-C(22)	0.0(5)
C(20)-C(21)-C(22)-C(23)	-0.5(5)
C(19)-C(18)-C(23)-C(22)	0.2(4)
S(1)-C(18)-C(23)-C(22)	-179.4(3)
C(21)-C(22)-C(23)-C(18)	0.4(5)
C(4)-C(3)-C(24)-C(25)	-173.3(2)
C(2)-C(3)-C(24)-C(25)	71.4(3)
C(3)-C(24)-C(25)-O(2)	23.7(4)
C(3)-C(24)-C(25)-C(26)	-157.8(2)

---

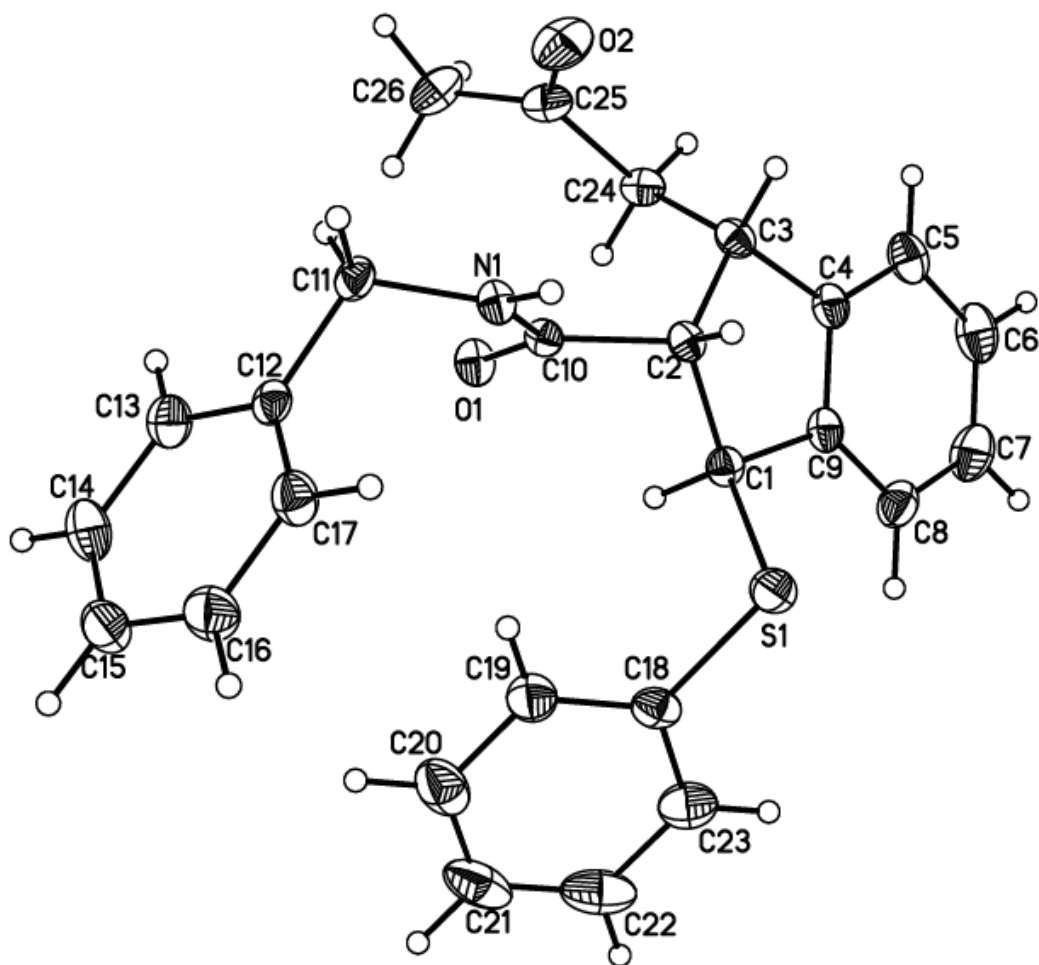
**Table 4.11.** Hydrogen bonds for **4.100a-BnNH<sub>2</sub>** [Å and °].

D-H...A	d(D-H)	d(H...A)	d(D...A)	<(DHA)
N(1)-H(1)...O(1)#1	0.88	2.05	2.783(3)	140.0
C(26)-H(26B)...O(2)#2	0.98	2.43	3.115(4)	126.2

Symmetry transformations used to generate equivalent atoms:

#1  $x-1, y, z$  #2  $x+1, y, z$

Projection view with 50% probability ellipsoids:



## 4.10 X-ray crystal structure of 4.100b

**Table 4.12.** Crystal data and structure refinement for **4.100b**.

Identification code	v21019/lt/venture/Straub-Birman	
Empirical formula	C <sub>24</sub> H <sub>18</sub> O <sub>2</sub> S	
Formula weight	370.44	
Temperature	100(2) K	
Wavelength	1.54178 Å	
Crystal system	Monoclinic	
Space group	P2 <sub>1</sub>	
Unit cell dimensions	a = 8.7451(4) Å	a = 90°.
	b = 5.0040(2) Å	b = 95.527(2)°.
	c = 21.5160(9) Å	g = 90°.
Volume	937.17(7) Å <sup>3</sup>	
Z	2	
Density (calculated)	1.313 Mg/m <sup>3</sup>	
Absorption coefficient	1.653 mm <sup>-1</sup>	
F(000)	388	
Crystal size	0.400 x 0.033 x 0.027 mm <sup>3</sup>	
Theta range for data collection	2.063 to 74.578°.	
Index ranges	-10 ≤ h ≤ 10, -5 ≤ k ≤ 6, -26 ≤ l ≤ 26	
Reflections collected	18969	
Independent reflections	3783 [R(int) = 0.0548]	
Completeness to theta = 67.679°	99.7 %	
Absorption correction	Semi-empirical from equivalents	
Max. and min. transmission	0.6627 and 0.5127	
Refinement method	Full-matrix least-squares on F <sup>2</sup>	
Data / restraints / parameters	3783 / 1 / 244	
Goodness-of-fit on F <sup>2</sup>	1.058	
Final R indices [I > 2σ(I)]	R1 = 0.0315, wR2 = 0.0818	
R indices (all data)	R1 = 0.0352, wR2 = 0.0834	
Absolute structure parameter	0.019(11)	
Largest diff. peak and hole	0.173 and -0.234 e.Å <sup>-3</sup>	

**Table 4.13.** Atomic coordinates ( $\times 10^4$ ) and equivalent isotropic displacement parameters ( $\text{\AA}^2 \times 10^3$ ) for **4.100b**.  $U(\text{eq})$  is defined as one third of the trace of the orthogonalized  $U^{ij}$  tensor.

	x	y	z	$U(\text{eq})$
S(1)	4489(1)	5844(1)	1189(1)	27(1)
O(1)	6947(2)	2768(3)	3396(1)	25(1)
O(2)	7189(2)	613(4)	2528(1)	24(1)
C(1)	6664(2)	2531(5)	2767(1)	20(1)
C(2)	5785(2)	4736(4)	2407(1)	19(1)
C(3)	4604(2)	6103(5)	2788(1)	21(1)
C(4)	5161(3)	6333(5)	3466(1)	23(1)
C(5)	6269(3)	4789(5)	3732(1)	21(1)
C(6)	4837(3)	3503(5)	1833(1)	21(1)
C(7)	3308(2)	2958(5)	2084(1)	21(1)
C(8)	2127(3)	1282(5)	1841(1)	27(1)
C(9)	828(3)	1043(6)	2165(1)	30(1)
C(10)	717(3)	2466(6)	2716(1)	31(1)
C(11)	1886(3)	4169(5)	2950(1)	26(1)
C(12)	3188(2)	4402(5)	2631(1)	21(1)
C(13)	6917(3)	4783(5)	4393(1)	22(1)
C(14)	6407(3)	6618(6)	4814(1)	34(1)
C(15)	6992(3)	6605(6)	5436(1)	35(1)
C(16)	8104(3)	4782(6)	5647(1)	32(1)
C(17)	8627(4)	2953(6)	5238(1)	40(1)
C(18)	8030(3)	2939(6)	4611(1)	33(1)
C(19)	6331(3)	6563(5)	957(1)	25(1)
C(20)	7675(3)	5191(5)	1162(1)	27(1)
C(21)	9061(3)	5965(6)	950(1)	31(1)
C(22)	9120(3)	8045(6)	533(1)	32(1)
C(23)	7782(3)	9380(6)	323(1)	35(1)
C(24)	6393(3)	8664(5)	534(1)	31(1)

**Table 4.14.** Bond lengths [ $\text{\AA}$ ] and angles [ $^\circ$ ] for **4.100b**.

---

S(1)-C(19)	1.769(3)
S(1)-C(6)	1.818(2)
O(1)-C(1)	1.359(3)
O(1)-C(5)	1.407(3)
O(2)-C(1)	1.200(3)
C(1)-C(2)	1.515(3)
C(2)-C(3)	1.540(3)
C(2)-C(6)	1.546(3)
C(2)-H(2)	1.0000
C(3)-C(4)	1.496(3)
C(3)-C(12)	1.514(3)
C(3)-H(3)	1.0000
C(4)-C(5)	1.326(3)
C(4)-H(4)	0.9500
C(5)-C(13)	1.478(3)
C(6)-C(7)	1.514(3)
C(6)-H(6)	1.0000
C(7)-C(8)	1.393(3)
C(7)-C(12)	1.395(3)
C(8)-C(9)	1.394(3)
C(8)-H(8)	0.9500
C(9)-C(10)	1.395(4)
C(9)-H(9)	0.9500
C(10)-C(11)	1.388(4)
C(10)-H(10)	0.9500
C(11)-C(12)	1.389(3)
C(11)-H(11)	0.9500
C(13)-C(18)	1.390(4)
C(13)-C(14)	1.394(4)
C(14)-C(15)	1.385(4)
C(14)-H(14)	0.9500
C(15)-C(16)	1.378(4)
C(15)-H(15)	0.9500
C(16)-C(17)	1.378(4)

C(16)-H(16)	0.9500
C(17)-C(18)	1.398(4)
C(17)-H(17)	0.9500
C(18)-H(18)	0.9500
C(19)-C(24)	1.395(3)
C(19)-C(20)	1.396(3)
C(20)-C(21)	1.390(3)
C(20)-H(20)	0.9500
C(21)-C(22)	1.379(4)
C(21)-H(21)	0.9500
C(22)-C(23)	1.385(4)
C(22)-H(22)	0.9500
C(23)-C(24)	1.385(4)
C(23)-H(23)	0.9500
C(24)-H(24)	0.9500

C(19)-S(1)-C(6)	104.81(11)
C(1)-O(1)-C(5)	121.99(17)
O(2)-C(1)-O(1)	117.1(2)
O(2)-C(1)-C(2)	124.1(2)
O(1)-C(1)-C(2)	118.78(19)
C(1)-C(2)-C(3)	112.61(18)
C(1)-C(2)-C(6)	108.92(18)
C(3)-C(2)-C(6)	105.50(17)
C(1)-C(2)-H(2)	109.9
C(3)-C(2)-H(2)	109.9
C(6)-C(2)-H(2)	109.9
C(4)-C(3)-C(12)	116.29(19)
C(4)-C(3)-C(2)	112.42(18)
C(12)-C(3)-C(2)	101.97(18)
C(4)-C(3)-H(3)	108.6
C(12)-C(3)-H(3)	108.6
C(2)-C(3)-H(3)	108.6
C(5)-C(4)-C(3)	122.2(2)
C(5)-C(4)-H(4)	118.9
C(3)-C(4)-H(4)	118.9



C(4)-C(5)-O(1)	121.5(2)
C(4)-C(5)-C(13)	127.9(2)
O(1)-C(5)-C(13)	110.55(19)
C(7)-C(6)-C(2)	102.23(17)
C(7)-C(6)-S(1)	107.37(15)
C(2)-C(6)-S(1)	112.89(16)
C(7)-C(6)-H(6)	111.3
C(2)-C(6)-H(6)	111.3
S(1)-C(6)-H(6)	111.3
C(8)-C(7)-C(12)	121.0(2)
C(8)-C(7)-C(6)	128.6(2)
C(12)-C(7)-C(6)	110.39(19)
C(7)-C(8)-C(9)	118.3(2)
C(7)-C(8)-H(8)	120.8
C(9)-C(8)-H(8)	120.8
C(8)-C(9)-C(10)	120.5(2)
C(8)-C(9)-H(9)	119.7
C(10)-C(9)-H(9)	119.7
C(11)-C(10)-C(9)	120.9(2)
C(11)-C(10)-H(10)	119.6
C(9)-C(10)-H(10)	119.6
C(10)-C(11)-C(12)	118.8(2)
C(10)-C(11)-H(11)	120.6
C(12)-C(11)-H(11)	120.6
C(11)-C(12)-C(7)	120.4(2)
C(11)-C(12)-C(3)	128.9(2)
C(7)-C(12)-C(3)	110.66(19)
C(18)-C(13)-C(14)	118.3(2)
C(18)-C(13)-C(5)	121.2(2)
C(14)-C(13)-C(5)	120.5(2)
C(15)-C(14)-C(13)	120.9(3)
C(15)-C(14)-H(14)	119.6
C(13)-C(14)-H(14)	119.6
C(16)-C(15)-C(14)	120.3(3)
C(16)-C(15)-H(15)	119.8
C(14)-C(15)-H(15)	119.8

C(17)-C(16)-C(15)	119.8(2)
C(17)-C(16)-H(16)	120.1
C(15)-C(16)-H(16)	120.1
C(16)-C(17)-C(18)	120.2(3)
C(16)-C(17)-H(17)	119.9
C(18)-C(17)-H(17)	119.9
C(13)-C(18)-C(17)	120.5(3)
C(13)-C(18)-H(18)	119.8
C(17)-C(18)-H(18)	119.8
C(24)-C(19)-C(20)	119.5(2)
C(24)-C(19)-S(1)	115.53(19)
C(20)-C(19)-S(1)	124.99(18)
C(21)-C(20)-C(19)	119.6(2)
C(21)-C(20)-H(20)	120.2
C(19)-C(20)-H(20)	120.2
C(22)-C(21)-C(20)	120.8(2)
C(22)-C(21)-H(21)	119.6
C(20)-C(21)-H(21)	119.6
C(21)-C(22)-C(23)	119.6(2)
C(21)-C(22)-H(22)	120.2
C(23)-C(22)-H(22)	120.2
C(22)-C(23)-C(24)	120.5(2)
C(22)-C(23)-H(23)	119.7
C(24)-C(23)-H(23)	119.7
C(23)-C(24)-C(19)	120.0(3)
C(23)-C(24)-H(24)	120.0
C(19)-C(24)-H(24)	120.0

---

**Table 4.15.** Anisotropic displacement parameters ( $\text{\AA}^2 \times 10^3$ ) for **4.100b**. The anisotropic displacement factor exponent takes the form:  $-2p^2[ h^2 a^*2U^{11} + \dots + 2 h k a^* b^* U^{12} ]$

	U11	U22	U33	U23	U13	U12
S(1)	26(1)	34(1)	22(1)	5(1)	3(1)	6(1)
O(1)	26(1)	24(1)	24(1)	-2(1)	-1(1)	6(1)
O(2)	18(1)	22(1)	32(1)	-4(1)	2(1)	1(1)
C(1)	13(1)	22(1)	25(1)	-1(1)	4(1)	-5(1)
C(2)	18(1)	18(1)	22(1)	0(1)	4(1)	-2(1)
C(3)	20(1)	19(1)	24(1)	0(1)	4(1)	2(1)
C(4)	21(1)	24(1)	25(1)	-2(1)	5(1)	1(1)
C(5)	19(1)	18(1)	25(1)	-1(1)	5(1)	-4(1)
C(6)	21(1)	21(1)	22(1)	1(1)	1(1)	1(1)
C(7)	16(1)	22(1)	25(1)	4(1)	1(1)	2(1)
C(8)	23(1)	26(1)	30(1)	-1(1)	-4(1)	2(1)
C(9)	18(1)	32(1)	39(1)	4(1)	-5(1)	-2(1)
C(10)	17(1)	42(2)	33(1)	7(1)	2(1)	0(1)
C(11)	19(1)	33(1)	25(1)	4(1)	3(1)	2(1)
C(12)	18(1)	22(1)	23(1)	3(1)	-1(1)	2(1)
C(13)	20(1)	23(1)	25(1)	2(1)	4(1)	-6(1)
C(14)	31(1)	40(2)	32(1)	-8(1)	-2(1)	4(1)
C(15)	32(1)	44(2)	29(1)	-9(1)	2(1)	-5(1)
C(16)	34(1)	37(1)	23(1)	1(1)	-2(1)	-12(1)
C(17)	47(2)	38(2)	32(1)	2(1)	-7(1)	7(1)
C(18)	37(1)	33(1)	27(1)	1(1)	0(1)	5(1)
C(19)	32(1)	26(1)	18(1)	-3(1)	5(1)	1(1)
C(20)	34(1)	24(1)	25(1)	2(1)	9(1)	5(1)
C(21)	33(1)	31(1)	32(1)	0(1)	10(1)	5(1)
C(22)	38(1)	34(1)	26(1)	-2(1)	11(1)	-5(1)
C(23)	44(2)	36(2)	25(1)	8(1)	4(1)	-6(1)
C(24)	36(1)	31(1)	25(1)	4(1)	0(1)	1(1)

**Table 4.16.** Hydrogen coordinates ( $\times 10^4$ ) and isotropic displacement parameters ( $\text{\AA}^2 \times 10^3$ ) for **4.100b**.

	x	y	z	U(eq)
H(2)	6517	6094	2267	23
H(3)	4397	7939	2617	25
H(4)	4706	7628	3713	28
H(6)	5318	1817	1696	25
H(8)	2205	326	1464	32
H(9)	12	-99	2009	36
H(10)	-170	2267	2934	37
H(11)	1798	5158	3322	31
H(14)	5648	7896	4673	41
H(15)	6624	7858	5718	42
H(16)	8508	4787	6073	38
H(17)	9396	1699	5382	48
H(18)	8387	1659	4333	39
H(20)	7644	3738	1445	33
H(21)	9979	5050	1095	38
H(22)	10072	8558	390	39
H(23)	7817	10799	31	42
H(24)	5482	9603	392	37

**Table 4.17.** Torsion angles [°] for **4.100b**.

---

C(5)-O(1)-C(1)-O(2)	-173.76(19)
C(5)-O(1)-C(1)-C(2)	9.1(3)
O(2)-C(1)-C(2)-C(3)	151.4(2)
O(1)-C(1)-C(2)-C(3)	-31.7(3)
O(2)-C(1)-C(2)-C(6)	34.7(3)
O(1)-C(1)-C(2)-C(6)	-148.38(18)
C(1)-C(2)-C(3)-C(4)	36.0(3)
C(6)-C(2)-C(3)-C(4)	154.6(2)
C(1)-C(2)-C(3)-C(12)	-89.3(2)
C(6)-C(2)-C(3)-C(12)	29.4(2)
C(12)-C(3)-C(4)-C(5)	96.1(3)
C(2)-C(3)-C(4)-C(5)	-20.9(3)
C(3)-C(4)-C(5)-O(1)	-2.4(3)
C(3)-C(4)-C(5)-C(13)	-179.4(2)
C(1)-O(1)-C(5)-C(4)	9.4(3)
C(1)-O(1)-C(5)-C(13)	-173.11(18)
C(1)-C(2)-C(6)-C(7)	92.5(2)
C(3)-C(2)-C(6)-C(7)	-28.6(2)
C(1)-C(2)-C(6)-S(1)	-152.48(15)
C(3)-C(2)-C(6)-S(1)	86.41(19)
C(19)-S(1)-C(6)-C(7)	176.07(16)
C(19)-S(1)-C(6)-C(2)	64.17(18)
C(2)-C(6)-C(7)-C(8)	-162.5(2)
S(1)-C(6)-C(7)-C(8)	78.5(3)
C(2)-C(6)-C(7)-C(12)	17.0(2)
S(1)-C(6)-C(7)-C(12)	-101.97(18)
C(12)-C(7)-C(8)-C(9)	-1.2(3)
C(6)-C(7)-C(8)-C(9)	178.3(2)
C(7)-C(8)-C(9)-C(10)	0.4(4)
C(8)-C(9)-C(10)-C(11)	0.7(4)
C(9)-C(10)-C(11)-C(12)	-1.1(4)
C(10)-C(11)-C(12)-C(7)	0.4(3)
C(10)-C(11)-C(12)-C(3)	180.0(2)
C(8)-C(7)-C(12)-C(11)	0.8(3)

C(6)-C(7)-C(12)-C(11)	-178.8(2)
C(8)-C(7)-C(12)-C(3)	-178.9(2)
C(6)-C(7)-C(12)-C(3)	1.6(3)
C(4)-C(3)-C(12)-C(11)	38.2(3)
C(2)-C(3)-C(12)-C(11)	160.9(2)
C(4)-C(3)-C(12)-C(7)	-142.2(2)
C(2)-C(3)-C(12)-C(7)	-19.5(2)
C(4)-C(5)-C(13)-C(18)	176.6(2)
O(1)-C(5)-C(13)-C(18)	-0.6(3)
C(4)-C(5)-C(13)-C(14)	-2.5(4)
O(1)-C(5)-C(13)-C(14)	-179.7(2)
C(18)-C(13)-C(14)-C(15)	-0.1(4)
C(5)-C(13)-C(14)-C(15)	179.1(2)
C(13)-C(14)-C(15)-C(16)	0.6(4)
C(14)-C(15)-C(16)-C(17)	-0.5(4)
C(15)-C(16)-C(17)-C(18)	-0.2(4)
C(14)-C(13)-C(18)-C(17)	-0.6(4)
C(5)-C(13)-C(18)-C(17)	-179.8(3)
C(16)-C(17)-C(18)-C(13)	0.7(4)
C(6)-S(1)-C(19)-C(24)	-169.80(18)
C(6)-S(1)-C(19)-C(20)	10.6(2)
C(24)-C(19)-C(20)-C(21)	1.1(4)
S(1)-C(19)-C(20)-C(21)	-179.34(19)
C(19)-C(20)-C(21)-C(22)	-1.0(4)
C(20)-C(21)-C(22)-C(23)	0.1(4)
C(21)-C(22)-C(23)-C(24)	0.7(4)
C(22)-C(23)-C(24)-C(19)	-0.7(4)
C(20)-C(19)-C(24)-C(23)	-0.2(4)
S(1)-C(19)-C(24)-C(23)	-179.9(2)

---

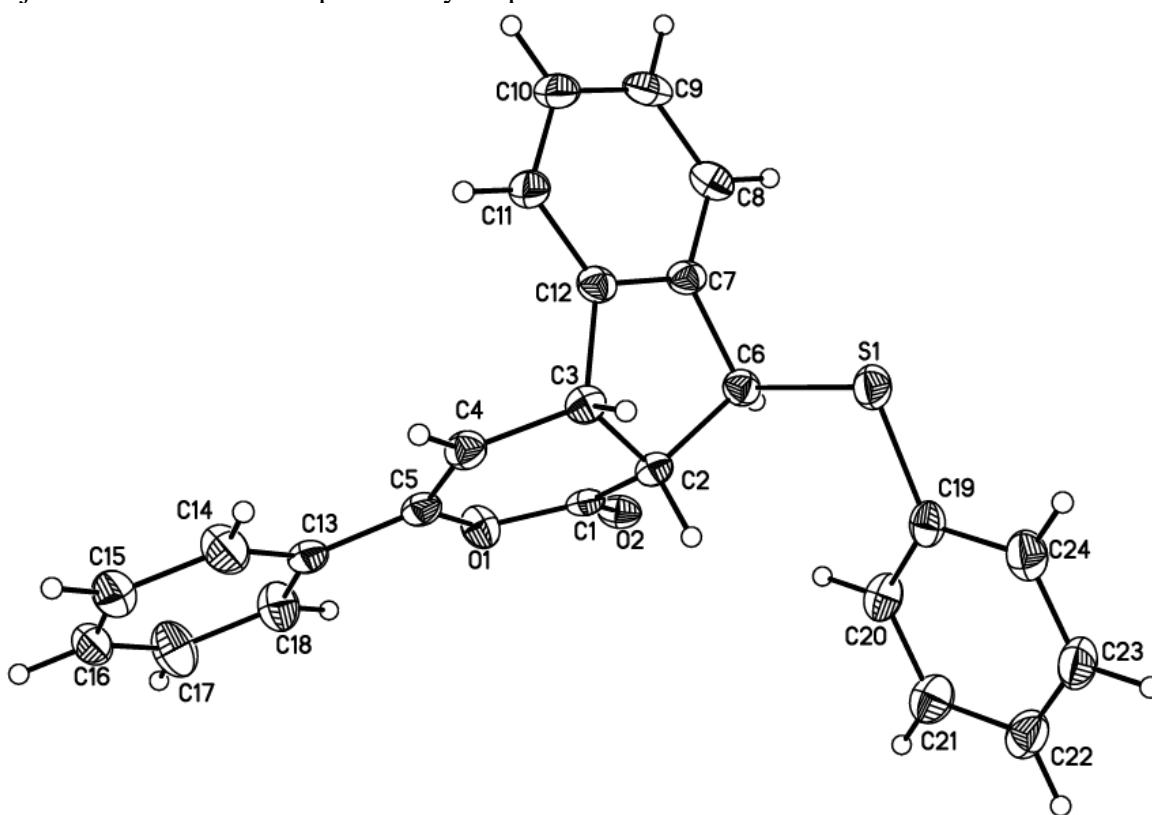
**Table 4.18.** Hydrogen bonds for **4.100b** [ $\text{\AA}$  and  $^\circ$ ].

D-H...A	d(D-H)	d(H...A)	d(D...A)	$\angle(\text{DHA})$
C(2)-H(2)...O(2)#1	1.00	2.39	3.188(3)	136.2

Symmetry transformations used to generate equivalent atoms:

#1  $x, y+1, z$

Projection view with 50% probability ellipsoids:



## 4.11 References

1. The results in this chapter were previously published: (a) Leace, D. M.; Straub, M. R.; Matz, B. A.; Birman, V. B. *J. Org. Chem.* **2019**, *84*, 7523. (b) Ahlemeyer, N. A.; Straub, M. R.; Leace, D. M.; Matz, B. A.; Birman, V. B. *J. Org. Chem.* **2021**, *86*, 1191.
2. Hoefle, G.; Steglich, W. *Synthesis* **1972**, 619.
3. (a) Müller, C. E.; Schreiner, P. R. *Angew. Chem., Int. Ed.* **2011**, *50*, 6012. (b) Denmark, S. E.; Beutner, G. L. *Angew. Chem. Int. Ed.* **2008**, *47*, 1560.
4. (a) Oriyama, T.; Hori, Y.; Imai, K.; Sasaki, R. *Tetrahedron Lett.* **1996**, *37*, 8543. (b) Ruble, J. C.; Latham, H. A.; Fu, G. C. *J. Am. Chem. Soc.* **1997**, *119*, 1492. (c) Vedejs, E.; Daugulis, O. *J. Am. Chem. Soc.* **1999**, *121*, 5813. (d) Jarvo, E. R.; Copeland, G. T.; Papaioannou, N.; Bonitatebus, P. J., Jr.; Miller, S. J. *J. Am. Chem. Soc.* **1999**, *121*, 11638. (e) Mizuta, S.; Sadamori, M.; Fujimoto, T.; Yamamoto, I. *Angew. Chem., Int. Ed.* **2003**, *42*, 3383. (f) Ishihara, K.; Kosugi, Y.; Akakura, M. *J. Am. Chem. Soc.* **2004**, *126*, 12212. (g) Kano, T.; Sasaki, K.; Maruoka, K. *Org. Lett.* **2005**, *7*, 1347. (h) Notte, G. T.; Sammakia, T.; Steel, P. J. *J. Am. Chem. Soc.* **2005**, *127*, 13502. (i) Notte, G. T.; Sammakia, T. *J. Am. Chem. Soc.* **2006**, *128*, 4230. (j) Duffey, T. A.; Shaw, S. A.; Vedejs, E. *J. Am. Chem. Soc.* **2009**, *131*, 14. (k) Uraguchi, D.; Koshimoto, K.; Miyake, S.; Ooi, T. *Angew. Chem., Int. Ed.* **2010**, *49*, 5567.
5. Birman, V. B. *Aldrimicha Acta* **2016**, *49*, 23.
6. (a) Ryan, S. J.; Candish, L.; Lupton, D. W. *J. Am. Chem. Soc.* **2009**, *131*, 14176 (b) Candish, L.; Levens, A.; Lupton, D. W. *J. Am. Chem. Soc.* **2014**, *136*, 14397.

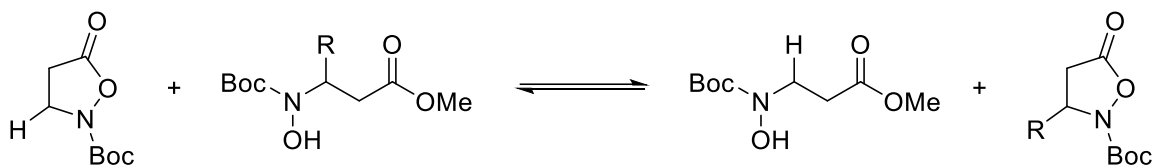


7. Fukata, Y.; Okamura, T.; Asano, K.; Matsubara, S. *Org. Lett.* **2014**, *16*, 2184.
8. Zhang, Y.; Birman, V. B. *Adv. Synth. Catal.* **2009**, *351*, 2525.
9. Ahlemeyer, N. A.; Birman, V. B. *Org. Lett.* **2016**, *18*, 3454.
10. Ahlemeyer, N. A.; Streff, E. V.; Muthupandi, P.; Birman, V. B. *Org. Lett.* **2017**, *19*, 6486.
11. Kobayashi, M.; Okamoto, S. *Tetrahedron Lett.* **2006**, *47*, 4347.
12. Birman, V. B.; Uffman, E. W.; Jiang, H.; Li, X.; Kilbane, C. J. *J. Am. Chem. Soc.* **2004**, *126*, 12226.
13. Lu, H.; Zhang, J.-L.; Liu, J.-Y.; Li, H.-Y.; Xu, P.-F. *ACS Catal.* **2017**, *7*, 7797.
14. (a) Duus, F. *Tetrahedron* **1981**, *37*, 2633. For a related aldol-based approach to tetrahydrothiophenes, see: (b) Brandau, S.; Maerten, E.; Jorgensen, K. A. *J. Am. Chem. Soc.* **2006**, *128*, 14986.
15. Okamoto, S.; Sakai, Y.; Watanabe, S.; Nishi, S.; Yoneyama, A.; Katsumata, H.; Kosaki, Y.; Sato, R.; Shiratori, M.; Shibuno, M.; Shishido, T. *Tetrahedron Lett.* **2014**, *55*, 1909.
16. For the use of 2,4,6-trichlorophenyl esters as acyl donors with amidine-based catalysts, see: Matviitsuk, A.; Taylor, J. E.; Cordes, D. B.; Slawin, A. M. Z.; Smith, A. D. *Chem. - Eur. J.* **2016**, *22*, 17748.
17. Lienard, B. M. R.; Garau, G.; Horsfall, L.; Karsisiotis, A. I.; Damblon, C.; Lassaux, P.; Papamicael, C.; Roberts, G. C. K.; Galleni, M.; Dideberg, O.; Frere, J. M.; Schofield, C. *J. Org. Biomol. Chem.* **2008**, *6*, 2282.

18. Joannesse, C.; Johnston, C. P.; Concellon, C.; Simal, C.; Philp, D.; Smith, A. D. *Angew. Chem. Int. Ed.* **2009**, *48*, 8914.
19. Birman, V. B.; Li, X. *Org. Lett.* **2006**, *8*, 1351.
20. Biswas, A.; De Sarkar, S.; Frohlich, R.; Studer, A. *Org. Lett.* **2011**, *13*, 4966.
21. All acids are known compounds and were obtained commercially or via the classical Knoevenagel–Doebner condensation: Koo, J.; Fish, M. S.; Walker, G. N.; Blake, J. *Org. Synth., Coll. Vol.* **1963**, *4*, 327.
22. p-Nitrophenyl-2-bromoethanone and (2-furyl)-2-bromoethanone are known compounds and were prepared by bromination of the corresponding methylketones with NBS and TsOH: Lee, J. C.; Bae, Y. H.; Chang, S.-K. *Bull. Korean Chem. Soc.* **2003**, *24*, 407.
23. Ueda, T.; Konishi, H.; Manabe, K. *Org. Lett.* **2012**, *14*, 5370.
24. (a) Augustine, J. K.; Bombrun, A.; Venkatachaliah, S.; Jothi, A. *Org. Biomol. Chem.* **2013**, *11*, 8065. (b) Vivier, D.; Soussia, I. B.; Rodrigues, N.; Lolignier, S.; Devilliers, M.; Chatelain, F. C.; Prival, L.; Chapuy, E.; Bourdier, G.; Bennis, K.; Lesage, F.; Eschalier, A.; Busserolles, J.; Ducki, S. *J. Med. Chem.* **2017**, *60*, 1076.
25. Dickman, D. A.; Chemburkar, S.; Konopacki, D. B.; Elisseou, E. M. *Synthesis* **1993**, *6*, 573.

# APPENDIX

## A.1 Isodesmic study: An attempt to elucidate the spontaneous ring closure of 3.44m-Me

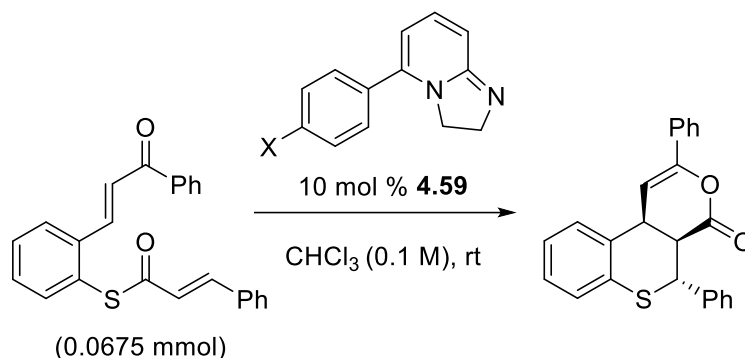


An isodesmic study of the hypothetical equation above was performed to study and compare the thermodynamic preferences of isoxazolidinones and their ring opened methyl esters. Geometry optimization of the isoxazolidinones and methyl esters (R = H, Me, Et, *i*-Pr, and *t*-Bu) was performed in Spartan '16 (Wavefunction, Inc.) at the B3LYP/6-31G\* level of theory using a gas phase model. The results are shown in the **Table A.1** below. Results show that as the steric bulk of R increases,  $\Delta H$  rel becomes more negative. This suggests that the ring closed form is more thermodynamically favored to the ring opened form as R increases in size.

**Table A.1.** Results of isodesmic study.

R	$\Delta H$ (isox) (kcal/mol)	$\Delta H$ (ester) (kcal/mol)	$\Delta\Delta H = \Delta H$ (ester)- $\Delta H$ (isox) (kcal/mol)	$\Delta H$ rel (kcal/mol)
H	-419368.49	-491995.64	-72627.15	0
Me	-444040.81	-516666.99	-72626.18	-0.97
Et	-468710.74	-541336.51	-72625.77	-1.38
<i>i</i> -Pr	-493380.1	-566004.56	-72624.46	-2.69
<i>t</i> -Bu	-518049.24	-590672.45	-72623.21	-3.94

## A.2 Kinetic data for 5-aryl DHIP derivatives



A published procedure was followed.<sup>10</sup> Each catalyst was tested in duplicate in the rearrangement of thioester **4.53a**. **Procedure:** 0.0675 mmol of thioester (25 mg) was dissolved in 575  $\mu$ L of CDCl<sub>3</sub>. Then, 100  $\mu$ L of 0.068 M catalyst in CDCl<sub>3</sub> (0.0068 mmol, 10 mol %) was added to create a final volume of 675  $\mu$ L (0.1 M in thioester). The contents were very quickly mixed and the reaction was analyzed by <sup>1</sup>H NMR. The conversions were calculated by comparing the integrations of starting material and product peaks. The results are summarized in Tables **A.1** and **A.2** below. The data are graphed in Figure **A.3**

**Table A.2.** Conversion data obtained for catalyst **4.59b**.

Time (minutes)	% conversion (Run 1)	% conversion (Run 2)	Average conversion	Error
2.5	14.38	14.18	14.28	0.1
4	18.45	19.31	18.88	0.43
5	22.17	21.6	21.89	0.29
6	26.39	25.38	25.89	0.51
7	28.9	28.33	28.62	0.29
8	32.05	31.06	31.56	0.5
9	33.78	33.67	33.73	0.06
10	36.76	36.63	36.7	0.07
12	41.84	40.82	41.33	0.51
13	44.44	43.67	44.06	0.39
14	46.08	44.84	45.46	0.62
15	48.78	48.31	48.55	0.24
17	51.55	51.55	51.55	0
19	54.95	55.25	55.1	0.15
20	57.8	57.14	57.47	0.33
22	60.61	59.52	60.07	0.55
24	63.69	63.29	63.49	0.2
26	65.79	66.67	66.23	0.44
28	68.03	68.49	68.26	0.23
30	70.42	69.93	70.18	0.25
33	74.63	74.07	74.35	0.28
36	75.76	75.76	75.76	0
39	78.74	77.52	78.13	0.61
42	80	79.37	79.69	0.32
45	83.33	81.97	82.65	0.68
50	84.75	84.03	84.39	0.36
55	87.72	86.21	86.97	0.76
60	88.5	86.96	87.73	0.77

**Table A.3.** Conversion data obtained for catalyst **4.59c**.

Time (minutes)	% conversion (Run 1)	% conversion (Run 2)	Average conversion	Error
3	17.51	17.99	17.75	0.24
5	24.1	23.64	23.87	0.23
6	27.32	26.53	26.93	0.4
7	30.58	29.85	30.22	0.37
8	33.11	33	33.06	0.06
9	36.36	36.1	36.23	0.13
10	39.37	38.02	38.7	0.68
12	44.05	43.48	43.77	0.29
13	46.95	46.08	46.52	0.44
14	49.26	48.54	48.9	0.36
15	51.28	50.76	51.02	0.26
17	55.87	54.05	54.96	0.91
19	59.17	58.14	58.66	0.52
20	60.98	60.24	60.61	0.37
22	63.69	63.69	63.69	0
24	66.67	67.11	66.89	0.22
26	68.97	68.97	68.97	0
28	70.92	71.94	71.43	0.51
30	74.07	74.07	74.07	0
33	75.76	76.92	76.34	0.58
36	78.74	78.74	78.74	0
39	81.3	80.65	80.98	0.33
42	82.64	82.64	82.64	0
45	84.03	84.75	84.39	0.36
50	85.47	86.96	86.22	0.74
55	88.5	88.5	88.5	0
60	90.09	90.09	90.09	0

The  $t_{1/2}$  values were calculated by choosing the two data points that 50 % conversion lay in between (these are highlighted in yellow in Tables **A.1** and **A.2** above). These two data points were plotted for each catalyst and the linear regression line was used to calculate the  $t_{1/2}$  value (see Figures **A.1** and **A.2** below). While this method of calculation assumes a linear correlation between conversion and time over the indicated time range, it is a good approximation for the  $t_{1/2}$  value.

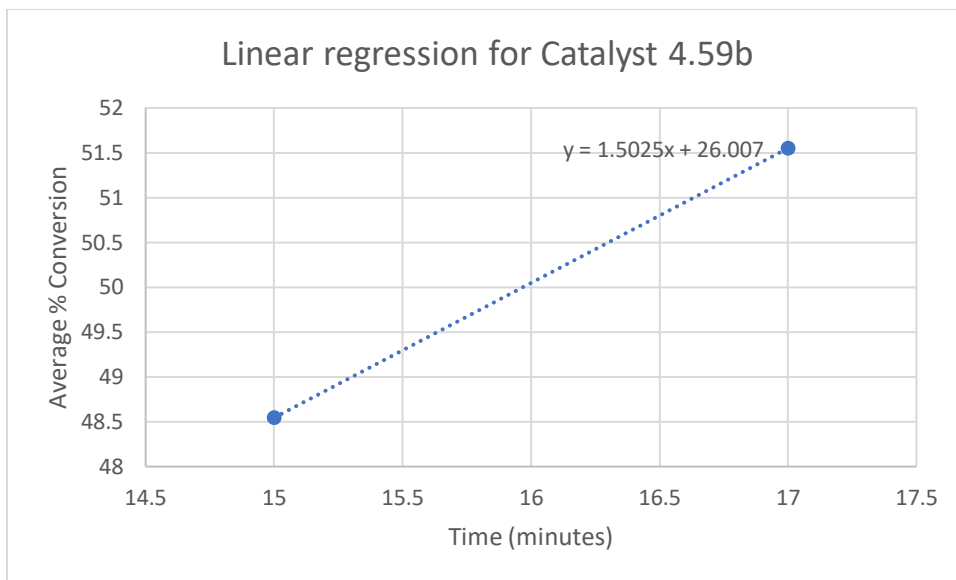


**Figure A.1.** Linear regression for Catalyst **4.59b**.

Thus, when  $y = 50\%$  conversion,  $x = 16$  minutes.

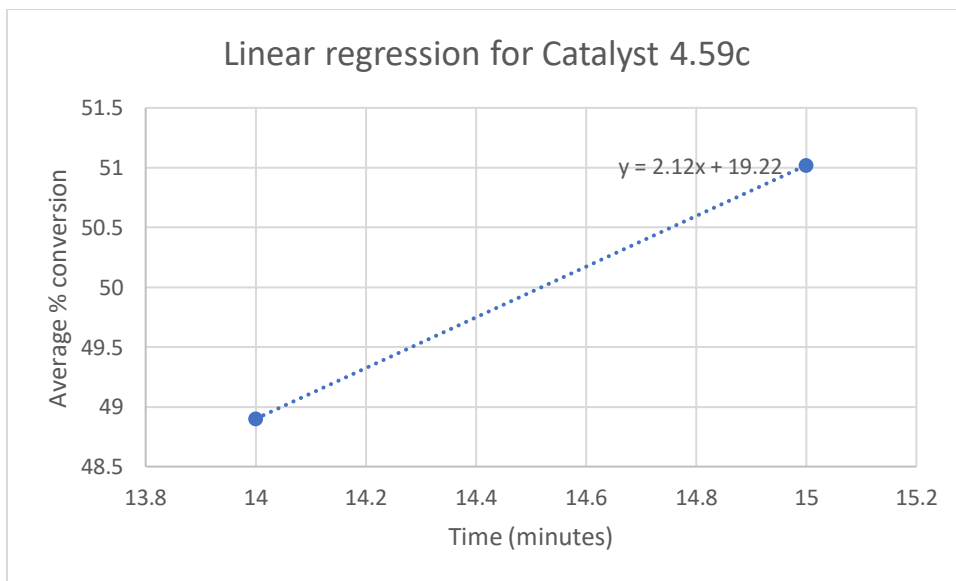


**Figure A.2.** Linear regression for catalyst **4.59c**.

Thus, when  $y = 50\%$  conversion,  $x = 14.5$  minutes.

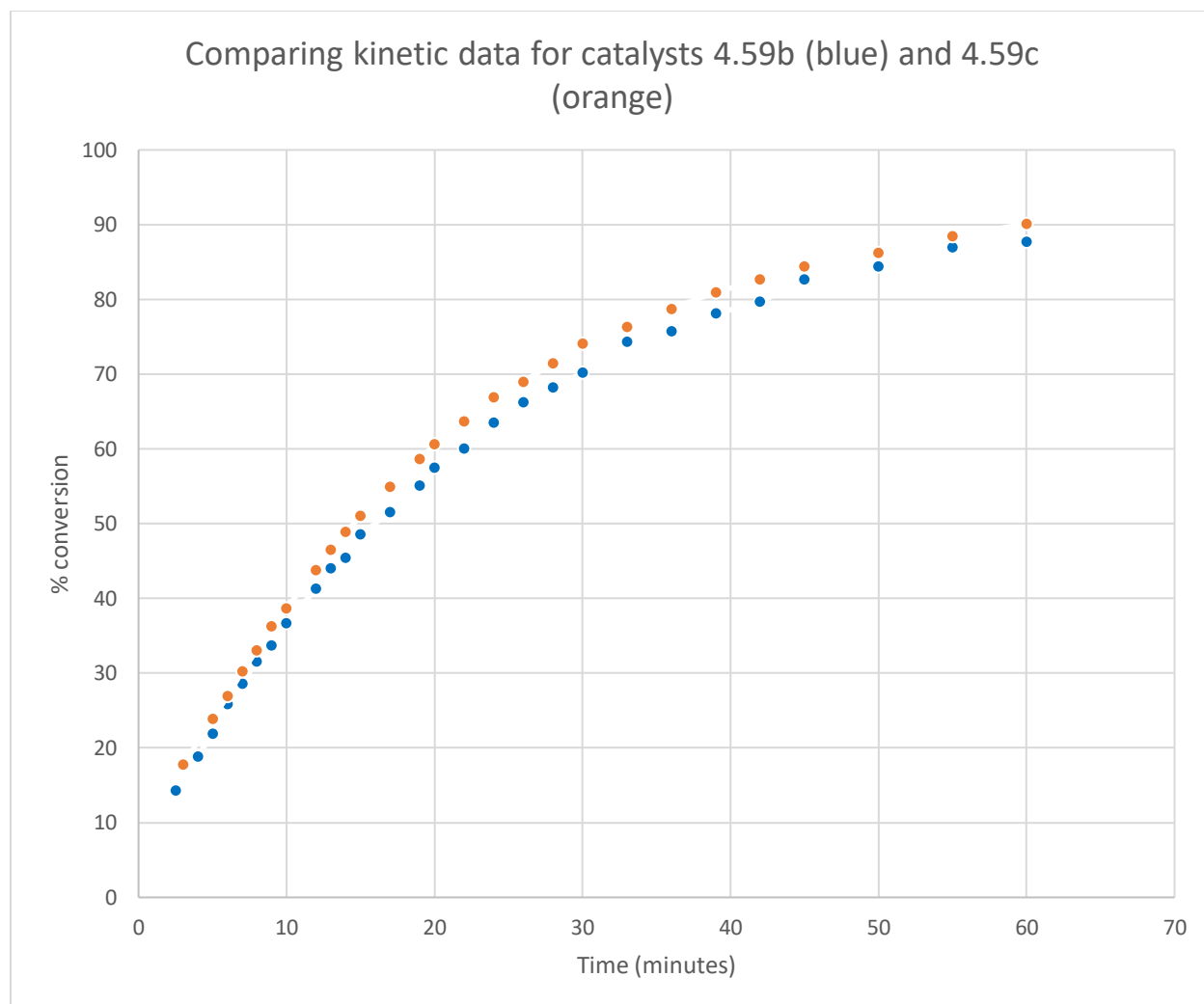


**Figure A.3.** Comparing the kinetics between catalysts 4.59b and 4.59c.



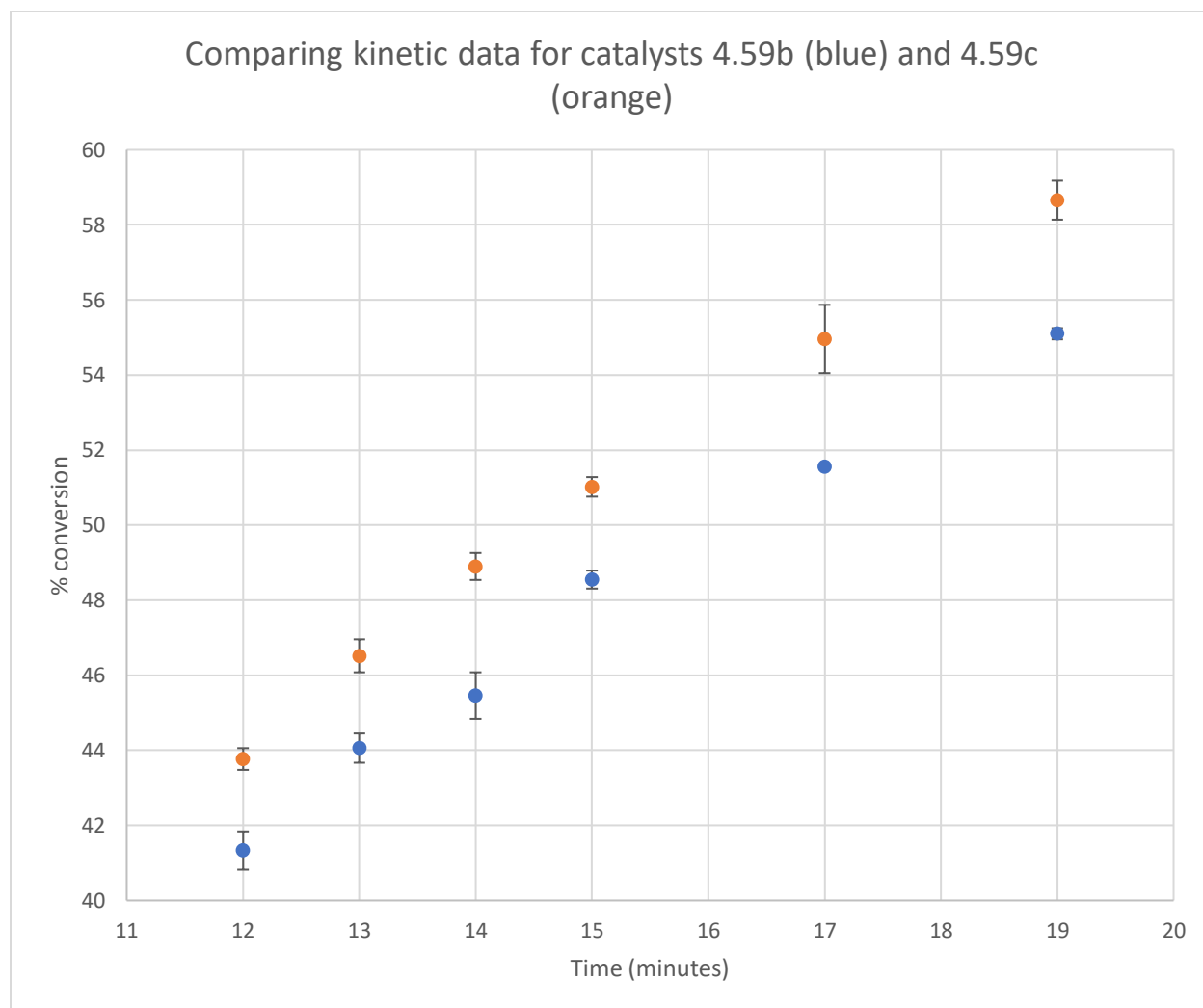
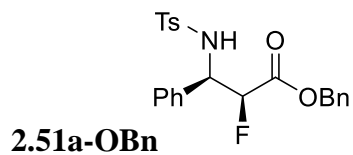
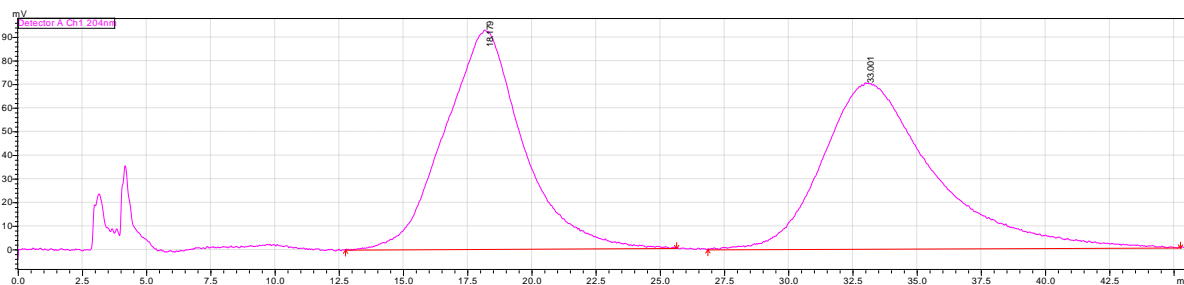


**Figure A.4.** Zoomed in graph with error bars.

## A.3 HPLC chromatograms

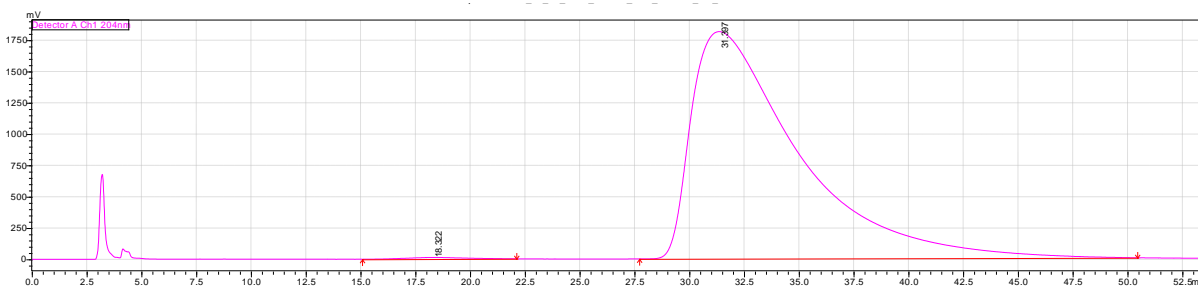


Reaction with catalyst DHPB **2.48a**



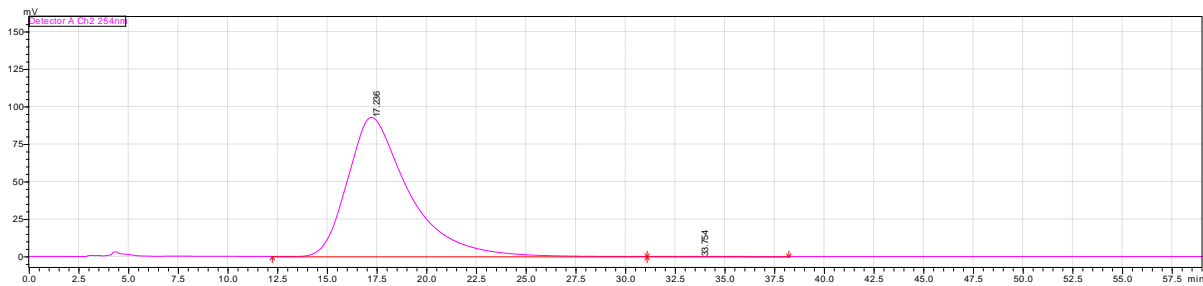
Peak#	Ret. Time	Area	Height	Area%
1	18.179	19537258	92719	48.091
2	33.001	21088265	70320	51.909
Total		40625523	163039	100

Reaction with catalyst **2.30** (Table 2.2, entry 1)



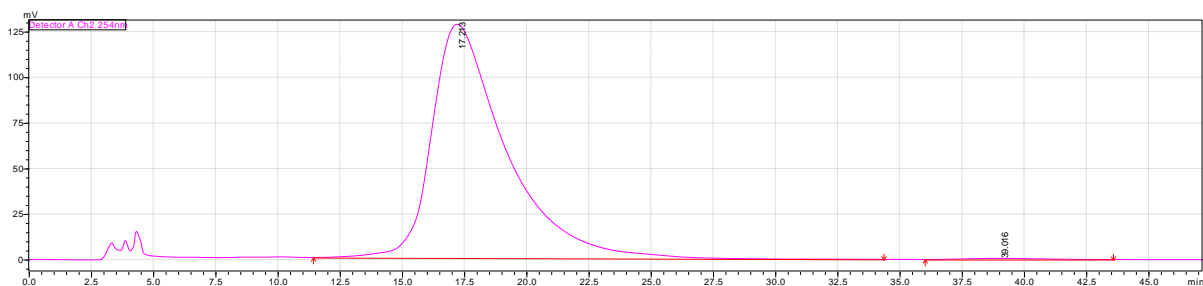
Peak#	Ret. Time	Area	Height	Area%
1	18.322	2612016	13432	0.421
2	31.397	6.17E+08	1814444	99.579
Total		6.2E+08	1827876	100

Reaction with catalyst **2.31c** (Table 2.2, entry 2)



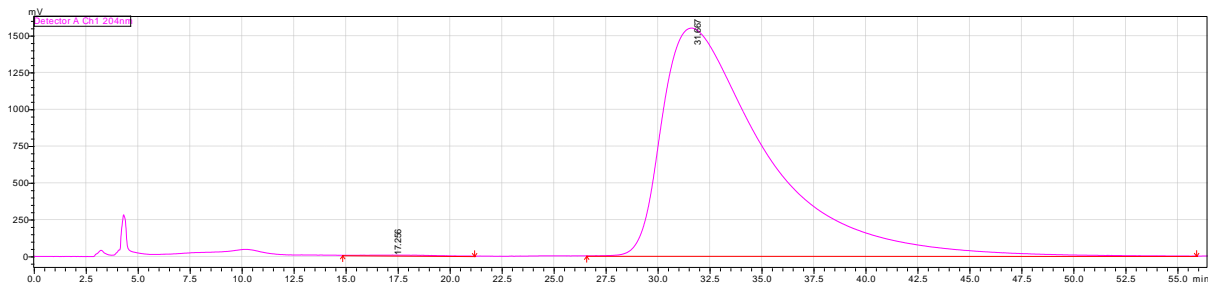
Peak#	Ret. Time	Area	Height	Area%
1	17.236	19736273	92725	99.984
2	33.754	3238	37	0.016
Total		19739510	92762	100

Reaction with catalyst **2.31a** (Table 2.2, entry 3)



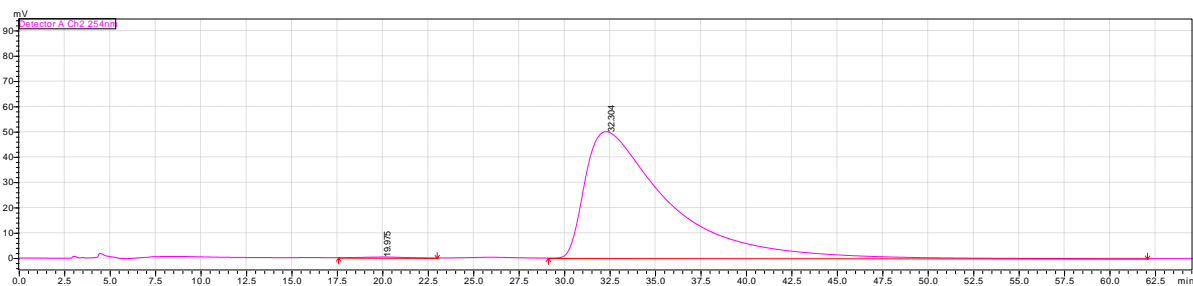
Peak#	Ret. Time	Area	Height	Area%
1	17.213	26542867	128138	99.492
2	39.016	135629	647	0.508
Total		26678497	128785	100

Reaction with **2.31b** (Table 2.2, entry 4)



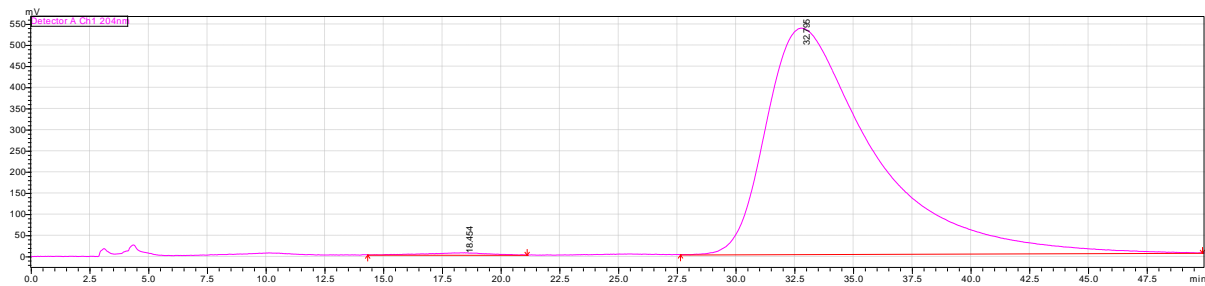
Peak#	Ret. Time	Area	Height	Area%
1	17.256	674012	3549	0.126
2	31.667	5.34E+08	1548451	99.874
Total		5.34E+08	1552000	100

Reaction with **2.31b** (Table 2.2, entry 8)



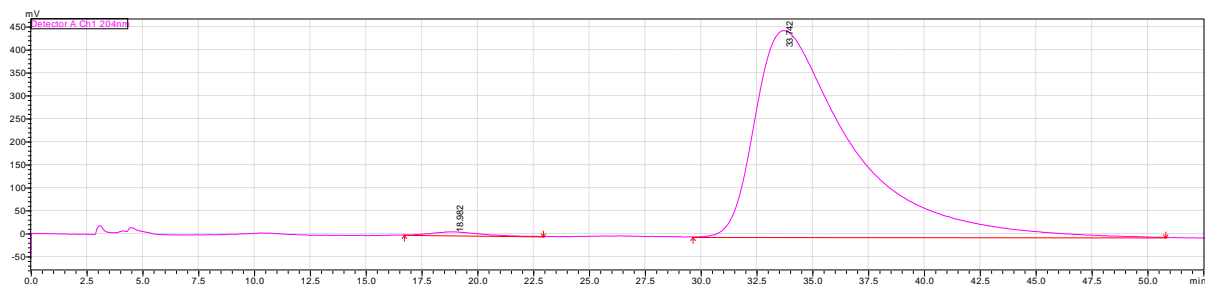
Peak#	Ret. Time	Area	Height	Area%
1	19.975	46286	320	0.291
2	32.304	15851440	49999	99.709
Total		15897726	50319	100

Reaction with catalyst **2.31b** (Table 2.2, entry 9)

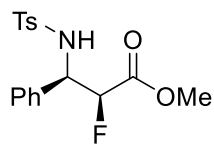


Peak#	Ret. Time	Area	Height	Area%
1	18.454	761260	4980	0.447
2	32.795	1.69E+08	534832	99.553
Total		1.7E+08	539811	100

Reaction with catalyst **2.31b** (Table 2.2, entry 10)

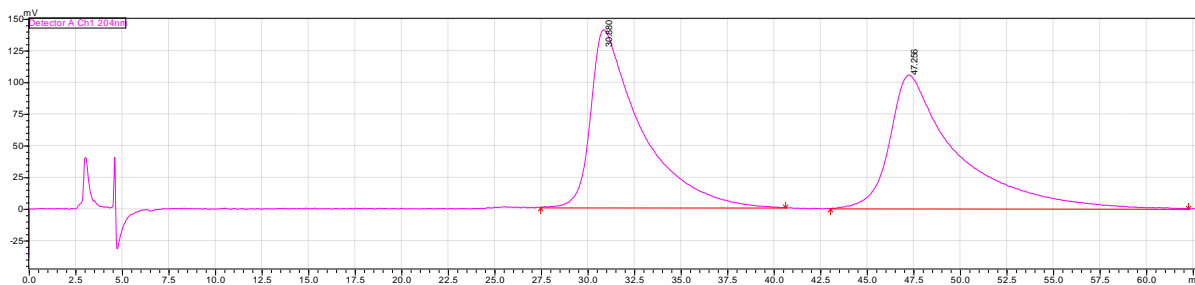


Peak#	Ret. Time	Area	Height	Area%
1	18.982	1062185	7898	0.785
2	33.742	1.34E+08	449095	99.215
Total		1.35E+08	456993	100

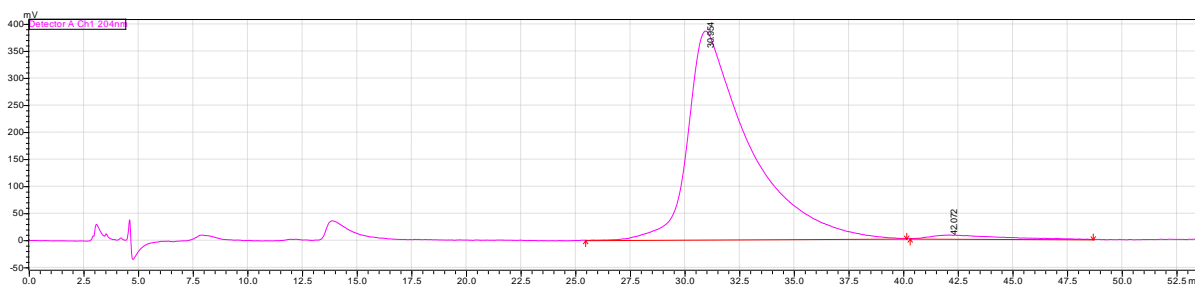


2.51a-OMe

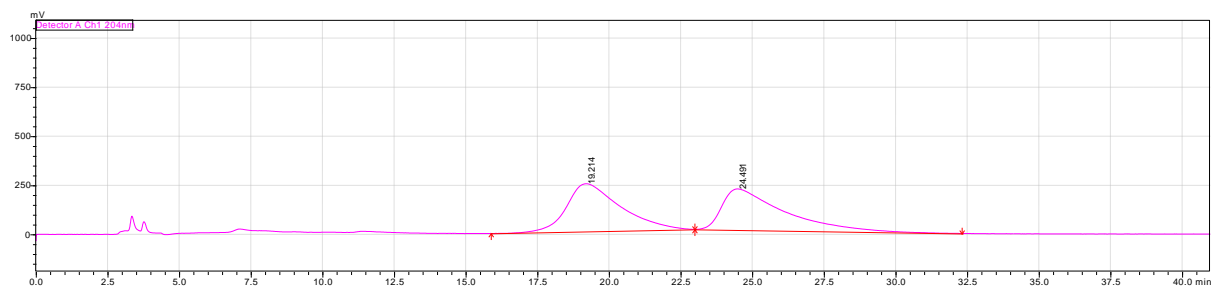
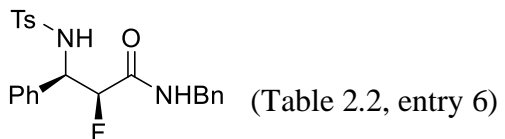
(Table 2.2, entry 5)



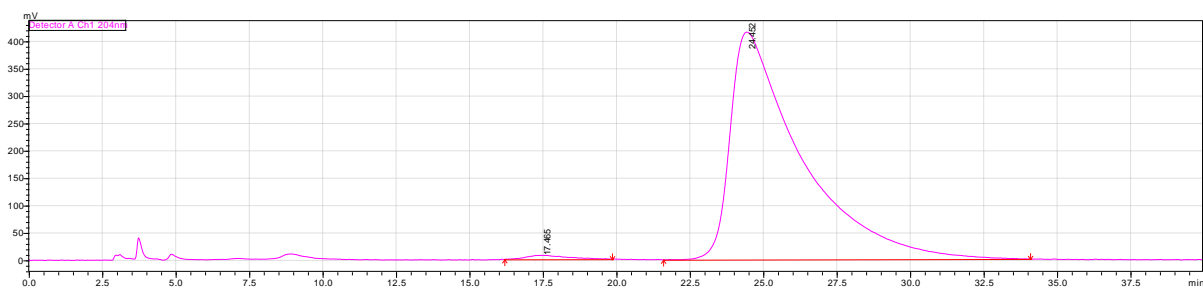
Peak#	Ret. Time	Area	Height	Area%
1	30.88	26157539	140162	49.663
2	47.256	26512154	105498	50.337
Total		52669692	245660	100



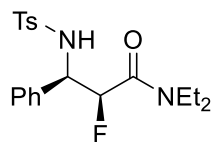
Peak#	Ret. Time	Area	Height	Area%
1	30.954	74565606	385418	98.08
2	42.072	1460035	6972	1.92
Total		76025642	392390	100

**2.51a-NHBn**

Peak#	Ret. Time	Area	Height	Area%
1	19.214	31812120	243133	50.298
2	24.491	31434603	209289	49.702
Total		63246723	452422	100

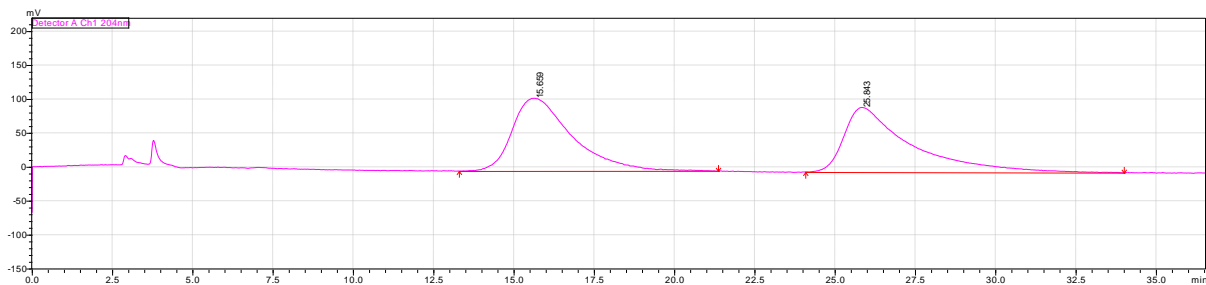


Peak#	Ret. Time	Area	Height	Area%
1	17.465	729624	7430	1.039
2	24.452	69524581	415400	98.961
Total		70254206	422831	100

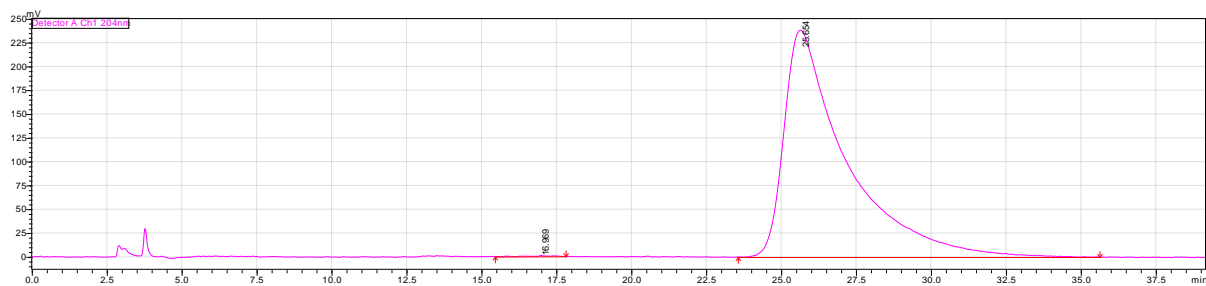


**2.51a-NEt<sub>2</sub>**

(Table 2.2, entry 7)



Peak#	Ret. Time	Area	Height	Area%
1	15.659	13829271	107060	50.267
2	25.843	13682126	95236	49.733
Total		27511397	202297	100



Peak#	Ret. Time	Area	Height	Area%
1	16.969	31575	1000	0.092
2	25.654	34191197	238384	99.908
Total		34222772	239384	100



2.51b-OBn

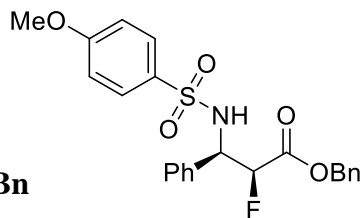
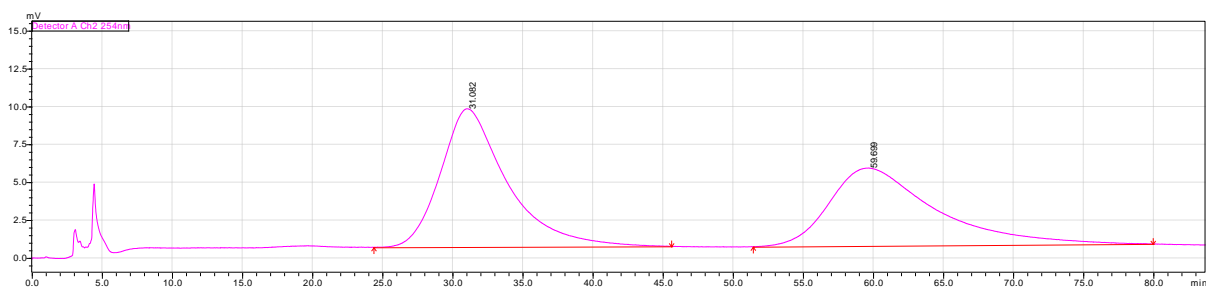
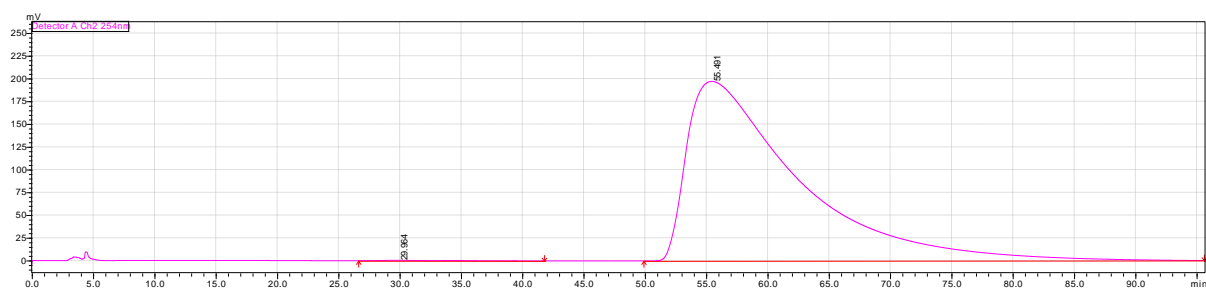


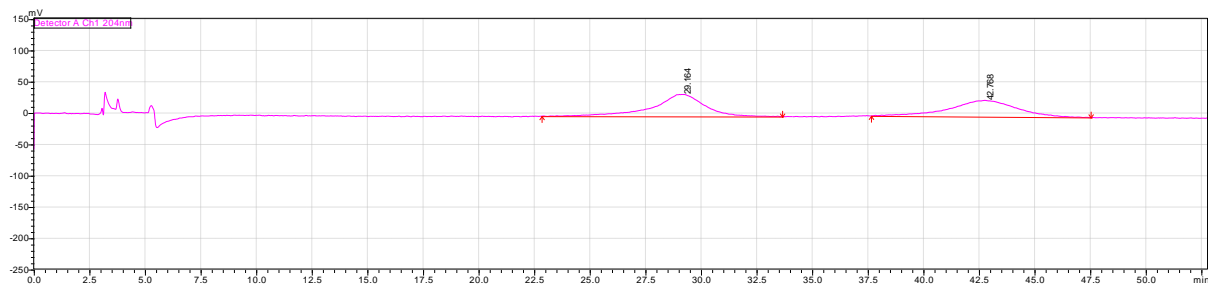
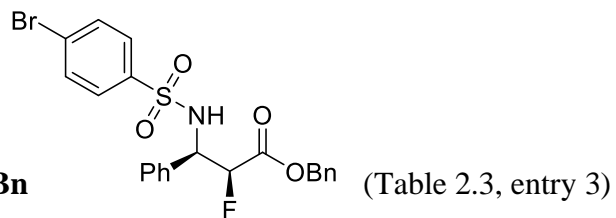
(Table 2.3, entry 2)



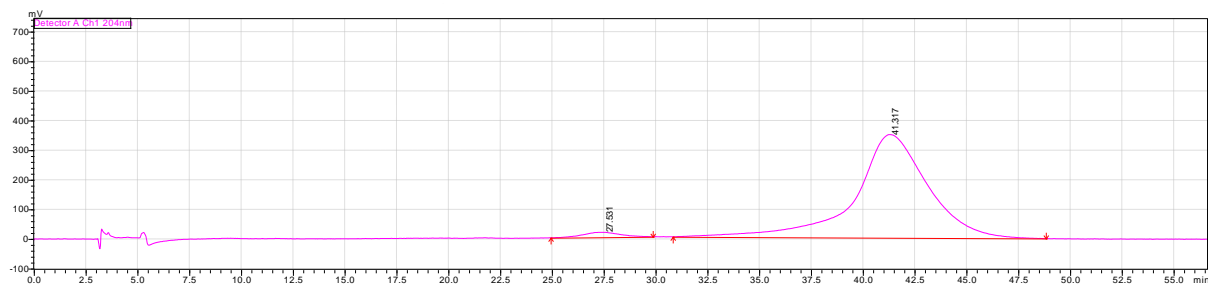
Peak#	Ret. Time	Area	Height	Area%
1	31.082	3016518	9133	52.819
2	59.699	2694544	5144	47.181
Total		5711062	14277	100



Peak#	Ret. Time	Area	Height	Area%
1	29.964	170756	434	0.138
2	55.491	123742048	197289	99.862
Total		123912805	197724	100

**2.51c-OBn**

Peak#	Ret. Time	Area	Height	Area%
1	29.164	5659186	35122	50.824
2	42.768	5475722	26161	49.176
Total		11134908	61283	100



Peak#	Ret. Time	Area	Height	Area%
1	27.531	2081685	16799	2.396
2	41.317	84809008	348442	97.604
Total		86890693	365241	100

2.51d-OBn

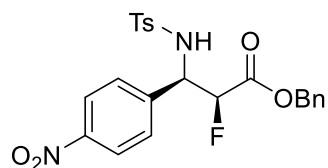
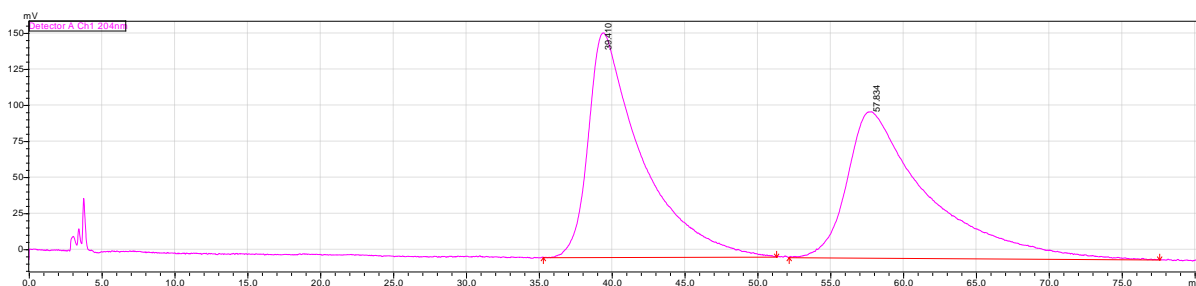
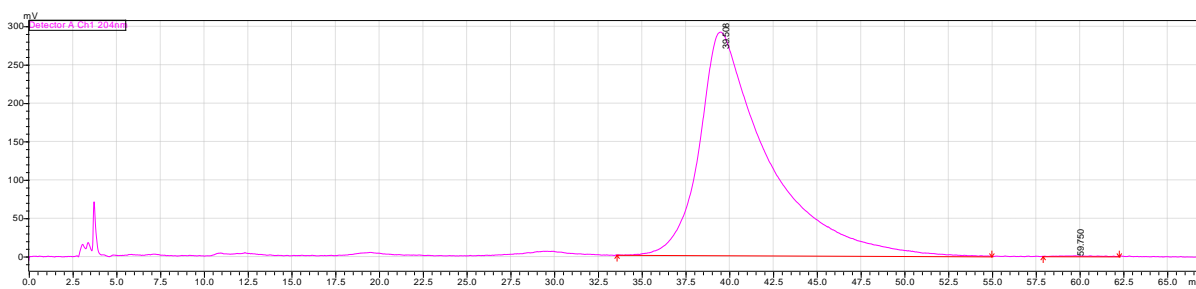


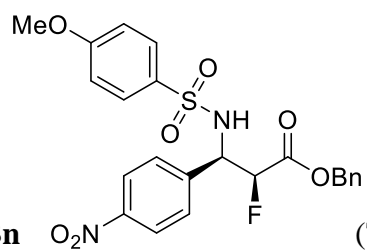
(Table 2.3, entry 5)



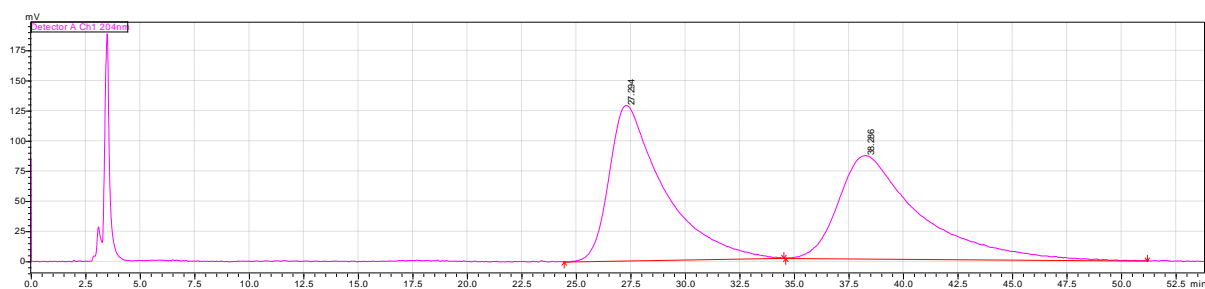
Peak#	Ret. Time	Area	Height	Area%
1	39.41	39273261	155484	50.357
2	57.834	38716174	101280	49.643
Total		77989435	256765	100



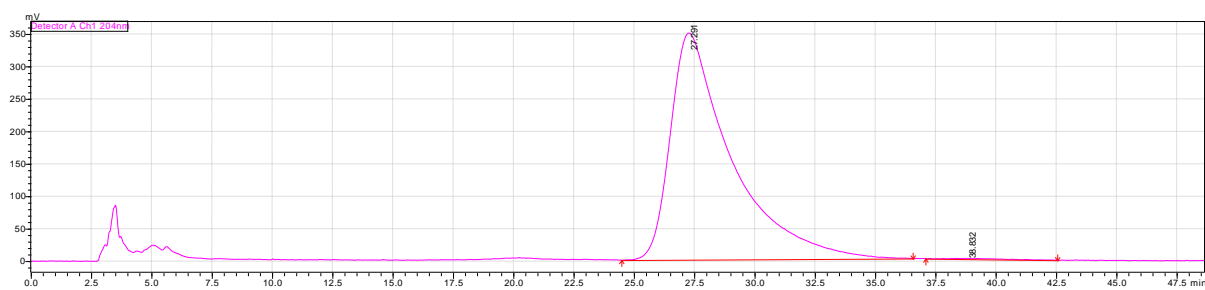
Peak#	Ret. Time	Area	Height	Area%
1	39.508	78564203	290755	99.931
2	59.75	54302	765	0.069
Total		78618505	291520	100



**2.51e-OBn** (Table 2.3, entry 6)

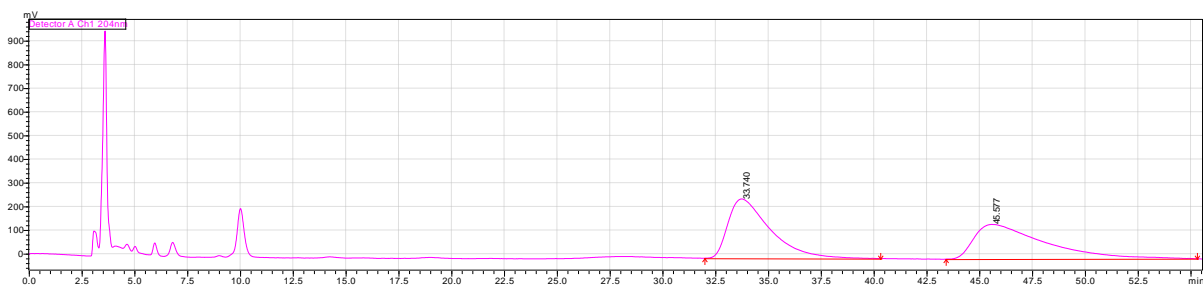
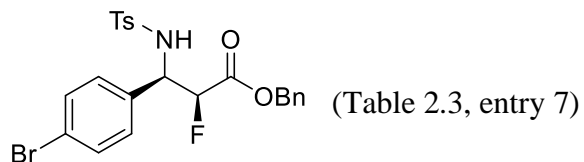


Peak#	Ret. Time	Area	Height	Area%
1	27.294	22301803	128520	50.603
2	38.286	21770214	85582	49.397
Total		44072017	214102	100

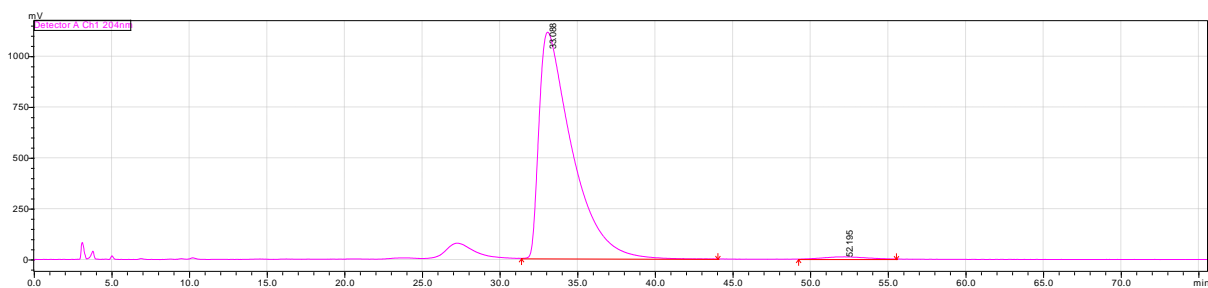


Peak#	Ret. Time	Area	Height	Area%
1	27.291	61274147	349427	99.741
2	38.832	158929	1259	0.259
Total		61433076	350686	100

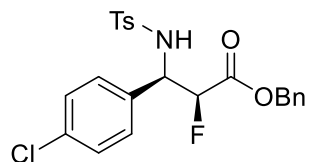
2.51f-OBn



Peak#	Ret. Time	Area	Height	Area%
1	33.74	34854387	251141	50.771
2	45.577	33796160	146151	49.229
Total		68650547	397291	100

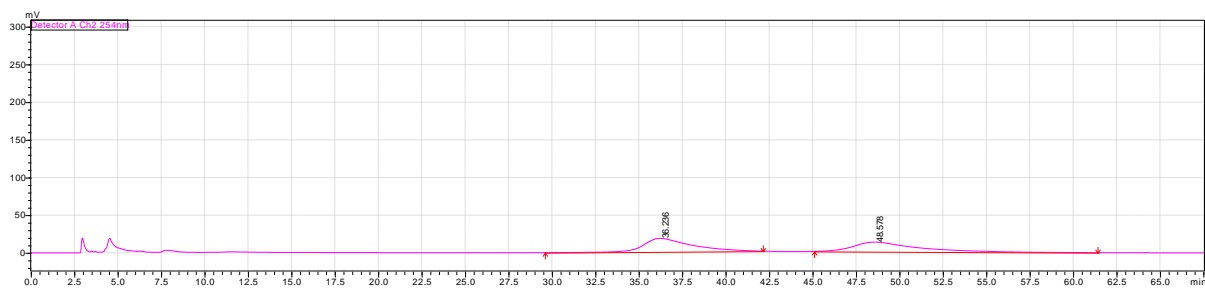


Peak#	Ret. Time	Area	Height	Area%
1	33.088	163089305	1112407	98.782
2	52.195	2010888	11085	1.218
Total		165100193	1123492	100

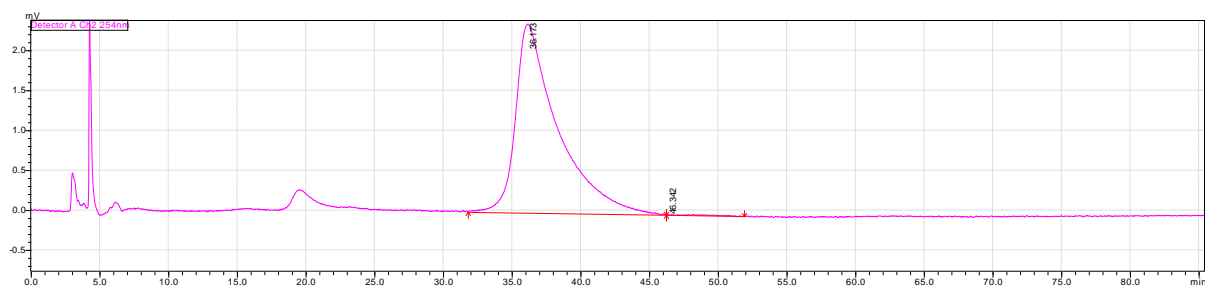


2.51g-OBn

(Table 2.3, entry 8)

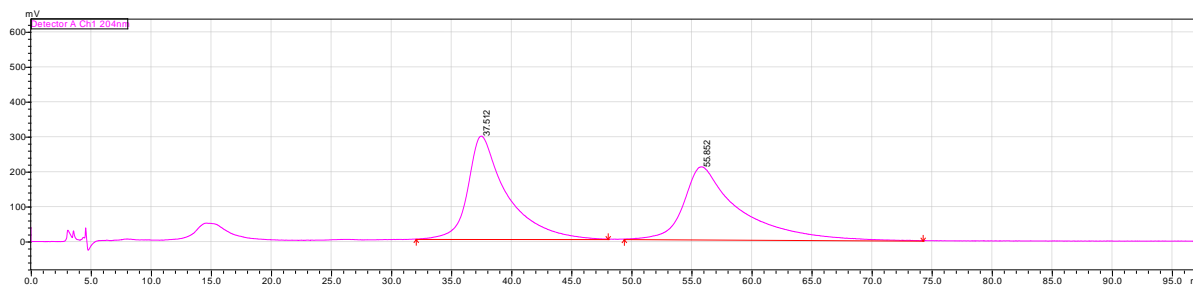
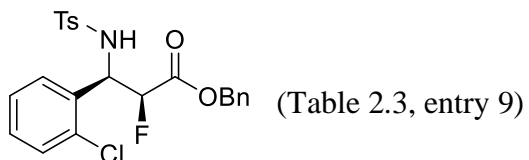


Peak#	Ret. Time	Area	Height	Area%
1	36.236	3434379	17936	51.738
2	48.578	3203646	12628	48.262
Total		6638025	30564	100

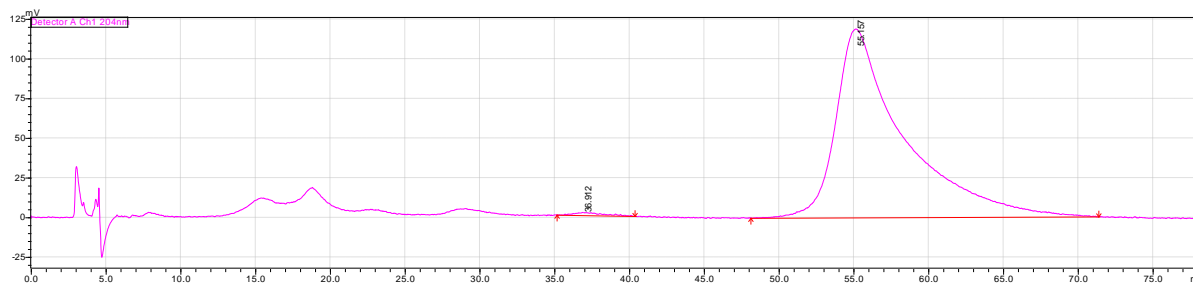


Peak#	Ret. Time	Area	Height	Area%
1	36.173	504467	2364	99.976
2	46.342	123	8	0.024
Total		504590	2372	100

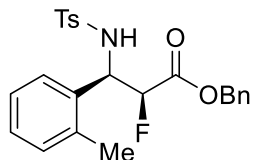
2.51h-OBn



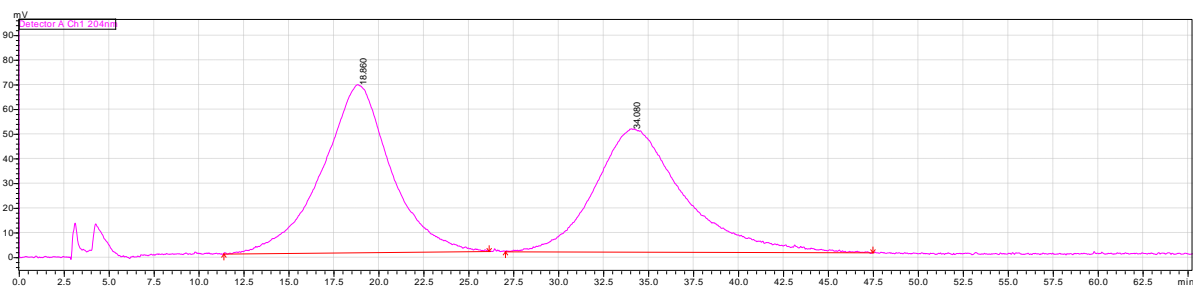
Peak#	Ret. Time	Area	Height	Area%
1	37.512	65972760	294434	49.883
2	55.852	66281978	207923	50.117
Total		132254738	502357	100



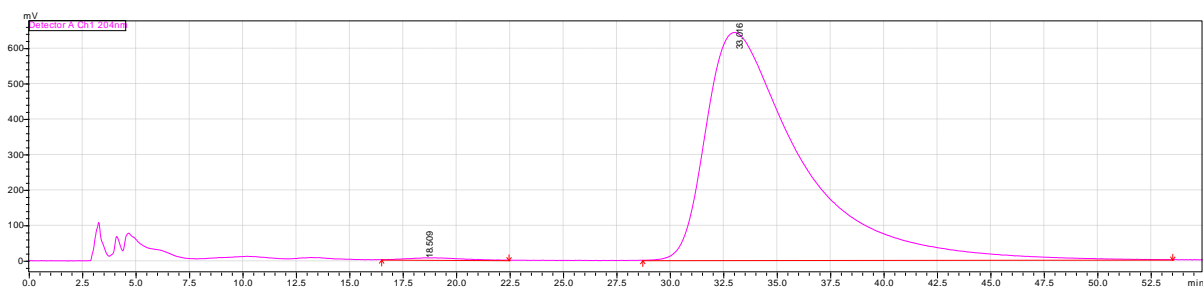
Peak#	Ret. Time	Area	Height	Area%
1	36.912	218936	1778	0.583
2	55.157	37359961	118785	99.417
Total		37578897	120563	100

**2.51i-OBn**

(Table 2.3, entry 10)



Peak#	Ret. Time	Area	Height	Area%
1	18.86	17982890	67960	51.353
2	34.08	17035283	49787	48.647
Total		35018173	117747	100



Peak#	Ret. Time	Area	Height	Area%
1	18.509	956430	5868	0.483
2	33.016	197062356	642349	99.517
Total		198018786	648216	100



2.51j-OBn

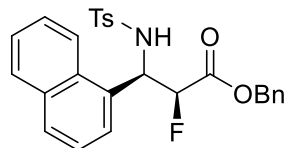
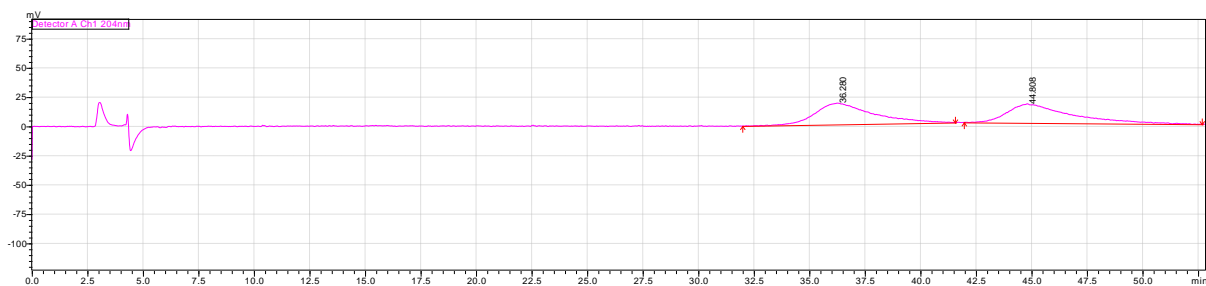
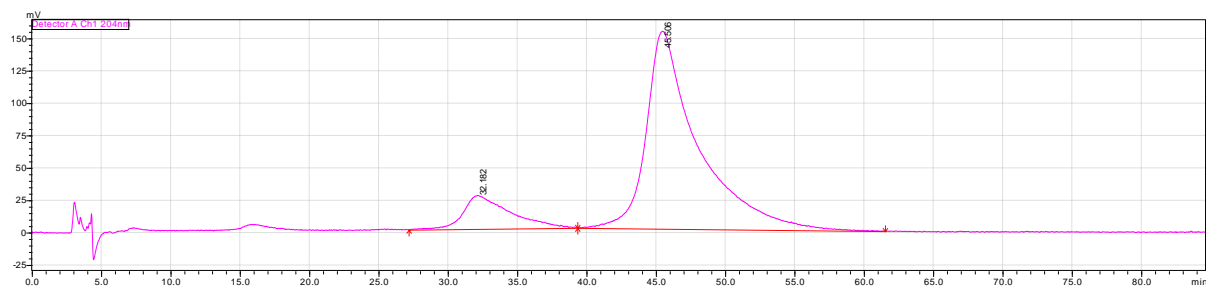


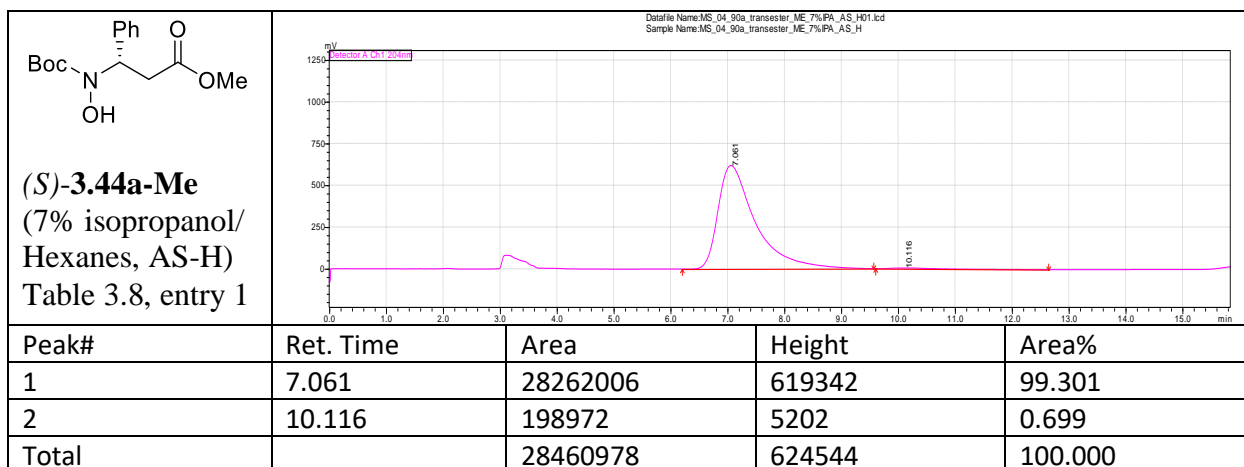
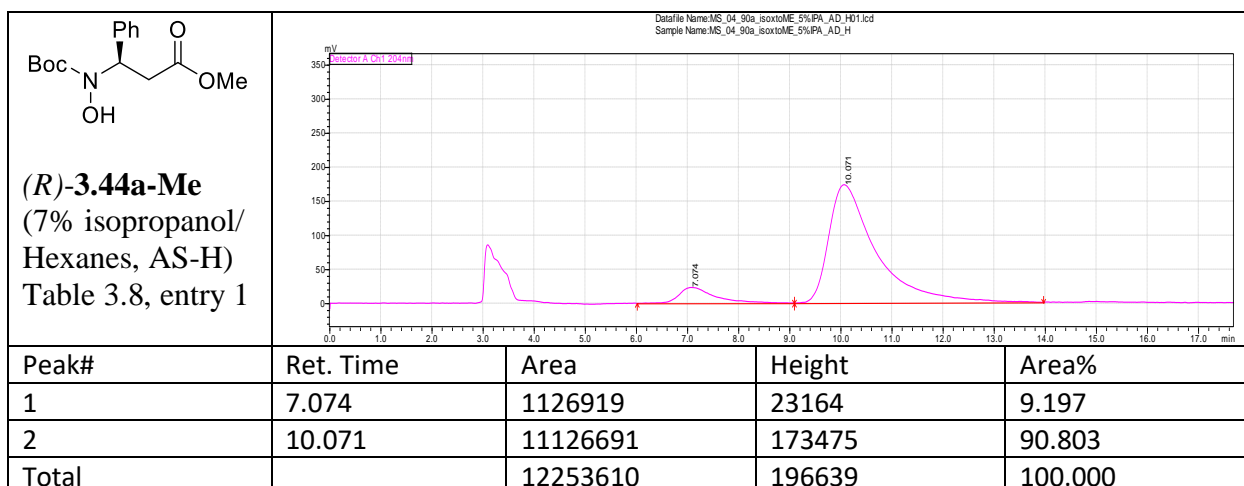
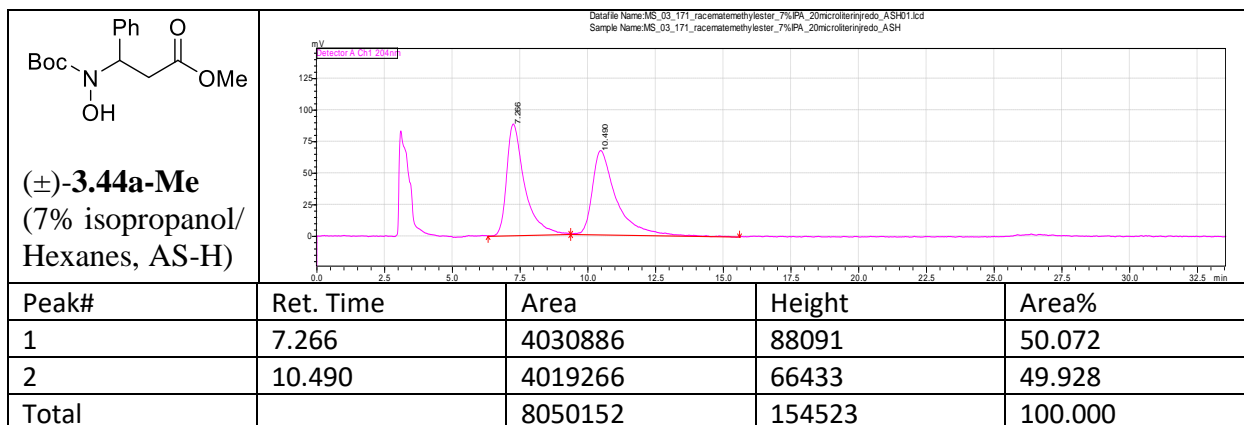
(Table 2.3, entry 11)

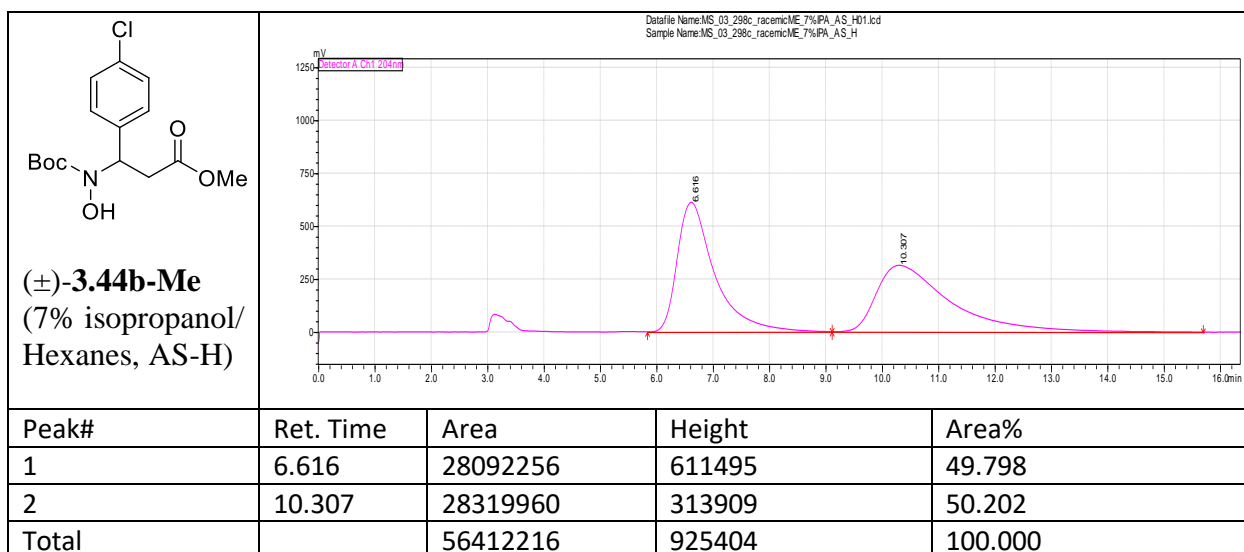
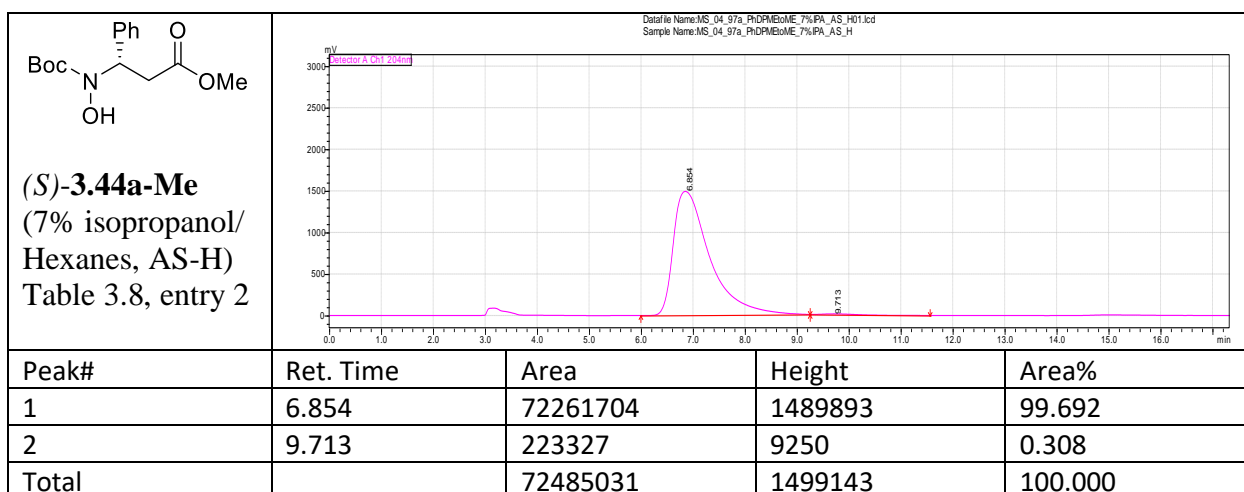
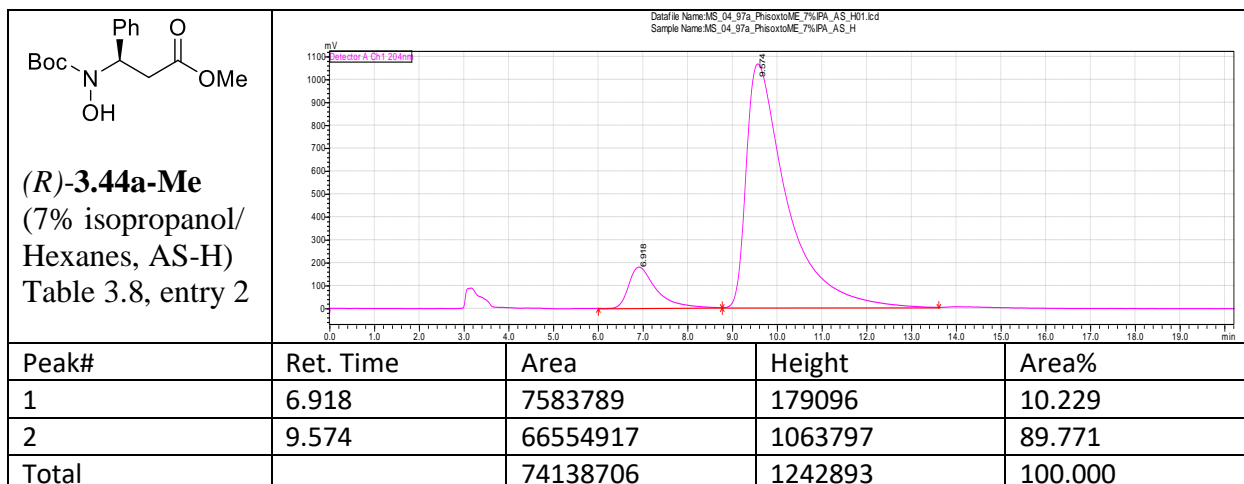


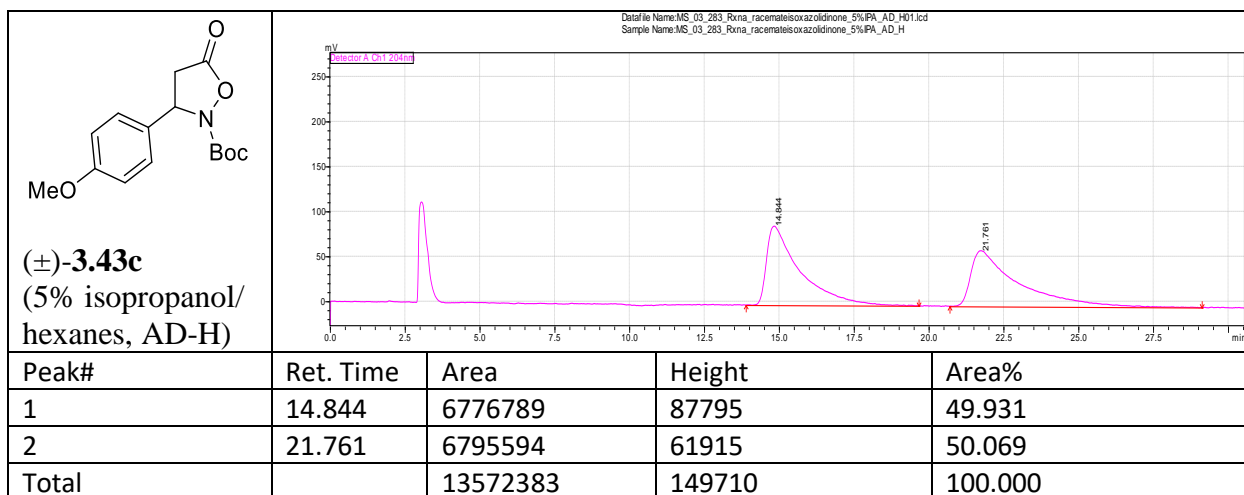
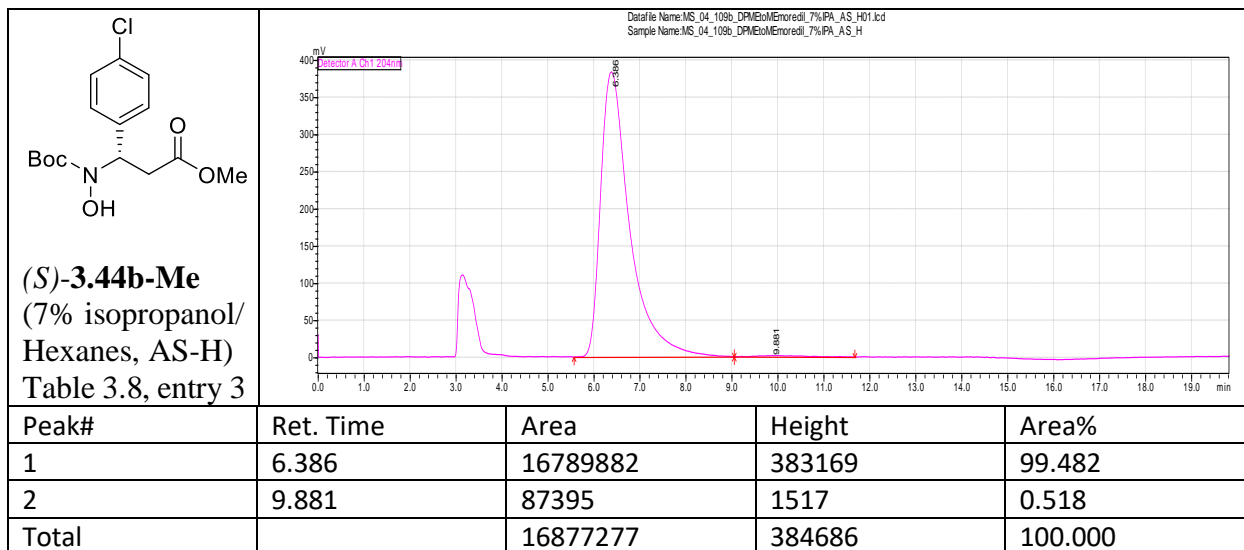
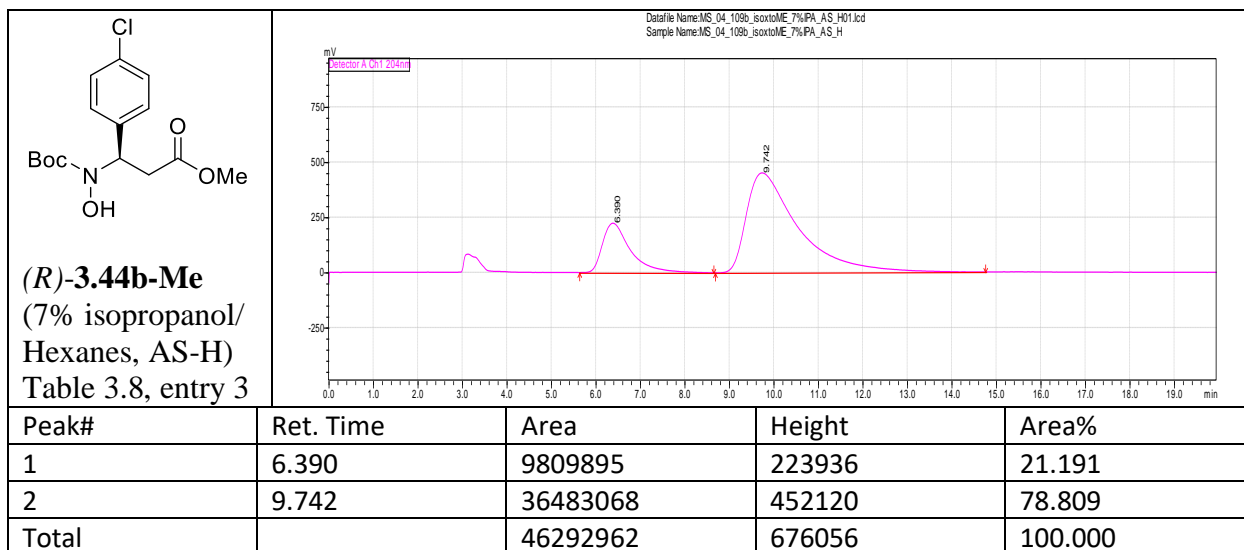
Peak#	Ret. Time	Area	Height	Area%
1	36.28	3288433	18181	50.718
2	44.808	3195369	16393	49.282
Total		6483802	34574	100

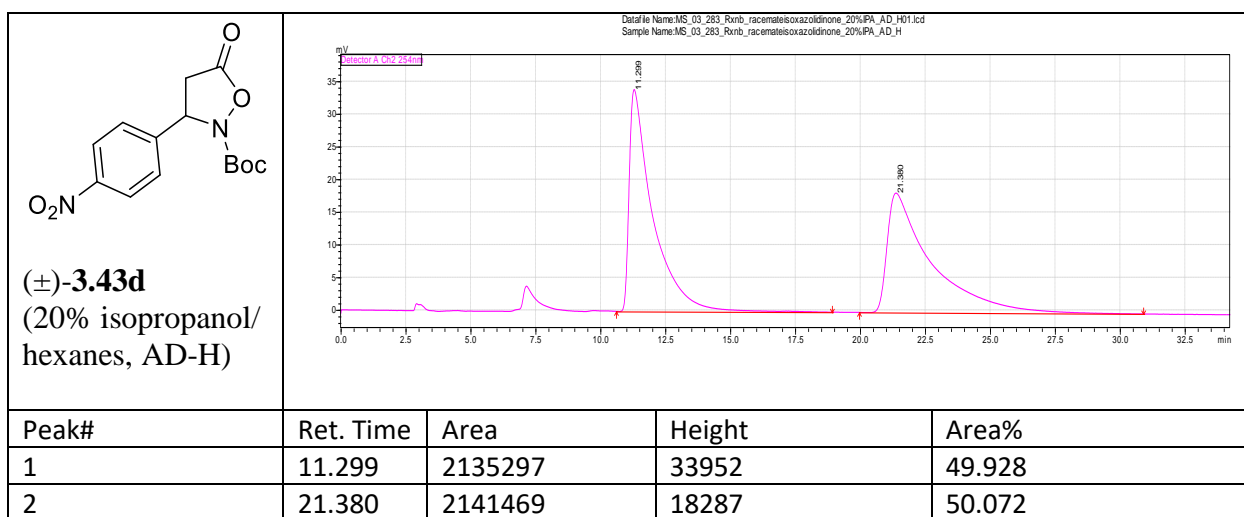
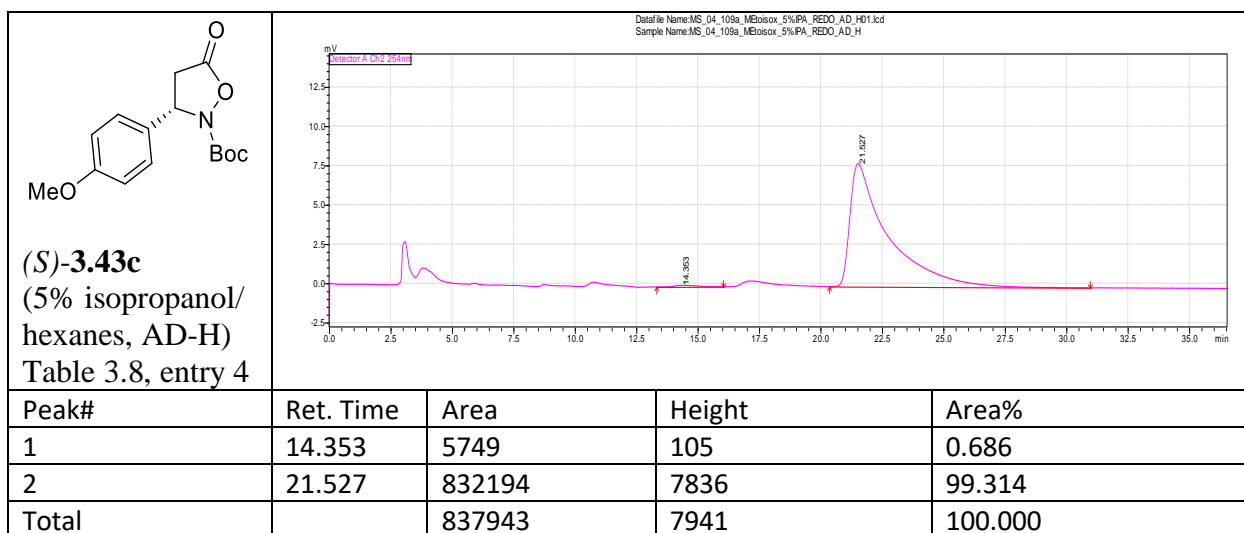
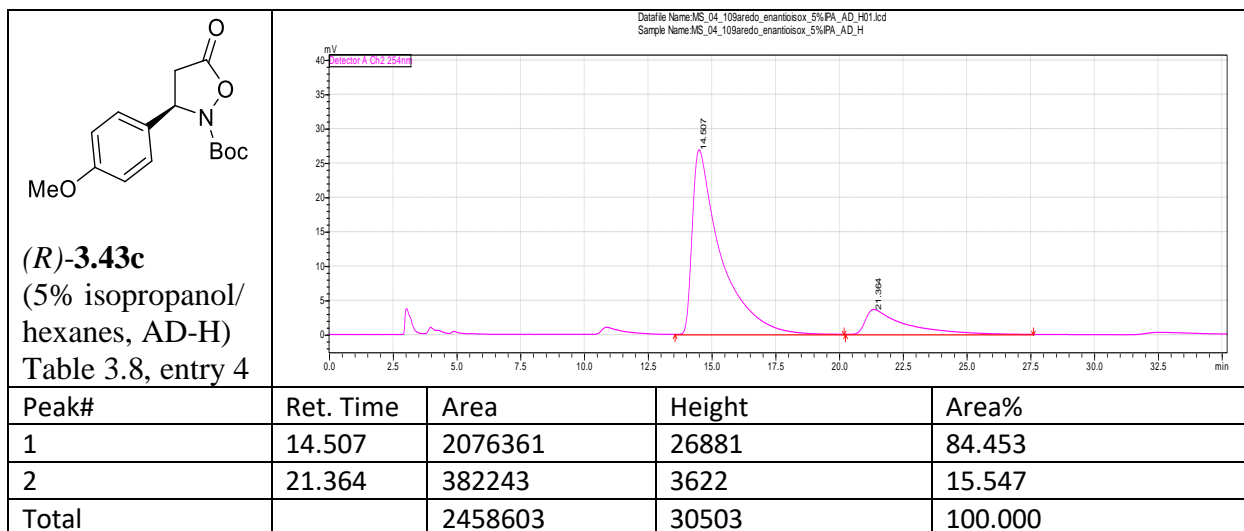


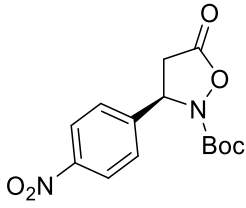
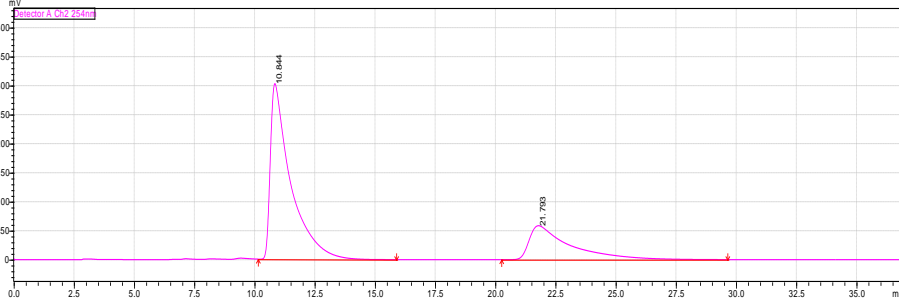
Peak#	Ret. Time	Area	Height	Area%
1	32.182	6053014	25834	13.259
2	45.506	39599267	152520	86.741
Total		45652281	178354	100

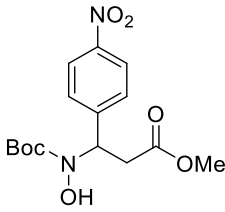
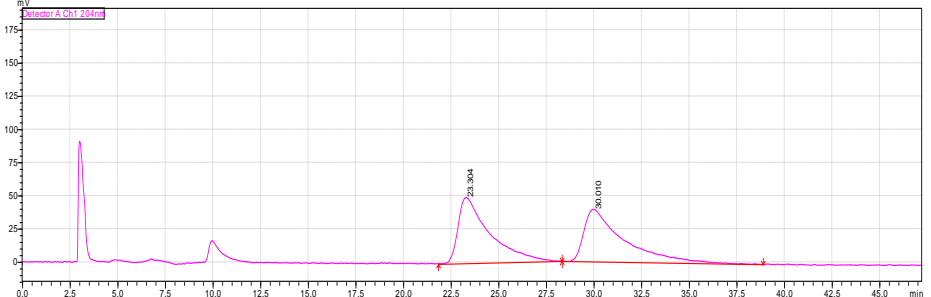


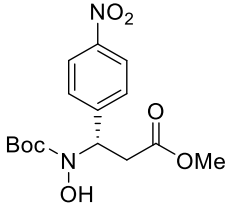
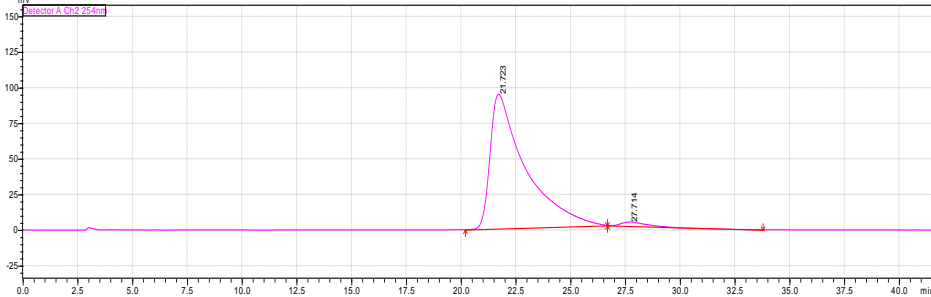


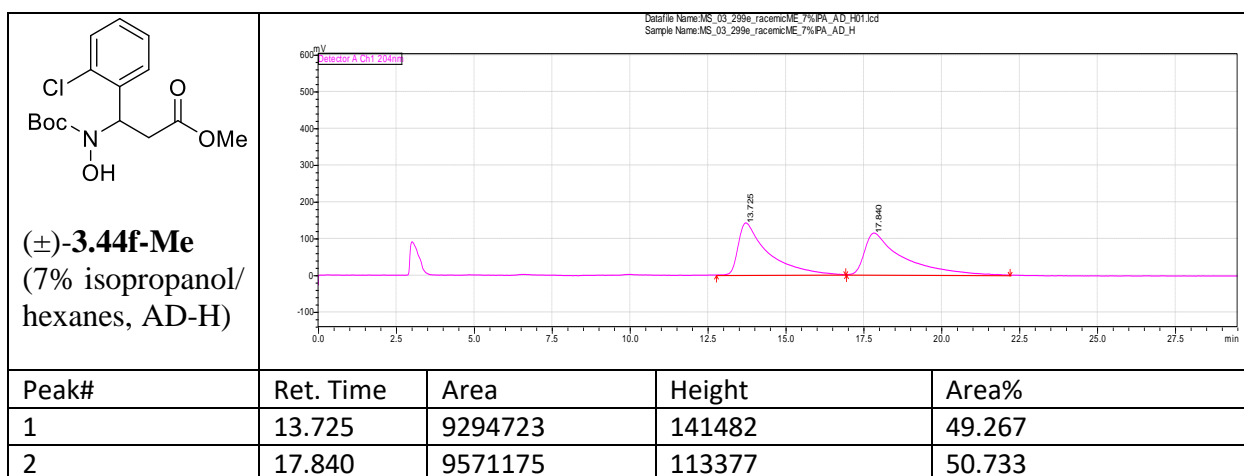
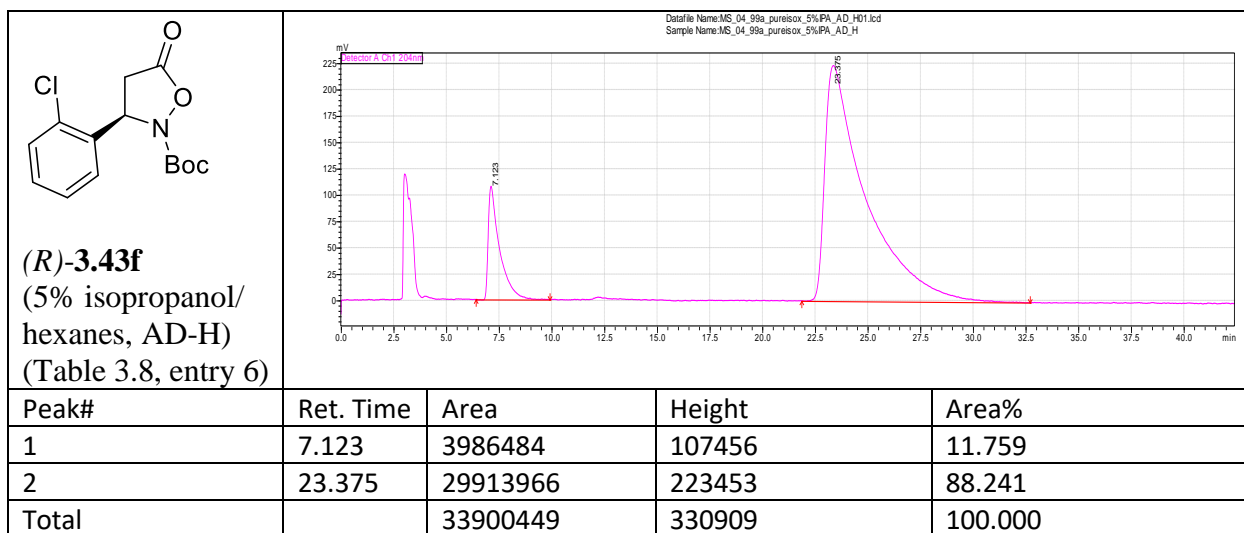
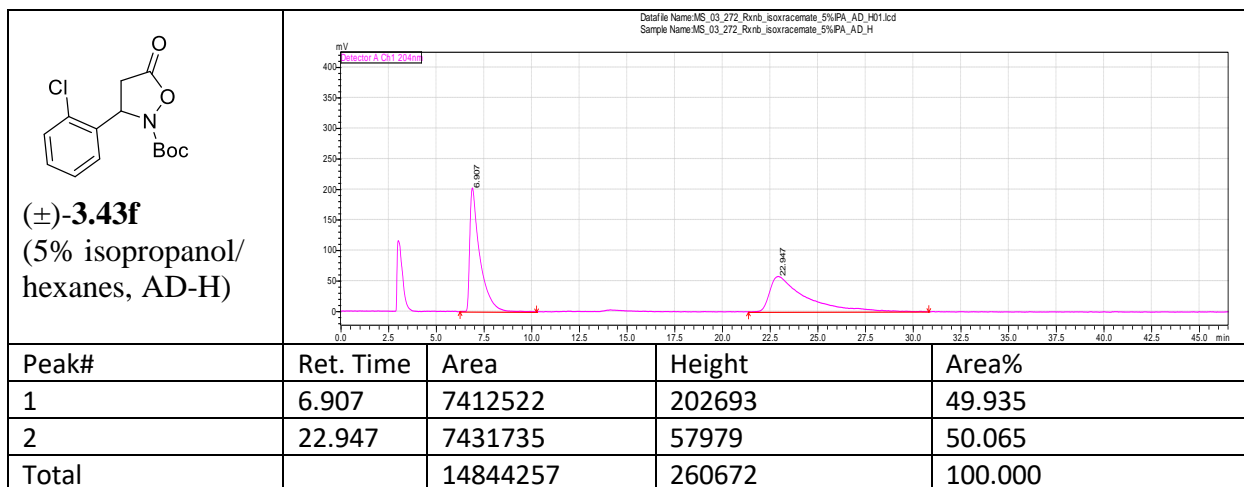




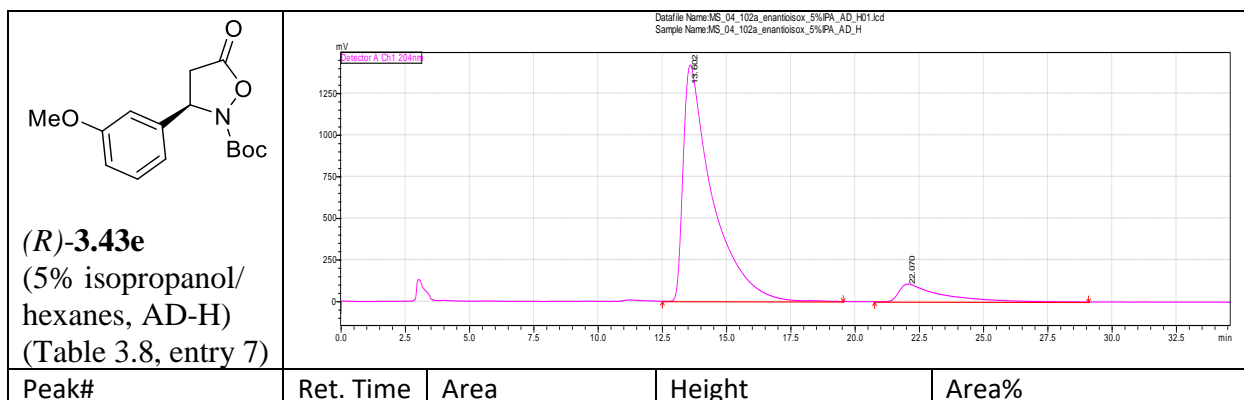
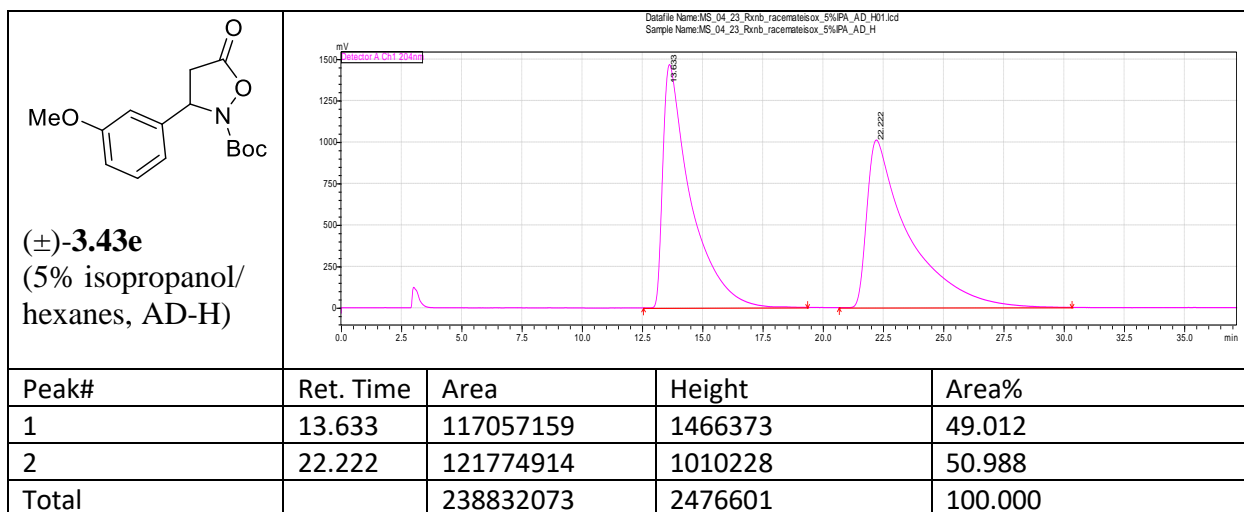
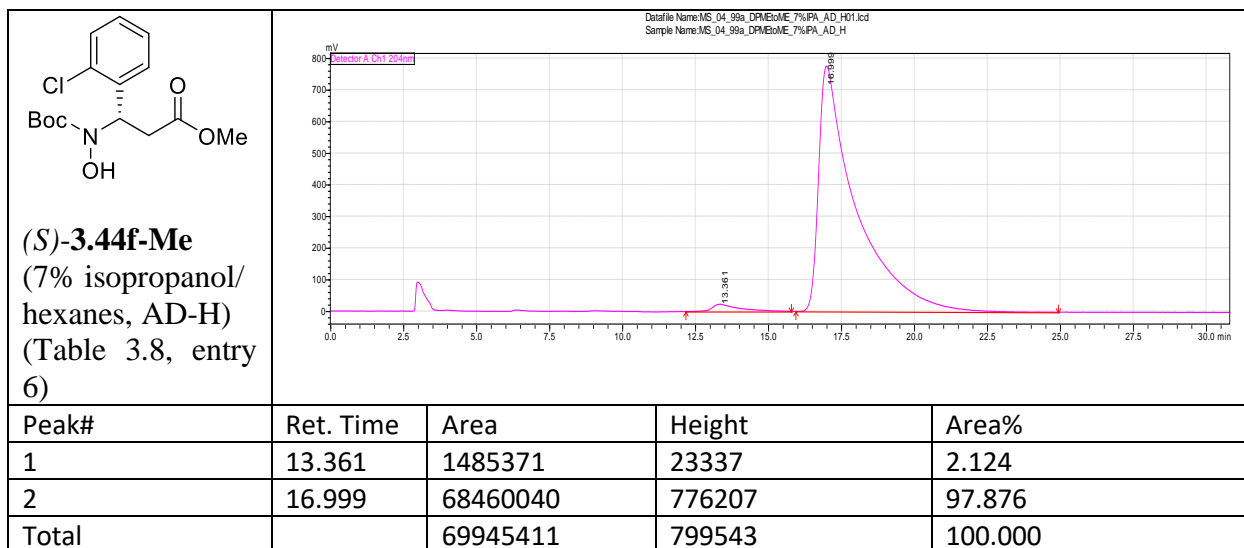
Total		4276766	52239	100.000
 <p><b>(R)-3.43d</b> (20% isopropanol/ hexanes, AD-H) Table 3.8, entry 5</p>	<p>Datefile Name: MS_04_114_enantioiox_20%IPA_AD_H01.lcd Sample Name: MS_04_114_enantioiox_20%IPA_AD_H</p> 			
	Peak#	Ret. Time	Area	Height
1	10.844	17655179	302586	72.157
2	21.793	6812431	58481	27.843
Total		24467610	361067	100.000

 <p><b>(±)-3.44d-Me</b> (7% isopropanol/ Hexanes, AD-H)</p>	<p>Datefile Name: MS_03_299b_raceincME_7%IPA_AD_H01.lcd Sample Name: MS_03_299b_raceincME_7%IPA_AD_H</p> 			
	Peak#	Ret. Time	Area	Height
1	23.304	5643838	49543	50.278
2	30.010	5581386	39282	49.722
Total		11225223	88825	100.000

 <p><b>(S)-3.44d-Me</b> (7% isopropanol/ Hexanes, AD-H) Table 3.8, entry 5</p>	<p>Datefile Name: MS_04_114_enantioME_morecil_2_7%IPA_AD_H01.lcd Sample Name: MS_04_114_enantioME_morecil_2_7%IPA_AD_H</p> 			
	Peak#	Ret. Time	Area	Height
1	21.723	10513496	94361	98.794
2	27.714	128372	2860	1.206
Total		10641868	97221	100.000



Total		18865898	254859	100.000
-------	--	----------	--------	---------





1	13.602	111060525	1418886	90.425
2	22.070	11759777	106293	9.575
Total		122820302	1525179	100.000

COC(=O)CC(O)N(C1=CC=C(OC)C=C1)C(=O)OC(C)C

**(±)-3.44e-Me**  
(7% isopropanol/  
hexanes, AS-H)

Datafile Name: MS\_04\_23Rrnb\_ME\_7%PA\_AS\_H01.lcd  
Sample Name: MS\_04\_23Rrnb\_ME\_7%PA\_AS\_H

Chromatogram showing two peaks at 10.003 and 14.239 minutes. The y-axis is mV (0 to 80) and the x-axis is minutes (0.0 to 25.0).

Peak#	Ret. Time	Area	Height	Area%
1	10.003	4540531	75644	50.537
2	14.239	4443997	56118	49.463
Total		8984527	131761	100.000

1	9.965	10534028	187432	99.418
2	13.552	61652	1339	0.582
Total		10595681	188771	100.000

COC(=O)CC(O)N(C1=CC=C(OC)C=C1)C(=O)OC(C)C

**(S)-3.44e-Me**  
(7% isopropanol/  
hexanes, AS-H)  
(Table 3.8, entry  
7)

Datafile Name: MS\_04\_102a\_DP(Eto)MeMorediluted\_7%PA\_AS\_H01.lcd  
Sample Name: MS\_04\_102a\_DP(Eto)MeMorediluted\_7%PA\_AS\_H

Chromatogram showing two peaks at 9.965 and 13.552 minutes. The y-axis is mV (0 to 175) and the x-axis is minutes (0.0 to 25.0).

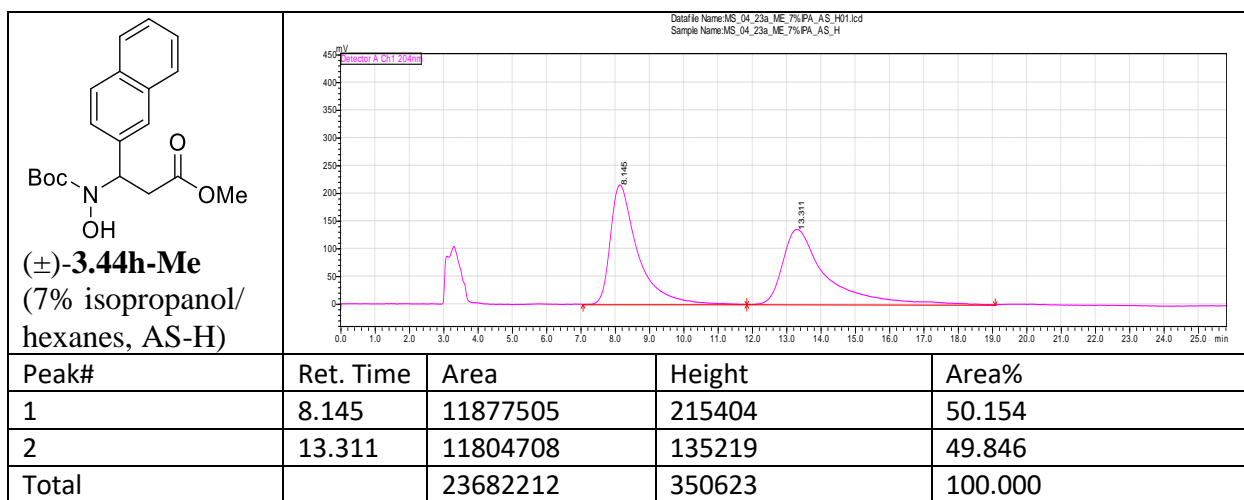
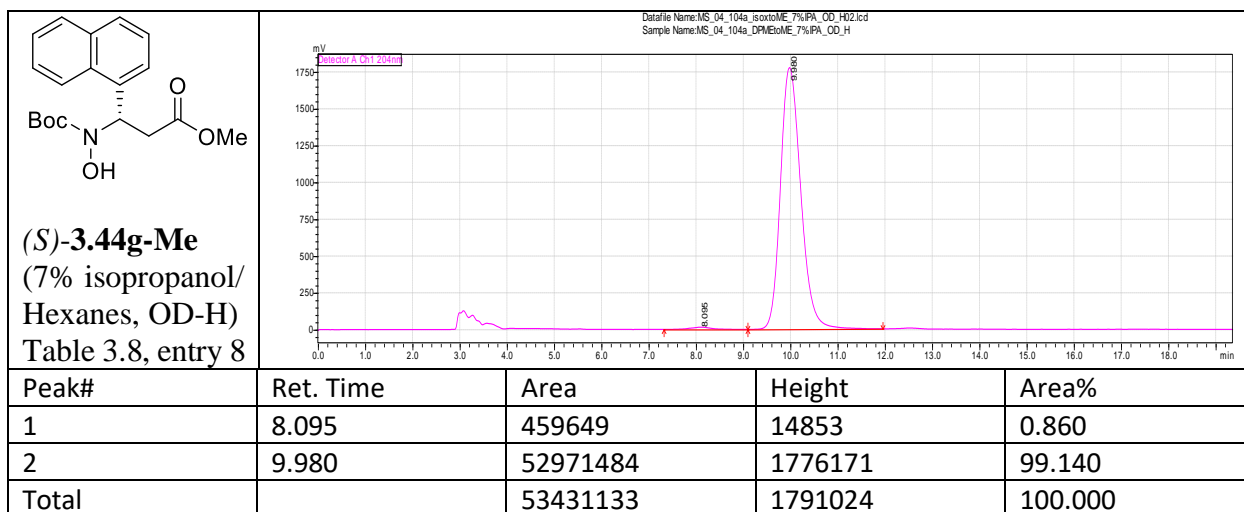
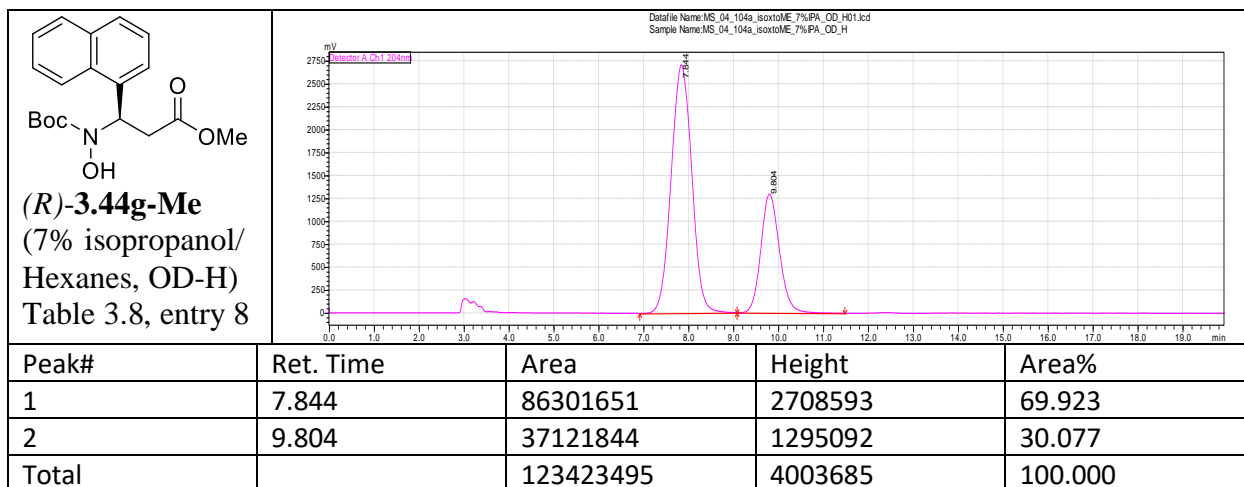
1	8.163	34530360	1208388	49.922
2	10.092	34637684	1234049	50.078
Total		69168044	2442437	100.000

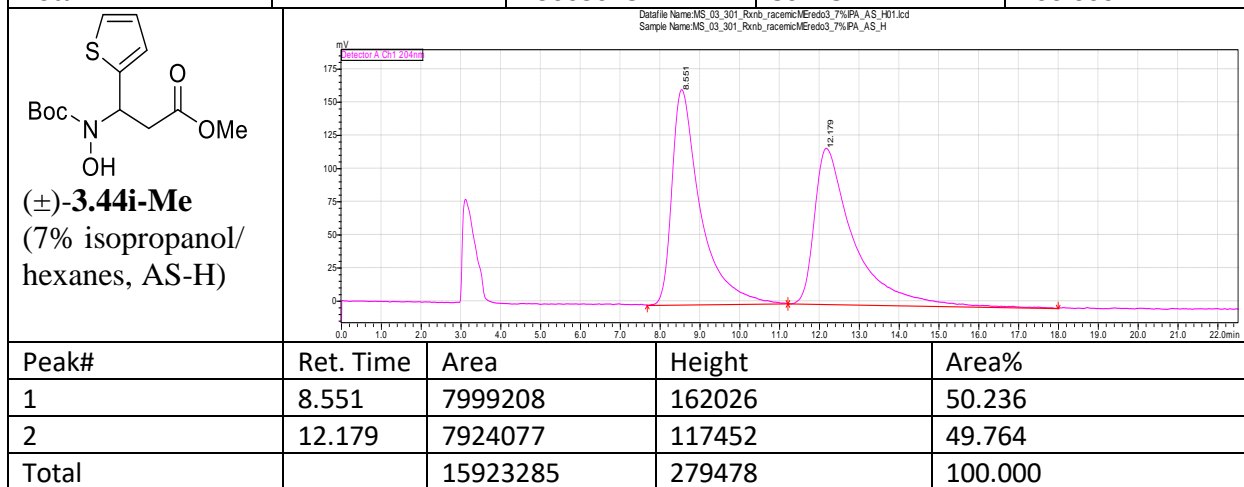
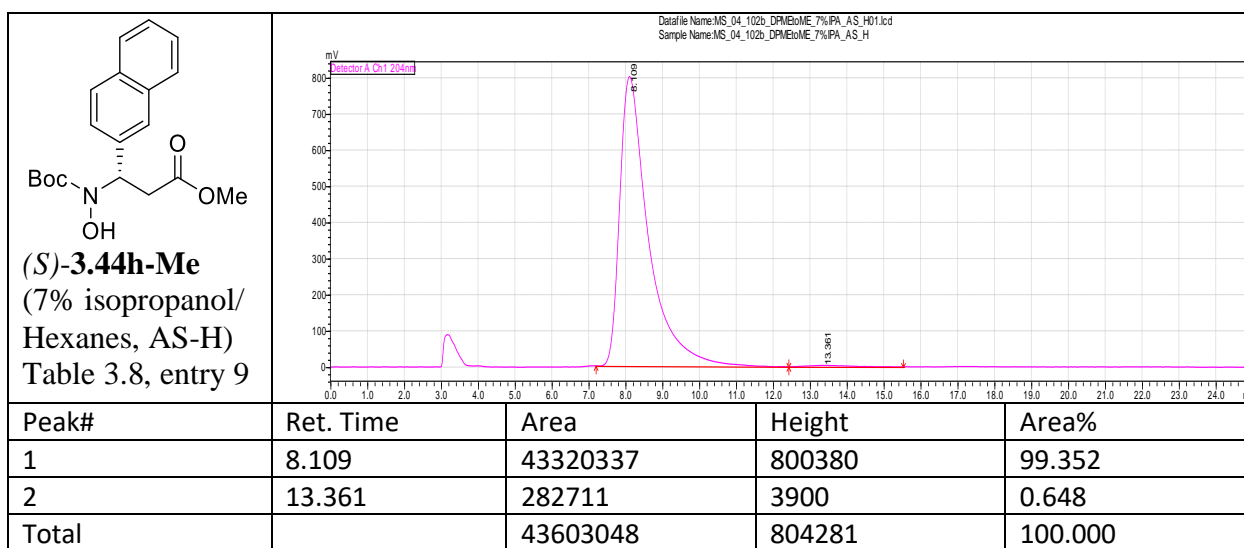
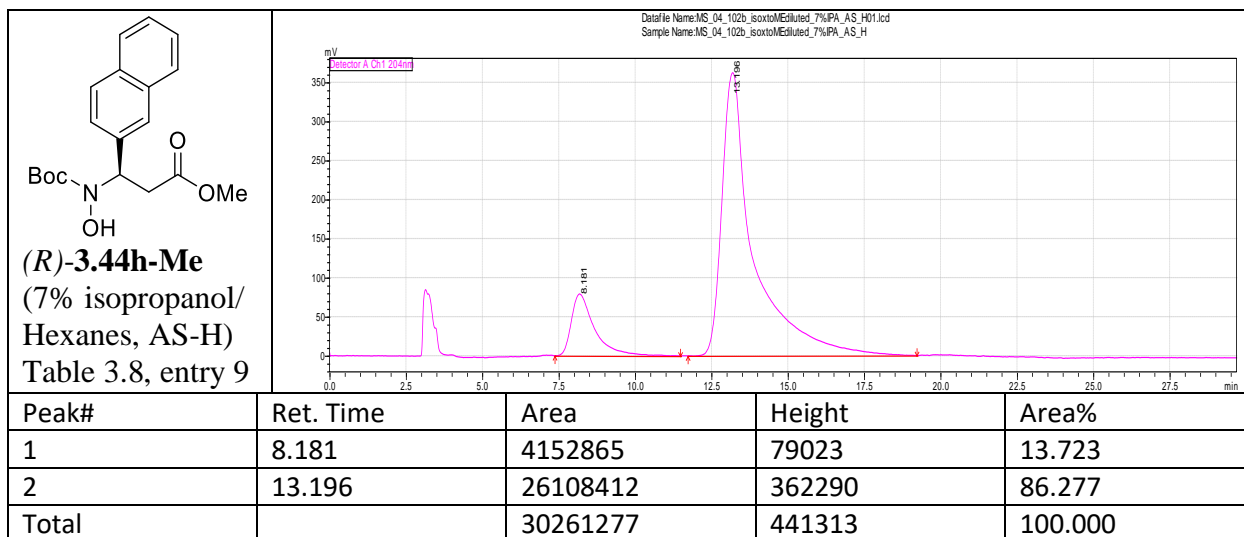
COC(=O)CC(O)N(C1=CC=C2C=CC=CC2=C1)C(=O)OC(C)C

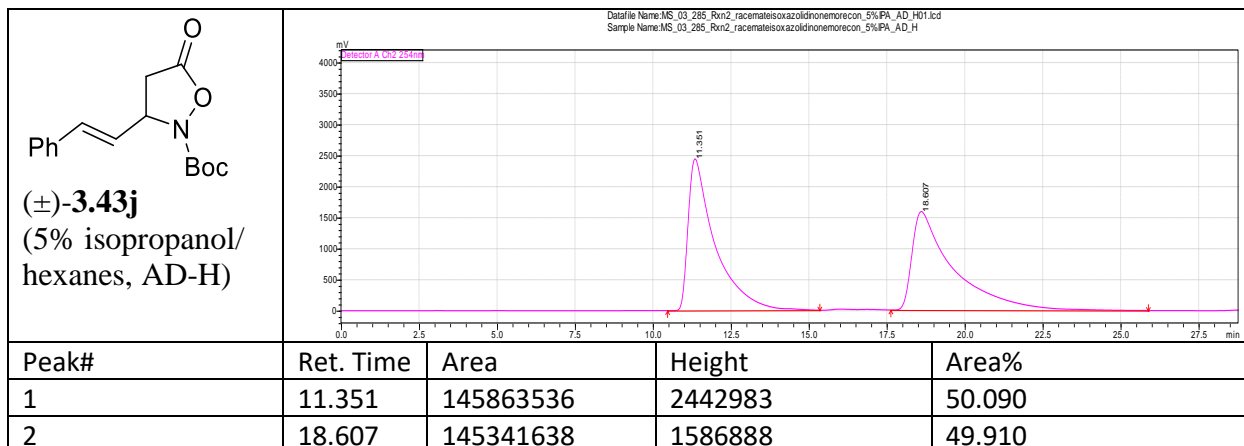
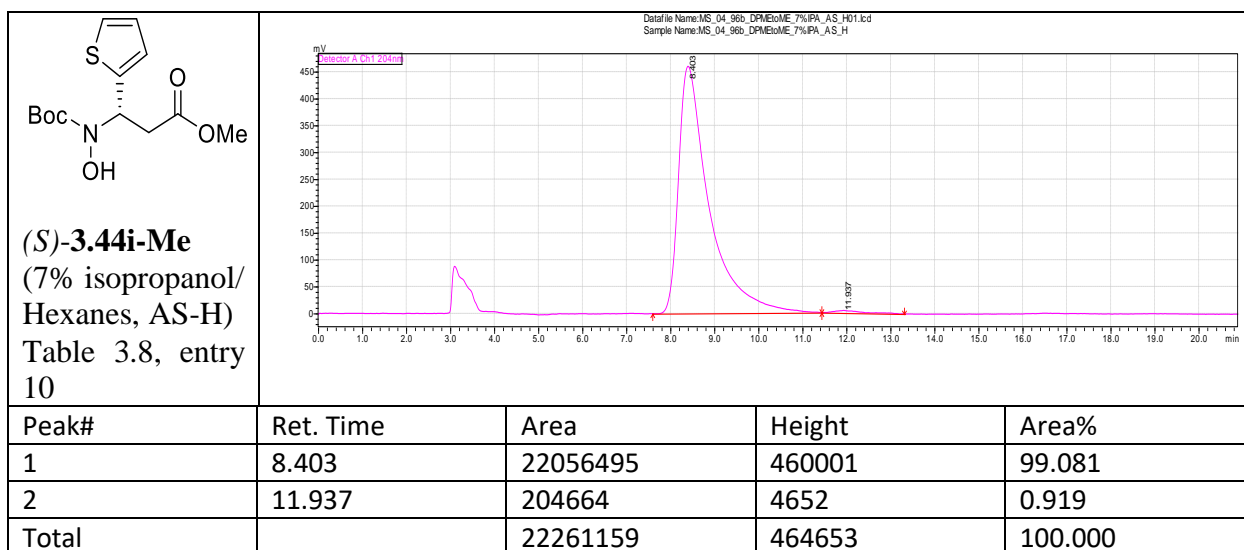
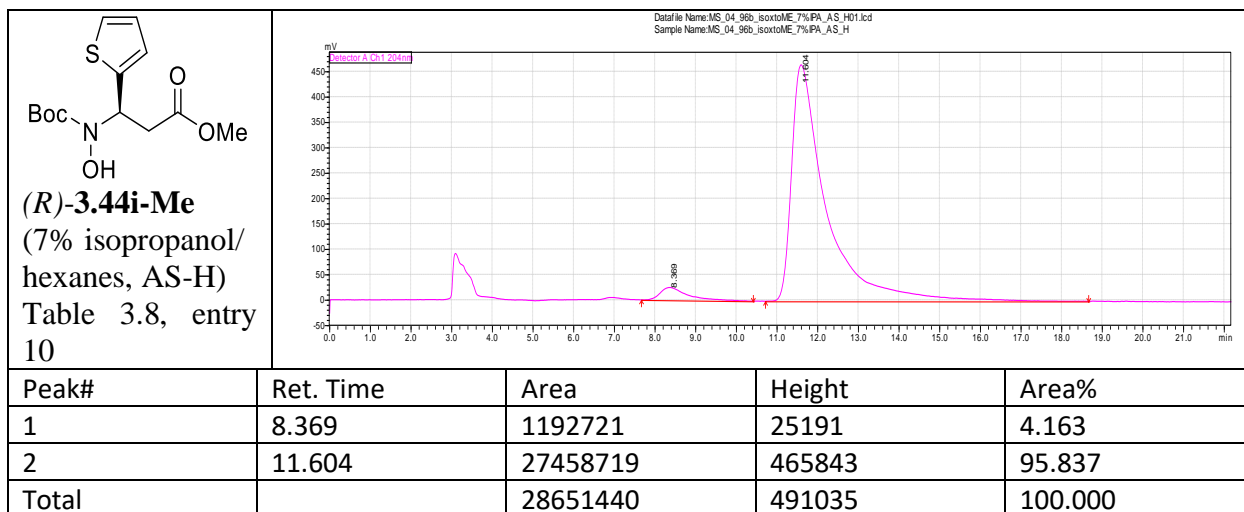
**(±)-3.44g-Me**  
(7% isopropanol/  
hexanes, OD-H)

Datafile Name: MS\_03\_299d\_raceMe\_7%PA\_OD\_H01.lcd  
Sample Name: MS\_03\_299d\_raceMe\_7%PA\_OD\_H

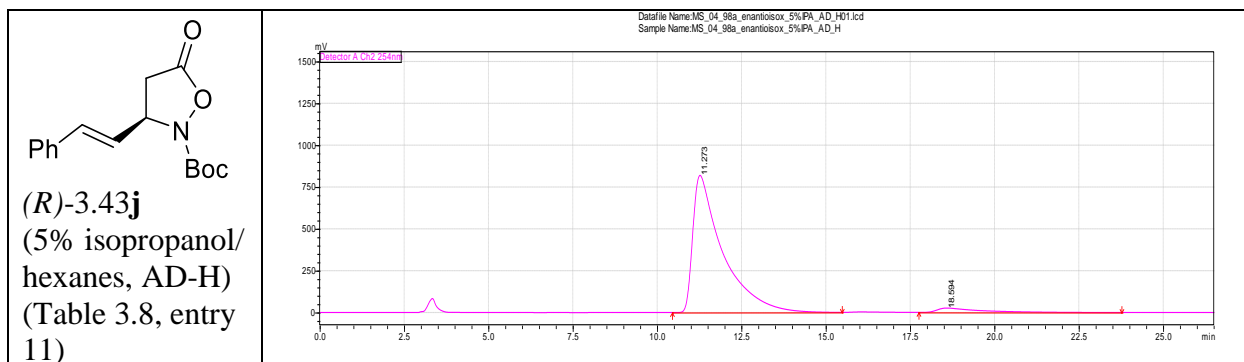
Chromatogram showing two peaks at 8.163 and 10.092 minutes. The y-axis is mV (0 to 2500) and the x-axis is minutes (0.0 to 15.0).



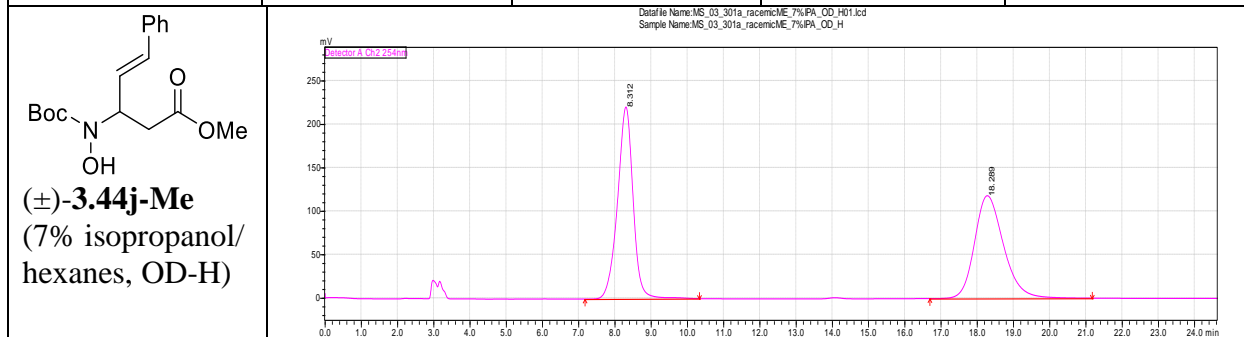




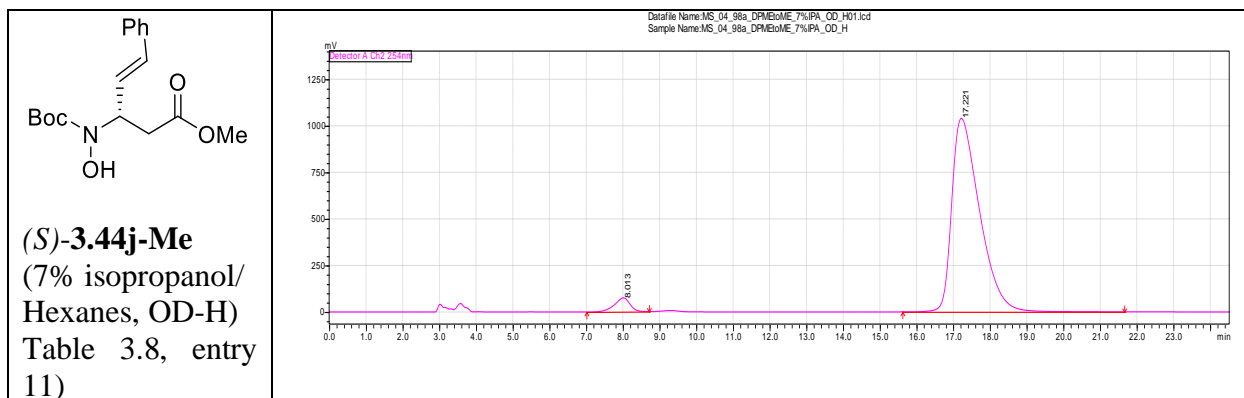
Total		291205175	4029871	100.000
-------	--	-----------	---------	---------



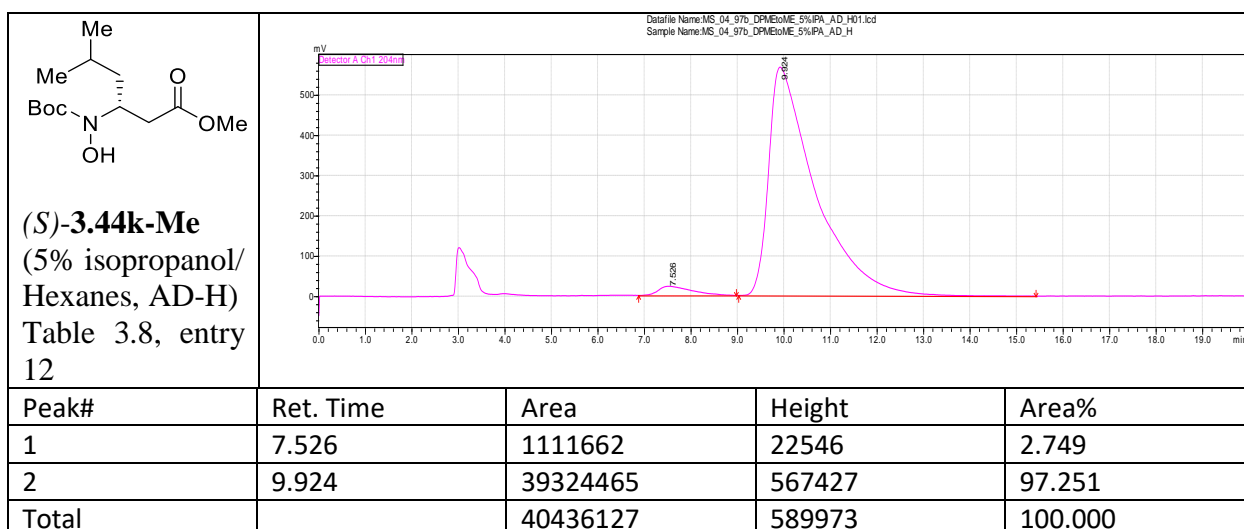
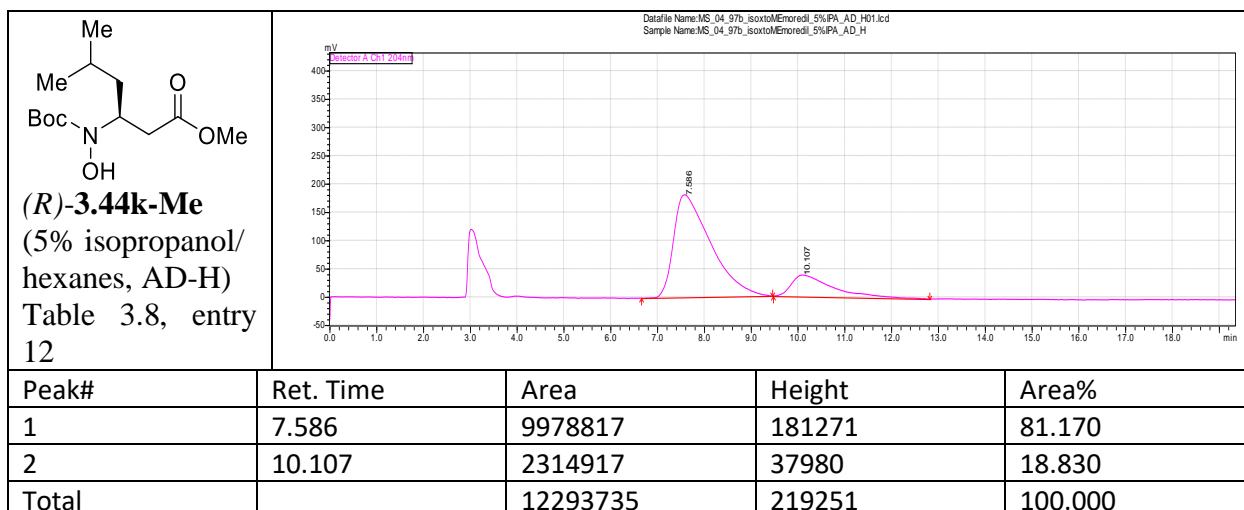
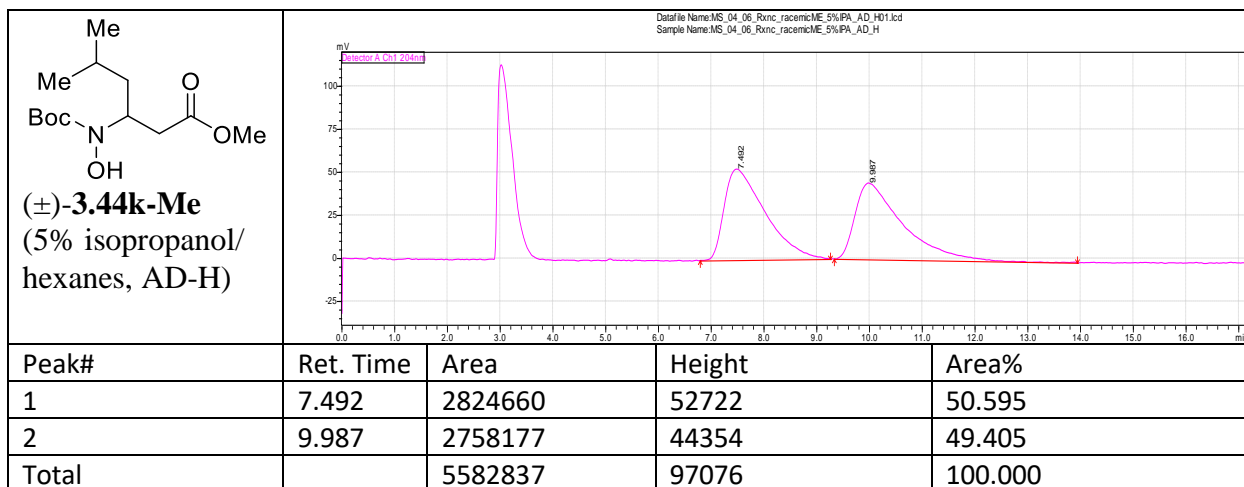
Peak#	Ret. Time	Area	Height	Area%
1	11.273	50294585	818986	95.625
2	18.594	2300825	26147	4.375
Total		52595410	845134	100.000

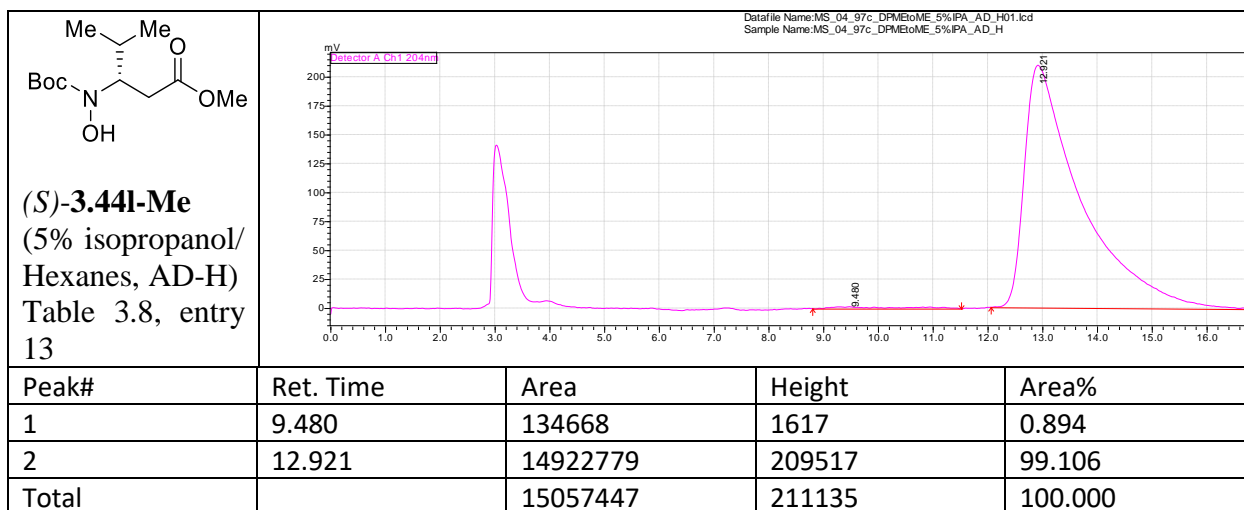
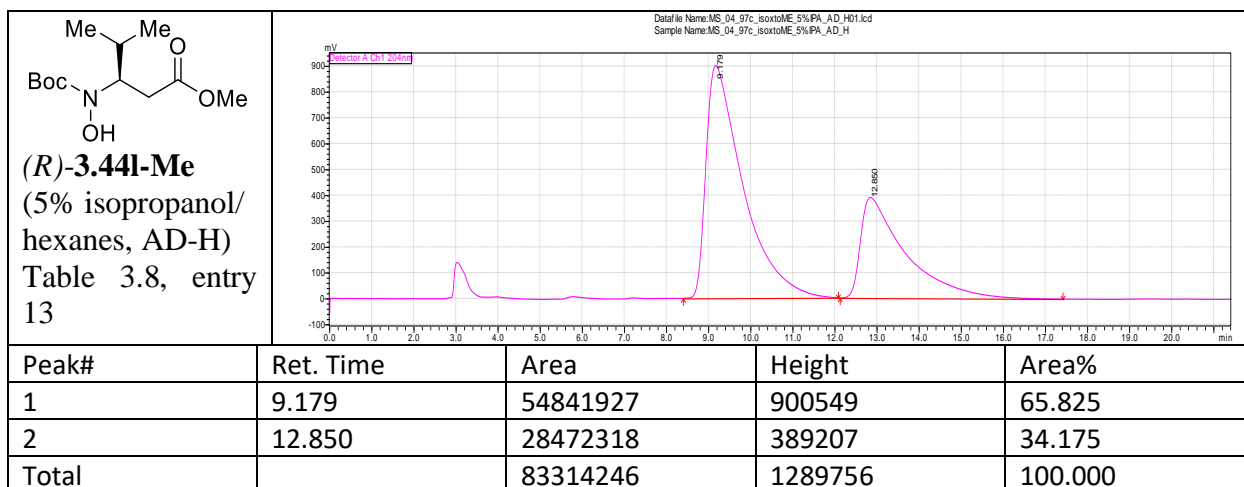
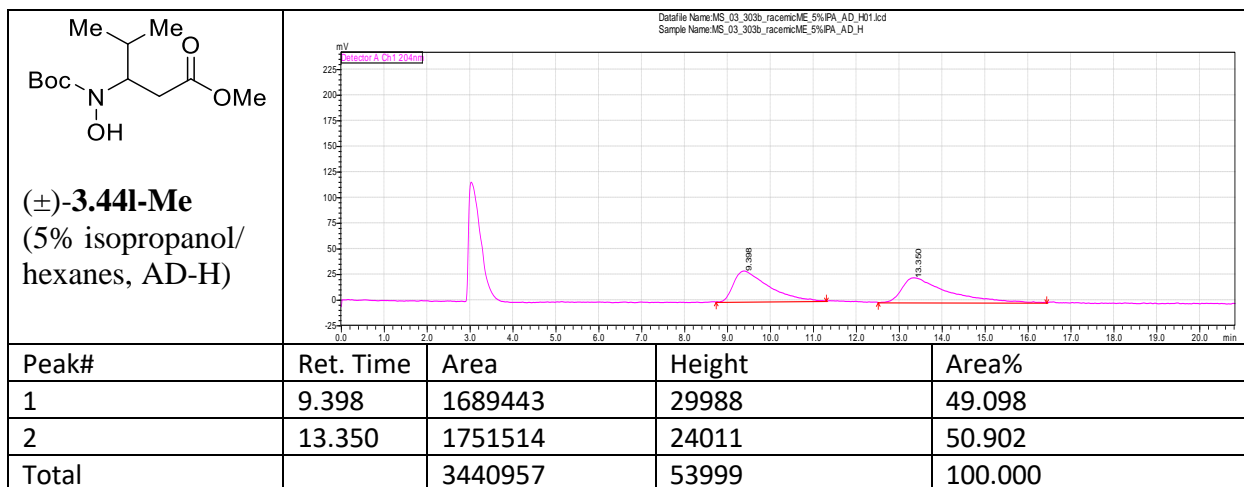


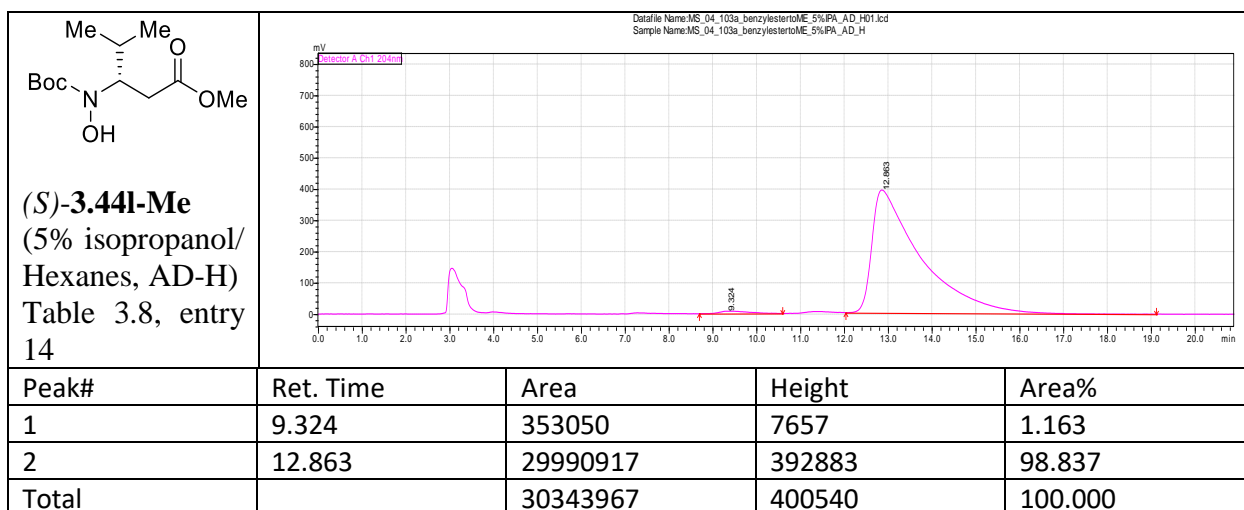
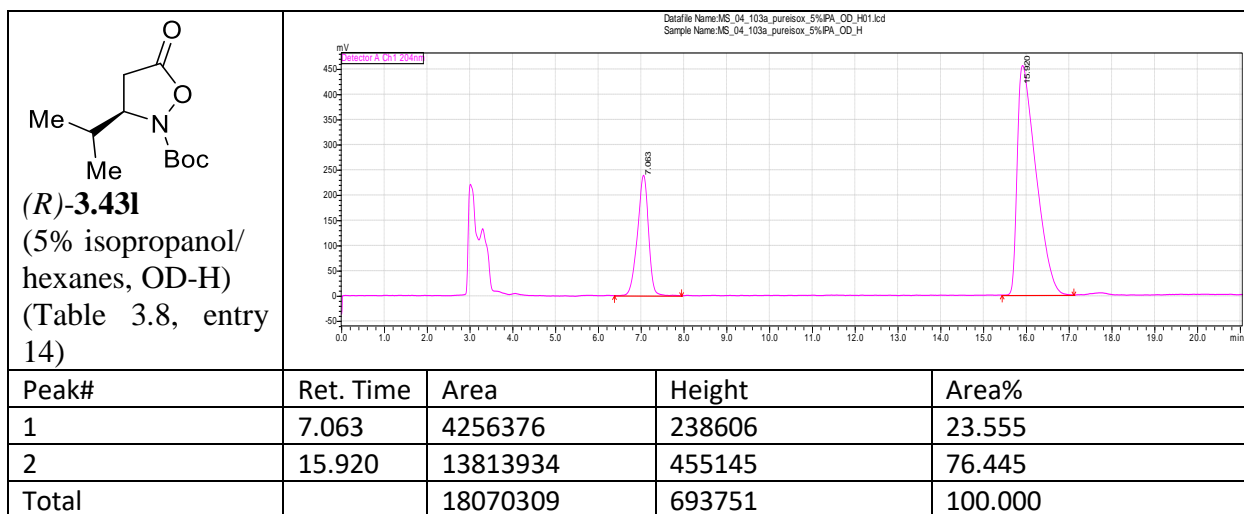
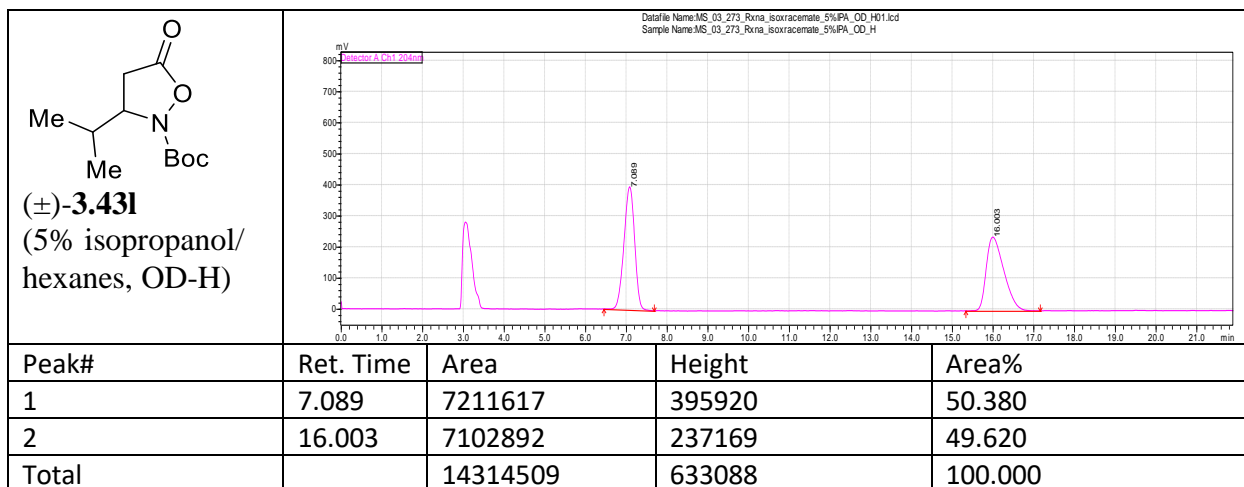
Peak#	Ret. Time	Area	Height	Area%
1	8.312	6607022	220888	50.124
2	18.289	6574231	118174	49.876
Total		13181253	339062	100.000



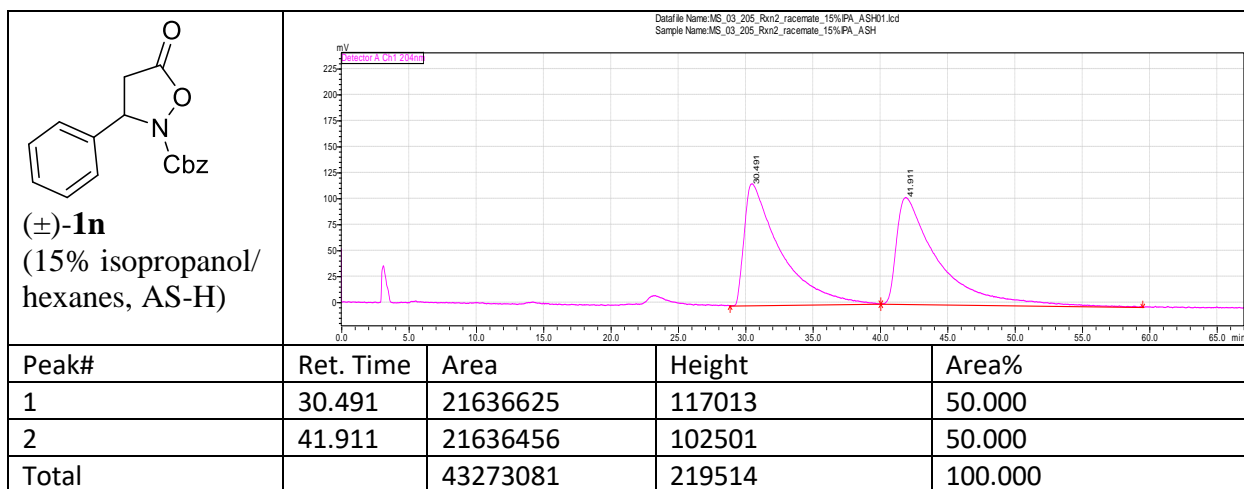
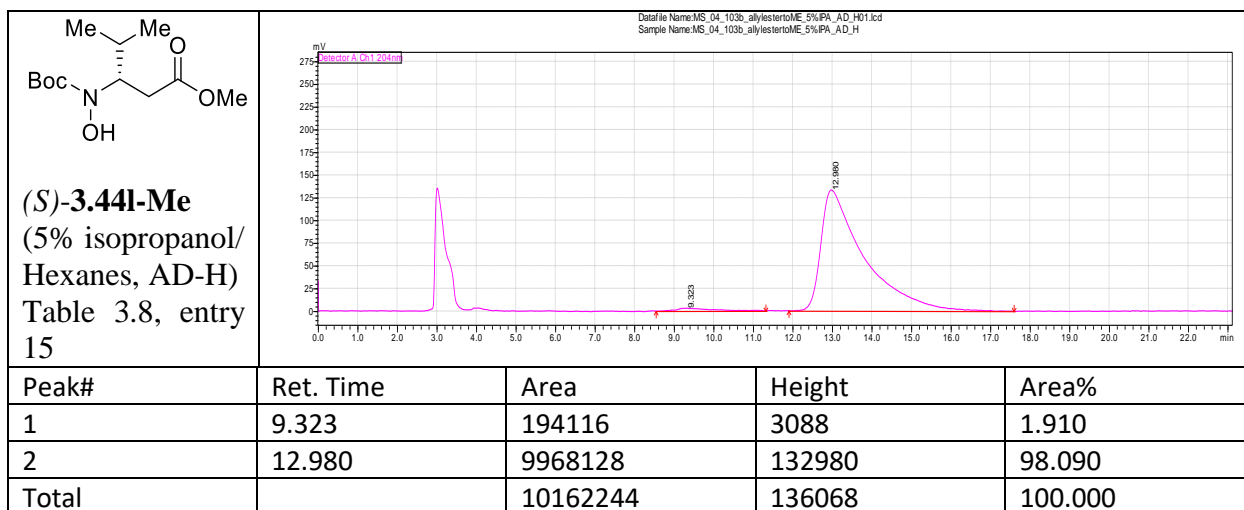
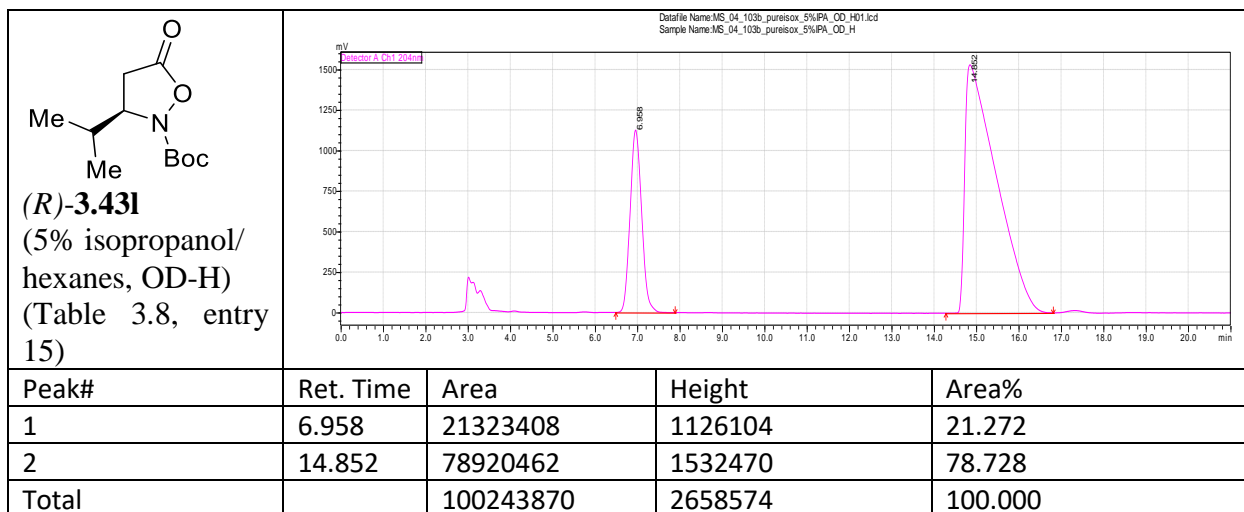
Peak#	Ret. Time	Area	Height	Area%
1	8.013	2183036	74389	3.839
2	17.221	54687323	1039945	96.161
Total		56870359	1114334	100.000

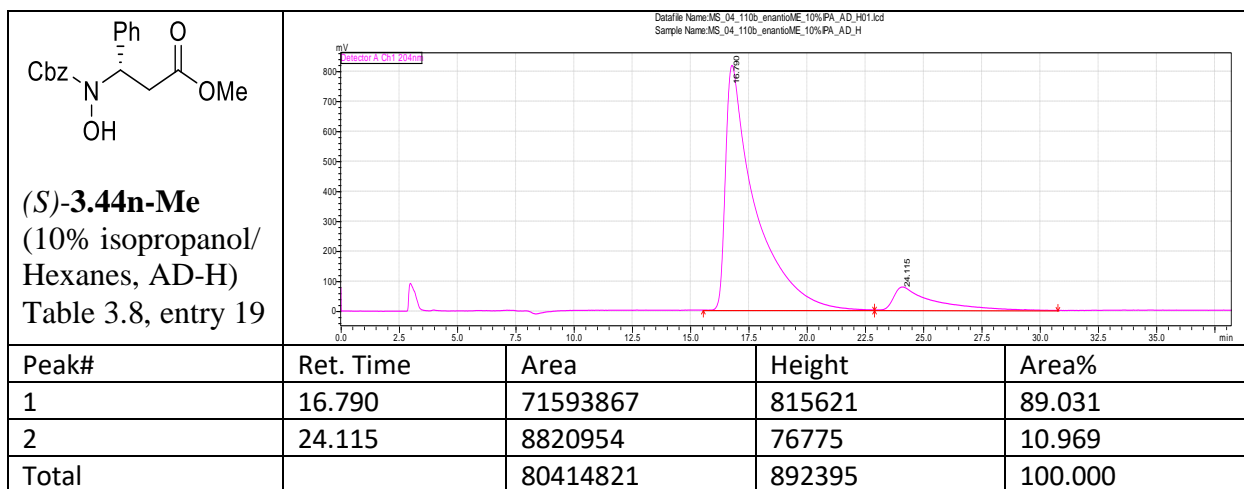
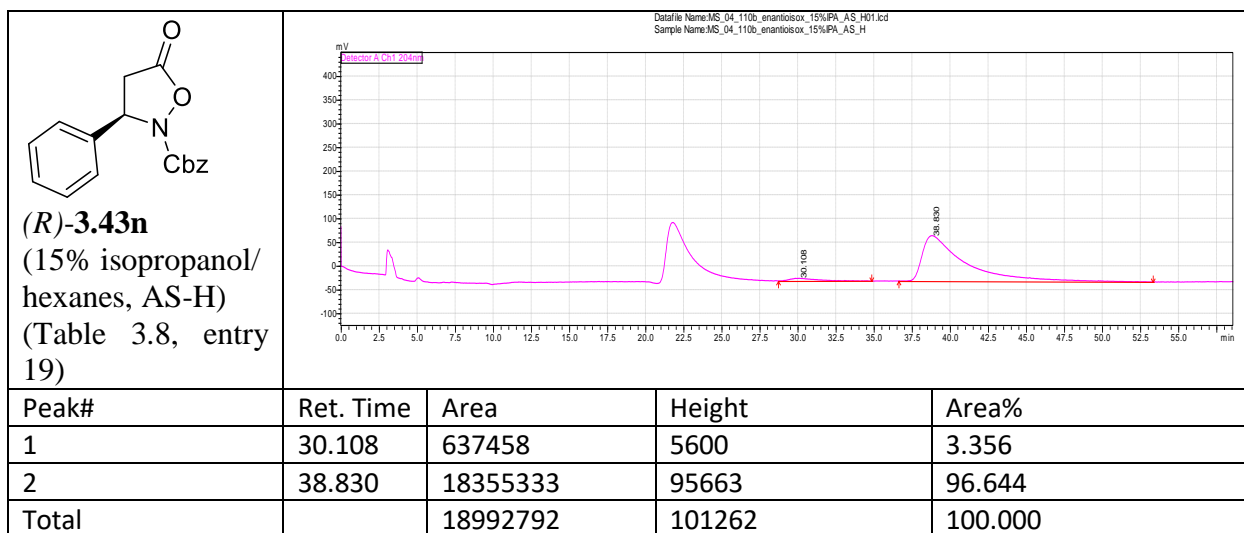
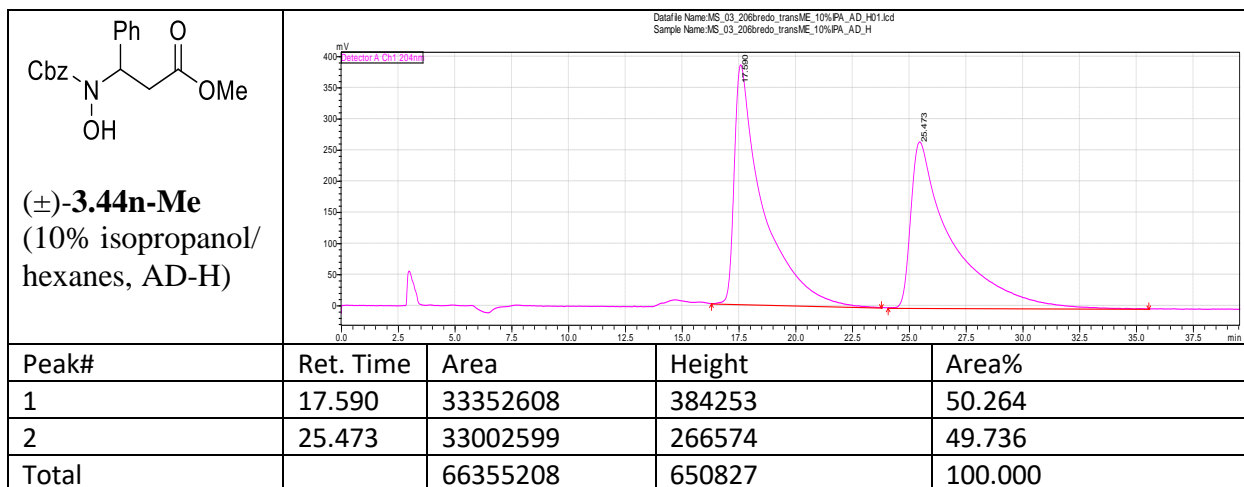


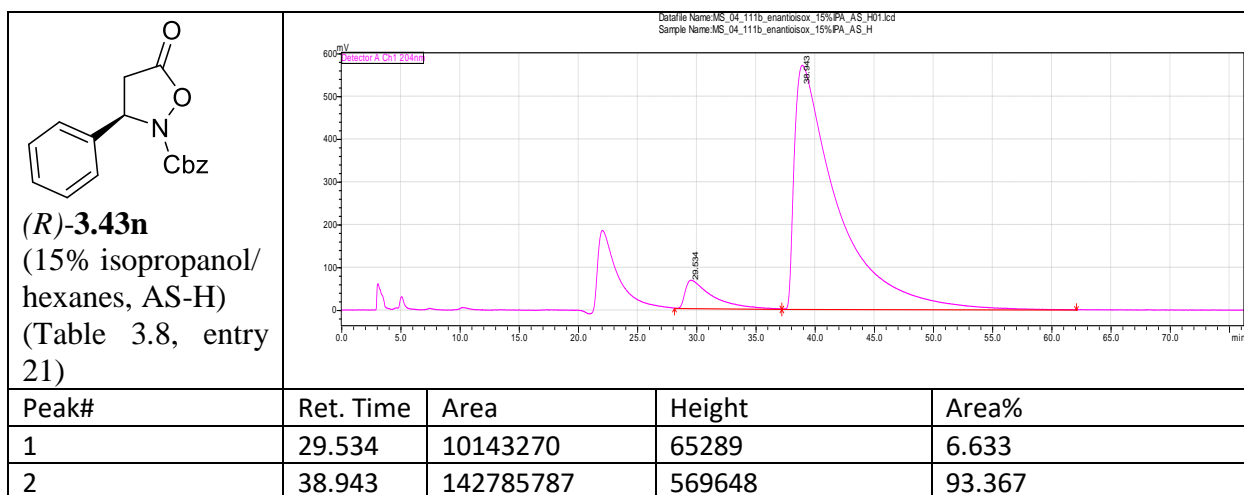
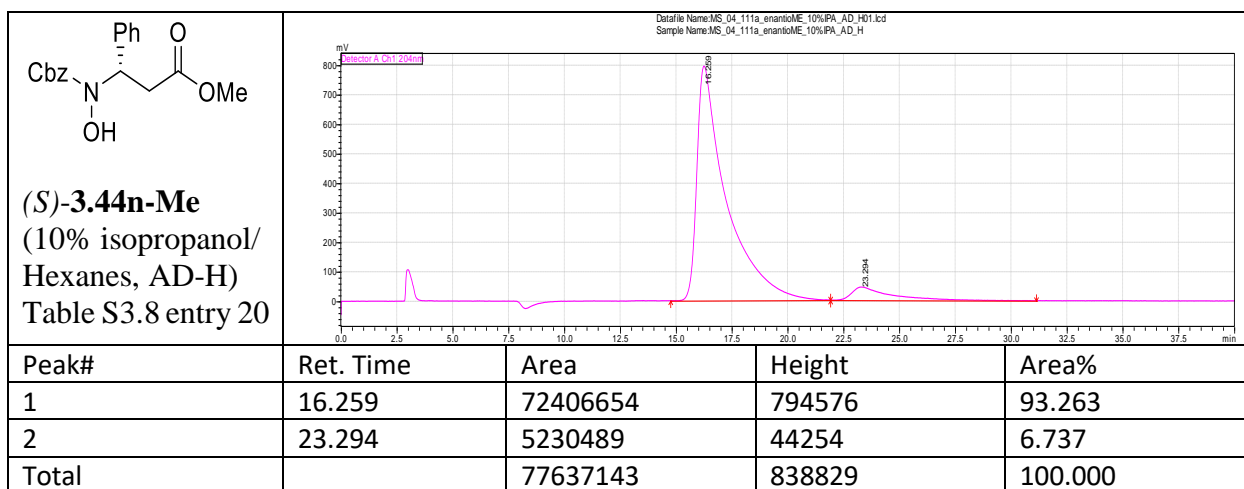
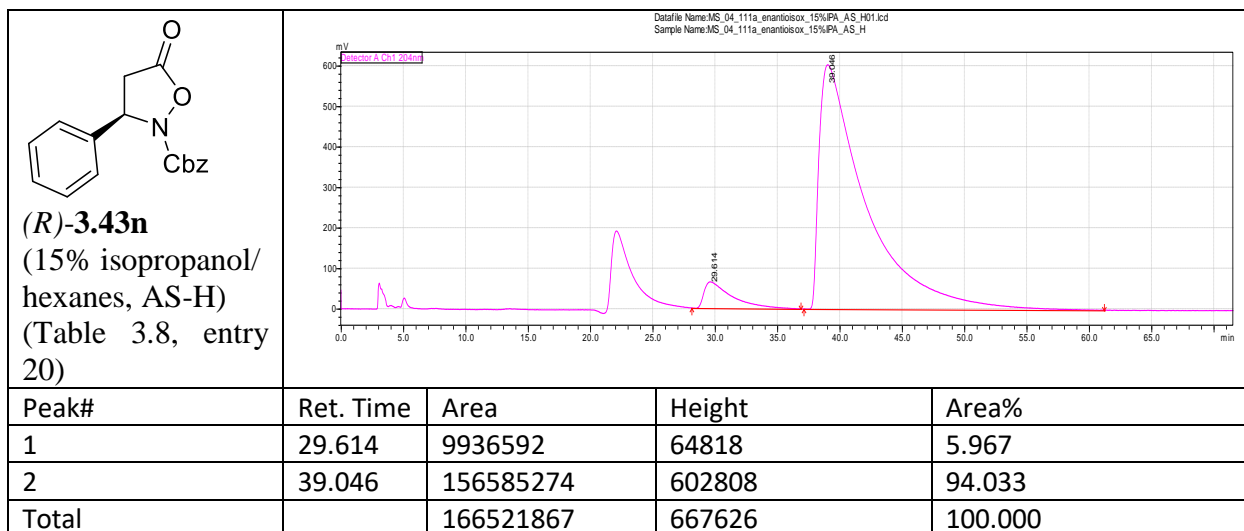




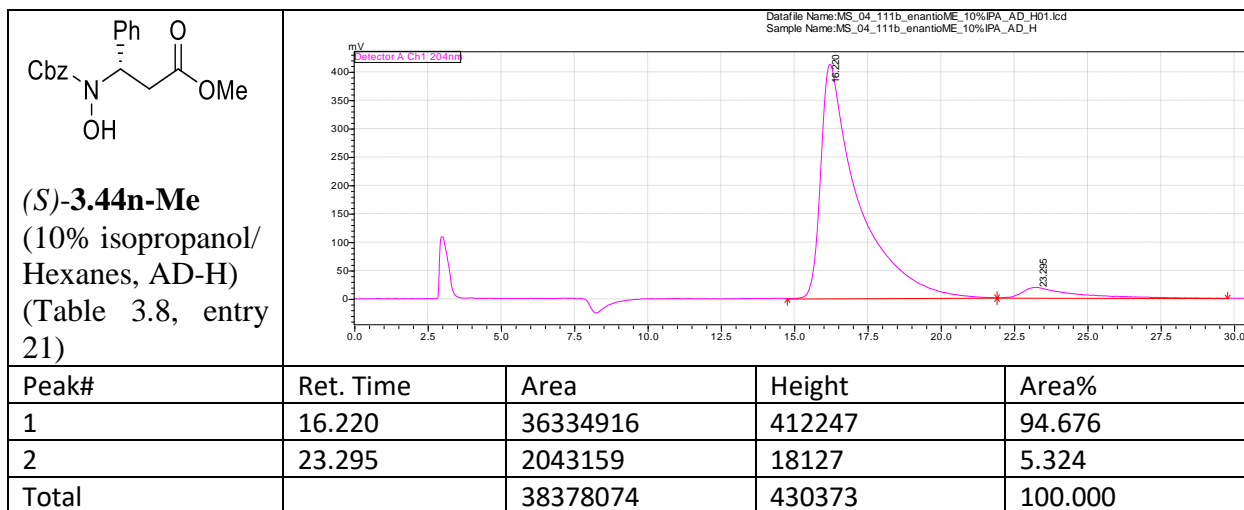


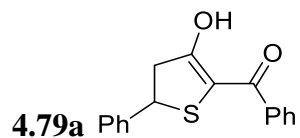




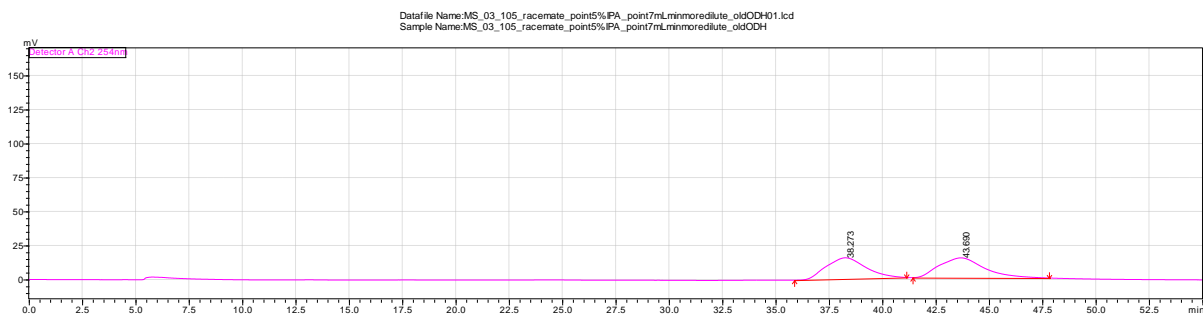


Total		152929057	634937	100.000
-------	--	-----------	--------	---------



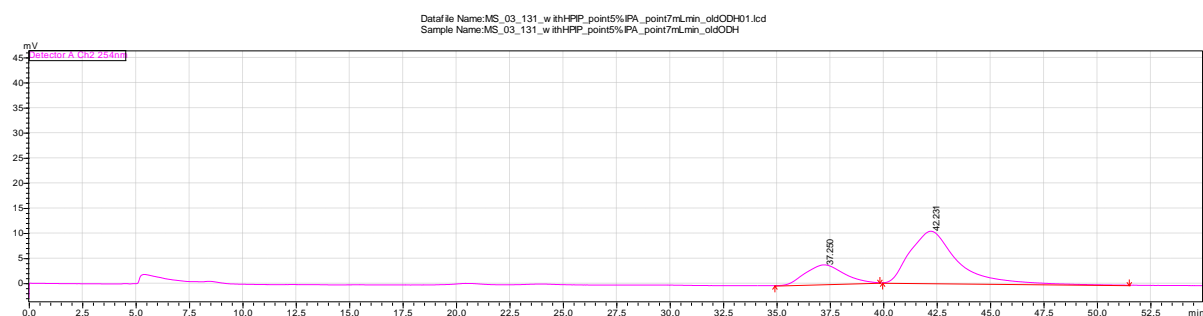


With catalyst **DHIP 4.59a**



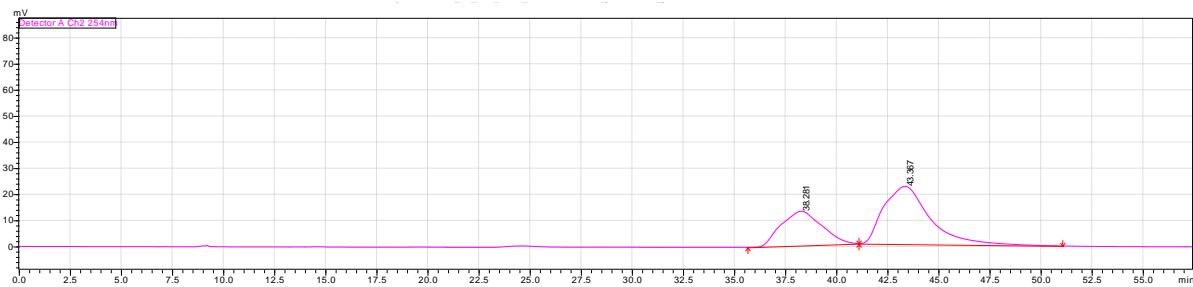
Peak#	Ret. Time	Area	Height	Area%
1	38.273	2004875	15564	48.334
2	43.69	2143115	14653	51.666
Total		4147989	30218	100

With catalyst **4.54** (Figure 4.16)



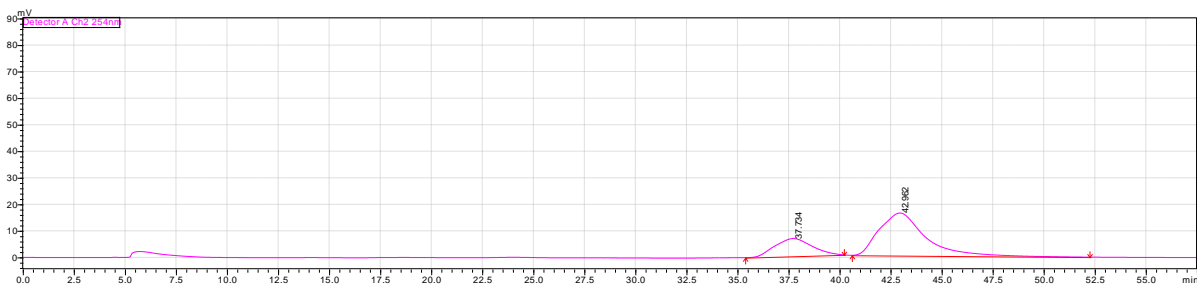
Peak#	Ret. Time	Area	Height	Area%
1	37.25	478894	3866	23.15
2	42.231	1589788	10369	76.85
Total		2068682	14235	100

With catalyst **4.69** (Figure 4.16)

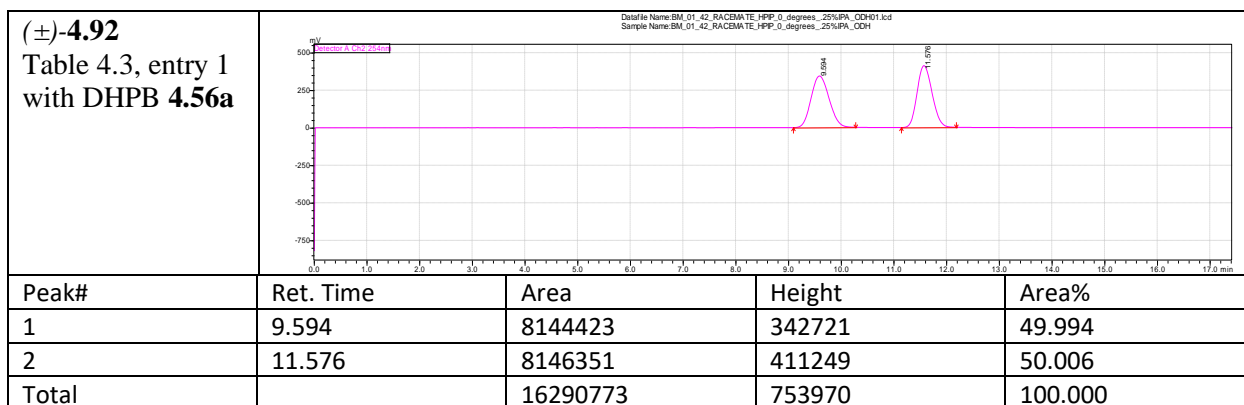
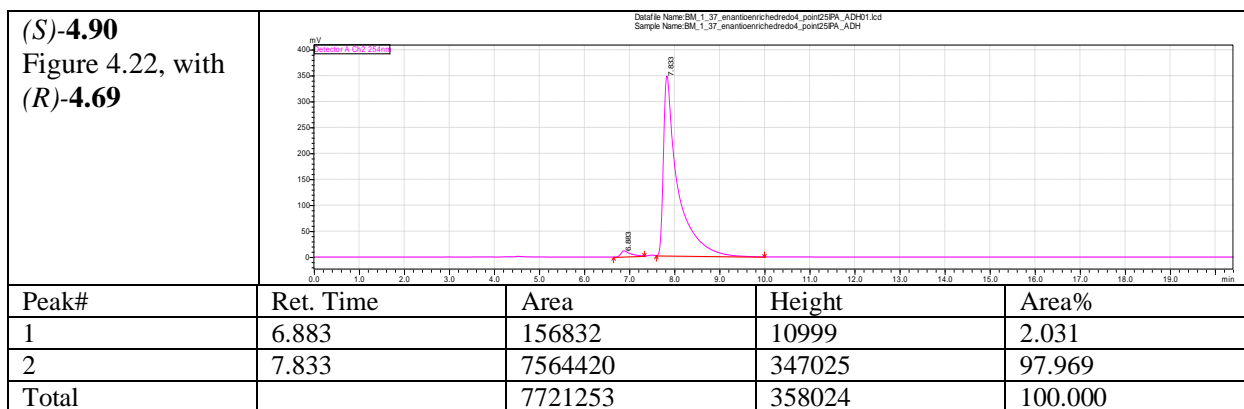
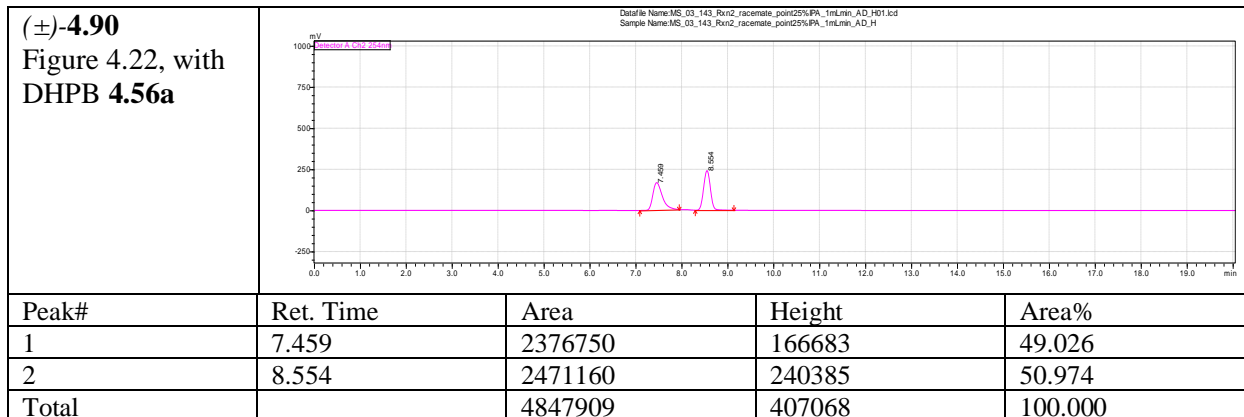


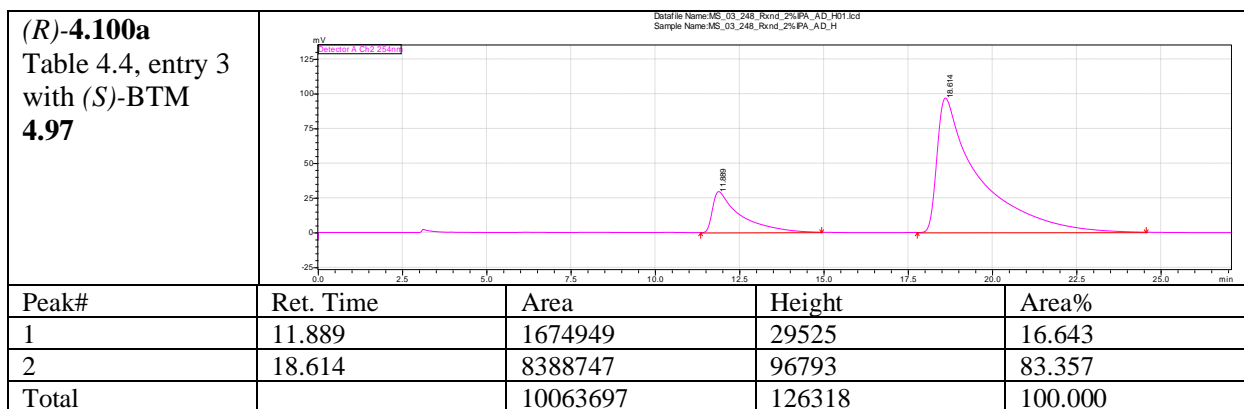
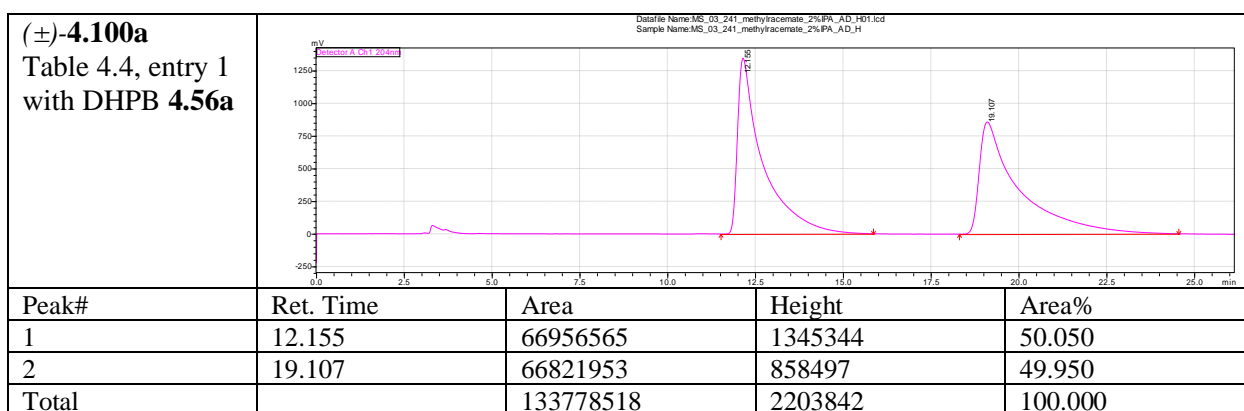
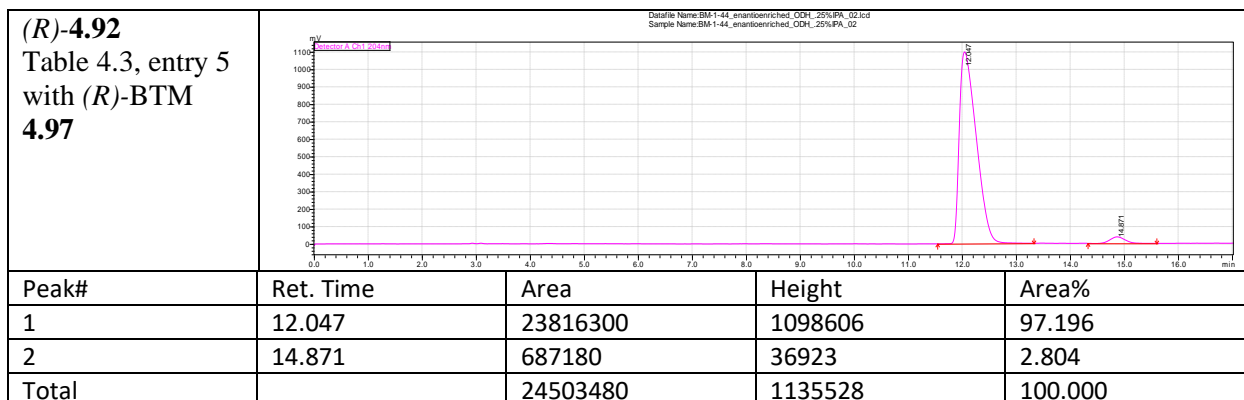
Peak#	Ret. Time	Area	Height	Area%
1	38.281	1806748	13149	34.104
2	43.367	3490995	22180	65.896
Total		5297743	35328	100

With catalyst **4.81** (Figure 4.16)



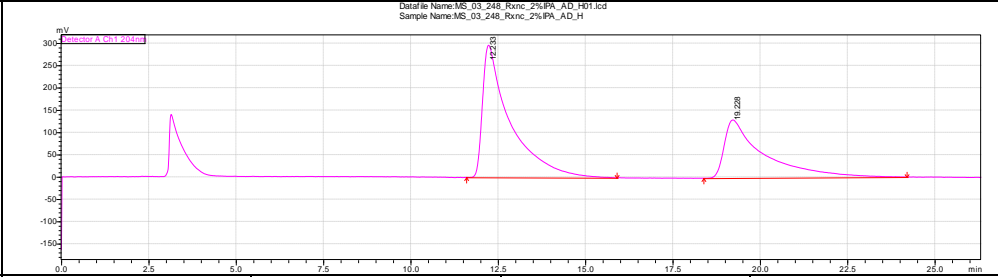
Peak#	Ret. Time	Area	Height	Area%
1	37.734	845452	6684	25.044
2	42.962	2530477	16068	74.956
Total		3375929	22752	100





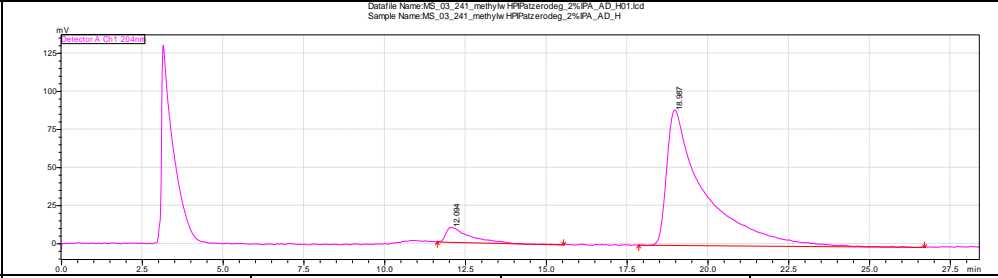


**(S)-4.100a**  
 Table 4.4, entry 5  
 with (S)-HBTM-  
 2.1 4.96



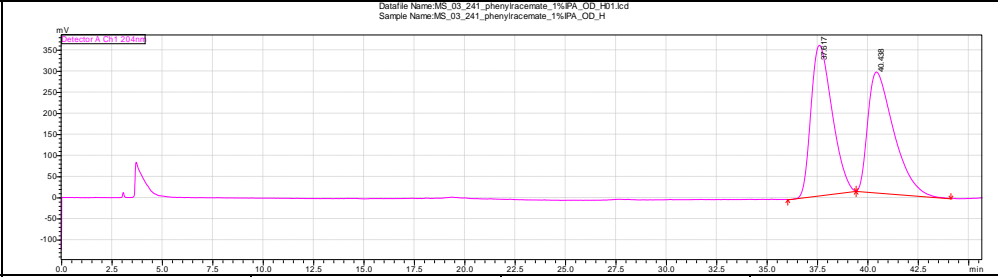
Peak#	Ret. Time	Area	Height	Area%
1	12.233	16248476	296709	61.334
2	19.228	10243160	130263	38.666
Total		26491636	426972	100.000

**(R)-4.100a**  
 Table 4.4, entry 7  
 with (R)-H-PIP  
 4.54

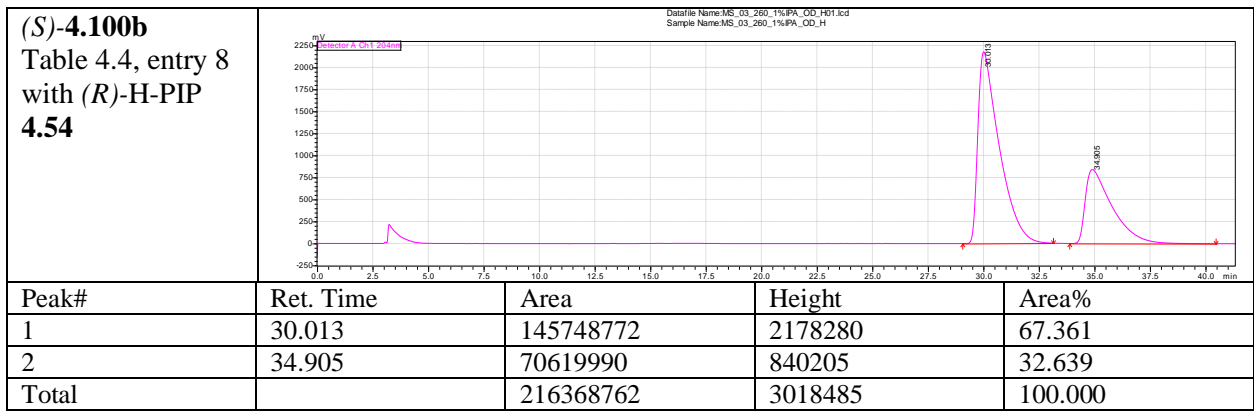
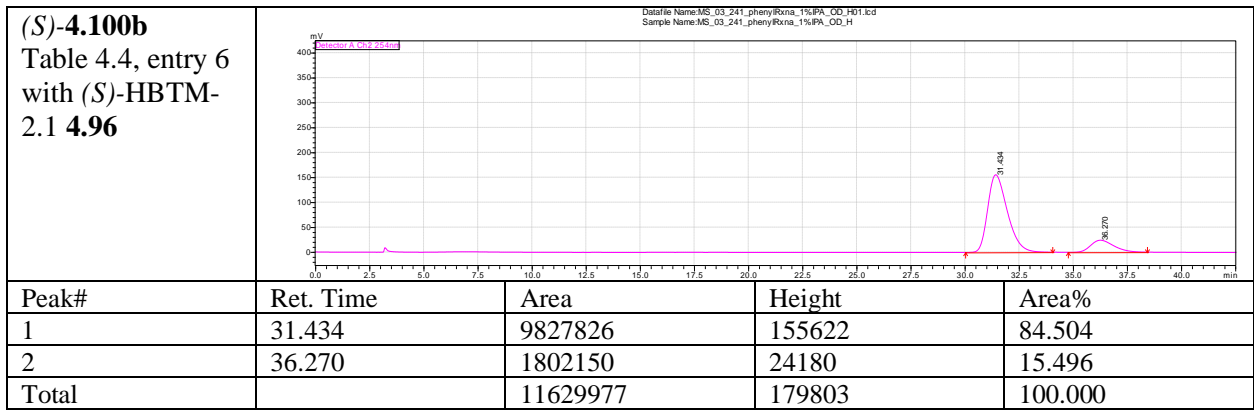
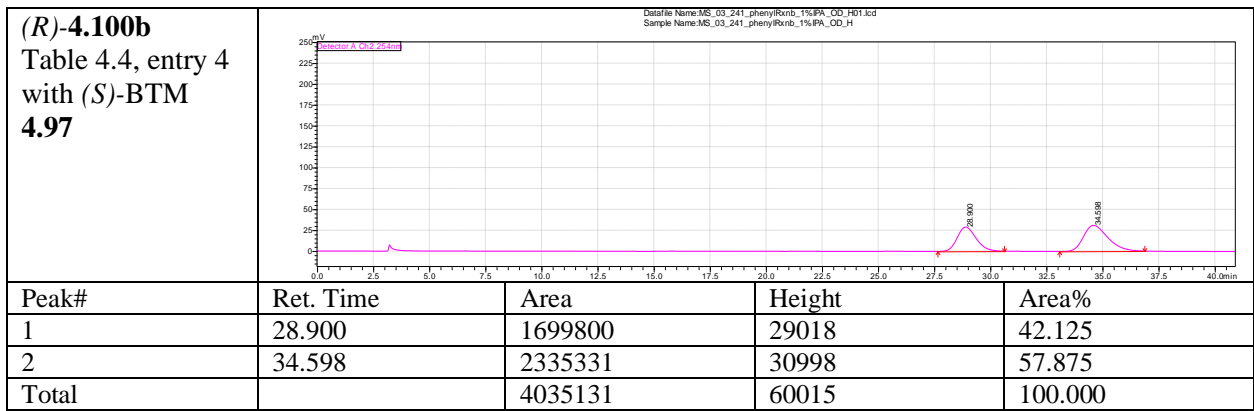


Peak#	Ret. Time	Area	Height	Area%
1	12.094	453445	9615	6.037
2	18.987	7057550	88554	93.963
Total		7510996	98169	100.000

**(±)-4.100b**  
 Table 4.4, entry 2  
 with DHPB 4.56a



Peak#	Ret. Time	Area	Height	Area%
1	37.617	25894316	356101	50.344
2	40.438	25540532	285918	49.656
Total		51434848	642019	100.000



## A.4 $^1\text{H}$ and $^{13}\text{C}$ NMR spectra

